Published June 29, 2015

Membrane potential and Ca^{2+} concentration dependence on pressure and vasoactive agents in arterial smooth muscle: A model

Arthur Karlin

Department of Biochemistry and Molecular Biophysics, Department of Physiology and Cellular Biophysics, and Department of Neurology, College of Physicians and Surgeons, Columbia University, New York, NY 10032

Arterial smooth muscle (SM) cells respond autonomously to changes in intravascular pressure, adjusting tension to maintain vessel diameter. The values of membrane potential (V_m) and sarcoplasmic Ca^{2+} concentration (Ca_{in}) within minutes of a change in pressure are the results of two opposing pathways, both of which use Ca^{2+} as a signal. This works because the two Ca^{2+}-signaling pathways are confined to distinct microdomains in which the Ca^{2+} concentrations needed to activate key channels are transiently higher than Ca_{in}. A mathematical model of an isolated arterial SM cell is presented that incorporates the two types of microdomains. The first type consists of junctions between cisternae of the peripheral sarcoplasmic reticulum (SR), containing ryanodine receptors (RyRs), and the sarcolemma, containing voltage- and Ca^{2+}-activated K^+ (BK) channels. These junctional microdomains promote hyperpolarization, reduced Ca_{in}, and relaxation. The second type is postulated to form around stretch-activated nonspecific cation channels and neighboring Ca^{2+}-activated Cl^- channels, and promotes the opposite (depolarization, increased Ca_{in}, and contraction). The model includes three additional compartments: the sarcoplasm, the central SR lumen, and the peripheral SR lumen. It incorporates 37 protein components. In addition to pressure, the model accommodates inputs of α- and β-adrenergic agonists, ATP, 11,12-epoxyeicosatrienoic acid, and nitric oxide (NO). The parameters of the equations were adjusted to obtain a close fit to reported V_m and Ca_{in} as functions of pressure, which have been determined in cerebral arteries. The simulations were insensitive to ±10% changes in most of the parameters. The model also simulated the effects of inhibiting RyR, BK, or voltage-activated Ca^{2+} channels on V_m and Ca_{in}. Deletion of BK β1 subunits is known to increase arterial–SM tension. In the model, deletion of β1 raised Ca_{in} at all pressures, and these increases were reversed by NO.

INTRODUCTION

Arteries are lined by endothelial cells and are wrapped by one or more layers of smooth muscle (SM) cells. There are electrical coupling and chemical signaling between SM cells and between SM cells and endothelial cells, and SM cells receive numerous neurotransmitter, endocrine, and paracrine signals that promote either contraction or relaxation. Independently of these signals, arterial SM cells respond autonomously to changes in sarcolemmal stretch caused by changes in intravascular pressure (McCarron et al., 1989). This phenomenon is called "myogenic reactivity." It has an early phase called the "myogenic response" and a sustained phase called "myogenic tone." The overall effect is to control luminal diameter in the face of changing luminal pressure. It is a vital background activity on top of which the many other stimuli have their effects.

The myogenic response is regulated by opposing circuits: one promoting an increase in sarcoplasmic Ca^{2+} concentration (Ca_{in}) and thereby an increase in tension and one promoting the opposite. Both circuits use Ca^{2+} (Ca) as a signal (Hill-Eubanks et al., 2011). The dual roles of Ca as a signal both for contraction and relaxation depend on the physical separation of opposing pathways afforded both by SM cellular architecture (Moore et al., 2004; van Breemen et al., 2013) and the widely different Ca sensitivities of the circuit-specific components. In the SM sarcoplasm, Ca_{in} varies between ∼100 and ∼400 nM, over which range myosin light chain kinase activity goes from low to half-maximal (Stull et al., 1998), and tension from low to maximal (Hill-Eubanks et al., 2011). The stretch-induced rise in Ca_{in} depends on the activity of voltage-dependent Ca (CaV) channels, principally those containing CaV1.2 (Moosmang et al., 2003; Navedo et al., 2007).

The activation of CaV channels is opposed by the hyperpolarizing activity of large-conductance, voltage- and Ca^{2+}-activated K^+ (BK) channels. In the range of

Correspondence to Arthur Karlin: ak12@columbia.edu

Abbreviations used in this paper: BK, large-conductance, voltage- and Ca^{2+}-activated K^+; Ca, Ca^{2+}; Ca_{in}, sarcoplasmic Ca^{2+} concentration; CaV, voltage-dependent Ca; Cl, Cl^-; ClA, Ca-activated Cl; DAG, diacylglycerol; EET, 11,12-epoxyeicosatrienoic acid; K, K^+; Na, Na^+; NCX, Na–Ca exchanger; NO, nitric oxide; rms, root mean square; SERCA, sarcoplasmic/endoplasmic reticulum Ca^{2+}-ATPase; SM, smooth muscle; STOCs, spontaneous, transient outward currents; TRP, transient receptor potential; V_m, membrane potential.

The Rockefeller University Press $30.00
J. Gen. Physiol. Vol. 146 No. 1 79–96
www.jgp.org/cgi/doi/10.1085/jgp.201511380

Supplemental Material can be found at:
http://jgp.rupress.org/content/suppl/2015/06/26/jgp.201511380.DC1.html

Published June 29, 2015

membrane potential (V_m) in SM cells, half-maximal activity of BK channels requires tens of micromolar Ca (Jaggar et al., 2000), which is obtained in narrow junctions between the peripheral SR and the sarcolemma (Moore et al., 2004; van Breemen et al., 2013). In these junctions, clusters of ryanodine receptors (RyRs) in the peripheral SR membrane are apposed to clusters of BK channels in the sarcolemma (Lifshitz et al., 2011). RyR releases Ca into the junctional gap, transiently raising the Ca concentration 10–100 times higher than that in the sarcoplasm (Jaggar et al., 2000), recruiting additional RyR activity and activating the apposed BK channels (Nelson et al., 1995). The junction is a microdomain, in which signaling is directed by proximity and the signal intensity is tailored to the sensitivities of the target components (Neher, 1998; Berridge et al., 2003; Rizzuto and Pozzan, 2006; Neves and Iyengar, 2009; Santana and Navedo, 2009; van Breemen et al., 2013).

The initiation of the myogenic response requires its own microdomain, albeit one that does not, at least to date, have a defined subcellular structure. Stretch-activated sarcolemmal cation–conducting channels have not been definitively identified. In the current model, they are taken to be transient receptor potential (TRP) channels (Earley et al., 2004; Sharif-Naeini et al., 2009; Earley and Brayden, 2010). These deliver Ca to neighboring Ca-activated Cl (ClA) channels formed by TMEM16A, of which the half-maximal activation occurs at micromolar Ca (Bulley et al., 2012; Jin et al., 2014). The ClA channel current depolarizes the SM cell, activating CaV channels.

I present a model of the short-term, pressure-induced responses of an isolated arterial SM cell. In small arteries, removal of the endothelium did not affect either pressure-induced responses or the block of key components (Knot and Nelson, 1998). The model SM cell contains five interconnected compartments for Ca: the sarcoplasm, the central SR, the peripheral SR, the combined junctional microdomains, and the combined stretch-transducing microdomains (Fig. 1). The model includes 37 protein components located within the compartments or embedded in their bounding membranes. The experimental evidence for the assigned roles and locations of the components is stronger for some than for others. The current model builds on previous models, none of which, however, included the junctional and the stretch-transducing microdomains or dealt with the myogenic response (Bennett et al., 2005; Yang et al., 2005; Kapela et al., 2008). The current model has a large number of parameters (number of molecules of each component, rate constants, dissociation constants, permeabilities, etc.), of which only some were constrained by experimental results. Most of the unconstrained "local" parameters were adjusted to give plausible properties to the individual components. The model was closely fit to V_m and Ca_{in} as functions of intravascular pressure, determined in cerebral arteries by Knot and Nelson (1998). The fit was achieved mainly by adjusting the numbers of molecules of each of the components, considered "global" parameters. There were not enough data to determine uniquely even the subset of parameters adjusted to obtain this fit, and given the complexity of the mechanism, a unique set of fitting parameters might not be obtainable (e.g., Hines et al., 2014). Nevertheless, the model simulated experimental data beyond those used to find the set of close-fit parameters, such as the effects of the block of key components on the relationships of V_m and Ca_{in} to pressure (Knot and Nelson, 1998; Knot et al., 1998) and the effects of the knockout of the BK β1 subunit (Brenner et al., 2000; Dong et al., 2008; Sachse et al., 2014). It also predicted the effects of selected vasoactive agents on the responses to pressure of an arterial SM cell after knockout of BK β1. In addition, the fit with plausible parameters of the model to experimental data demonstrated the feasibility of its speculative components as, for example, stretch-transducing microdomains.

MATERIALS AND METHODS

Physical model. The model of an arterial SM cell (Fig. 1) includes compartments and components relevant to the control of V_m and Ca_{in} by intravascular pressure. It also includes the targets for a few exemplary endocrine and paracrine inputs to SM. The compartments are the sarcoplasm (subscript "in"), the central SR (SR_{cen}), the peripheral SR (SR_{per}), the junctional microdomain (subscript "jun"), and the postulated stretch-transducing microdomain (subscript "str"). There are hundreds of junctional microdomains per SM cell (Moore et al., 2004) between the sarcolemma and apposing peripheral SR cisternae. I assume that there are also a similar number of stretch-transducing microdomains. In my initial estimates of the rate constants for the relaxation by diffusion of concentration differences between these microdomains and the domains to which they are connected, their approximate dimensions were taken into account. Otherwise, they were treated as single composite compartments with uniform concentrations and with volumes that are the sums of the individual microdomains.

Inorganic ions and second messengers. The key ion is Ca. Its concentrations in the different domains are Ca_{in}, Ca_{jun}, Ca_{SRcen}, Ca_{SRper}, and Ca_{NSCstr}. The microdomains are relatively small volumes into which Ca influxes are transiently greater than Ca effluxes (Sobie et al., 2002). Both the stretch microdomains and the junctional microdomains have paths to the cytoplasm, and Ca in these domains equilibrates by diffusion with Ca in the sarcoplasm (see supplementary equations Seqs. D1 and D3). Similarly, Ca in the SR_{cen} equilibrates with Ca in the SR_{per} by diffusion (Seq. D2). The cytoplasmic concentrations of Na, K, and Cl, designated "Na_{in}," "K_{in}," and "Cl_{in}," are also taken to be the concentrations in the other intracellular domains. All of the intracellular ion concentrations are functions of time (Seqs. J31 and J36–J41). The extracellular ion concentrations, Ca_{ex}, Na_{ex}, K_{ex}, and Cl_{ex}, are fixed. The diffusible second messengers, cAMP, cGMP, and IP3, are distributed uniformly in the cytoplasm and in the stretch and junctional microdomains. Diacylglycerol (DAG), no doubt almost completely confined to lipid membranes, for simplicity is also treated as if it were soluble and uniformly distributed in all

Published June 29, 2015

domains. The concentrations of the second messengers vary with time (Seqs. J2, J10, J21, and J29).

Protein components

αAR (α1-adrenergic receptor). αAR binds α-adrenergic agonist reversibly, activates $G\alpha_q\beta\gamma$, and is phosphorylated, internalized, and recycled (Schöfl et al., 1993; Bennett et al., 2005). These processes are represented as simplified reactions (see supplementary reaction schemes), the time courses of which are determined by Seqs. J11–J15 and J25.

AC (adenylate cyclase). AC6 is the major subtype involved in β-adrenergic vasodilator signaling in arterial SM cells (Nelson et al., 2011). AC is activated by $G\alpha_{s\_GTP}$ and converts ATP to cAMP (Dessauer and Gilman, 1997) (see supplementary reaction schemes), as governed by Seqs. J9, J10, and J46–J49. In the model, PKA inactivates AC, representing feedback inhibition (Vandamme et al., 2012). The time courses of the phosphorylated and dephosphorylated states are determined by Seqs. J8 and J49.

βAR (β-adrenergic receptor). β1AR is the predominant subtype in small resistance arteries (Garland et al., 2011). The reaction scheme (see supplementary reaction schemes) mirrors that for αAR, except that βAR activates $G\alpha_s\beta\gamma$. The time courses are determined by Seqs. J42–J45.

BK channel. BK channel consists of four pore-forming α subunits and four modulatory β1 subunits (Butler et al., 1993; Knaus et al.,

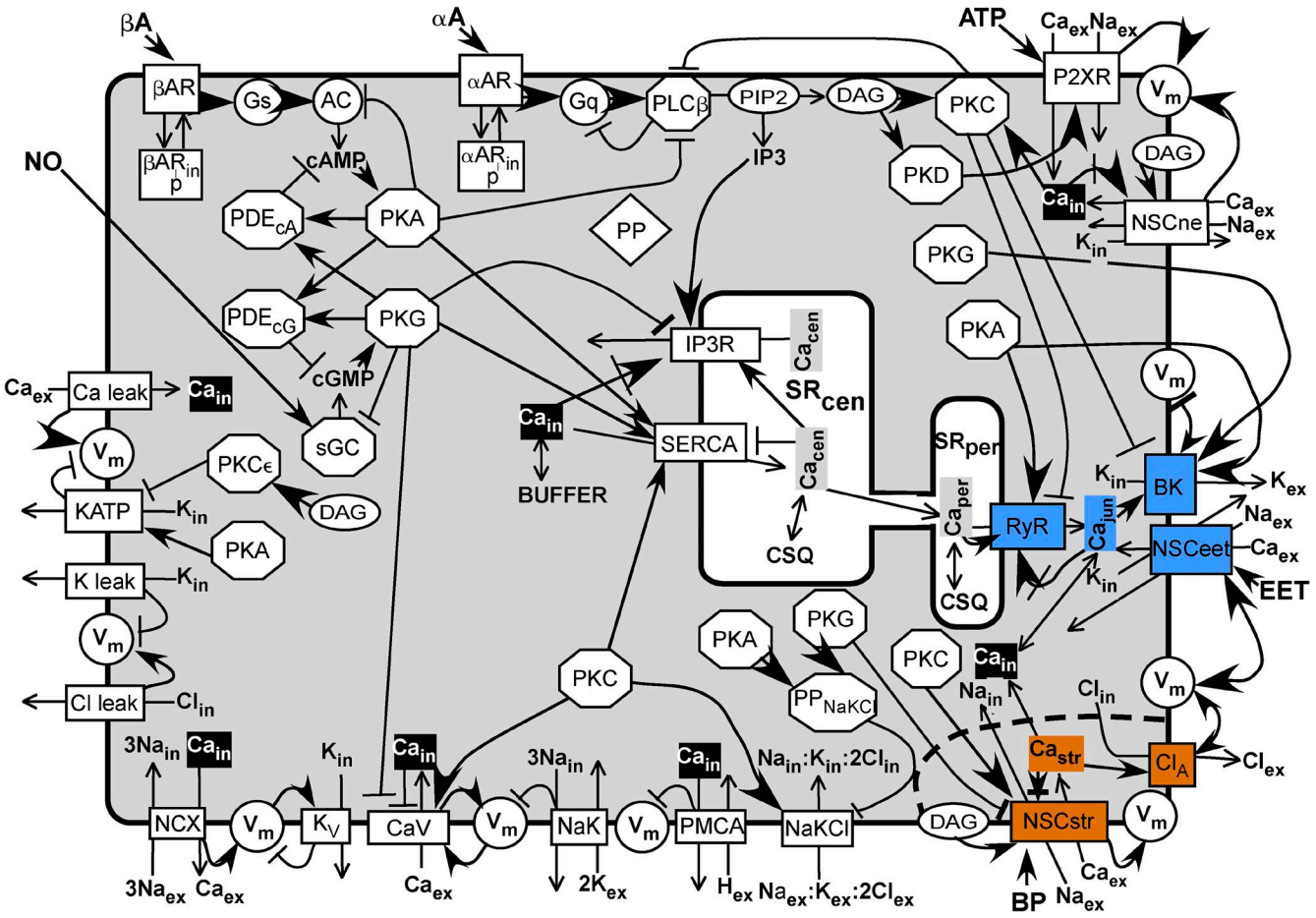

Figure 1. Scheme of model. A SM cell sarcolemma contains channels, receptors, and transporters shown as rectangles spanning the membrane. Enzymes are represented as circles or octagons. Membrane-bound substrate PIP2 and effector DAG are shown as ovals. A common Ca buffer (BUFFER) is uniformly distributed throughout the cell except in the central SR (SR_{cen}) and the peripheral SR (SR_{per}), in which the Ca buffer is uniformly CSQ. Inorganic ions are shown without their charges and subscripted to indicate their compartment. Subscript "ex" refers to the extracellular milieu, "in" refers to the sarcoplasm, "jun" refers to the junction between the SRper and the sarcolemma, "str" refers to the postulated Ca microdomain around the stretch-activated channel (NSCstr), "cen" refers to the central SR, and "per" refers to the peripheral SR. (The longer subscripts NSCstr, SRper, and SRcen are used in the text and in the program.) The components associated with the junction are highlighted in blue, and those associated with the stretch microdomain are highlighted in orange. Ca_{in}, considered uniformly distributed in the sarcoplasm except for the microdomains, is highlighted in black. Other soluble components and effectors are shown in bold lettering. Most components are shown once. The kinases are repeated to be close to their targets, and the inorganic ions are repeated to be close to their sources and sinks. All abbreviations are defined in Materials and methods. A line ending in a closed arrowhead indicates activation; a line ending in a bar indicates inhibition. A closed arrow head pointing at an encircled V_m indicates depolarization, and a barred line indicates hyperpolarization. A line ending in a closed arrow crossed by a bar indicates activation followed by inhibition. A line ending in an open arrowhead indicates a flux between compartments or an enzyme reaction.

Published June 29, 2015

1994; Wang et al., 2002). The steady-state dependence of P_{BK} on V_m ("v" in steady-state equations) and Ca_{in} ("c" in steady-state equations) (Seqs. E1–E3) is based on the model of Horrigan et al. (1999) as modified for the complex with β1 (Bao and Cox, 2005). The complex enhancement of BK channel activity by PKA and PKG and its suppression by PKC (Zhou et al., 2008, 2010) are represented simply by changes in L_{BK} (Seqs. E6, E9, and E12). In the model, BK channel phosphorylation by one kinase blocks phosphorylation by another. The time courses of the phosphorylated states are governed by Seqs. J22–J24 and J27. The potentiation of BK channels by PKG and PKA via enhanced trafficking of β1 to the sarcolemma (Leo et al., 2014) is not included: the BK complex is assumed to contain a full complement of four β1 subunits.

BUFFER. BUFFER stands in for all protein and nonprotein Ca buffers in the sarcoplasm, junctions, and the stretch-transducing microdomains, and is assumed to be uniformly distributed.

CaV channel (voltage-activated Ca channel containing the CaV1.2 α subunit together with additional subunits). CaV1.2-containing CaV channel plays a dominant role in SM control of Ca and of tension (Moosmang et al., 2003). Steady-state P_{open} for CaV channel, called P_{CaV}, increases with increasing V_m (Rubart et al., 1996) and decreases with increasing Ca_{in} (Zühlke et al., 1999) (Seqs. E17–E19). Potentiation of CaV channel activity by PKC phosphorylation (Navedo et al., 2006) is modeled as a negative shift in the midpoint of the dependence of P_{CaV} on V_m, from V_{CaV} for the dephosphorylated channel to V_{CaV_PKC} (Seqs. E22 and E23). Suppression of CaV channel activity by PKG phosphorylation (Yang et al., 2007) is modeled as a positive shift from V_{CaV} to V_{CaV_PKG} (Seqs. E26 and E27). The time courses of the phosphorylated states are governed by Seqs. J57–J59. The steady-state Ca flux and current are given by Seqs. E20 and E21, E24 and E25, and E28–E30.

ClA channel (TMEM16A). ClA channel contributes to the myogenic response in resistance-size cerebral arteries (Bulley et al., 2012). Furthermore, ClA channel is activated by locally elevated Ca_{in} conducted by nearby nonspecific cation channels (Bulley et al., 2012), which are designated here as "NSCstr channels" and share the stretch-transducing microdomain with ClA channel in the model (Fig. 1). The EC50 for Ca decreases with depolarization, and the channel is inhibited by high Ca_{in} (Yang et al., 2008). These characteristics are represented by the steady-state equations for P_{ClA} (Seqs. E31–33). The steady-state Cl flux and current are given by Seqs. E34–E36.

CSQ (calsequestrin). CSQ stands in for all Ca buffers in the central and peripheral SR.

G_q ($G\alpha_q\beta\gamma$). G_q is primed by αAR to exchange GTP for GDP. $G\alpha_{q\_GTP}$ activates PLC and slowly hydrolyzes bound GTP, a reaction accelerated by PLC (Waldo et al., 2010) (supplementary reaction schemes). Time courses of G_q forms are determined by Seqs. J14, J15, J17–J21, J25, J26, and J28.

G_s ($G\alpha_s\beta\gamma$). G_s is primed by βAR to exchange GTP for GDP. $G\alpha_{s\_GTP}$ activates AC and slowly hydrolyzes bound GTP (supplementary reaction schemes), as governed by Seqs. J9, J42, and J45–J49.

IP3R (IP3 receptor, Ca release channel). These tetrameric Ca release channels are located principally in the SR_{cen} membrane (Fig. 1) (Narayanan et al., 2012). IP3R contains stimulatory sarcoplasmic Ca sites, inhibitory sarcoplasmic Ca sites (Seq. F5), and stimulatory luminal Ca sites (Seq. F6) (Bezprozvanny et al., 1991). Binding of IP3 increases the affinity of the stimulatory sarcoplasmic Ca sites (Seqs. F1 and F3) and may also decrease the Ca affinity of the inhibitory sites (Taylor and Prole, 2012), although the latter effect is neglected here. ATP is a coregulator of the Ca affinity of the stimulatory sites (Mak et al., 2001), but because sarcoplasmic ATP concentration is assumed here to be constant, its effect on IP3R is implicit. PKG phosphorylation is modeled as suppressing IP3R activity by lowering its affinity for IP3 (Seqs. F2 and F4) (Desch et al., 2010). The time courses of the phosphorylated states are governed by Seqs. J50 and J51.The steady-state Ca flux and current are given by Seqs. F9–F12.

KATP (Kir6/SUR). KATP channels in resistance artery SM are activated by PKA, causing hyperpolarization and vasodilation, and inhibited by PKCε, causing depolarization and vasoconstriction (Quayle et al., 1997; Aziz et al., 2012). Sarcoplasmic ATP, the concentration of which is assumed to be constant, acts as a low-affinity inhibitor. In the model, the open probability, P_{KATP_PKA}, of PKA-phosphorylated KATP is greater than P_{KATP} of dephosphorylated KATP; P_{open} of PKCε-phosphorylated KATP is assumed to be zero. Furthermore, phosphorylation by PKA and phosphorylation by PKCε are assumed to be mutually exclusive. The time courses of the phosphorylated states are governed by Seq. J73-J75. The steady-state K flux and current are given by Seq. E37-E42.

K_V (voltage-dependent K) channels. One type of voltage-dependent K channel, with the properties of Kv1.5, is incorporated in the model (McGahon et al., 2007; Kapela et al., 2008; Hald et al., 2012). The steady-state K flux and current are given by Seqs. E44 and E45.

Leak channels Ca_{leak}, Cl_{leak}, and K_{leak}. These are postulated conductors of background Ca, K, and Cl currents. The model has equations for a Na leak (Seqs. E50 and E51), but this leak was set to zero in all simulations presented here. The steady-state fluxes and currents are given by Seqs. E46–E54.

NaK (Na, K-ATPase). The relative driving force for transport is taken as the electrochemical free energy change for the transport of 3 mol of Na outward plus 2 mol of K inward plus the free energy change caused by the hydrolysis of 1 mol of ATP ($\Delta\mu_{ATP}$), all normalized by $\Delta\mu_{ATP}$ (Seq. G1). The net current depends on Hill functions of Na_{in} and K_{ex} (Kapela et al., 2008) multiplied by the relative driving force and by the maximum NaK current per cell (Seq. G2).

NaKCl (Na-K-Cl cotransporter NKCC1). NaKCl is essential for the maintenance of the relatively high Cl_{in} in SM cells (Chipperfield and Harper, 2000). It is modeled as containing four ion-binding sites: one for Na, one for K, and two for Cl (supplementary reaction schemes). There are two accessibility states: all sites facing outward and all sites facing inward. Isomerization between these states occurs only when all sites are empty or when all sites are occupied. These isomerizations are governed by rate constants. Ion binding to the sites is ordered in single file (first on, first off) (Lytle et al., 1998) and is governed by three equilibrium-binding constants. These are unchanged by changes in site accessibility. The steady-state net inward flux of the fully occupied transporter is given by Seq. G7 (derivation not shown). This model is based on that of Benjamin and Johnson (1997) but with fewer parameters. Because the binding constants are the same in the two conformations, the isomerization rate constants are constrained by microscopic reversibility, as shown in Seq. G3. NaKCl transport is potentiated by PKC (Chipperfield and Harper, 2000), and in the model the rate constants for the isomerization of the occupied, phosphorylated NaKCl are multiplied by an enhancement factor (Seq. G8). The transport is suppressed by both PKA and PKG (Chipperfield and Harper, 2000), and in the model these kinases

Published June 29, 2015

activate a hypothetical protein phosphatase specific for PKC-phosphorylated NaKCl. (This is a simplifying logical device permitting just one NaKCl phosphorylation site.) The time courses of phosphorylation and dephosphorylation are governed by Seqs. J66 and J67. The net inward fluxes of Cl, Na, and K are given by Seqs. G10–G13. Notwithstanding that the sum of the Cl, Na, and K currents via NaKCl is zero, the Cl flux is also expressed as current (Seq. G13) for convenient comparison with other currents.

NCX (Na–Ca exchanger). In one of three possible functional modes, NCX exchanges three Na for one Ca (Kang and Hilgemann, 2004). In a relatively simple model of this major mode (supplementary reaction schemes), NCX is activated by Ca_{in} binding cooperatively to regulatory sites (Seq. G15) (Reeves and Condrescu, 2008). Furthermore, NCX has one transport site for Ca and three transport sites for Na. The transport Ca site and the Na sites are simultaneously accessible only on opposite sides of the membrane. Association and dissociation are ordered: the three Na associate before the Ca and dissociate after the Ca. Binding is always at equilibrium. Only NCX with empty transport sites or with fully occupied transport sites can switch the accessibilities of the transport sites. In the model, unoccupied NCX has two net negative charges in its Ca transport site and three net negative charges in its three Na transport sites. When these unoccupied sites switch their accessibilities to opposite sides of the membrane, the equivalent of one negative charge crosses the membrane, and the free energy changes by $\pm FV_m$, depending on the direction of transport. No net charge is transported when the fully loaded sites switch their accessibilities. It is assumed that the effect of V_m is on the rate constants for switching accessibilities and that the transition state is halfway through the potential drop; thus, the rate constant for the isomerization for Na sites–out and Ca site–in to Na sites–in and Ca site–out, α'_{NCX_0}, contains the factor $\exp[F*V_m/(2RT)]$, and the rate constant for the opposite isomerization, β'_{NCX_0}, contains the factor $\exp[-F*V_m/(2RT)]$ (supplementary reaction schemes; Seq. G16). Microscopic reversibility applies to the isomerization rate constants at $V_m = 0$ (Seq. G14). In the steady state, the total fluxes of Na sites, both empty and occupied, in the two directions must be equal. This and the equilibrium-binding equations yield the steady-state transport rate of three Na outward and one Ca inward minus three Na inward and one Ca outward (Seq. G19) and the net current (Seq. G20).

NSCeet (nonspecific cation channels activated by 11,12-epoxyeicosatrienoic acid [EET], an endothelium-derived hyperpolarizing factor). NSCeet includes TRPV4, which acts as an EET receptor in a signaling microdomain with BK channel and RyR (Earley et al., 2005, 2009). In the model, NSCeet is located in the junctional microdomains. EET binding activates NSCeet (Seq. E56). When activated, it increases Ca_{jun}, activating BK channel and RyR. TRPV4 is also activated by depolarization in the absence of ligand, but nP_o is low at V_m of less than −40 mV (Loukin et al., 2010). One way to simulate both the V dependence of TRPV4 in the absence of EET and its significant activation by EET in the physiologically relevant range of V_m of less than −40 mV is to allow EET binding to shift the V_{50} to the left (Seq. E55). The steady-state Na, K, and Ca fluxes and currents are given by Seqs. E57–E63.

NSCne (receptor-activated nonspecific cation) channels. In mesenteric artery SM, NSCne channel is close to α1-adrenergic receptors and activated by phenylephrine and by DAG, but not by PKC (Hill et al., 2006). NSCne channel is composed of TRPC6 and possibly TRPC3 or TRPC1 (Saleh et al., 2006). NSCne channel open probability is modeled as activated by DAG and both activated and inhibited by Ca_{in} (Seq. E64). The steady-state Na, K, and Ca fluxes and currents are given by Seqs. E65–E71.

NSCstr (stretch-activated nonspecific cation) channels. These channels share the stretch-transducing microdomains with ClA channels (see above). Several types of TRP channels, including TRPM4, are candidates for roles in the myogenic response to intramural pressure (Sharif-Naeini et al., 2009; Earley and Brayden, 2010), and the NSCstr channels might be hetero-oligomeric complexes of TRP types (Earley et al., 2004). Because TRPM4 alone does not conduct Ca, it is unlikely to be the sole component of NSCstr channels. Piezo1 and Piezo2 are unlikely candidates for stretch-activated channels in SM: Piezo 1, half-maximally activated at 28 mm Hg and maximally activated at 60 mm Hg, is too sensitive, and Piezo 2 desensitizes too quickly (Coste et al., 2010). NSCstr channels are modeled as activated by stretch and DAG (Seq. E72), and both are activated (Seqs. E73–E75) and inhibited (Seq. E76) by Ca_{NSCstr}. P_{open} for NSCstr, called "P_{NSCstr}," is a product of these factors (Seqs. E77–E79). Potentiation by PKC (Earley et al., 2007) is modeled as a decreased EC50 (K.NSCstr_PKC_Ca_act) for activation by Ca (Seq. E74), and suppression by PKG (Takahashi et al., 2008) is modeled as an increased EC50 (K.NSCstr_PKG_Ca_act) for Ca (Seq. E75). The time courses of the phosphorylated states are determined by Seqs. J70–J72. The steady-state Na, K, and Ca fluxes and currents are given by Seqs. E80–E105.

PDE_{cA} and PDE_{cG} (generic phosphodiesterases specific for cAMP and cGMP, respectively). These are modeled as activated by binding of their cognate substrate at an allosteric site, as described by equilibrium Hill functions (Seqs. H1–H4) (Francis et al., 2011). They can be potentiated by both PKA and PKG (Vandamme et al., 2012). In the model, they each can be phosphorylated at a single site by either PKA or PKG (Fig. 1), and this phosphorylation increases the affinities of their allosteric sites. The time courses of phosphorylation are determined by Seqs. J62–J65. The cAMP and cGMP hydrolysis reactions are modeled as second order (Seqs. J2 and J10), i.e., at low extents of saturation of the catalytic sites, as opposed to the allosteric sites.

PKA. The allosteric activation of PKA by cAMP is modeled as a Hill function with a Hill coefficient >1 (Herberg et al., 1994; Boettcher et al., 2011) (Seq. H5). In the model, all kinases are assumed to be in one-to-one complexes with their targets (Santana and Navedo, 2009; Kholodenko et al., 2010; Gold et al., 2011; Schlossmann and Desch, 2011), with reaction rate constants specific for these targets.

PKC. This is a generic, conventional PKC requiring both DAG and Ca for activity (Nishizuka, 1995). The relative activity is modeled as a product of two Hill functions (Seq. H6).

PKCε. PKCε is a DAG-dependent, Ca-independent subtype, which targets KATP (Aziz et al., 2012). Its relative activity is given by Seq. H7.

PKD. PKD is another DAG-dependent, Ca-independent subtype, which targets P2XR (Ase et al., 2005). Its relative activity is given by Seq. H8.

PKG. PKG is activated by cGMP, as given by Seq. H9.

PLC (PLCβ). PLC is activated by $G_{\alpha q\_GTP}$ and hydrolyzes PIP2 to DAG and IP3. In the model, PLC has low basal activity. PLC acts as a GAP and hastens the hydrolysis of GTP by $G_{\alpha q\_GTP}$ (Waldo et al., 2010). PLC activity is suppressed by both PKA and PKC (Yue et al., 2000; Huang et al., 2007), which is simplified in the model as direct phosphorylation of PLC resulting in the lowering of its affinity for $G_{\alpha q\_GTP}$. These reactions are shown in supplementary

Published June 29, 2015

reaction schemes (α-Adrenergic signaling), and the time courses are governed by Seqs. J16–J21.

PMCA (sarcolemmal Ca-ATPase). PMCA exchanges one Ca for one or more protons with the hydrolysis of one ATP (Brini and Carafoli, 2011). In the model, it is assumed that Ca/H is 1:1, so that the 1 net charge is transferred per cycle (Seq. G21). PMCA is disinhibited by Ca-calmodulin at $K_d < 1$ μM for Ca. This is simplified in the model as a dependence of activity on a Hill function in Ca (Seq. G22).

PP (generic protein phosphatase). PP is modeled to be in a complex with each component that is a target of a kinase and to be constitutively active.

PP_NaKCl. This is a hypothetical protein phosphatase specific for NaKCl. PP_NaKCl is modeled as activated by PKA and PKC. This is a simple mechanism for the suppression of NaKCl activity by these kinases (Chipperfield and Harper, 2000). The time courses of PP_NaKCl and of PP_NaKCl_P are determined by Seqs. J68 and J69.

P2XR (P2X1 receptor). This receptor is activated by ATP coreleased with norepinephrine in pulses from proximal sympathetic nerve varicosities (Nausch et al., 2012) (see supplementary reaction schemes). The rate constants of the upper cycle are constrained by microscopic reversibility. Desensitization is from the open state (Kaczmarek-Hájek et al., 2012), and PKD potentiation is modeled as increasing the rate of recovery from desensitization (Ase et al., 2005). The time courses of all forms are governed by Seqs. J76–J82. The steady-state Na, K, and Ca fluxes and currents are given by Seqs. E106–E112.

RyR (Ca release channel type 2). In the model, only RyR channels located in the peripheral SR are considered. RyR is both activated and inhibited (Seqs. F15 and F16) by Ca_{jun} binding to separate junctional sites (Bezprozvanny et al., 1991). Significant binding of Ca in the physiological range to the latter site likely involves calmodulin (Xu and Meissner, 2004), which is implicit in the model. RyR is potentiated by Ca_{SRper} binding to an SR-luminal site (Sobie et al., 2002; Launikonis et al., 2006). This potentiation is modeled as Ca_{SRper} lowering the dissociation constant of the activating junctional site (Seqs. F13 and F14). In the model, PKA potentiates RyR (Shan et al., 2010) by increasing the affinity of the activating site (Seqs. F17–F19). In contrast, PKC suppresses RyR (Liu et al., 2009; Peng et al., 2010) by decreasing the affinity for Ca_{jun} (Seqs. F20–F22). PKA and PKC phosphorylation are modeled as mutually exclusive. The time courses of the phosphorylated states are determined by Seqs. J54–J56. The steady-state Ca flux and current are given by Seqs. F23–F27.

SERCA (Sarcoplasmic/endoplasmic reticulum Ca^{2+}-ATPase). SERCA is restricted in the model to the central SR. It is activated by Ca_{in} and inhibited by Ca_{SRcen} (Wray and Burdyga, 2010) (Seq. G23). PKA, PKG, and PKC phosphorylate phospholamban causing disinhibition, thereby increasing the apparent affinity of SERCA for Ca_{in} (Colyer, 1998; Wray and Burdyga, 2010). These modulations are simplified in the model, in which direct phosphorylation of SERCA by these kinases increases the affinity for Ca_{in} (Seq. G24). Two Ca are transported and approximately two protons are counter-transported per ATP hydrolyzed (Tran et al., 2009) (Seqs. G25–G29). Because the SR V_m and the proton concentration gradient are both assumed zero, the energy cost of transport is the result of the Ca concentration gradient alone. The time courses of the phosphorylated forms are governed by Seqs. J60 and J61.

sGC (soluble guanylate cyclase). sGC is the target for nitric oxide (NO), modeled as in supplementary reaction schemes. The binding of one NO activates sGC; the binding of a second NO accelerates this activation (Yang et al., 2005). Feedback inhibition of sGC by PKG (Murthy, 2004) is modeled as exclusive phosphorylation of the active state to yield an inactive state incapable of binding NO. Seqs. J2–J7 govern the time courses of the sGC states and the concentration of cGMP.

Mathematical representation

The core of the program is a solve block of 63 nonlinear ordinary differential equations and 18 algebraic equations (Seqs. J2–J82) that generate the time courses of 81 variables. These include V_m; the concentrations of Ca in all compartments; the concentrations of Na, K, Cl, cAMP, cGMP, IP3, and DAG; the states of occupation and activity of receptors for αA, ATP, βA, and NO; the states of AC, G_s, G_q, sGC, and PLC; the states of phosphorylation of all modulated components; and the states of occupation of Ca buffers. The equations in the solve block call 180 steady-state equations (in which time is not an explicit argument) that determine for all channels and transporters their open-state probabilities or activities and the currents and fluxes conducted or transported by them and, in addition, the relative activities of all kinases and phosphodiesterases. The time courses of the applications of effectors are described by functions (Seqs. C1–C16), the parameters of which are given in Table S1.

The equations were written and solved in PTC Mathcad 15.0 M010. The differential equations and algebraic equations in the solve block were solved with the radau option for stiff differential equations. In a typical run with the normal parameter set (Table S6), the time courses over 300 s of 81 variables, and of additional functions of these variables, were solved at 6 values of intravascular pressure. For each variable (and functions of variables like fluxes and currents) at each intravascular pressure, 12,000 points were retained for the calculation of mean values of the variables and for plotting. On a computer with an Intel Core i7-3770K cpu, calculations and plotting were completed in ∼35 min.

Parameters

The equations of the model involved a large number of adjustable parameters (Table S6). Parameters that determined the behavior of the individual components were considered local; the parameters specifying the total numbers of molecules, or concentrations, or maximum currents of the components were considered global. Parameter values were (a) experimentally determined; (b) adjusted to give local model output that approximated the observed behavior of individual components; or (c) biochemically reasonable guesses calculated to give behavior of the components consistent with their expected roles and, if rate constants, to give steady states within a few minutes. In case (a), the local models and their parameters were taken from the literature. Local models were extended to simulate the reported qualitative effects of phosphorylation. In case (b), the local model was different from any published model, and its parameters could not have been obtained previously even if the experimental data existed. For some of these components, there are experimentally derived composite parameters such as EC50s, desensitization rates, and so on. For this subset of components, parameter values were initially adjusted to simulate the observed properties. These values, however, were often ballpark approximations because, for example, arterial constriction might have been determined experimentally, whereas the ultimate outputs of the model are Ca_{in} and V_m; furthermore, these outputs are not determined by a single component. Also, published experiments were performed with a variety of species, cell types, and conditions, and different values have been reported for the same composite parameter.

Published June 29, 2015

Many of the parameters, excluding the few well-established ones, were adjusted to achieve a close simulation of the primary experimental targets, V_m and Ca_{in}, as functions of intravascular pressure (Knot and Nelson, 1998). Because the number of adjustable parameters relevant just to the fit of the Knot and Nelson data was very large (189), it was impractical to search for the best fit over all parameters simultaneously. Instead, the fit was selective and iterative. The parameters of the components with the largest impacts (identified below) were adjusted one at a time, first to improve the global fit while maintaining realistic local properties. The fit was quantified separately for V_m and for Ca_{in} by calculating, first, the difference between the simulated value and experimental value for each of six pressures; second, each difference divided by the experimental value to get the relative difference; and, finally, the square root of the mean of the squares of the relative differences (rmsRelErr). The primary goal was to minimize rmsRelErr_Ca_{in}. With a few exceptions, the parameter values were determined to only one or two significant places. This was justified by the shallowness of the minimum (see Robustness below). A parameter set, called the "normal" parameter set (Table S6), minimized rmsRelErr_Ca_{in} and, within a small margin, rmsRelErr_V_m as well.

The sensitivity of the fit to changes in 24 global parameters was quantified as rmsRelErr_V_m and rmsRelErr_Ca_{in} after changing each parameter, one at a time, to 0.8, 0.9, 1.1, and 1.2 times their normal values. These were in all cases compared with the rmsRelErrs after elimination of the component. In addition, the sensitivities of the simulations of V_m and Ca_{in} and the output of the individual components to changes in 97 local parameters were calculated based on the differences between perturbed simulated values and normal simulated values (for details see legends of Figs. S8–S10).

Online supplemental material

Model equations (Mathcad program) are available in a PDF file. A PDF file of reaction schemes for α-adrenergic signaling, β-adrenergic signaling, NaKCl cotransporter, NCX exchanger, and P2XR is also available. Figs. S1–S10 and Tables S1–S6 are part of the online supplemental material. Figs. S1–S5 show the time courses of 15 variables, each at 20, 60, and 100 mm Hg. Figs. S6 and S7 show the sensitivities to variations in the global parameters of the fit of simulated $\langle V_m \rangle$ to V_{exp} and of simulated $\langle Ca_{in} \rangle$ to Ca_{exp}. Figs. S8–S10 show the sensitivities of $\langle V_m \rangle$, $\langle Ca_{in} \rangle$, and the outputs of individual components to variations in 97 global and local parameters. Table S1 shows the set of parameters determining the application of intravascular pressure and concentrations of chemical effectors. Table S2 shows the values of selected variables from a run with the normal set of parameters. Table S3 shows the effects of varying and/or holding constant key variables and parameters on the output oscillations. Table S4 shows the fractional changes in $\langle V_m \rangle$, $\langle Ca_{in} \rangle$, and the local component output per millivolt change in additive parameters that set the midpoints of voltage dependence. Table S5 shows the dose–response parameters characterizing the simulated responses to chemical effectors. Table S6 gives the values of the normal set of parameters and their derivations. The online supplemental material is available at http://www.jgp.org/cgi/content/full/jgp.201511380/DC1.

RESULTS

Simulations of V_m and Ca_{in} as functions of intravascular pressure

Simulations were run for 300 s, with pressure applied gradually starting at 10 s, reaching a steady value by 15 s, and sustained to 300 s. With most sets of parameter values tested, the simulated variables oscillated (Figs. S1–S5). To compare the simulated V_m and Ca_{in} with the experimentally determined V_{exp} and Ca_{exp} (Knot and Nelson, 1998), I took as the responses to pressure the means $\langle V_m \rangle$ and $\langle Ca_{in} \rangle$ over the last 50 s of the 300-s simulation. The means changed little over this last 50 s. A set of parameters that gave a close fit (see Materials and methods) of $\langle V_m \rangle$ and $\langle Ca_{in} \rangle$ to V_{exp} and Ca_{exp} (Fig. 2) was designated the normal set (Table S6). The root mean square (rms)-relative differences over the six experimentally tested intravascular pressures were 1.25% for V_m and 3.21% for Ca_{in}. Variations of most of the parameters by ±10% had little effect on the rms errors of the fits (see Robustness below).

Means were also calculated for all other variables and for all fluxes or currents. For each trial run, automatic plots of the means as functions of intravascular pressure

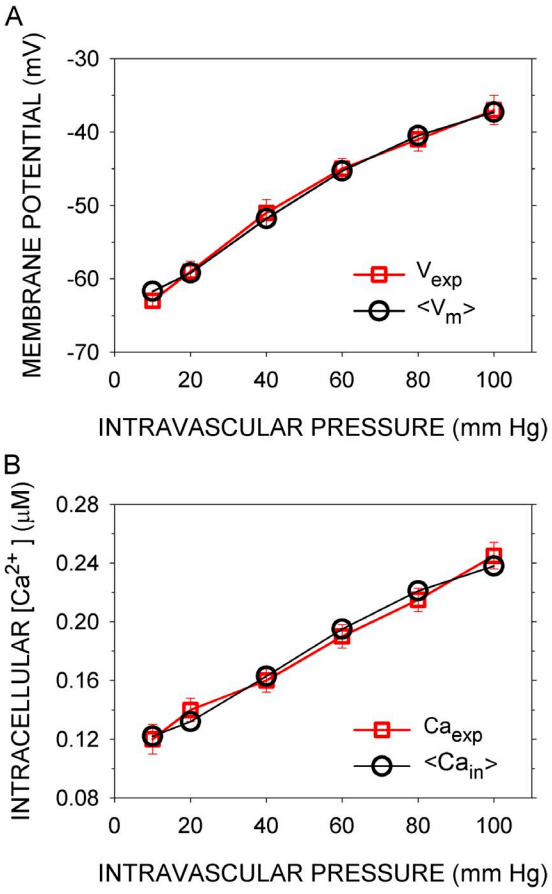

Figure 2. Simulated and experimental V_m and sarcoplasmic Ca concentration as functions of intramural pressure. (A) V_{exp} (red squares) are the means over 30 s of the observed V_ms after steady-state responses to the indicated intramural pressures were reached, recorded in rat cerebral arteries (Knot and Nelson, 1998). $\langle V_m \rangle$ (black circles) are the means of V_m over the last 50 s of a 300-s simulation with the normal parameter set (Table S6). In the simulations, the indicated intramural pressures were applied starting at 10 s. (B) Ca_{exp} (red squares) are the mean Ca concentrations recorded under the conditions in A, and $\langle Ca_{in} \rangle$ (black circles) are the means of Ca_{in} calculated as in A. Error bars represent standard deviations of the experimental data.

Published June 29, 2015

provided insight into the effects of changing parameter values. The means of the salient variables and currents from a run with the normal parameters, in the absence of all effectors except intravascular pressure, are shown in Table S2. In many cases, for example Ca_{jun} and I_{BK_ALL}, the means are much smaller than the peak values (Figs. S4 H, inset, and S5 E, inset; the peaks are sharper in the insets than in the main panel because the plotting density is greater). In the absence of chemical effectors, the concentrations of second messengers and the activities of phosphodiesterases and kinases remain at their basal levels. Even in the absence of chemical effectors, however, PKC activity changes with Ca_{in}.

Simulations of the effects of inhibiting BK, RyR, and CaV channels

Knot et al. (1998) determined the effects on V_{exp} and Ca_{exp} of the inhibition of three key components: BK channels by iberiotoxin, RyR channels by ryanodine, and CaV channels by nisoldipine. In the model, reduction of the number of BK channels (BK_T) to between 1 and 10% of the normal value simulated the effects of 100 nM iberiotoxin on V_{exp} and Ca_{exp} at 60 mm Hg (Fig. 3, A and B). In the model, reducing the number of RyR channels (RyR_T) to 50% of the normal value and reducing it to 1% had nearly the same effect on $<V_m>$, and both overlap with V_{exp} at 60 mm Hg in the presence of 10 µM ryanodine (Fig. 4 A). (There may be three distinct ryanodine-binding sites on RyR2, binding to each of which promotes a distinct state of the channel [Bidasee et al., 2003]. At 10 µM ryanodine, however, the "shut" state predominates.) The mean effect of ryanodine on Ca_{exp} was simulated by the reduction of RyR_T to between 80 and 50% of the normal value, but 1% of the normal value gave $<Ca_{in}>$ within the experimental error in Ca_{exp} (Fig. 4 B). Finally, reduction of CaV_T to 1% of the normal value simulated the small effect of 10 nM nisoldipine on V_m at 80 mm Hg but not at 40 mm Hg, where the reduction of CaV_T generated a hyperpolarization not observed experimentally (Fig. 5 A). Reduction of CaV_T to 1% or to 0.1% of its

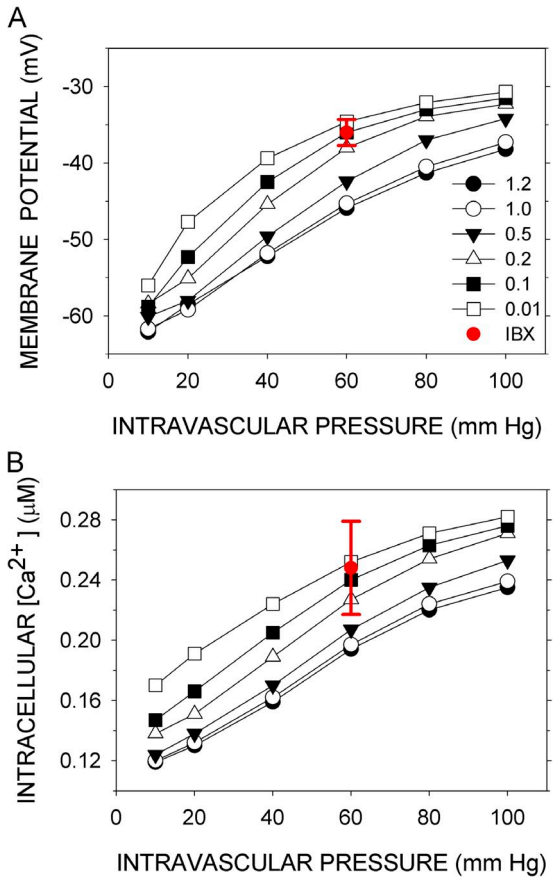

Figure 3. Simulation of the effects of inhibiting BK. (A) V_{exp} and (B) Ca_{exp} (red circles with error bars) were recorded at 60 mm Hg in the presence of 100 nM iberiotoxin (Knot et al., 1998). V_m and Ca_{in} were simulated with the number of BK molecules (BK_T) set at the indicated multiples (1–120%) of its normal value. $<V_m>$ and $<Ca_{in}>$ are the means over the last 50 s of a 300-s simulation (black symbols). Except for BK_T, the parameters were normal. Error bars represent standard deviations of the experimental data.

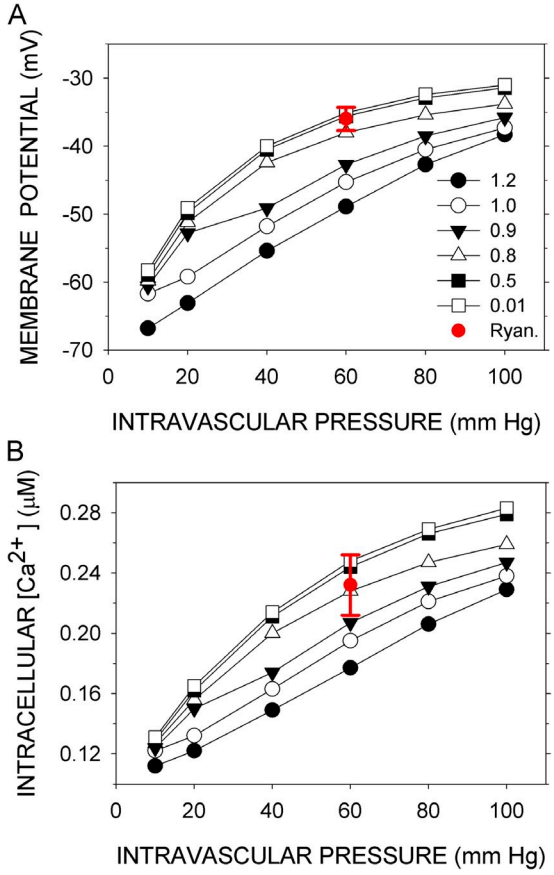

Figure 4. Simulation of the effects of inhibiting RyR. (A) V_{exp} and (B) Ca_{exp} (red circles with error bars) were recorded at 60 mm Hg in the presence of 10 µM ryanodine (Knot et al., 1998). V_m and Ca_{in} were simulated with RyR_T set at the indicated multiples (1–120%) of its normal value. $<V_m>$ and $<Ca_{in}>$ are the means over the last 50 s of a 300-s simulation (black symbols). Except for RyR_T, the parameters were normal. Error bars represent standard deviations of the experimental data.

Published June 29, 2015

normal value simulated, at least qualitatively, the effect of nisoldipine on Ca_{exp}; namely, the increase in Ca_{in} with pressure is completely abrogated over the entire pressure range (Fig. 5 B).

Ca concentrations in different compartments

The Ca concentrations in the five compartments included in the model spanned three orders of magnitude. For example, during the interval from 250 to 300 s at 60 mm Hg, the mean concentrations (μM) are 0.195 $<Ca_{in}>$, 108 $<Ca_{SRcen}>$, 82.3 $<Ca_{SRper}>$, 0.7 $<Ca_{jun}>$, and 0.53 $<Ca_{NSCstr}>$, and the peak values in the smaller compartments (microdomains), namely of Ca_{SRper}, Ca_{jun}, and Ca_{NSCstr}, were considerably higher than their means. These concentrations were in the ranges of activation of compartment-specific targets or functions; e.g., Ca_{in} activates myosin light chain kinase, Ca_{NSCstr} activates ClA, Ca_{jun} activates RyR and BK, Ca_{SRcen} is a reservoir for IP3R and replenishes Ca_{SRper}, and Ca_{SRper} both sensitizes RyR and feeds Ca_{jun} (Fig. 1).

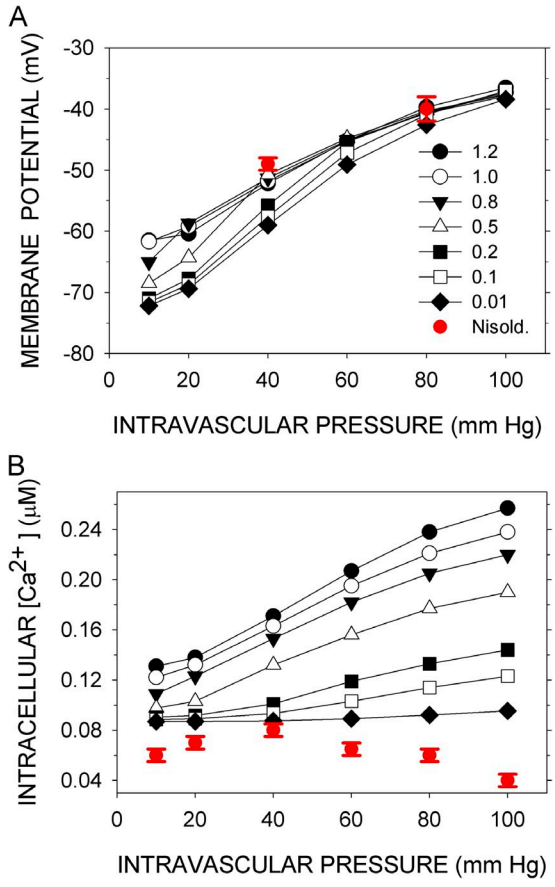

Figure 5. Simulation of the effects of inhibiting CaV channels. (A) V_{exp} and (B) Ca_{exp} (red circles with error bars) were recorded at various intravascular pressures in the presence of 10 nM nisoldipine (Knot and Nelson, 1998). V_m and Ca_{in} were simulated with CaV_T set at the indicated multiples (1–120%) of its normal value. $<V_m>$ and $<Ca_{in}>$ are the means over the last 50 s of a 300-s simulation (black symbols). Except for CaV_T, the parameters were normal. Error bars represent standard deviations of the experimental data.

Oscillations

V_m, Ca_{in}, and other of the simulated variables showed sustained, synchronous oscillations (Figs. S1–S5). Such synchronous oscillations, however, are not seen experimentally. Rather, there are sporadic, localized spikes in Ca ("sparks") and, imperfectly correlated with them, spontaneous, transient outward currents ("STOCs") (Nelson et al., 1995; Lifshitz et al., 2011). Sparks and STOCs result from the activation of RyR and BK channels, respectively. Sparks and the correlated STOCs occur at individual junctions and are stochastic. Their properties depend on the gating kinetics and spatial distributions of RyR and BK channels (Lifshitz et al., 2011), on the diffusion of Ca, and on the electrotonic spread of changes in V_m. In the model, however, all individual channels of a type were simultaneously in the same state determined by the steady-state equation for P_{open}. There were no delays in the transitions between steady states. Nonetheless, the underlying mechanism driving the irregular spikes of experimentally observed sparks and STOCs and of the regular oscillations in the simulation are likely the same.

The mechanism as it applies to RyR and sparks is analogous to the flushing of a toilet. The flapper stays up (i.e., RyR continues to open) until the tank (SRper) nearly empties (but see Sobie et al., 2002). This toilet analogy needs the refinement that the filling of the tank beyond a certain level promotes the opening of the flapper (RyR), and the filling of the bowl (junctional domain) keeps the flapper up (RyR open). The spikes in Ca_{jun} drive the spikes in I_{BK}, i.e., the STOCs (Hill-Eubanks et al., 2011). Although this mechanism for sparks and STOCs is too simple, because not all sparks result in STOCs, and not all STOCs are correlated with sparks (Lifshitz et al., 2011), it should suffice for the correlated sparks and STOCs.

The mechanisms promoting and sustaining the oscillations in the model are illuminated by the effects of changes in component parameters on the frequency of oscillations (Table S3). In the model with the normal set of parameters, all variables oscillated synchronously, albeit with widely different amplitudes (Figs. S1–S5). During the interval from 150 to 155 s (for illustration) and at an intravascular pressure of 60 mm Hg, the common frequency was 2.9 Hz. The rate of refilling of SRper depended on the rate of SERCA pumping Ca into the SRcen: the frequency decreased to 2.2 Hz when I_{SERCA_MAX} was set at 80% of its normal value and increased to 3.3 Hz when I_{SERCA_MAX} was set at 120% of its normal value. It has been observed that inhibition of SERCA decreases the frequency of sparks (Vandier et al., 1998).

The refilling also depended directly on the Ca gradient between SRcen and SRper. Although normally Ca_{SRcen}

Published June 29, 2015

oscillated with a small amplitude (Fig. S4, A–C), this oscillation was not required for oscillation in Ca_{SRper} and Ca_{jun}. Fixing Ca_{SRcen} at 108 µM, its normal mean value at 60 mm Hg, yielded a frequency of 3.0 Hz in the other variables. Fixing Ca_{SRcen} at 97.2 µM, 90% of its normal value, eliminated the oscillations. Fixing Ca_{NSCcen} at 110% of its normal value, 118.8 µM, however, increased the frequency to 5.3 Hz, consistent with the more rapid refilling of SRper. At 129.6 µM Ca_{NSCcen}, 120% of its normal value, there was again no oscillation, and the rate of refilling of SRper equaled the rate of its emptying via RyR.

Consistent with the idea that the periodic drop in Ca_{SRper} drives the oscillation, fixing Ca_{SRper} either at its normal mean value (82.3 µM) or at 65.8 µM (80% of normal) or at 98.8 µM (120% of normal) eliminated all oscillations. It follows that the frequency should increase as the rates of emptying and refilling of SRper increases, and these will increase as VOL_{SRper} decreases, and vice versa. In the simulation, the frequency increased when VOL_{SRper} was decreased to 80% of normal, and the frequency decreased when VOL_{SRper} was increased to 120% of normal.

The drop in Ca_{SRper} and the rise in Ca_{jun} depend on Ca flux through the open RyR channel, the opening of which depends on both of these concentrations. Decreased numbers of RyR compared with normal resulted in decreased Ca flux and decreased frequency, whereas increased numbers of RyR resulted in increased frequency. In the model, Ca_{SRper} binding promotes RyR activity by decreasing the dissociation constant, $K_{RyR\_Ca\_act}$, from $K_{RyR\_Ca\_max}$ toward $K_{RyR\_Ca\_min}$. With these three parameters fixed at a low value of 6.0 µM, promoting RyR activity, the frequency was 5.4 Hz. At an intermediate value of 7.5 µM, the frequency was 2.2 Hz, and at a high value of 9.0 µM (low RyR activity), there was no sustained oscillation; rather, a steady state was reached.

The oscillation of Ca_{jun} was necessary but not sufficient for all other oscillations. Both RyR and BK channels are activated by Ca_{jun}. Allowing Ca_{jun} to oscillate as usual but fixing just the input to RyR of Ca_{jun} at its normal mean value, 0.7 µM, or at 80% (0.56 µM) or 120% (0.84 µM) of its mean value eliminated all oscillations. It follows that there are no other oscillations without oscillation in RyR activity. On the other hand, if Ca_{jun} input to RyR was allowed to vary with time as usual and only the input to BK channels was fixed (Table S3, bottom), oscillations in I_{RyR_ALL}, Ca_{SRper}, and Ca_{jun} continued, albeit with frequencies changed as expected, but there was no oscillation in I_{BK_ALL}, V_m, or in any sarcolemmal currents. These last currents are all dependent on the electrochemical potential, and some are also carried by voltage-activated channels. RyR oscillations entrain BK channels, and BK channel oscillations entrain V_m. There is also strong negative feedback on BK channel activity of the hyperpolarization caused by I_{BK}, which contributes to the sharpness of the spikes of simulated I_{BK} and also of experimentally observed STOCs.

Robustness

Robustness is the insensitivity of the output of a mechanism to changes in its components. The mathematical model of a mechanism is robust to the extent that its output is insensitive to changes in the parameters of its governing equations. As in the well-known case of bacterial chemotaxis, in which adaptation was insensitive to parameter changes but tumbling rate was not (Alon et al., 1999), a mechanism and a model can have both robust and sensitive outputs. Also, of course, a model is likely to be more sensitive to changes in some parameters than in others.

Sensitivity was examined in two ways. In the first, the effects of changes in parameters on the rms-relative differences between V_{exp} and $<V_m>$ (Fig. S6) and between Ca_{exp} and $<Ca_{in}>$ (Fig. S7) were determined at six intramural pressures (Materials and methods). The parameters changed were the numbers of functional molecules of each component. These numbers represent the expression levels, which are likely to vary among cells. The parameters were changed, one at a time, to 0.8, 0.9, 1.1, and 1.2 times their normal values. In addition, they were set to zero. The model lacks redundancy, so that insensitivity of the simulations to 10 and 20% changes in expression levels is pertinent to robustness only if complete removal of the component has a significant effect on the fit.

The perturbed rms-relative errors are also compared with the normal rms-relative errors, $rmsRelErr\_V_m$ and $rmsRelErr\_Ca_{in}$, which were 1.25 and 3.21%, respectively, and indicated by dashed red lines in Figs. S6 and S7. Also shown as reference lines for a moderately perturbed state are the rms-relative errors simulated with the parameters for the channel composed of BK channel α subunits alone, i.e., in the absence of β1 subunits (Bao and Cox, 2005). These are 16.7 and 21.0%, respectively.

The rms-relative errors were obtained for perturbed expression levels of 24 components. The model has 37 protein components, but some are not active in these simulations because chemical effectors are absent, and some are enzymes assumed to be in 1:1 complexes with their targets and, hence, with no separate parameter for expression. The rms-relative errors were insensitive to the total elimination of AC, KATP, and sGC because, in the absence of chemical effectors, these components were active only at a basal level. There were 14 components, of which the elimination of any one resulted in an rms-relative error in either V_m or Ca_{in} >10%. For eight of these (BK, Ca_{leak}, Cl_A, Cl_{leak}, IP3R, NaK, NSCne, and BUF_{jun}), altering the number per cell by ±20% yielded rms-relative errors in V_m and Ca_{in} <5%. These components play significant roles in the model, and yet $<V_m>$ and $<Ca_{in}>$ were relatively insensitive to their expression levels. The simulations of V_{exp} and Ca_{exp} were more sensitive to changes in the numbers of CaV, NSCstr, PLC, PMCA, RyR, and SERCA; altering the number

Published June 29, 2015

of any one of them by ±20% yielded an rms-relative error in V_m or Ca_{in} >5%. Only for PLC, however, did the rms-relative errors exceed those obtained in the absence of BK β1. Sensitivity to variation in PLC_T is caused by the dependence of NSCstr, NSCne, and PKC on the basal level of DAG, the regulation of which in the model is highly simplified. Overall, the rms-relative errors in the simulations were moderately insensitive to changes in the expression levels of most of the components.

In a second approach, I looked at the sensitivity of the simulations to changes by ±10% of 97 parameters, including the expression levels and the kinetic parameters of the components (Figs. S8–S10). I calculated global sensitivities as the absolute values of the relative changes $|(\langle V_m\rangle_{norm} - \langle V_m\rangle_{perturbed})/\varepsilon\langle V_m\rangle_{norm}|$ and $|(\langle Ca_{in}\rangle_{norm} - \langle Ca_{in}\rangle_{perturbed})/\varepsilon\langle Ca_{in}\rangle_{norm}|$, where ε is 0.1, the fractional change in the parameter, and averaged these over six intramural pressures. In addition, I calculated the fractional change in the output of the cognate component (e.g., I_{BK} for BK channel parameters, I_{CaV} for CaV channel parameters, etc.) per fractional change in each parameter. These were the local sensitivities. Calculated this way, sensitivity approximates the mean of the absolute value of the partial derivative $\partial[\ln(Z)]/\partial[\ln(\text{parameter})]$, where Z is $\langle V_m\rangle$, $\langle Ca_{in}\rangle$, or the mean output of the cognate component. A sensitivity of 1 indicates, for example, that a 10% change in a given parameter results in a 10% change in output.

For most of the 97 parameters considered, the global sensitivities are far <1 and also less than the sensitivities of the cognate components (Figs. S8–S10). For $\langle V_m\rangle$ and $\langle Ca_{in}\rangle$, the sensitivities are ≤0.1 for 54 and 53 parameters, respectively, whereas the component sensitivities are ≥0.4 for 65 parameters. Five additional parameters, V_x (where x is the relevant component), appear as the expression $(V_m - V_x)$ in exponentials. These were perturbed by ±2 mV, and a modified sensitivity was calculated (Table S4). Except for the sensitivity of $\langle Ca_{in}\rangle$ to V_{CaV_act}, the sensitivities of $\langle V_m\rangle$ and $\langle Ca_{in}\rangle$ were far less than the component sensitivities. Thus, at least in the vicinity of the normal set, the effects of most parameter changes on $\langle V_m\rangle$ and $\langle Ca_{in}\rangle$ are small both absolutely and relatively compared with their effects on the outputs of their cognate components. The model is buffered against changes in many of its parameters and can be considered robust.

Chemical effectors

α-adrenergic input.

The effects on $\langle V_m\rangle$ and $\langle Ca_{in}\rangle$ of an α-adrenergic agonist (αA) were simulated at 60–mm Hg intravascular pressure and normal parameters (Fig. 6, A and B). The association and dissociation rate constants of αA were selected so that its equilibrium dissociation constant was 10 µM, characteristic of norepinephrine (see Table S6). αA was added alone or simultaneously with the same concentration of extracellular ATP. Also, the addition was either steady or pulsatile (Fig. 6 C), with the latter simulating release from sympathetic neurovascular junctions (Todorov et al., 1999). The EC50 for the increase in $\langle Ca_{in}\rangle$ caused by the steady application of αA was 0.41 µM (Table S5). The EC50 for norepinephrine-induced

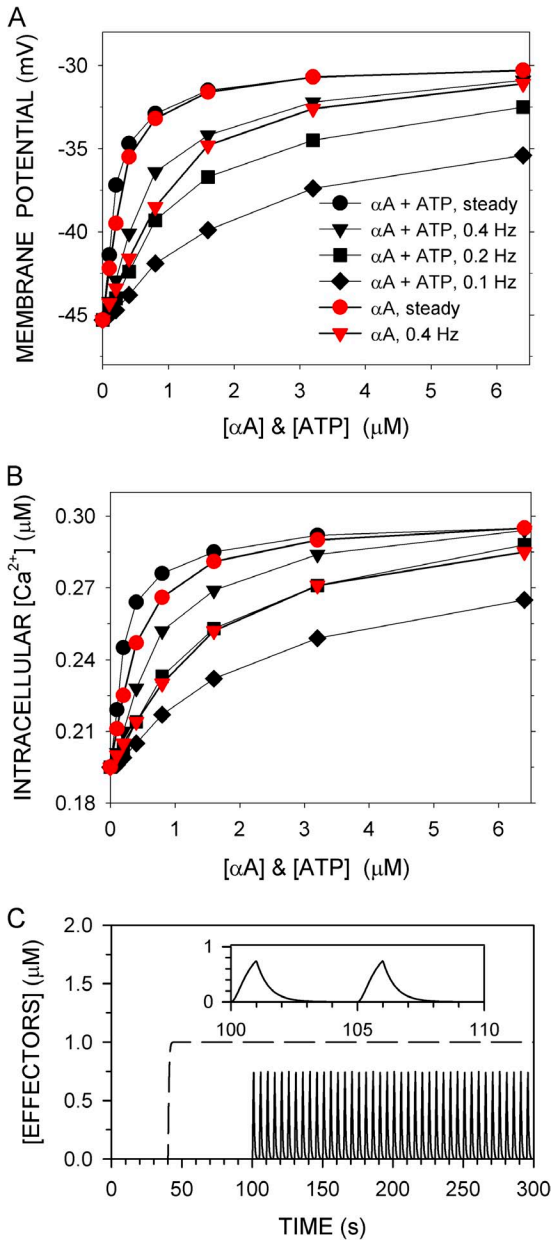

Figure 6. Effects of α-adreneric agonist (αA) and ATP on $\langle V_m\rangle$ and $\langle Ca_{in}\rangle$ at 60 mm Hg. (A) $\langle V_m\rangle$ and (B) $\langle Ca_{in}\rangle$ are the means over the last 50 s of a 300-s simulation computed with normal parameters. αA alone (red symbols) or αA and ATP together at the same concentration (black symbols) were added either steadily from t = 40–300 s (C; dashed line) or in pulses from t = 100–300 s (C; solid line). Pulses were on for 1 s and were off for 1.5 s (0.4 Hz), 4 s (0.2 Hz), or 9 s (0.1 Hz). The rate constant for both the rise and fall of a pulse was 2/s. (C) Nominally 1-µM pulses at 0.2 Hz and (inset) two cycles on expanded scale (solid line) are shown, at a steady application of 1 µM (dashed line).

Published June 29, 2015

contraction of isolated rat mesenteric arteries pressurized to 60 mm Hg was 0.25 µM (Enouri et al., 2011). The EC50 for the effects of the steady application of αA plus ATP was lower than that for αA alone, more so for the effects on $<Ca_{in}>$ than on $<V_m>$ (Table S5). The maximum depolarizations and maximum increases in Ca_{in}, however, were nearly identical for αA alone and αA plus ATP. Thus, ATP enhanced the effects of αA more at lower than at higher concentrations. With pulsatile application, the EC50s for the effects of αA plus ATP were also lower than the EC50s for the effects of αA alone.

Pulsatile application was both effective and economical. For example, 80 1-s pulses over 200 s (i.e., at 0.4 Hz) of nominally 3.2 µM αA plus ATP increased $<Ca_{in}>$ by 89 µM, whereas steady application of 3.2 µM αA plus ATP increased $<Ca_{in}>$ by 97 µM. The quantity of αA added in pulses, however, was cumulatively only 15% of that added during steady application. Note that the effector concentration in a pulse reached only ∼75% of the nominal concentration after 1 s, when the pulse turned off (Fig. 6 C).

βA, EET, and NO input. These three effectors hyperpolarize V_m and lower Ca_{in} by overlapping pathways. They all promote BK channel activity, among other channels that are modulated (Fig. 1). The effects of their steady application on $<V_m>$ and $<Ca_{in}>$ were simulated at 60–mm Hg intravascular pressure and normal parameters (Fig. 7, A and B). For βA, the EC50s for the two variables (Table S5) were similar to the EC50s for epinephrine determined in rat mesenteric arteries in the presence of the αAR blocker prazocin at ∼60 mm Hg, namely, 0.79 µM for hyperpolarization and 0.25 µM for relaxation (Garland et al., 2011). In the model, elimination of KATP suppressed the βA-induced hyperpolarization, simulating the observed effect of the KATP inhibitor glibenclamide (Garland et al., 2011). In the model, however, elimination of KATP suppressed the βA-induced decrease in $<Ca_{in}>$, counter to the observed lack of effect of glibenclamide on relaxation (Garland et al., 2011). The model lacks additional significant pathways for the lowering of tension by PKA.

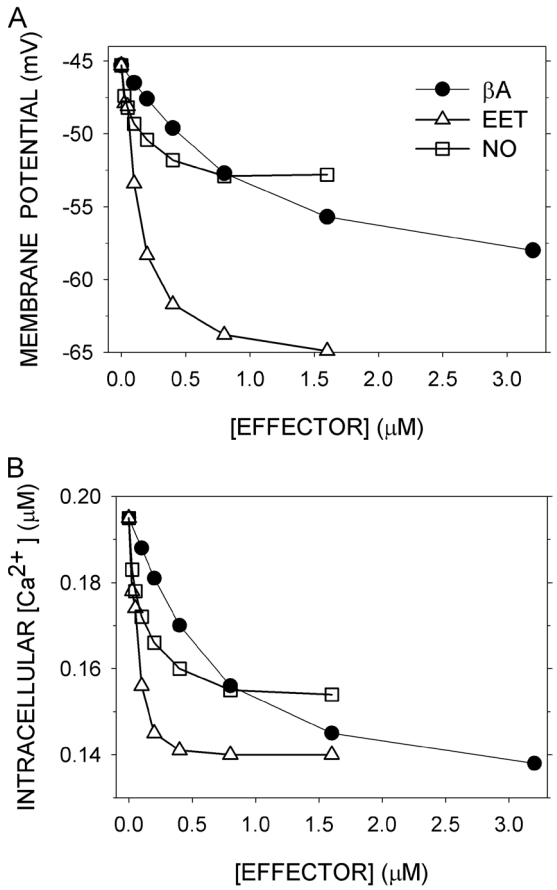

Figure 7. Effects of β-adrenergic agonist (βA), EET, and NO on $<V_m>$ and $<Ca_{in}>$ at 60 mm Hg. (A) $<V_m>$ and (B) $<Ca_{in}>$ were computed as before with normal parameters. Effectors were added steadily from t = 40–300 s.

For EET, the EC50s for $<V_m>$ and $<Ca_{in}>$ from the simulation were 0.54 and 0.24 µM (Table S5). The EC50 for 11,12-EET–induced vasodilation of pressurized mesenteric arteries, however, was far lower, in the range of 1 to 10 nM (Earley et al., 2005). For NO, the EC50s for $<V_m>$ and $<Ca_{in}>$ were 0.46 and 0.40 µM (Table S5). The observed EC50s for relaxation were higher, ∼8 µM for aorta and ∼5 µM for femoral artery (Nimmegeers et al., 2007). Roles for sGC-independent NO effects (Nimmegeers et al., 2007; Yuill et al., 2010) were not considered in the model.

Mitigating the effects of the loss of BK β1

In mice, knockout of BK β1 subunit reduces the Ca sensitivity and shifts the G-V curve of the BK channel to the right so that STOCs are less efficiently activated by Ca sparks (Brenner et al., 2000; Bao and Cox, 2005). Low expression of BK β1 results in increased arterial SM tone and increased blood pressure (Brenner et al., 2000), although the latter effect depends on the mouse strain (Sachse et al., 2014). In the simulation with BK channel parameters appropriate for channels composed of α alone (Horrigan and Aldrich, 2002), $<V_m>$ and $<Ca_{in}>$ are higher at all pressures than $<V_m>$ and $<Ca_{in}>$ simulated with the normal parameters, which include those for BK α in complex with β1 (Bao and Cox, 2005) (Fig. 8). SM tension is directly related to $<Ca_{in}>$, and thus the myogenic response is predicted to be abnormal in the absence of β1.

βA, EET, and NO all brought $<V_m>$ and $<Ca_{in}>$ closer to their normal values and hence should have a normalizing effect on the myogenic response. At least in the simulation, one vasorelaxant is more effective than the others (Fig. 8). For effector concentrations approximately optimal for shifting the BK β1 knockout curves toward the normal curve, the mean over six intramural pressures of $|(<Ca_{in}> - <Ca_{in,norm}>)/<Ca_{in,norm}>|$ for the β1 knockout with no effector was 19.3%, with 0.1 µM

Published June 29, 2015

βA it was 15.1%, with 0.2 µM EET it was 6.4%, and with 0.4 µM NO it was 3.7%. Among these vasorelaxants, NO is the most effective in restoring global Ca concentrations to near-normal over the tested range of intramural pressure.

DISCUSSION

The model should be evaluated based on whether it simulates experimental data, whether it does so with credible mechanisms and parameters, whether it incorporates all components known to be significant in the short-term control of V_m and Ca_{in} in arterial SM cells (and excludes components not present in these cells), and whether the architecture of an arterial SM cell and the distribution of components in this architecture are adequately represented. Obviously, the equations should represent the model adequately and should be solvable over the relevant ranges of inputs and time. These criteria concern the testability and conformity of the model to properties of arterial SM inferred from experiments. If the model satisfies these criteria, it consolidates and tests the consistency of these inferences. Where the model fills in or goes beyond previously proposed mechanisms, it predicts that these mechanisms will be verified experimentally.

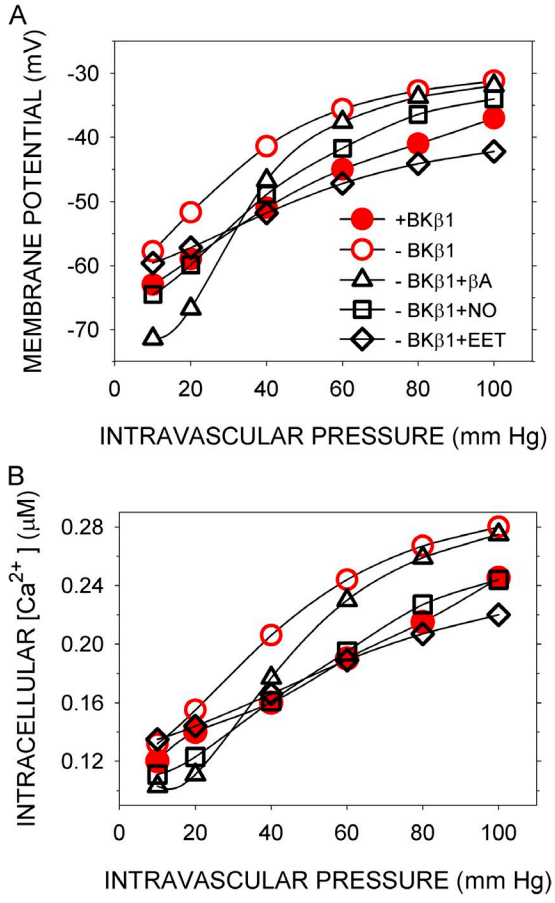

Figure 8. Effects of intravascular pressure and vasorelaxants on $\langle V_m \rangle$ and $\langle Ca_{in} \rangle$ in the absence of BK β1. (A) $\langle V_m \rangle$ and (B) $\langle Ca_{in} \rangle$ were computed as before either with normal parameters (closed red circles), which include those appropriate for the BK channel containing both α and β1 subunits (+BKβ1) (Bao and Cox, 2005), or with parameters appropriate for BK α alone (−BKβ1) (Horrigan and Aldrich, 2002), in the absence (open red circles) or presence (open black symbols) of effectors. 0.1 µM βA (open black triangles), 0.4 µM NO (open black squares), or 0.2 µM EET (open black diamonds) was added steadily from t = 40–300 s.

A set of parameters (the "normal" set) was obtained that resulted in a close fit of the model-generated V_m and Ca_{in} to the experimentally determined V_{exp} and Ca_{exp} as functions of intravascular pressure (Knot and Nelson, 1998) (Fig. 2). With the same normal parameters, except that the number of molecules of the target component was progressively decreased, the model also simulated, at least qualitatively, the experimentally determined effects of inhibiting, one at a time, RyR, BK, and CaV channels (Knot et al., 1998) (Figs. 3–5). This conformity of the model to experimental data beyond those used to derive the normal parameters is, at the very least, the absence of its invalidation; i.e., the model is possibly a valid mathematical representation. Nevertheless, the normal set of parameter values cannot be considered well determined or providing a unique fit to the limited experimental data available. Even if there were more data, unique best-fit parameter values for the complex of mechanisms constituting the model would be elusive (Hines et al., 2014). The existence of even one set of normal parameters, however, confirms that the combination of reasonably behaving components as in the model can result in global behavior that simulates experimentally observed behavior. Again, the model is possibly a valid representation of arterial SM cell function in the limited range of the myogenic response.

The activities of all channels, transporters, kinases, phosphatases, and phosphodiesterases are represented by steady-state equations (not explicitly dependent on time). These include all of the components involved in the control of V_m and Ca_{in} by pressure in the absence of other effectors. The steady-state equations are called by the differential equations that determine as functions of time V_m and all ion concentrations, among other variables. In this approach, the faster processes are governed by steady-state equations, and the slower processes are governed by differential equations (Saucerman and McCulloch, 2004). For most components, the steady-state equations differ from those used in previously published models of SM. Here, all fluxes and currents through channels are driven by the Goldman–Hodgkin–Katz constant-field integral of the Nernst–Planck equation, which is at least a thermodynamically consistent simplification. Primary transporters are driven by the negative free energy change per mole of the overall reaction, including hydrolysis of ATP ($\Delta\mu_{ATP}$). Cotransporters, NCX and NaKCl, are modeled with thermodynamically valid reaction schemes and parameters. The model here for NCX,

Published June 29, 2015

in particular, is more complicated than that in Kapela et al. (2008) and less complicated than that in Kang and Hilgemann (2004). The equations for the open probability of BK channels are taken from Horrigan and Aldrich (2002), and those for CaV channels are from Rubart et al. (1996). For other channels, the local mechanisms incorporated the reported qualitative effects of V_m, Ca, and DAG on open probabilities. Similarly, for all modulated channels and transporters, the reported qualitative effects of phosphorylation were represented quantitatively. The data did not exist to train these local models and to obtain local best-fit parameters. At most, a partial set of related parameters was available (Table S6). For rate constants unconstrained by experiment, I used values within the range of biochemical reaction rate constants and also consistent with the reactions reaching a steady state within ∼200 s.

The disparate signaling roles of Ca require separate microdomains (see Introduction). The model contains two types: the junctional microdomains and the stretch-transducing microdomains. Junctions between the peripheral SR and the sarcolemma were identified in electron micrographs of urinary bladder SM, where they contain RyR and CaV channels and promote contraction (Moore et al., 2004). In the model, I have assumed that similar subcellular structures exist in arterial SM but that their role is to promote relaxation. There is close apposition of the peripheral SR and caveolae in arterial SM (Shaw et al., 2006). One role suggested for such structures is the direct coupling, independent of Ca release, of IP3R and TRPC3 (Adebiyi et al., 2010). Thus, physically restricted spaces that could serve as microdomains for Ca exist in arterial SM. Furthermore, at least in airway myocytes, arrays of RyR in SR and arrays of BK channels in the sarcolemma are close, although not overlapping (Lifshitz et al., 2011).

There is no evidence for stretch-transducing microdomains formed by apposing membranes, but this arrangement is not required for a Ca microdomain. NSCstr and ClA channels are in the same membrane, with 1 NSCstr channel per approximately 10 ClA channels according to the fitted normal set of parameters. If the ClA channels were arrayed in close proximity to the NSCstr channel, the local Ca concentration could be transiently elevated enough (Rizzuto and Pozzan, 2006) to activate the ClA channel sufficiently to depolarize V_m. If instead ClA channels were sensing Ca delivered directly into the global sarcoplasmic pool, the Ca concentration needed to activate ClA channels sufficiently would also strongly activate myosin light chain kinase and cause maximum contraction. Furthermore, experimentally, the Ca current via NSCstr channels does not contribute significantly to Ca_{in}, which is almost entirely caused by influx via CaV channels, as seen in Fig. 5 B. Thus, if Ca influx via NSCstr channels need be limited and yet achieve concentrations greater than Ca_{in}, NSCstr channels must release this Ca signal into a restricted volume, a microdomain, also containing the ClA channels.

A simplification of the model is that each channel and transporter is found only in the membrane bounding one compartment; e.g., RyR is exclusively in the peripheral SR membrane bounding the junctional microdomain, and IP3R is exclusively in the central SR membrane (c.f. Kapela et al., 2008). In arterial SM, however, RyR is also found in the central SR, and IP3R is likely also in the peripheral SR membrane (Adebiyi et al., 2010). Moreover, not all BK channels are directly apposed to RyR (Lifshitz et al., 2011). Would the output of the model differ significantly if it included more realistic distributions of components? BK channels outside the junctions exposed to global Ca_{in} would have very low open probabilities. Active RyR channels in the central SR would raise Ca_{in}, opposing the lowering of Ca_{in} by junctional RyR acting through BK and CaV channels. Given that inhibiting RyR with 10 µM ryanodine raised Ca_{in} (Fig. 4), RyR must be active predominantly in junctions in arterial SM.

In the model, NCX is in the sarcolemma facing the sarcoplasm. Given the simulated values of Na_{in}, Ca_{in}, and V_m, NCX transports Na inward and Ca outward. NCX makes small contributions to the control of V_m and Ca_{in} (Table S2 and Figs. S6 and S7). There is, however, evidence that NCX makes a significant contribution to the maintenance of arterial SM tone (Zhang, 2013). To do so, NCX would need to run in reverse mode, transporting Na outward and Ca inward. In the range of V_m in the SM cell and if Ca_{in} were 0.2–1 µM, Na_{in} would need to be >16–25 mM to drive influx of Ca. More relevant to the control of Ca_{in} by pressure is the possibility that NCX is present in the stretch-transducing microdomains, amplifying the activation of NSCstr channels and the resulting influx of Na by increasing Ca_{NSCstr}. In that case, Ca_{NSCstr} would be ∼0.5 µM, and Na_{NSCstr} would need to be >20 mM to get influx of Ca via NCX. I have simulated the addition of NCX to the NSCstr microdomain and found that with reasonable rates of diffusive equilibration of Na_{NSCstr} with Na_{in} and plausible VOL_{NSCstr}, the I_{NSCstr} needed to obtain Na_{NSCstr} of >20 mM would in itself depolarize V_m to approximately −30 mV and raise Ca_{in} to ∼300 nM without much contribution from NCX. A major role of NCX in the short-term myogenic response seems unlikely. There is, however, evidence that NCX runs in reverse mode in a microdomain shared with NSCne (Zhang, 2013), which I have not explored in the current model.

The model incorporates only pared-down versions of signaling via α- and β-adrenergic receptors and G proteins. Cyclic nucleotide–independent effects via Gβγ, which can promote vasoconstriction (Zhou et al., 2008) or vasorelaxation (Meens et al., 2012), depending on the terminal components of the circuits, are neglected. Including Gβγ effects would require a fine-grained approach beyond the scope of the present model.

Published June 29, 2015

The model makes two types of predictions. The first type is explicit, and such predictions can be tested by straightforward experiments. For example, the model predicts the sensitivities of V_m and Ca_{in} as functions of pressure to partial block of components (Figs. S6 and S7). These predictions can be tested by measurements of V_{exp} and Ca_{exp} in pressurized arteries over a range of concentrations of specific inhibitors, combined with assays for the residual activities of the target components. It also predicts that observables, such as V_{exp} and Ca_{exp}, will be buffered against modest changes in the properties of components (Figs. S8–S10); i.e., like the model, SM cell responses to perturbations are predicted to be robust. It predicts the effects of changes in the activities and properties of SERCA, RyR, and BK channels on the frequency of sparks and STOCs. It predicts the effects of the knockout of the BK β1 subunit (Brenner et al., 2000; Dong et al., 2008; Sachse et al., 2014) on the myogenic response as reflected in V_m and Ca_{in} and the effects of selected vasoactive agents on the myogenic response after knockout of BK β1. Among these vasoactive agents, it predicts that NO will be most effective in restoring the normal functional relationship between Ca_{in} and pressure over its entire range.

The second type of prediction is implicit in the postulated mechanisms included in the model. Two of these are the pressure-transducing microdomains containing NSCstr and ClA channels and the core mechanism of spiking Ca concentrations (sparks) and spiking V_m (STOCs). These predictions are just a short step beyond what others have observed and inferred, made concrete by their mathematical expression.

I thank Steven Marx, Mark Nelson, David Clapham, and two anonymous reviewers for helpful comments.

This work was supported in part by research grant NS054946 from the National Institute of Neurological Disorders and Stroke.

The author declares no competing financial interests.

Richard W. Aldrich served as editor.

Submitted: 11 February 2015
Accepted: 26 May 2015

REFERENCES

Adebiyi, A., G. Zhao, D. Narayanan, C.M. Thomas-Gatewood, J.P. Bannister, and J.H. Jaggar. 2010. Isoform-selective physical coupling of TRPC3 channels to IP3 receptors in smooth muscle cells regulates arterial contractility. *Circ. Res.* 106:1603–1612. http://dx.doi.org/10.1161/CIRCRESAHA.110.216804

Alon, U., M.G. Surette, N. Barkai, and S. Leibler. 1999. Robustness in bacterial chemotaxis. *Nature.* 397:168–171. http://dx.doi.org/10.1038/16483

Ase, A.R., R. Raouf, D. Bélanger, E. Hamel, and P. Séguéla. 2005. Potentiation of P2X1 ATP-gated currents by 5-hydroxytryptamine 2A receptors involves diacylglycerol-dependent kinases and intracellular calcium. *J. Pharmacol. Exp. Ther.* 315:144–154. http://dx.doi.org/10.1124/jpet.105.089045

Aziz, Q., A.M. Thomas, T. Khambra, and A. Tinker. 2012. Regulation of the ATP-sensitive potassium channel subunit, Kir6.2, by a Ca^{2+}-dependent protein kinase C. *J. Biol. Chem.* 287:6196–6207. http://dx.doi.org/10.1074/jbc.M111.243923

Bao, L., and D.H. Cox. 2005. Gating and ionic currents reveal how the BK_{Ca} channel's Ca^{2+} sensitivity is enhanced by its β1 subunit. *J. Gen. Physiol.* 126:393–412. http://dx.doi.org/10.1085/jgp.200509346

Benjamin, B.A., and E.A. Johnson. 1997. A quantitative description of the Na-K-2Cl cotransporter and its conformity to experimental data. *Am. J. Physiol.* 273:F473–F482.

Bennett, M.R., L. Farnell, and W.G. Gibson. 2005. A quantitative description of the contraction of blood vessels following the release of noradrenaline from sympathetic varicosities. *J. Theor. Biol.* 234:107–122. http://dx.doi.org/10.1016/j.jtbi.2004.11.013

Berridge, M.J., M.D. Bootman, and H.L. Roderick. 2003. Calcium signalling: dynamics, homeostasis and remodelling. *Nat. Rev. Mol. Cell Biol.* 4:517–529. http://dx.doi.org/10.1038/nrm1155

Bezprozvanny, I., J. Watras, and B.E. Ehrlich. 1991. Bell-shaped calcium-response curves of Ins(1,4,5)P3- and calcium-gated channels from endoplasmic reticulum of cerebellum. *Nature.* 351:751–754. http://dx.doi.org/10.1038/351751a0

Bidasee, K.R., L. Xu, G. Meissner, and H.R. Besch Jr. 2003. Diketopyridylryanodine has three concentration-dependent effects on the cardiac calcium-release channel/ryanodine receptor. *J. Biol. Chem.* 278:14237–14248. http://dx.doi.org/10.1074/jbc.M208372200

Boettcher, A.J., J. Wu, C. Kim, J. Yang, J. Bruystens, N. Cheung, J.K. Pennypacker, D.A. Blumenthal, A.P. Kornev, and S.S. Taylor. 2011. Realizing the allosteric potential of the tetrameric protein kinase A RIα holoenzyme. *Structure.* 19:265–276. http://dx.doi.org/10.1016/j.str.2010.12.005

Brenner, R., G.J. Peréz, A.D. Bonev, D.M. Eckman, J.C. Kosek, S.W. Wiler, A.J. Patterson, M.T. Nelson, and R.W. Aldrich. 2000. Vasoregulation by the beta1 subunit of the calcium-activated potassium channel. *Nature.* 407:870–876. http://dx.doi.org/10.1038/35038011

Brini, M., and E. Carafoli. 2011. The plasma membrane Ca^{2+} ATPase and the plasma membrane sodium calcium exchanger cooperate in the regulation of cell calcium. *Cold Spring Harb. Perspect. Biol.* 3:a004168. http://dx.doi.org/10.1101/cshperspect.a004168

Bulley, S., Z.P. Neeb, S.K. Burris, J.P. Bannister, C.M. Thomas-Gatewood, W. Jangsangthong, and J.H. Jaggar. 2012. TMEM16A/ANO1 channels contribute to the myogenic response in cerebral arteries. *Circ. Res.* 111:1027–1036. http://dx.doi.org/10.1161/CIRCRESAHA.112.277145

Butler, A., S. Tsunoda, D.P. McCobb, A. Wei, and L. Salkoff. 1993. mSlo, a complex mouse gene encoding "maxi" calcium-activated potassium channels. *Science.* 261:221–224. http://dx.doi.org/10.1126/science.7687074

Chipperfield, A.R., and A.A. Harper. 2000. Chloride in smooth muscle. *Prog. Biophys. Mol. Biol.* 74:175–221. http://dx.doi.org/10.1016/S0079-6107(00)00024-9

Colyer, J. 1998. Phosphorylation states of phospholamban. *Ann. NY Acad. Sci.* 853:79–91. http://dx.doi.org/10.1111/j.1749-6632.1998.tb08258.x

Coste, B., J. Mathur, M. Schmidt, T.J. Earley, S. Ranade, M.J. Petrus, A.E. Dubin, and A. Patapoutian. 2010. Piezo1 and Piezo2 are essential components of distinct mechanically activated cation channels. *Science.* 330:55–60. http://dx.doi.org/10.1126/science.1193270

Desch, M., K. Sigl, B. Hieke, K. Salb, F. Kees, D. Bernhard, A. Jochim, B. Spiessberger, K. Höcherl, R. Feil, et al. 2010. IRAG determines nitric oxide- and atrial natriuretic peptide-mediated smooth muscle relaxation. *Cardiovasc. Res.* 86:496–505. http://dx.doi.org/10.1093/cvr/cvq008

Dessauer, C.W., and A.G. Gilman. 1997. The catalytic mechanism of mammalian adenylyl cyclase. Equilibrium binding and kinetic analysis of P-site inhibition. *J. Biol. Chem.* 272:27787–27795. http://dx.doi.org/10.1074/jbc.272.44.27787

Dong, L., Y.M. Zheng, D. Van Riper, R. Rathore, Q.H. Liu, H.A. Singer, and Y.X. Wang. 2008. Functional and molecular evidence for impairment of calcium-activated potassium channels in type-1 diabetic cerebral artery smooth muscle cells. *J. Cereb. Blood Flow Metab.* 28:377–386.

Earley, S., and J.E. Brayden. 2010. Transient receptor potential channels and vascular function. *Clin. Sci.* 119:19–36.

Earley, S., B.J. Waldron, and J.E. Brayden. 2004. Critical role for transient receptor potential channel TRPM4 in myogenic constriction of cerebral arteries. *Circ. Res.* 95:922–929. http://dx.doi.org/10.1161/01.RES.0000147311.54833.03

Earley, S., T.J. Heppner, M.T. Nelson, and J.E. Brayden. 2005. TRPV4 forms a novel Ca^{2+} signaling complex with ryanodine receptors and BKCa channels. *Circ. Res.* 97:1270–1279. http://dx.doi.org/10.1161/01.RES.0000194321.60300.d6

Earley, S., S.V. Straub, and J.E. Brayden. 2007. Protein kinase C regulates vascular myogenic tone through activation of TRPM4. *Am. J. Physiol. Heart Circ. Physiol.* 292:H2613–H2622. http://dx.doi.org/10.1152/ajpheart.01286.2006

Earley, S., T. Pauyo, R. Drapp, M.J. Tavares, W. Liedtke, and J.E. Brayden. 2009. TRPV4-dependent dilation of peripheral resistance arteries influences arterial pressure. *Am. J. Physiol. Heart Circ. Physiol.* 297:H1096–H1102. http://dx.doi.org/10.1152/ajpheart.00241.2009

Enouri, S., G. Monteith, and R. Johnson. 2011. Characteristics of myogenic reactivity in isolated rat mesenteric veins. *Am. J. Physiol. Regul. Integr. Comp. Physiol.* 300:R470–R478. http://dx.doi.org/10.1152/ajpregu.00491.2010

Francis, S.H., M.A. Blount, and J.D. Corbin. 2011. Mammalian cyclic nucleotide phosphodiesterases: Molecular mechanisms and physiological functions. *Physiol. Rev.* 91:651–690. http://dx.doi.org/10.1152/physrev.00030.2010

Garland, C.J., P.L. Yarova, F. Jiménez-Altayó, and K.A. Dora. 2011. Vascular hyperpolarization to β-adrenoceptor agonists evokes spreading dilatation in rat isolated mesenteric arteries. *Br. J. Pharmacol.* 164:913–921. http://dx.doi.org/10.1111/j.1476-5381.2011.01224.x

Gold, M.G., F. Stengel, P.J. Nygren, C.R. Weisbrod, J.E. Bruce, C.V. Robinson, D. Barford, and J.D. Scott. 2011. Architecture and dynamics of an A-kinase anchoring protein 79 (AKAP79) signaling complex. *Proc. Natl. Acad. Sci. USA.* 108:6426–6431. http://dx.doi.org/10.1073/pnas.1014400108

Hald, B.O., J.C. Jacobsen, T.H. Braunstein, R. Inoue, Y. Ito, P.G. Sørensen, N.H. Holstein-Rathlou, and L.J. Jensen. 2012. BKCa and KV channels limit conducted vasomotor responses in rat mesenteric terminal arterioles. *Pflugers Arch.* 463:279–295. http://dx.doi.org/10.1007/s00424-011-1049-8

Herberg, F.W., W.R. Dostmann, M. Zorn, S.J. Davis, and S.S. Taylor. 1994. Crosstalk between domains in the regulatory subunit of cAMP-dependent protein kinase: Influence of amino terminus on cAMP binding and holoenzyme formation. *Biochemistry.* 33:7485–7494. http://dx.doi.org/10.1021/bi00189a057

Hill, A.J., J.M. Hinton, H. Cheng, Z. Gao, D.O. Bates, J.C. Hancox, P.D. Langton, and A.F. James. 2006. A TRPC-like non-selective cation current activated by alpha 1-adrenoceptors in rat mesenteric artery smooth muscle cells. *Cell Calcium.* 40:29–40. http://dx.doi.org/10.1016/j.ceca.2006.03.007

Hill-Eubanks, D.C., M.E. Werner, T.J. Heppner, and M.T. Nelson. 2011. Calcium signaling in smooth muscle. *Cold Spring Harb. Perspect. Biol.* 3:a004549. http://dx.doi.org/10.1101/cshperspect.a004549

Hines, K.E., T.R. Middendorf, and R.W. Aldrich. 2014. Determination of parameter identifiability in nonlinear biophysical models: A Bayesian approach. *J. Gen. Physiol.* 143:401–416. http://dx.doi.org/10.1085/jgp.201311116

Horrigan, F.T., and R.W. Aldrich. 2002. Coupling between voltage sensor activation, Ca^{2+} binding and channel opening in large conductance (BK) potassium channels. *J. Gen. Physiol.* 120:267–305. http://dx.doi.org/10.1085/jgp.20028605

Horrigan, F.T., J. Cui, and R.W. Aldrich. 1999. Allosteric voltage gating of potassium channels I. Mslo ionic currents in the absence of Ca^{2+}. *J. Gen. Physiol.* 114:277–304. http://dx.doi.org/10.1085/jgp.114.2.277

Huang, J., H. Zhou, S. Mahavadi, W. Sriwai, and K.S. Murthy. 2007. Inhibition of $G\alpha_q$-dependent PLC-β1 activity by PKG and PKA is mediated by phosphorylation of RGS_4 and GRK2. *Am. J. Physiol. Cell Physiol.* 292:C200–C208. http://dx.doi.org/10.1152/ajpcell.00103.2006

Jaggar, J.H., V.A. Porter, W.J. Lederer, and M.T. Nelson. 2000. Calcium sparks in smooth muscle. *Am. J. Physiol. Cell Physiol.* 278:C235–C256.

Jin, X., S. Shah, X. Du, H. Zhang, and N. Gamper. 2014. Activation of Ca^{2+}-activated Cl^- channel ANO1 by localized Ca^{2+} signals. *J. Physiol.* In press.

Kaczmarek-Hájek, K., E. Lörinczi, R. Hausmann, and A. Nicke. 2012. Molecular and functional properties of P2X receptors—recent progress and persisting challenges. *Purinergic Signal.* 8:375–417. http://dx.doi.org/10.1007/s11302-012-9314-7

Kang, T.M., and D.W. Hilgemann. 2004. Multiple transport modes of the cardiac Na^+/Ca^{2+} exchanger. *Nature.* 427:544–548. http://dx.doi.org/10.1038/nature02271

Kapela, A., A. Bezerianos, and N.M. Tsoukias. 2008. A mathematical model of Ca^{2+} dynamics in rat mesenteric smooth muscle cell: Agonist and NO stimulation. *J. Theor. Biol.* 253:238–260. http://dx.doi.org/10.1016/j.jtbi.2008.03.004

Kholodenko, B.N., J.F. Hancock, and W. Kolch. 2010. Signalling ballet in space and time. *Nat. Rev. Mol. Cell Biol.* 11:414–426. http://dx.doi.org/10.1038/nrm2901

Knaus, H.G., K. Folander, M. Garcia-Calvo, M.L. Garcia, G.J. Kaczorowski, M. Smith, and R. Swanson. 1994. Primary sequence and immunological characterization of beta-subunit of high conductance Ca^{2+}-activated K^+ channel from smooth muscle. *J. Biol. Chem.* 269:17274–17278.

Knot, H.J., and M.T. Nelson. 1998. Regulation of arterial diameter and wall $[Ca^{2+}]$ in cerebral arteries of rat by membrane potential and intravascular pressure. *J. Physiol.* 508:199–209. http://dx.doi.org/10.1111/j.1469-7793.1998.199br.x

Knot, H.J., N.B. Standen, and M.T. Nelson. 1998. Ryanodine receptors regulate arterial diameter and wall $[Ca^{2+}]$ in cerebral arteries of rat via Ca^{2+}-dependent K^+ channels. *J. Physiol.* 508:211–221. http://dx.doi.org/10.1111/j.1469-7793.1998.211br.x

Launikonis, B.S., J. Zhou, D. Santiago, G. Brum, and E. Ríos. 2006. The changes in Ca^{2+} sparks associated with measured modifications of intra-store Ca^{2+} concentration in skeletal muscle. *J. Gen. Physiol.* 128:45–54. http://dx.doi.org/10.1085/jgp.200609545

Leo, M.D., J.P. Bannister, D. Narayanan, A. Nair, J.E. Grubbs, K.S. Gabrick, F.A. Boop, and J.H. Jaggar. 2014. Dynamic regulation of β1 subunit trafficking controls vascular contractility. *Proc. Natl. Acad. Sci. USA.* 111:2361–2366. http://dx.doi.org/10.1073/pnas.1317527111

Lifshitz, L.M., J.D. Carmichael, F.A. Lai, V. Sorrentino, K. Bellvé, K.E. Fogarty, and R. ZhuGe. 2011. Spatial organization of RYRs and BK channels underlying the activation of STOCs by Ca^{2+} sparks in airway myocytes. *J. Gen. Physiol.* 138:195–209. http://dx.doi.org/10.1085/jgp.201110626

Liu, Q.H., Y.M. Zheng, A.S. Korde, X.Q. Li, J. Ma, H. Takeshima, and Y.X. Wang. 2009. Protein kinase C-epsilon regulates local calcium signaling in airway smooth muscle cells. *Am. J. Respir. Cell Mol. Biol.* 40:663–671. http://dx.doi.org/10.1165/rcmb.2008-0323OC

Loukin, S., X. Zhou, Z. Su, Y. Saimi, and C. Kung. 2010. Wild-type and brachyolmia-causing mutant TRPV4 channels respond directly to stretch force. *J. Biol. Chem.* 285:27176–27181. http://dx.doi.org/10.1074/jbc.M110.143370

Lytle, C., T.J. McManus, and M. Haas. 1998. A model of Na-K-2Cl cotransport based on ordered ion binding and glide symmetry. *Am. J. Physiol.* 274:C299–C309.

Mak, D.O., S. McBride, and J.K. Foskett. 2001. ATP regulation of recombinant type 3 inositol 1,4,5-trisphosphate receptor gating. *J. Gen. Physiol.* 117:447–456. http://dx.doi.org/10.1085/jgp.117.5.447

McCarron, J.G., G. Osol, and W. Halpern. 1989. Myogenic responses are independent of the endothelium in rat pressurized posterior cerebral arteries. *Blood Vessels.* 26:315–319.

McGahon, M.K., J.M. Dawicki, A. Arora, D.A. Simpson, T.A. Gardiner, A.W. Stitt, C.N. Scholfield, J.G. McGeown, and T.M. Curtis. 2007. Kv1.5 is a major component underlying the A-type potassium current in retinal arteriolar smooth muscle. *Am. J. Physiol. Heart Circ. Physiol.* 292:H1001–H1008. http://dx.doi.org/10.1152/ajpheart.01003.2006

Meens, M.J., N.J. Mattheij, P.B. van Loenen, L.J. Spijkers, P. Lemkens, J. Nelissen, M.G. Compeer, A.E. Alewijnse, and J.G. De Mey. 2012. G-protein βγ subunits in vasorelaxing and anti-endothelinergic effects of calcitonin gene-related peptide. *Br. J. Pharmacol.* 166:297–308. http://dx.doi.org/10.1111/j.1476-5381.2011.01774.x

Moore, E.D., T. Voigt, Y.M. Kobayashi, G. Isenberg, F.S. Fay, M.F. Gallitelli, and C. Franzini-Armstrong. 2004. Organization of Ca^{2+} release units in excitable smooth muscle of the guinea-pig urinary bladder. *Biophys. J.* 87:1836–1847. http://dx.doi.org/10.1529/biophysj.104.044123

Moosmang, S., V. Schulla, A. Welling, R. Feil, S. Feil, J.W. Wegener, F. Hofmann, and N. Klugbauer. 2003. Dominant role of smooth muscle L-type calcium channel Cav1.2 for blood pressure regulation. *EMBO J.* 22:6027–6034. http://dx.doi.org/10.1093/emboj/cdg583

Murthy, K.S. 2004. Modulation of soluble guanylate cyclase activity by phosphorylation. *Neurochem. Int.* 45:845–851. http://dx.doi.org/10.1016/j.neuint.2004.03.014

Narayanan, D., A. Adebiyi, and J.H. Jaggar. 2012. Inositol trisphosphate receptors in smooth muscle cells. *Am. J. Physiol. Heart Circ. Physiol.* 302:H2190–H2210. http://dx.doi.org/10.1152/ajpheart.01146.2011

Nausch, L.W., A.D. Bonev, T.J. Heppner, Y. Tallini, M.I. Kotlikoff, and M.T. Nelson. 2012. Sympathetic nerve stimulation induces local endothelial Ca^{2+} signals to oppose vasoconstriction of mouse mesenteric arteries. *Am. J. Physiol. Heart Circ. Physiol.* 302:H594–H602. http://dx.doi.org/10.1152/ajpheart.00773.2011

Navedo, M.F., G.C. Amberg, M. Nieves, J.D. Molkentin, and L.F. Santana. 2006. Mechanisms underlying heterogeneous Ca^{2+} sparklet activity in arterial smooth muscle. *J. Gen. Physiol.* 127:611–622. http://dx.doi.org/10.1085/jgp.200609519

Navedo, M.F., G.C. Amberg, R.E. Westenbroek, M.J. Sinnegger-Brauns, W.A. Catterall, J. Striessnig, and L.F. Santana. 2007. $Ca_v1.3$ channels produce persistent calcium sparklets, but $Ca_v1.2$ channels are responsible for sparklets in mouse arterial smooth muscle. *Am. J. Physiol. Heart Circ. Physiol.* 293:H1359–H1370. http://dx.doi.org/10.1152/ajpheart.00450.2007

Neher, E. 1998. Vesicle pools and Ca^{2+} microdomains: New tools for understanding their roles in neurotransmitter release. *Neuron.* 20:389–399. http://dx.doi.org/10.1016/S0896-6273(00)80983-6

Nelson, C.P., R.D. Rainbow, J.L. Brignell, M.D. Perry, J.M. Willets, N.W. Davies, N.B. Standen, and R.A. Challiss. 2011. Principal role of adenylyl cyclase 6 in K^+ channel regulation and vasodilator signalling in vascular smooth muscle cells. *Cardiovasc. Res.* 91:694–702. http://dx.doi.org/10.1093/cvr/cvr137

Nelson, M.T., H. Cheng, M. Rubart, L.F. Santana, A.D. Bonev, H.J. Knot, and W.J. Lederer. 1995. Relaxation of arterial smooth muscle by calcium sparks. *Science.* 270:633–637. http://dx.doi.org/10.1126/science.270.5236.633

Neves, S.R., and R. Iyengar. 2009. Models of spatially restricted biochemical reaction systems. *J. Biol. Chem.* 284:5445–5449. http://dx.doi.org/10.1074/jbc.R800058200

Nimmegeers, S., P. Sips, E. Buys, P. Brouckaert, and J. Van de Voorde. 2007. Functional role of the soluble guanylyl cyclase α_1 subunit in vascular smooth muscle relaxation. *Cardiovasc. Res.* 76:149–159. http://dx.doi.org/10.1016/j.cardiores.2007.06.002

Nishizuka, Y. 1995. Protein kinase C and lipid signaling for sustained cellular responses. *FASEB J.* 9:484–496.

Peng, H., G.C. Yaney, and M.T. Kirber. 2010. Modulation of Ca^{2+} release through ryanodine receptors in vascular smooth muscle by protein kinase Cα. *Pflugers Arch.* 460:791–802. http://dx.doi.org/10.1007/s00424-010-0850-0

Quayle, J.M., M.T. Nelson, and N.B. Standen. 1997. ATP-sensitive and inwardly rectifying potassium channels in smooth muscle. *Physiol. Rev.* 77:1165–1232.

Reeves, J.P., and M. Condrescu. 2008. Ionic regulation of the cardiac sodium-calcium exchanger. *Channels (Austin).* 2:322–328. http://dx.doi.org/10.4161/chan.2.5.6897

Rizzuto, R., and T. Pozzan. 2006. Microdomains of intracellular Ca^{2+}: Molecular determinants and functional consequences. *Physiol. Rev.* 86:369–408. http://dx.doi.org/10.1152/physrev.00004.2005

Rubart, M., J.B. Patlak, and M.T. Nelson. 1996. Ca^{2+} currents in cerebral artery smooth muscle cells of rat at physiological Ca^{2+} concentrations. *J. Gen. Physiol.* 107:459–472. http://dx.doi.org/10.1085/jgp.107.4.459

Sachse, G., J. Faulhaber, A. Seniuk, H. Ehmke, and O. Pongs. 2014. Smooth muscle BK channel activity influences blood pressure independent of vascular tone in mice. *J. Physiol.* 592:2563–2574. http://dx.doi.org/10.1113/jphysiol.2014.272880

Saleh, S.N., A.P. Albert, C.M. Peppiatt, and W.A. Large. 2006. Angiotensin II activates two cation conductances with distinct TRPC1 and TRPC6 channel properties in rabbit mesenteric artery myocytes. *J. Physiol.* 577:479–495. http://dx.doi.org/10.1113/jphysiol.2006.119305

Santana, L.F., and M.F. Navedo. 2009. Molecular and biophysical mechanisms of Ca^{2+} sparklets in smooth muscle. *J. Mol. Cell. Cardiol.* 47:436–444. http://dx.doi.org/10.1016/j.yjmcc.2009.07.008

Saucerman, J.J., and A.D. McCulloch. 2004. Mechanistic systems models of cell signaling networks: a case study of myocyte adrenergic regulation. *Prog. Biophys. Mol. Biol.* 85:261–278. http://dx.doi.org/10.1016/j.pbiomolbio.2004.01.005

Schlossmann, J., and M. Desch. 2011. IRAG and novel PKG targeting in the cardiovascular system. *Am. J. Physiol. Heart Circ. Physiol.* 301:H672–H682. http://dx.doi.org/10.1152/ajpheart.00198.2011

Schöfl, C., G. Brabant, R.D. Hesch, A. von zur Mühlen, P.H. Cobbold, and K.S. Cuthbertson. 1993. Temporal patterns of alpha 1-receptor stimulation regulate amplitude and frequency of calcium transients. *Am. J. Physiol.* 265:C1030–C1036.

Shan, J., A. Kushnir, M.J. Betzenhauser, S. Reiken, J. Li, S.E. Lehnart, N. Lindegger, M. Mongillo, P.J. Mohler, and A.R. Marks. 2010. Phosphorylation of the ryanodine receptor mediates the cardiac fight or flight response in mice. *J. Clin. Invest.* 120:4388–4398. http://dx.doi.org/10.1172/JCI32726

Sharif-Naeini, R., J.H. Folgering, D. Bichet, F. Duprat, I. Lauritzen, M. Arhatte, M. Jodar, A. Dedman, F.C. Chatelain, U. Schulte, et al. 2009. Polycystin-1 and -2 dosage regulates pressure sensing. *Cell.* 139:587–596. http://dx.doi.org/10.1016/j.cell.2009.08.045

Shaw, L., M.A. Sweeney, S.C. O'Neill, C.J. Jones, C. Austin, and M.J. Taggart. 2006. Caveolae and sarcoplasmic reticular coupling in smooth muscle cells of pressurised arteries: The relevance for Ca^{2+} oscillations and tone. *Cardiovasc. Res.* 69:825–835. http://dx.doi.org/10.1016/j.cardiores.2005.12.016

Sobie, E.A., K.W. Dilly, J. dos Santos Cruz, W.J. Lederer, and M.S. Jafri. 2002. Termination of cardiac Ca^{2+} sparks: An investigative

mathematical model of calcium-induced calcium release. *Biophys. J.* 83:59–78. http://dx.doi.org/10.1016/S0006-3495(02)75149-7

Stull, J.T., P.J. Lin, J.K. Krueger, J. Trewhella, and G. Zhi. 1998. Myosin light chain kinase: functional domains and structural motifs. *Acta Physiol. Scand.* 164:471–482. http://dx.doi.org/10.1111/j.1365-201X.1998.tb10699.x

Takahashi, S., H. Lin, N. Geshi, Y. Mori, Y. Kawarabayashi, N. Takami, M.X. Mori, A. Honda, and R. Inoue. 2008. Nitric oxide-cGMP-protein kinase G pathway negatively regulates vascular transient receptor potential channel TRPC6. *J. Physiol.* 586:4209–4223. http://dx.doi.org/10.1113/jphysiol.2008.156083

Taylor, C.W., and D.L. Prole. 2012. Ca^{2+} signalling by IP_3 receptors. *Subcell. Biochem.* 59:1–34.

Todorov, L.D., S.T. Mihaylova-Todorova, R.A. Bjur, and D.P. Westfall. 1999. Differential cotransmission in sympathetic nerves: Role of frequency of stimulation and prejunctional autoreceptors. *J. Pharmacol. Exp. Ther.* 290:241–246.

Tran, K., N.P. Smith, D.S. Loiselle, and E.J. Crampin. 2009. A thermodynamic model of the cardiac sarcoplasmic/endoplasmic Ca^{2+} (SERCA) pump. *Biophys. J.* 96:2029–2042. http://dx.doi.org/10.1016/j.bpj.2008.11.045

van Breemen, C., N. Fameli, and A.M. Evans. 2013. Pan-junctional sarcoplasmic reticulum in vascular smooth muscle: nanospace Ca^{2+} transport for site- and function-specific Ca^{2+} signalling. *J. Physiol.* 591:2043–2054. http://dx.doi.org/10.1113/jphysiol.2012.246348

Vandamme, J., D. Castermans, and J.M. Thevelein. 2012. Molecular mechanisms of feedback inhibition of protein kinase A on intracellular cAMP accumulation. *Cell. Signal.* 24:1610–1618. http://dx.doi.org/10.1016/j.cellsig.2012.04.001

Vandier, C., M. Delpech, and P. Bonnet. 1998. Spontaneous transient outward currents and delayed rectifier K^+ current: effects of hypoxia. *Am. J. Physiol.* 275:L145–L154.

Waldo, G.L., T.K. Ricks, S.N. Hicks, M.L. Cheever, T. Kawano, K. Tsuboi, X. Wang, C. Montell, T. Kozasa, J. Sondek, and T.K. Harden. 2010. Kinetic scaffolding mediated by a phospholipase C-β and G_q signaling complex. *Science.* 330:974–980. http://dx.doi.org/10.1126/science.1193438

Wang, Y.W., J.P. Ding, X.M. Xia, and C.J. Lingle. 2002. Consequences of the stoichiometry of Slo1 alpha and auxiliary beta subunits on functional properties of large-conductance Ca^{2+}-activated K^+ channels. *J. Neurosci.* 22:1550–1561.

Wray, S., and T. Burdyga. 2010. Sarcoplasmic reticulum function in smooth muscle. *Physiol. Rev.* 90:113–178. http://dx.doi.org/10.1152/physrev.00018.2008

Xu, L., and G. Meissner. 2004. Mechanism of calmodulin inhibition of cardiac sarcoplasmic reticulum Ca^{2+} release channel (ryanodine receptor). *Biophys. J.* 86:797–804. http://dx.doi.org/10.1016/S0006-3495(04)74155-7

Yang, J., J.W. Clark, R.M. Bryan, and C.S. Robertson. 2005. Mathematical modeling of the nitric oxide/cGMP pathway in the vascular smooth muscle cell. *Am. J. Physiol. Heart Circ. Physiol.* 289:H886–H897. http://dx.doi.org/10.1152/ajpheart.00216.2004

Yang, L., G. Liu, S.I. Zakharov, A.M. Bellinger, M. Mongillo, and S.O. Marx. 2007. Protein kinase G phosphorylates Cav1.2 alpha1c and beta2 subunits. *Circ. Res.* 101:465–474. http://dx.doi.org/10.1161/CIRCRESAHA.107.156976

Yang, Y.D., H. Cho, J.Y. Koo, M.H. Tak, Y. Cho, W.S. Shim, S.P. Park, J. Lee, B. Lee, B.M. Kim, et al. 2008. TMEM16A confers receptor-activated calcium-dependent chloride conductance. *Nature.* 455:1210–1215. http://dx.doi.org/10.1038/nature07313

Yue, C., C.Y. Ku, M. Liu, M.I. Simon, and B.M. Sanborn. 2000. Molecular mechanism of the inhibition of phospholipase C beta 3 by protein kinase C. *J. Biol. Chem.* 275:30220–30225. http://dx.doi.org/10.1074/jbc.M004276200

Yuill, K.H., A.J. McNeish, Y. Kansui, C.J. Garland, and K.A. Dora. 2010. Nitric oxide suppresses cerebral vasomotion by sGC-independent effects on ryanodine receptors and voltage-gated calcium channels. *J. Vasc. Res.* 47:93–107. http://dx.doi.org/10.1159/000235964

Zhang, J. 2013. New insights into the contribution of arterial NCX to the regulation of myogenic tone and blood pressure. *Adv. Exp. Med. Biol.* 961:329–343.

Zhou, X.B., I. Wulfsen, S. Lutz, E. Utku, U. Sausbier, P. Ruth, T. Wieland, and M. Korth. 2008. M_2 muscarinic receptors induce airway smooth muscle activation via a dual, Gβγ-mediated inhibition of large conductance Ca^{2+}-activated K^+ channel activity. *J. Biol. Chem.* 283:21036–21044. http://dx.doi.org/10.1074/jbc.M800447200

Zhou, X.B., I. Wulfsen, E. Utku, U. Sausbier, M. Sausbier, T. Wieland, P. Ruth, and M. Korth. 2010. Dual role of protein kinase C on BK channel regulation. *Proc. Natl. Acad. Sci. USA.* 107:8005–8010. http://dx.doi.org/10.1073/pnas.0912029107

Zühlke, R.D., G.S. Pitt, K. Deisseroth, R.W. Tsien, and H. Reuter. 1999. Calmodulin supports both inactivation and facilitation of L-type calcium channels. *Nature.* 399:159–162. http://dx.doi.org/10.1038/20200

Karlin et al., http://www.jgp.org/content/full/jgp.201511380/DC1

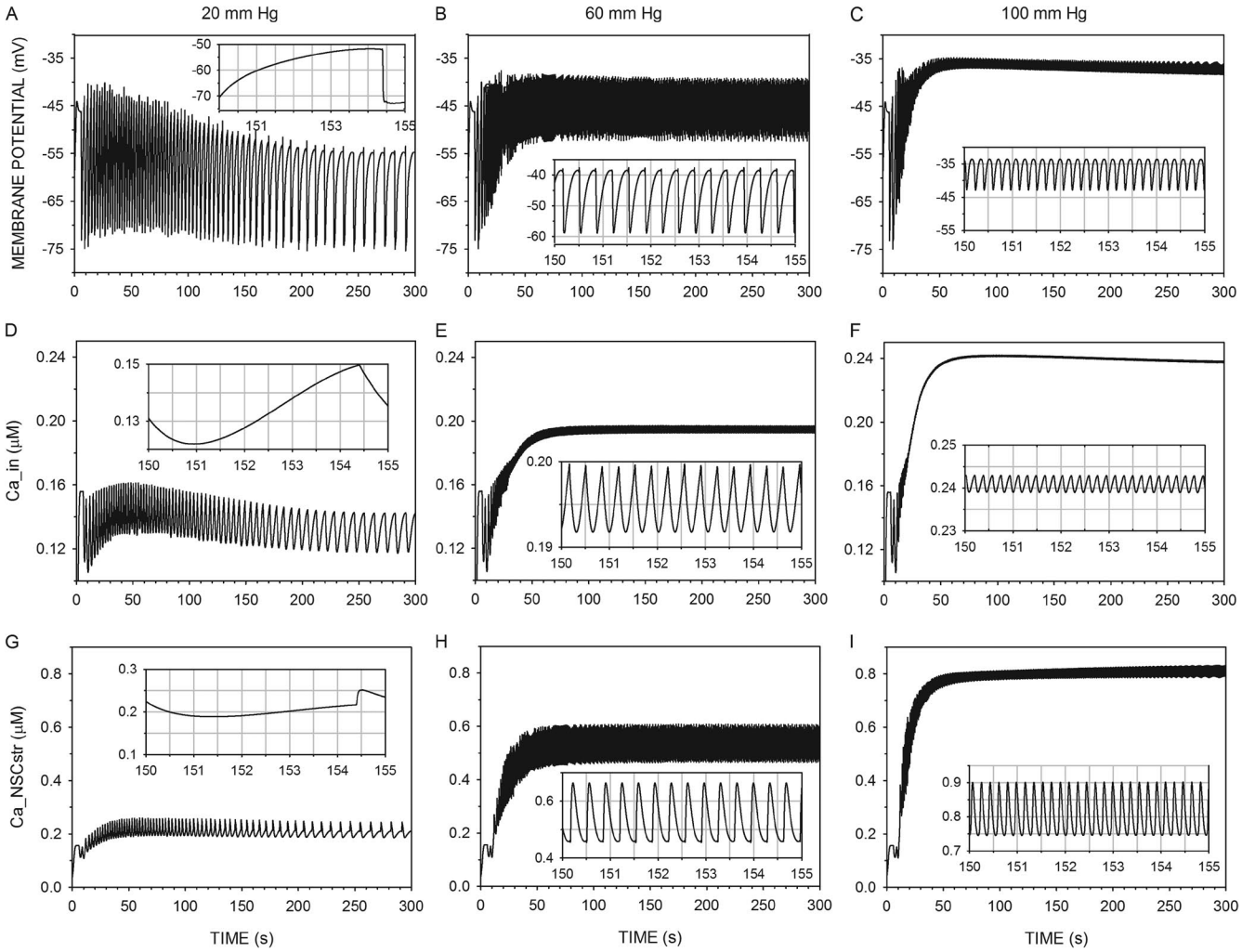

Figure S1. Simulation of time courses of V_m (A–C), Ca_{in} (D–F), and Ca_{NSCstr} (G–I) with normal parameters from t = 0–300 s. Insets show time courses from t = 150–155 s. Intravascular pressure is 20 mm Hg (A, D, and G), 60 mm Hg (B, E, and H), and 100 mm Hg (C, F, and I).

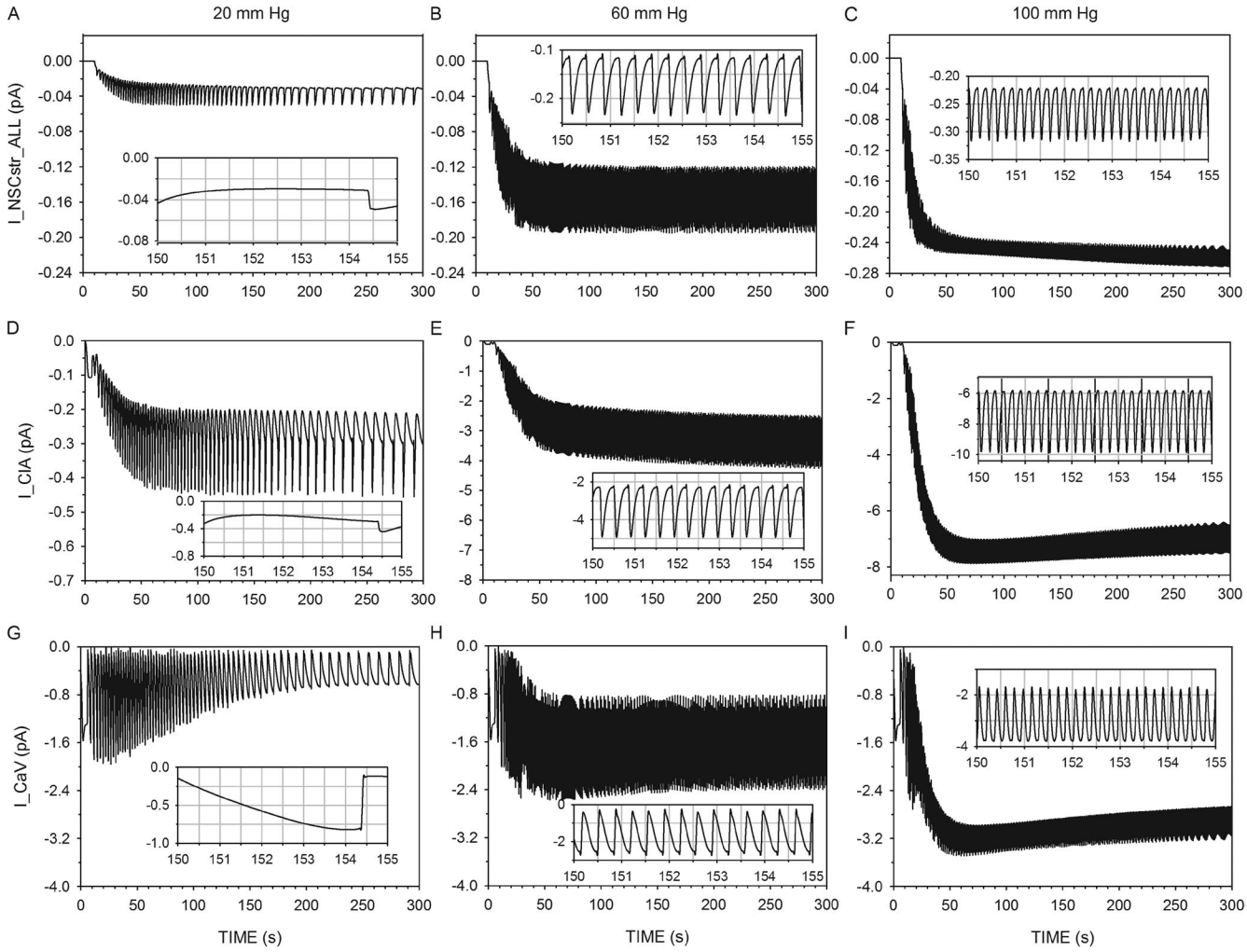

Figure S2. Simulation of time courses of I_{NSCstr_ALL} (A–C), I_{ClA} (D–F), and I_{CaV_ALL} (G–I) with normal parameters from t = 0–300 s. Insets show time courses from t = 150–155 s. Intravascular pressure is 20 mm Hg (A, D, and G), 60 mm Hg (B, E, and H), and 100 mm Hg (C, F, and I).

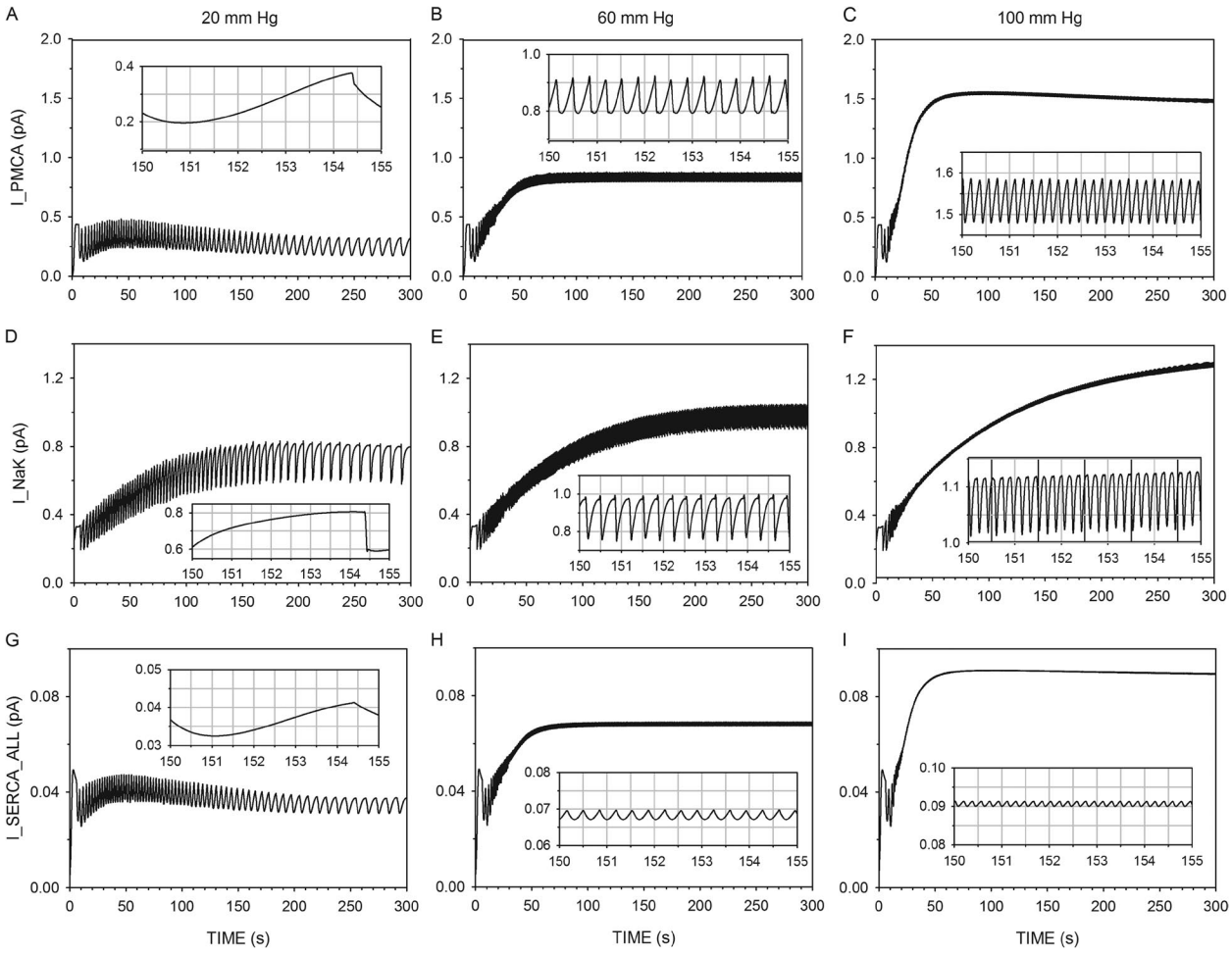

Figure S3. Simulation of time courses of I_{PMCA} (A–C), I_{NaK} (D–F), and I_{SERCA_ALL} (G–I) with normal parameters from t = 0–300 s. Insets show time courses from t = 150–155 s. Intravascular pressure is 20 mm Hg (A, D, and G), 60 mm Hg (B, E, and H), and 100 mm Hg (C, F, and I).

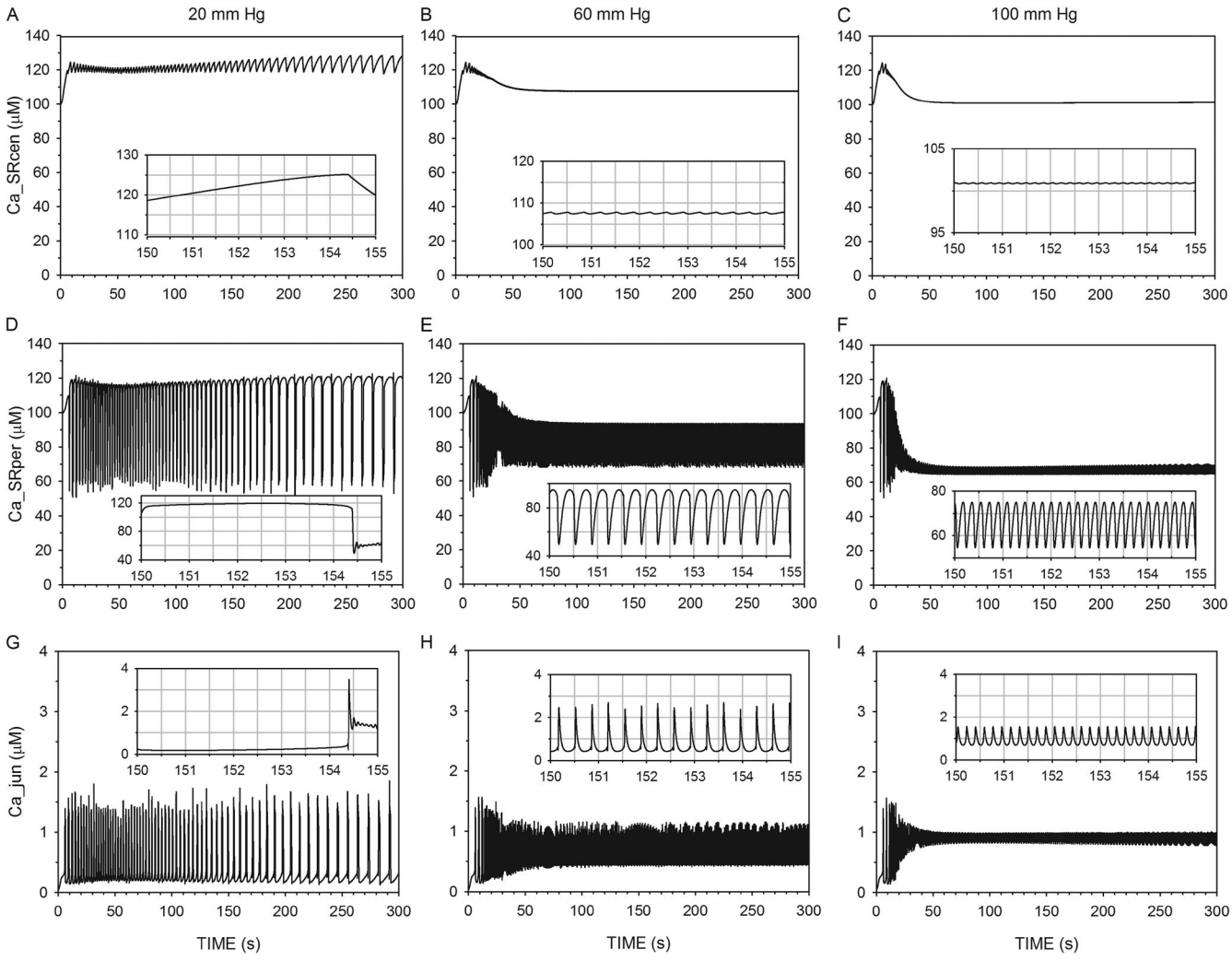

Figure S4. Simulation of time courses of Ca_{SRcen} (A–C), Ca_{SRper} (D–F), and Ca_{jun} (G–I) with normal parameters from t = 0–300 s. Insets show time courses from t = 150–155 s. Intravascular pressure is 20 mm Hg (A, D, and G), 60 mm Hg (B, E, and H), and 100 mm Hg (C, F, and I).

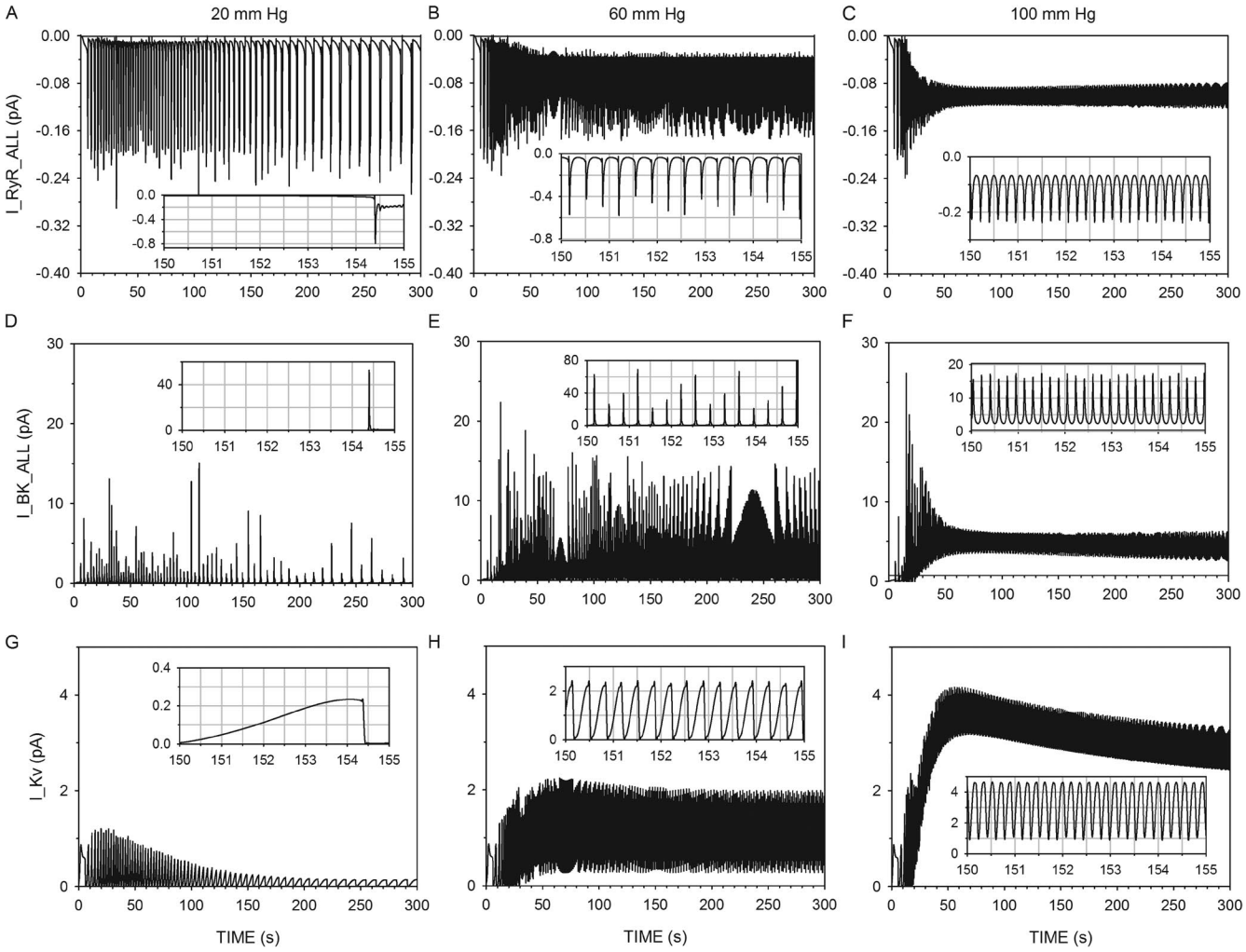

Figure S5. Simulation of time courses of I_{RyR_ALL} (A–C), I_{BK_ALL} (D–F), and I_{Kv} (G–I) with normal parameters from t = 0–300 s. Insets show time courses from t = 150–155 s. Intravascular pressure is 20 mm Hg (A, D, and G), 60 mm Hg (B, E, and H), and 100 mm Hg (C, F, and I).

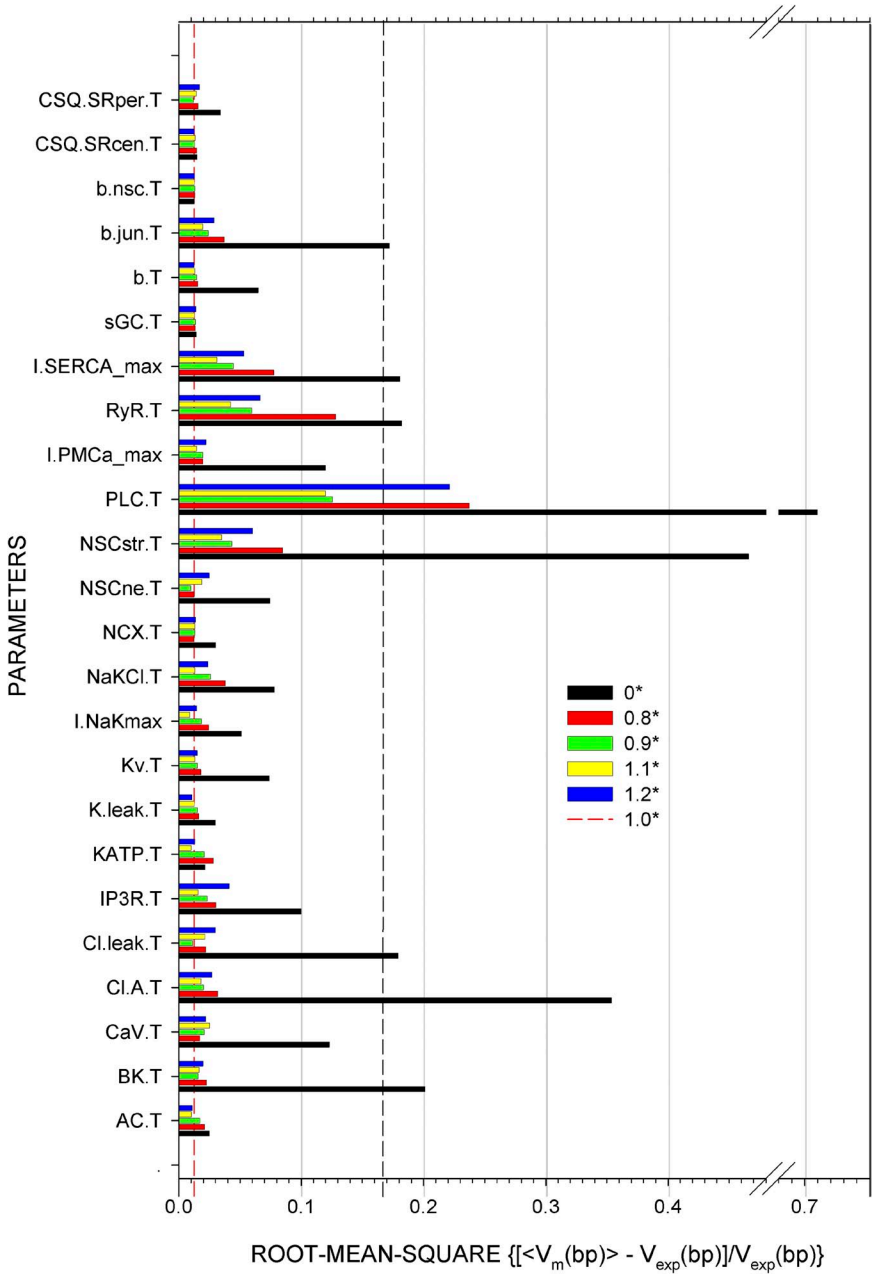

Figure S6. Sensitivity of the fit of $\langle V_m \rangle$ to V_{exp} on variation in the number of molecules of each component. The total number of molecules or the maximum current of each component of relevance in the absence of chemical effectors was changed one at a time by a factor of 0 (or 0.001 in some cases to avoid dividing by zero), 0.8, 0.9, 1.1, and 1.2 times their normal values. (Most enzymes were excluded because they are assumed to be in 1:1 complexes with their targets.) At each of six intravascular pressures (as in Fig. 2), $(\langle V_m \rangle - V_{exp})/V_{exp}$ was calculated; these relative differences were squared, the six values were averaged, and the square root was taken to obtain the rms-relative error in $\langle V_m \rangle$. With the normal parameters, this was 1.25% (dashed red line). The rms-relative error in $\langle V_m \rangle$ simulated with the parameters relevant to BK channel function in the absence of its β1 subunit (see Fig. 8) is 16.7% (black dashed line). Abbreviations are defined in Table S6.

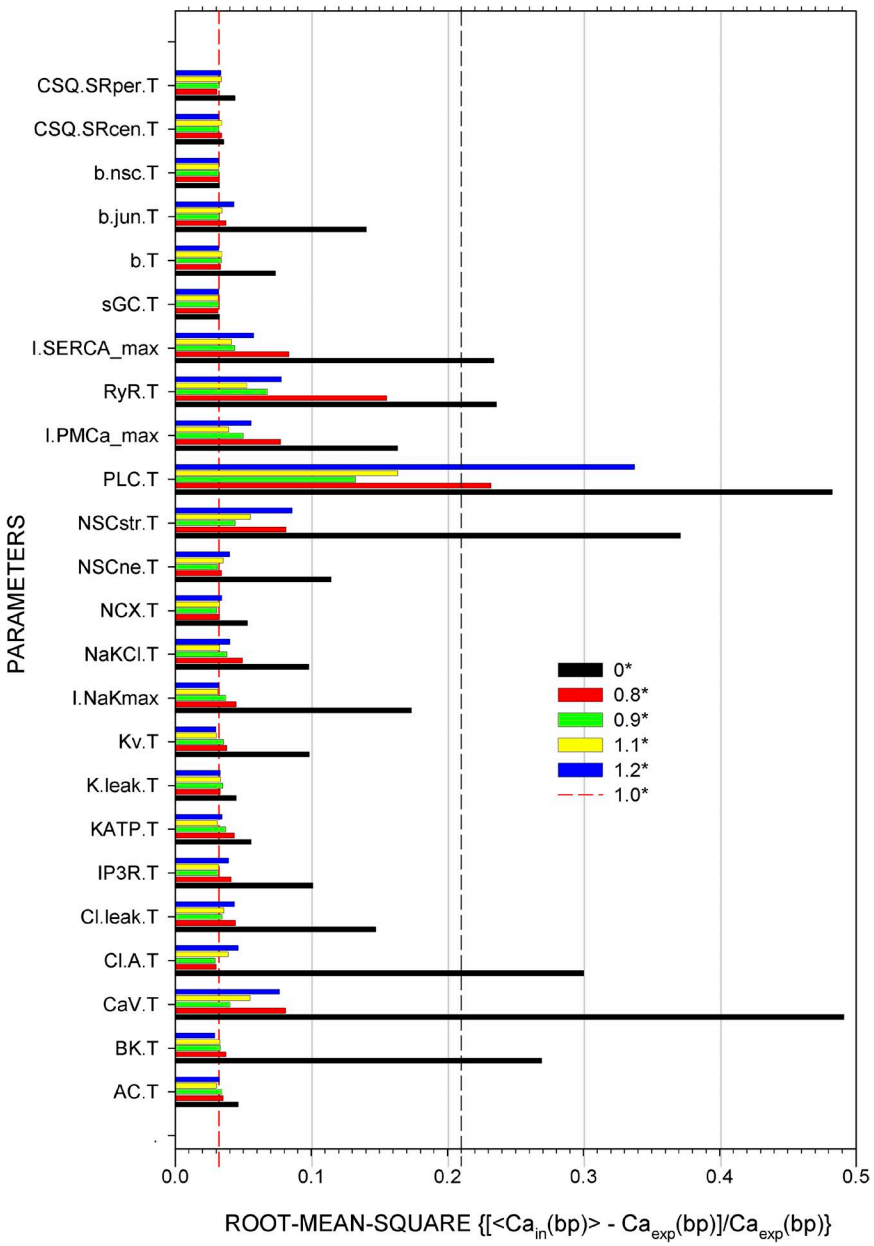

Figure S7. Sensitivity of the fit of of $\langle Ca_{in} \rangle$ to Ca_{exp} on variation in the number of molecules of each component. The rms-relative error in $\langle Ca_{in} \rangle$ was calculated as in Fig. S6. With the normal parameter set, this was 3.21% (dashed red line). The rms-relative error in $\langle Ca_{in} \rangle$ simulated with the parameters relevant to BK channel function in the absence of its β1 subunit (see Fig. 8) is 21.0% (black dashed line).

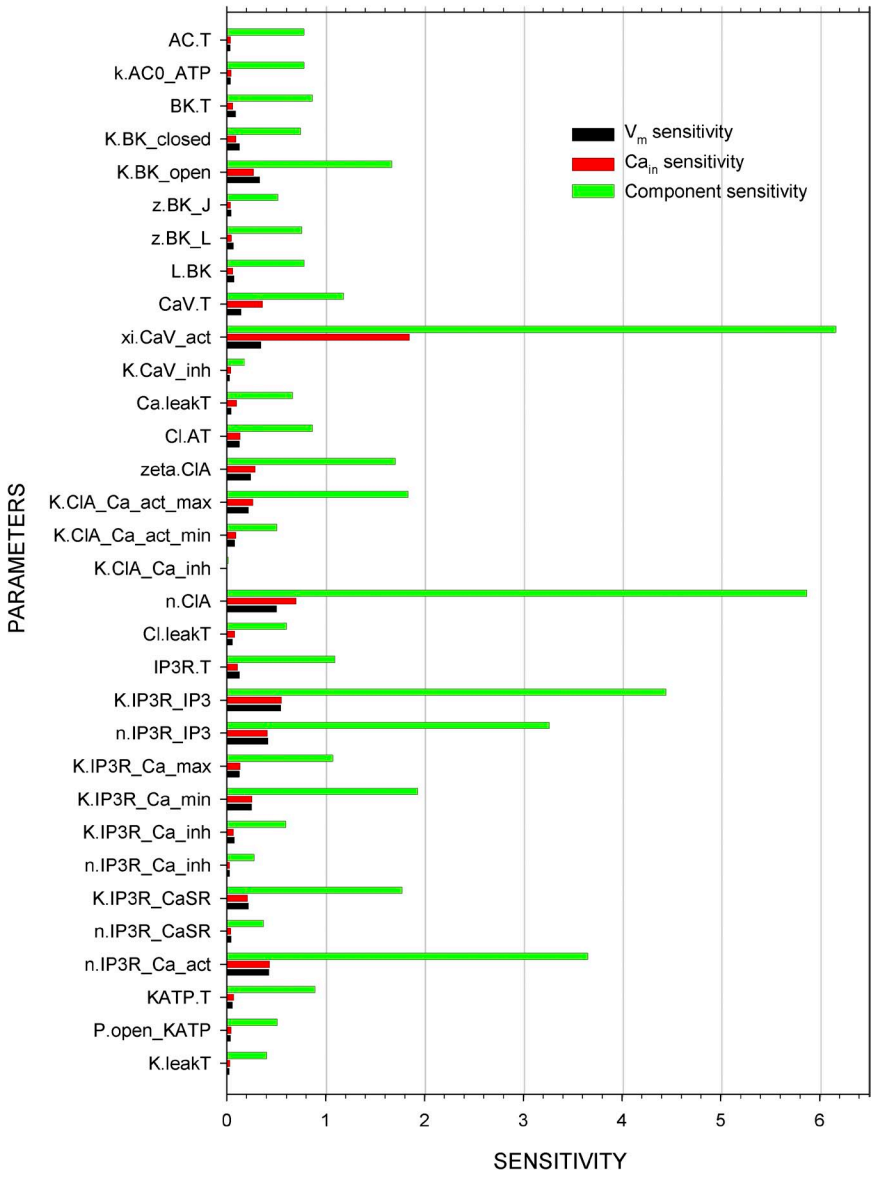

Figure S8. Sensitivities of $\langle V_m \rangle$, $\langle Ca_{in} \rangle$, and components to parameters. Sensitivity is calculated as the mean over six intramural pressures, and for $\pm\varepsilon$, of $|(\langle Z \rangle - \langle Z_{norm} \rangle)/\langle Z_{norm} \rangle|/|\varepsilon|$, where Z is $\langle V_m \rangle$, $\langle Ca_{in} \rangle$, or the immediate output of the cognate component, e.g., $\langle I_{BK\_ALL} \rangle$ for the parameters relevant to BK channel function. The subscript "norm" indicates the value obtained with normal parameters. ε is the fractional change in the parameter, which in these cases are ±0.1. Sensitivity so defined is approximately the mean of the absolute values of the partial derivative of ln(Z) with respect to ln(parameter) in the vicinity of the normal parameters.

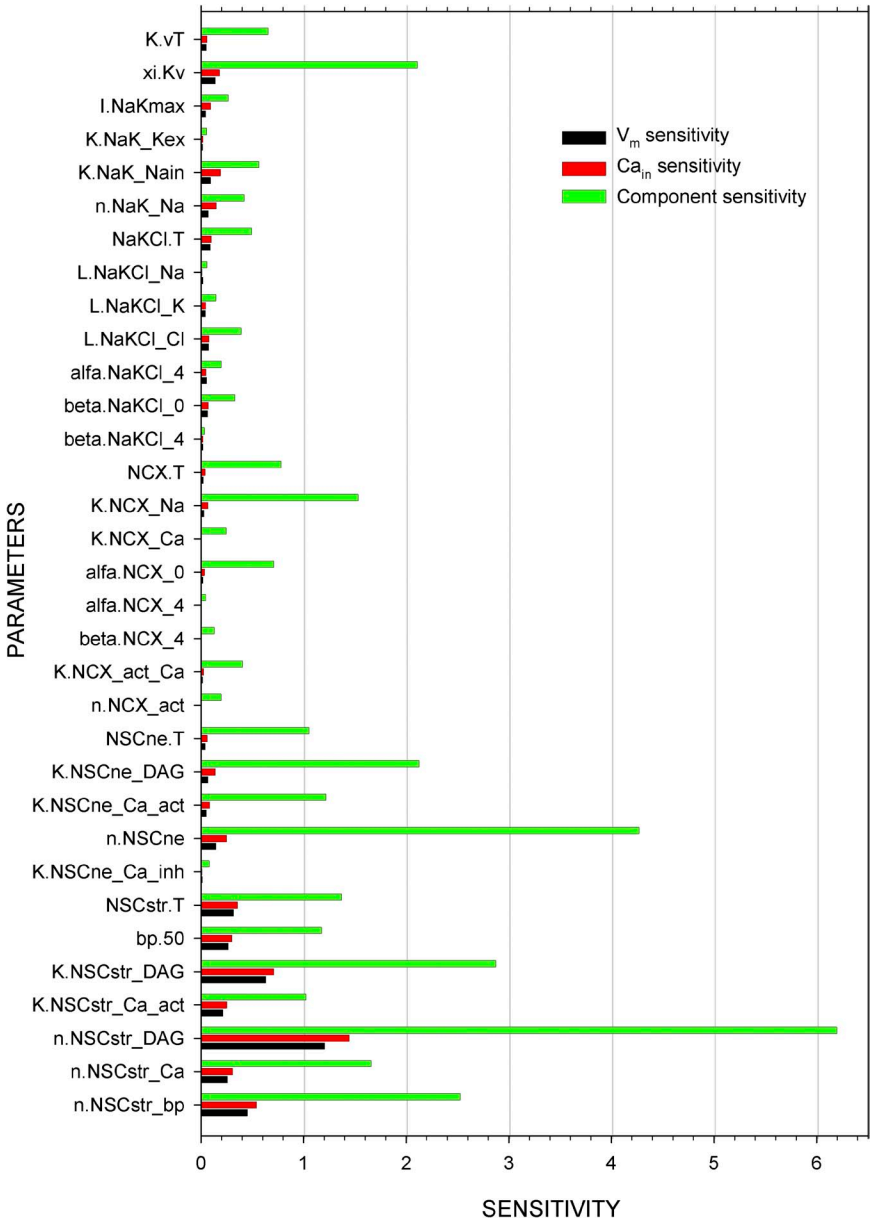

Figure S9. Sensitivities of $\langle V_m \rangle$, $\langle Ca_{in} \rangle$, and components to parameters. Sensitivity is calculated as the mean over six intramural pressures, and for $\pm\varepsilon$, of $|(\langle Z \rangle - \langle Z_{norm} \rangle)/\langle Z_{norm} \rangle|/|\varepsilon|$, where Z is $\langle V_m \rangle$, $\langle Ca_{in} \rangle$, or the immediate output of the cognate component, e.g., $\langle I_{BK\_ALL} \rangle$ for the parameters relevant to BK channel function. The subscript "norm" indicates the value obtained with normal parameters. ε is the fractional change in the parameter, which in these cases are ±0.1. Sensitivity so defined is approximately the mean of the absolute values of the partial derivative of ln(Z) with respect to ln(parameter) in the vicinity of the normal parameters.

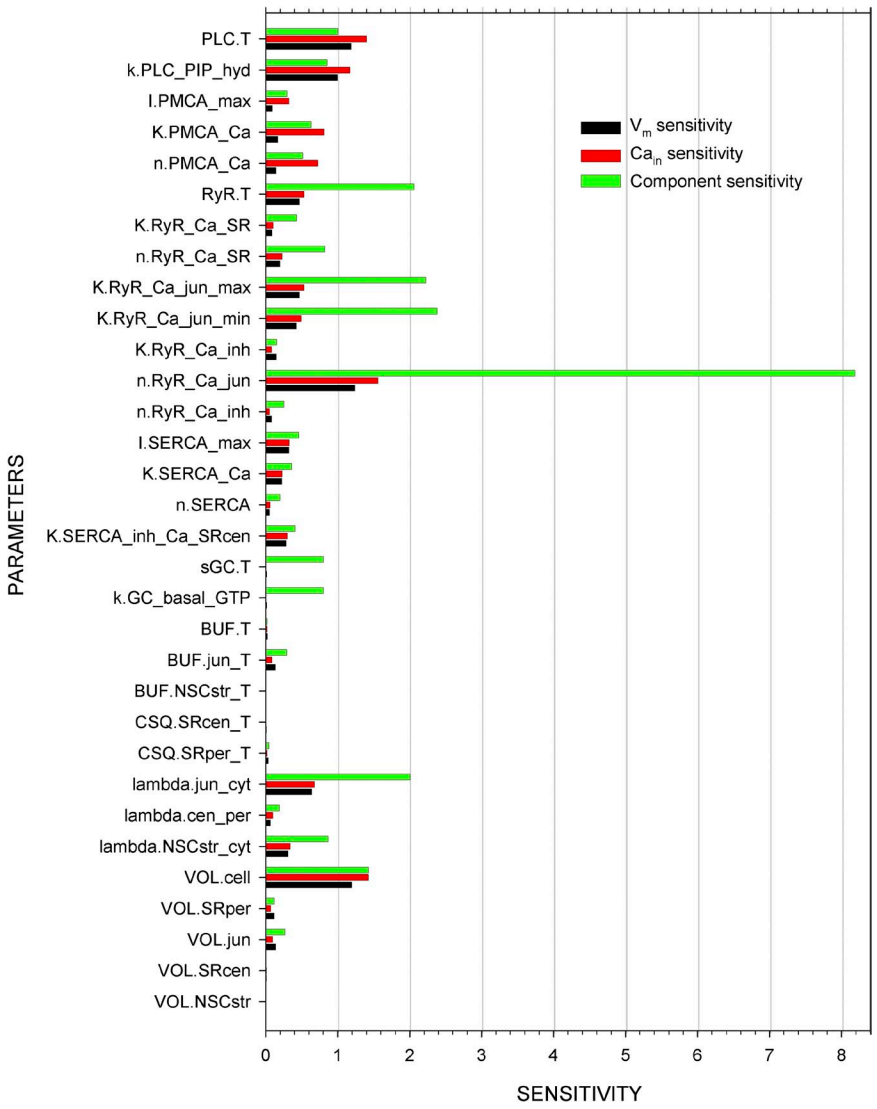

Figure S10. Sensitivities of $\langle V_m \rangle$, $\langle Ca_{in} \rangle$, and components to parameters. Sensitivity is calculated as the mean over six intramural pressures, and for $\pm\varepsilon$, of $|(\langle Z \rangle - \langle Z_{norm} \rangle)/\langle Z_{norm} \rangle|/|\varepsilon|$, where Z is $\langle V_m \rangle$, $\langle Ca_{in} \rangle$, or the immediate output of the cognate component, e.g., $\langle I_{BK\_ALL} \rangle$ for the parameters relevant to BK channel function. The subscript "norm" indicates the value obtained with normal parameters. ε is the fractional change in the parameter, which in these cases are ±0.1. Sensitivity so defined is approximately the mean of the absolute values of the partial derivative of ln(Z) with respect to ln(parameter) in the vicinity of the normal parameters.

TABLE S1

Effector application parameters

Parameters	Units	Values	Parameters	Units	Values
αA.0[a]	μM	0	κ.βA1	1/s	2
αA.1	μM	0	κ.βA2	1/s	2
τ.αA1	s	4.00E + 01	BP.0	mm Hg	0.00E + 00
τ.αA2	s	5.00E + 01	BP.1	mm Hg	10
τ.αA3	s	3.00E + 02	τ.BP1	s	1.00E + 01
κ.αA1	1/s	2	τ.BP2	s	1.50E + 01
κ.αA2	1/s	2	τ.BP3	s	3.00E + 02
ATP.0	μM	0	κ.BP1	1/s	2
ATP.1	μM	0	κ.BP2	1/s	2
τ.pulse_init	s	100	EET.0	μM	0
Δτ.pulse_on	s	1	EET.1	μM	0
Δτ.pulse_off	s	9	τ.EET1	s	4.00E + 01
n.cycles		20	τ.EET2	s	6.00E + 01
τ.ATP1	s	4.00E + 01	τ.EET3	s	3.00E + 02
τ.ATP2	s	5.00E + 01	κ.EET1	1/s	2.00E − 01
τ.ATP3	s	3.00E + 02	κ.EET2	1/s	2.00E + 00
κ.ATP1	1/s	2	NO.0	μM	0
κ.ATP2	1/s	2	NO.1	μM	0
βA.0	μM	0.00E + 00	τ.NO1	s	4.00E + 01
βA.1	μM	0	τ.NO2	s	5.00E + 01
τ.βA1	s	4.00E + 01	τ.NO3	s	3.00E + 02
τ.βA2	s	5.00E + 01	κ.NO1	1/s	2
τ.βA3	s	3.00E + 02	κ.NO2	1/s	2

The values shown are for application of intravascular pressure (BP) alone; the concentrations of all other effectors are zero. For each effector, X, two concentrations are given, X.0, the initial and base concentration, and X.1, the second concentration. X.0 is applied from t = 0 to t = τ.X1, when the concentration rises (or falls) to X.1 with a rate constant of κ.X1 until t = τ.X2. The concentration of X remains constant from τ.X2 to τX3, when it begins to fall (or rise) to X.0 with a rate constant of κ.X2. One or more effectors can be thus added in the same run. In addition, multiple consecutive runs with different concentrations of any one of the effectors are initiated with a vector of consecutive concentrations of the effector (see supplementary equations, section A). All other effector parameters remain the same for each of these runs. For pulsatile addition of any effector, the first pulse starts at t = τ.pulse_init, and each pulse is on for Δτ.pulse_on, off for Δτ.pulse_off, and repeated n.cycles times.

[a]Text preceded by a period in the table is subscripted in the program.

TABLE S2

Means of selected variables from 250 to 300 s in a run with normal parameters

bp	mm Hg	10	20	40	60	80	100
Variables	Units						
V.m	mV	−6.17E + 01	−5.92E + 01	−5.18E + 01	−4.53E + 01	−4.05E + 01	−3.73E + 01
Ca.in	μM	1.22E − 01	1.32E − 01	1.63E − 01	1.95E − 01	2.21E − 01	2.38E − 01
Ca.NSCstr	μM	1.51E − 01	2.04E − 01	3.60E − 01	5.32E − 01	6.83E − 01	8.12E − 01
Ca.jun	μM	2.37E − 01	3.63E − 01	5.11E − 01	7.00E − 01	8.41E − 01	9.17E − 01
Ca.SRper	μM	1.35E + 02	1.13E + 02	9.99E + 01	8.23E + 01	7.21E + 01	6.72E + 01
Ca.SRcen	μM	1.41E + 02	1.24E + 02	1.17E + 02	1.08E + 02	1.03E + 02	1.01E + 02
Cl.in	mM	6.19E + 01	6.16E + 01	6.02E + 01	5.65E + 01	5.21E + 01	4.86E + 01
K.in	mM	1.49E + 02	1.48E + 02	1.46E + 02	1.41E + 02	1.36E + 02	1.31E + 02
Na.in	mM	9.65E + 00	9.69E + 00	9.69E + 00	9.84E + 00	1.01E + 01	1.03E + 01
I.BK_ALL[a]	pA	3.10E − 02	1.40E − 01	1.09E + 00	2.34E + 00	3.79E + 00	4.67E + 00
I.CaV_ALL[a]	pA	−3.33E − 01	-4.70E − 01	−9.45E − 01	−1.64E + 00	−2.36E + 00	−2.89E + 00
I.ClA	pA	−1.23E − 01	−2.76E − 01	−1.24E + 00	−3.30E + 00	−5.52E + 00	−7.11E + 00
I.Kv	pA	3.80E − 02	8.97E − 02	3.92E − 01	1.13E + 00	2.11E + 00	2.84E + 00
I.NSCstr_ALL[b]	pA	−1.35E − 02	−3.33E − 02	−9.08E − 02	−1.55E − 01	−2.10E − 01	−2.61E − 01
I.NSCne_ALL[b]	pA	−2.12E − 01	−2.27E − 01	−2.60E − 01	−2.77E − 01	−2.79E − 01	−2.75E − 01
I_KATP_ALL[a]	pA	1.96E − 01	2.24E − 01	3.01E − 01	3.65E − 01	4.06E − 01	4.29E − 01
I.Ca_leak	pA	−1.87E − 01	−1.80E − 01	−1.59E − 01	−1.41E − 01	−1.28E − 01	−1.20E − 01
I.Cl_leak	pA	−2.72E − 01	−2.31E − 01	−2.48E − 01	−1.68E − 01	−1.57E − 01	−9.06E − 02
I.K_leak	pA	4.70E − 02	2.80E − 02	1.14E − 01	1.03E − 01	1.48E − 01	1.19E − 01
I.NaK	pA	7.21E − 01	7.57E − 01	8.46E − 01	9.79E − 01	1.13E + 00	1.27E + 00
I.PMCA	pA	1.93E − 01	2.54E − 01	4.84E − 01	8.34E − 01	1.20E + 00	1.49E + 00
I.NCX	pA	−8.56E − 02	−8.99E − 02	−9.89E − 02	−9.38E − 02	−7.95E − 02	−6.49E − 02
I.NaK_Cl[c]	pA	3.33E + 00	3.39E + 00	3.74E + 00	4.54E + 00	5.58E + 00	6.51E + 00
I.IP3R_ALL[a]	pA	− 3.47E − 02	−3.28E − 02	−4.75E − 02	−5.83E − 02	−6.77E − 02	−7.44E − 02
I.RyR_jun_ALL[a]	pA	−1.79E − 02	−3.56E − 02	−5.45E − 02	−7.80E − 02	−9.58E − 02	−1.05E − 01
I.SERCA_ALL[a]	pA	2.63E − 02	3.50E − 02	5.00E − 02	6.82E − 02	8.16E − 02	8.96E − 02
PLC_PIP	#	4.62E + 02	4.62E + 02	4.62E + 02	4.62E + 02	4.62E + 02	4.62E + 02
IP3	μM	1.70E − 01	1.70E − 01	1.70E − 01	1.70E − 01	1.70E − 01	1.70E − 01
DAG	μM	1.70E − 01	1.70E − 01	1.70E − 01	1.70E − 01	1.70E − 01	1.70E − 01
cGMP	μM	2.12E − 01	2.12E − 01	2.12E − 01	2.12E − 01	2.12E − 01	2.12E − 01
AC0	#	5.99E + 03	5.99E + 03	5.99E + 03	5.99E + 03	5.99E + 03	5.99E + 03
AC_p	#	1.00E + 01	1.00E + 01	1.00E + 01	1.00E + 01	1.00E + 01	1.00E + 01
cAMP	μM	2.12E − 01	2.12E − 01	2.12E − 01	2.12E − 01	2.12E − 01	2.12E − 01
PDE_cA	μM	9.92E − 03	9.92E − 03	9.92E − 03	9.92E − 03	9.92E − 03	9.92E − 03
PDE_cA_P	μM	7.72E − 05	7.72E − 05	7.72E − 05	7.72E − 05	7.72E − 05	7.72E − 05
PDE_cG	μM	9.92E − 03	9.92E − 03	9.92E − 03	9.92E − 03	9.92E − 03	9.92E − 03
PDE_cG_P	μM	7.72E − 05	7.72E − 05	7.72E − 05	7.72E − 05	7.72E − 05	7.72E − 05
relPKA	none	2.80E − 03	2.80E − 03	2.80E − 03	2.80E − 03	2.80E − 03	2.80E − 03
relPKG	none	4.99E − 03	4.99E − 03	4.99E − 03	4.99E − 03	4.99E − 03	4.99E − 03
relPKC	none	6.86E − 02	7.70E − 02	1.01E − 01	1.24E − 01	1.40E − 01	1.49E − 01
relPKC	none	9.11E − 02	9.11E − 02	9.11E − 02	9.11E − 02	9.11E − 02	9.11E − 02
BK	#	1.29E + 03	1.29E + 03	1.24E + 03	1.21E + 03	1.20E + 03	1.20E + 03
BK_PKA	#	3.61E + 00	3.60E + 00	3.45E + 00	3.39E + 00	3.36E + 00	3.35E + 00
BK_PKC	#	1.92E + 02	1.96E + 02	2.48E + 02	2.71E + 02	2.82E + 02	2.87E + 02
BK_PKG	#	1.29E + 01	1.29E + 01	1.23E + 01	1.21E + 01	1.20E + 01	1.20E + 01
CaV	#	2.78E + 03	2.76E + 03	2.70E + 03	2.65E + 03	2.61E + 03	2.59E + 03
CaV_PKC	#	1.91E + 02	2.12E + 02	2.73E + 02	3.27E + 02	3.64E + 02	3.86E + 02
CaV_PKG	#	2.78E + 01	2.76E + 01	2.70E + 01	2.64E + 01	2.60E + 01	2.58E + 01
NaKCl	#	9.36E + 03	9.29E + 03	9.09E + 03	8.91E + 03	8.78E + 03	8.71E + 03
NaKCl_PKC	#	6.38E + 02	7.10E + 02	9.12E + 02	1.09E + 03	1.22E + 03	1.29E + 03
NSCstr	#	2.52E + 02	2.49E + 02	2.44E + 02	2.42E + 02	2.42E + 02	2.41E + 02
NSCstr_PKC	#	6.95E + 00	9.64E + 00	1.41E + 01	1.61E + 01	1.69E + 01	1.73E + 01
NSCstr_PKG	#	2.51E + 00	2.48E + 00	2.44E + 00	2.42E + 00	2.41E + 00	2.41E + 00

bp	mm Hg	10	20	40	60	80	100
PP_NaKCl	#	9.92E + 03	9.92E + 03	9.92E + 03	9.92E + 03	9.92E + 03	9.92E + 03
PP_P_NaKCl	#	7.73E + 01	7.73E + 01	7.73E + 01	7.73E + 01	7.73E + 01	7.73E + 01
IP3R	#	1.99E + 03	1.99E + 03	1.99E + 03	1.99E + 03	1.99E + 03	1.99E + 03
IP3R_IRAG_PKG	#	9.93E + 00	9.93E + 00	9.93E + 00	9.93E + 00	9.93E + 00	9.93E + 00
SERCA	#	9.29E + 02	9.22E + 02	9.02E + 02	8.84E + 02	8.72E + 02	8.64E + 02
SERCA_P	#	7.10E + 01	7.81E + 01	9.82E + 01	1.16E + 02	1.28E + 02	1.36E + 02
KATP	#	1.55E + 02	1.55E + 02	1.55E + 02	1.55E + 02	1.55E + 02	1.55E + 02
KATP_PKA	#	4.24E + 00	4.24E + 00	4.24E + 00	4.24E + 00	4.24E + 00	4.24E + 00
KATP_PKC	#	1.41E + 02	1.41E + 02	1.41E + 02	1.41E + 02	1.41E + 02	1.41E + 02

#, the number of molecules.
[a]ALL here indicates the sum of the currents conducted by dephosphorylated and all phosphorylated species.
[b]ALL here indicates the sum of all ionic currents.
[c]Just the Cl current; the total current carried by NaKCl is zero.

TABLE S3
Determinants of oscillations

Parameter/Variable	Normal value	Altered value	I.RyR_ALL, Ca. jun, Ca.SRper	I.BK_ALL, V.m, I.CaV_ALL
			Frequency[a]	Frequency[a]
			(1/s)	(1/s)
NORM			2.9	2.9
I.SERCA_max	0.8 pA	0.64 pA	2.2	2.2
I.SERCA_max	0.8 pA	0.96 pA	3.3	3.3
Ca.SRcen	variable	97.2 µM	0	0
Ca.SRcen	variable	108 µM	3.0	3.0
Ca.SRcen	variable	118.8 µM	5.3	5.3
Ca.SRcen	variable	129.6 µM	0	0
Ca.SRper	variable	65.8 µM	0	0
Ca.SRper	variable	82.3 µM	0	0
Ca.SRper	variable	98.8 µM	0	0
VOL.SRper	0.56 fL	0.45 fL	3.1	3.1
VOL.SRper	0.56 fL	0.67 fL	2.8	2.8
RyR.T	3,000 #/cell	3,600 #/cell	3.9	3.9
RyR.T	3,000 #/cell	3,300 #/cell	3.4	3.4
RyR.T	3,000 #/cell	2,700 #/cell	2.3	2.3
RyR.T	3,000 #/cell	2,400 #/cell	0	0
K.RyR_Ca_min; …_max	4 µM; 10 µM	6.0 µM	5.4	5.4
K.RyR_Ca_min; …_max	4 µM; 10 µM	7.5 µM	2.2	2.2
K.RyR_Ca_min; …_max	4 µM; 10 µM	9.0 µM	0	0
Ca.jun input to RyR	variable	0.56 µM	0	0
Ca.jun activation of RyR	variable	0.7 µM	0	0
Ca.jun activation of RyR	variable	0.84 µM	0	0
K.RyR_Ca_inh	3 µM	2.4 µM	3.1	3.1
K.RyR_Ca_inh	3 µM	3.6 µM	2.9	2.9
K.RyR_Ca_inh	3 µM	100 µM	2.8	2.8
VOL.jun	0.13 fL	0.104 fL	3.2	3.2
VOL.jun	0.13 fL	0.156 fL	2.6	2.6
Ca.jun_fixed input to BK	variable	0.56 µM	4.8	0
Ca.jun_fixed input to BK	variable	0.7 µM	4.0	0
Ca.jun_fixed input to BK	variable	0.84 µM	2.8	0

[a]Frequency in the interval from 150 to 155 s during a 300-s simulation at 60 mm Hg.

TABLE S4

Fractional changes in V_m, Ca_{in}, and individual components per change in parameter

Parameter	<V.m>	<Ca.in>	Local output	Local output
	Fractional changes[a]	Fractional changes[a]		Fractional changes[b]
	(1/mV)	(1/mV)		(1/mV)
V.Kv	0.59%	0.70%	I.Kv	8.13%
V.ClA	0.53%	0.58%	I.ClA	3.42%
V.CaV_act	0.66%	3.14%	I.CaV_ALL	10.16%
V.BK_closed	0.11%	0.05%	I.BK_ALL	3.11%
V.BK_open	0.34%	0.27%	I.BK_ALL	4.08%

[a]V.m and Ca.in were simulated at six intravascular pressures with the parameters increased and decreased by 2 mV to obtain the perturbed values. The mean of the six values of {|(z.perturbed − z.normal)/z.normal|}/2, where z is either V.m or Ca.in, was calculated. The average of the means for 2 and −2 mV are presented.

[b]As in footnote a, except that z is the value of the individual component dependent on the parameter.

TABLE S5

Dose–response parameters for αA, αA + ATP, βA, EET, and NO

Effectors	Frequency	Variable (Z)	EC_{50}	Z_{inf}-Z_0	*n*
	hz		*μM*	*mV or μM*	
αA	steady	V	0.27	15.1	1.36
		Ca.in	0.41	0.103	1.20
αA+ATP	steady	V	0.20	14.9	1.28
		Ca.in	0.22	0.100	1.26
αA	0.1	V	2.73	12.3	1.46
		Ca.in	2.79	0.065	1.52
αA	0.2	V	1.67	14.4	1.34
		Ca.in	2.22	0.092	1.29
αA	0.4	V	0.93	15.3	1.30
		Ca.in	1.30	0.101	1.24
αA+ATP	0.1	V	1.59	11.2	1.33
		Ca.in	1.68	0.079	1.36
αA+ATP	0.2	V	1.16	14.0	1.42
		Ca.in	1.25	0.103	1.23
αA+ATP	0.4	V	0.72	15.1	1.39
		Ca.in	0.73	0.103	1.25
βA	steady	V	0.83	−15.1	1.21
		Ca.in	0.57	−0.064	1.23
EET	steady	V	0.54	−20.0	1.45
		Ca.in	0.24	−0.057	1.39
NO	steady	V	0.46	−8.7	0.81
		Ca.in	0.40	−0.046	0.79

Parameters of the Hill equation, $\Delta Z = \Delta Z_{inf} a^n/(Q^n + a^n)$, where $\Delta Z = Z - Z_0$, Z_0 = variable at 0 effector, Z_{inf} = variable at infinite effector concentration, a = [agonist], Q = EC50, and *n* = the Hill coefficient, were obtained by a nonlinear least-squares error fit of simulated data (see Fig. 6).

Table S6 is available as a Word document.

Model equations (Mathcad program) are available in a PDF file.

A PDF file of reaction schemes for *α*-adrenergic signaling, *β*-adrenergic signaling, NaKCl cotransporter, NCX exchanger, and P2XR is also available.

Table S6
Normal parameters

Parameter	Units	Values	Notes
t1	s	300	0 to t1 is solution interval.
N1		12000	Number of points saved for calculations and plotting.
TOL		1.00E-05	Precision of derivatives and integrals; convergence criterion in a solve block.
CTOL		1.00E-03	Criterion for acceptable deviation from a constraint in a solve block.
a	s	250	Start-time of means.
b	s	300	End-time of means.
αAR			
αAR.T	#/cell	6.00E+03	Calculated from ~100 fmol/mg protein in rat aorta (Faber et al., 2001).
k.αAR_on	1/(μM*s)	1.00E+00	From k.αAR_off/ k.αAR_on = 10 μM (Bennett et al., 2005).
k.αAR_off	1/s	1.00E+01	From k.αAR_off/ k.αAR_on = 10 μM (Bennett et al., 2005).
k.αAR_P	1/s	2.00E-02	0.1 (Bennett et al., 2005).
k.αAR_endo	1/s	2.00E-02	0.006 in ref (Bennett et al., 2005).
k.αAR_recyc	1/s	1.00E-02	(Schofl et al., 1993).
AC			
AC.T	#	6.00E+03	Assume AC.T = βAR.T.
k.AC0_Gs_on	cell/(#*s)	4.00E-05	Local fit[c] of βAR dose response (Garland et al., 2011).
k.AC1_Gs_off	1/s	5.00E-01	Local fit of βAR dose response.
k.AC1_ATP	1/s	2.00E+02	From ~100/s (Dessauer and Gilman, 1997)
k.PKA_AC	1/s	1.00E-02	Local fit of βAR dose response.
k.PP_AC	1/s	1.00E-02	Local fit of βAR dose response.
k.AC0_ATP	1/s	1.00E-01	Compatible with basal [cAMP] = ~0.2 μM in PKA microdomain (Iancu et al., 2008).
βAR			
βAR.T	#/cell	6.00E+03	Assume = alphaR.T.
k.βAR_on	1/(μM*s)	2.00E-01	Local fit (Garland et al., 2011).
k.βAR_off	1/s	4.00E+00	Local fit.
k.βAR_P	1/s	4.00E-03	Local fit.
k.βAR_endo	1/s	4.00E-03	Local fit.
k.βAR_recyc	1/s	4.00E-03	Local fit.
BK			
BK.T	#/cell	1.50E+03	Global fit[b]; ~3000 channels per cell (Wellman and Nelson, 2003).
perm.BK	cm^3/(#*s)	4.00E-13	From γ = 212 pS in symmetrical 140 mM K^+ (Mistry and Garland, 1998).
K.BK_closed	μM	4.72E+00	(Bao and Cox, 2005)
K.BK_open	μM	8.00E-01	(Bao and Cox, 2005)
V.BK_open	mV	-3.40E+01	(Bao and Cox, 2005)
V.BK_closed	mV	8.00E+01	(Bao and Cox, 2005)
z.BK_J	alg. chrg	5.70E-01	(Bao and Cox, 2005)
z.BK_L	alg. chrg	4.10E-01	(Bao and Cox, 2005)
L.BK	none	2.50E-06	(Bao and Cox, 2005)
L.BK_PKA	none	7.50E-06	Hypothetical.[d]
L.BK_PKC	none	8.33E-07	Hypothetical.

L.BK_PKG	none	7.50E-06	Hypothetical.
k.PKA_BK	1/s	2.00E+01	Hypothetical.
k.PKC_BK	1/s	2.00E+01	Hypothetical.
k.PKG_BK	1/s	4.00E+01	Hypothetical.
k.PP_BK	1/s	2.00E+01	Hypothetical.
CaV			
CaV.T	#/cell	3.00E+03	Global fit.
perm.CaV	$cm^3/(\#*s)$	1.21E-13	From γ = 3.5 pS at 2 mM Ca^{2+} externally (Rubart et al., 1996).
V.CaV_act	mV	6.20E+00	(Rubart et al., 1996)
ξ.CaV_act	mV	9.30E+00	(Rubart et al., 1996)
V.CaV_PKC_act	mV	1.20E+00	Hypothetical.
V.CaV_PKG_act	mV	1.12E+01	Hypothetical.
K.CaV_inh	μM	1.20E-00	Global fit.
k.PKC_CaV	1/s	2.00E+01	Hypothetical.
k.PKG_CaV	1/s	4.00E+01	Hypothetical.
k.PP_CaV	1/s	2.00E+01	Hypothetical.
Cl.A=Cl(Ca)			
Cl.AT	#/cell	2.50E+03	Global fit.
perm.ClA	$cm^3/(\#*s)$	1.60E-14	From γ = 8.3 pS with symmetrical 140 mM Cl^- (Yang et al., 2008).
zeta.ClA	alg. chrg.	2.00E+00	Local fit (Yang et al., 2008).
V.ClA	mV	0.00E+00	Local fit.
K.ClA_Ca_act_max	μM	4.10E+00	Local fit.
K.ClA_Ca_act_min	μM	3.00E-01	Local fit.
K.ClA_Ca_inh	μM	4.00E+01	Local fit.
n.ClA	none	2.60E+00	Local fit.
G.q			
G.qT	#/cell	6.00E+03	Assumed equal to αAR.T
k.Gq0_GDP_αAR_on	cell/(#*s)	2.00E-05	Local fit to obtain αR dose-response (Bennett et al., 2005).
k.Gq1_GDP_αAR_off	1/s	1.00E+00	Local fit to obtain αR dose-response.
k.Gq1_GDP_GTP_exch	1/s	1.00E+00	Local fit to obtain αR dose-response.
k.Gq_GTPase	1/s	5.00E-02	Local fit to obtain αR dose-response.
G.s			
G.sT	#/cell	6.00E+03	Assumed equal to βAR.T
k.Gs0_GDP_βAR_on	cell/(#*s)	1.00E-05	Local fit to obtain βR dose-response.
k.Gs1_GDP_βAR_off	1/s	5.00E-01	Local fit to obtain βR dose-response.
k.Gs1_GDP_GTP_exch	1/s	1.00E+00	Local fit to obtain βR dose-response.
k.Gs_GTPase	1/s	5.00E-02	Local fit to obtain βR dose-response.
IP3R			
IP3.T	#/cell	2.00E+03	Global fit.
perm.IP3R	$cm^3/(s*\#)$	1.10E-13	From γ = 80 pS in symmetrical 50 mM Ba^{2+} (Tu et al., 2005).
K.IP3R_IP3	μM	3.50E-01	~0.3 μM (IP3R type 1) (Narayanan et al., 2012).
K.IP3R_IRAG_PKG_IP3	μM	8.00E-01	Hypothetical.
n.IP3R_IP3	none	3.00E+00	Hypothetical.
K.IP3R_Ca_max	μM	1.00E+00	Hypothetical.
K.IP3R_Ca_min	μM	1.00E-01	~0.2 μM (Narayanan et al., 2012)
K.IP3R_Ca_inh	μM	3.00E-01	~0.4 μM (Narayanan et al., 2012)
n.IP3R_Ca_inh	none	2.50E+00	Hypothetical.
K.IP3R_CaSR	μM	1.40E+02	Hypothetical.

n.IP3R_CaSR	none	2.50E+00	Hypothetical.
n.IP3R_Ca_act	none	3.00E+00	Hypothetical.
k.PKG_IP3R_IRAG	1/s	2.00E+01	Hypothetical.
k.PP_IP3R_IRAG_PKG	1/s	2.00E+01	Hypothetical.
KATP			
KATP.T	#/cell	3.00E+02	Global fit. Upper limit ~500/cell (Quayle et al., 1997).
P.open_KATP	none	5.00E-03	Hypothetical.
P.open_KATP_PKA	none	1.20E-01	Hypothetical.
k.PKA_KATP	1/s	2.00E+00	Hypothetical.
k.PKCε_KATP	1/s	2.00E+00	Hypothetical.
k.PP_KATP_PKA	1/s	2.00E-01	Hypothetical.
k.PP_KATP_PKCε	1/s	2.00E-01	Hypothetical.
perm.KATP	$cm^3/(\#*s)$	7.00E-14	From γ = 35 pS in symmetrical 140 mM KCl (Quayle et al., 1997).
Kv			
Kv.T	#/cell	2.70E+02	Global fit.
perm.Kv	$cm^3/(\#*s)$	2.50E-14	From γ = 12 pS ,130 mM KCl inside, 3.5 mM outside (Kwan et al., 2006).
V.Kv	mV	-2.00E+01	(Ledwell and Aldrich, 1999; Zhang et al., 2001)
ξ.Kv	mV	7.00E+00	(Ledwell and Aldrich, 1999)
LEAKS			
Na.leakT	#/cell	0.00E+00	Global fit.
perm.Na_leak	$cm^3/(s*\#)$	1.00E-15	Hypothetical.
K.leakT	#/cell	2.00E+01	Global fit.
perm.K_leak	$cm^3/(s*\#)$	1.00E-15	Hypothetical.
Cl.leakT	#/cell	2.20E+01	Global fit.
perm.Cl_leak	$cm^3/(s*\#)$	1.00E-15	Hypothetical.
Ca.leakT	#/cell	1.30E+01	Global fit.
perm.Ca_leak	$cm^3/(s*\#)$	1.00E-14	Hypothetical.
NaK			
I.NaKmax	pA/cell	6.00E+01	2.3 A/Farad * 25 pFarad/cell (Kapela et al., 2008).
K.NaK_Kex	mM	1.60E+00	(Kapela et al., 2008)
K.NaK_Nain	mM	2.20E+01	(Kapela et al., 2008)
n.NaK_Na	none	2.50E+00	Adjusted from 1.7 (Kapela et al., 2008).
n.NaK_K	none	1.10E+00	(Kapela et al., 2008)
Δμ..ATP	J/mol	-5.00E+04	(Bergman, 2010)
NaKCl			
NaKCl.T	#/cell	1.00E+04	Global fit.
L.NaKCl_Na	mM	3.20E+01	Adjusted from 18 mM (Somasekharan et al., 2012).
L.NaKCl_K	mM	2.70E+01	Adjusted from 1.6 mM (Somasekharan et al., 2012).
L.NaKCl_Cl	mM	6.30E+01	Adjusted from 48 mM (Somasekharan et al., 2012).
α.NaKCl_4	1/s	5.00E+04	Hypothetical. Note that α.NaKCl_0 = β.NaKCl_0*α.NaKCl_4/β.NaKCl_4.
β.NaKCl_0	1/s	5.00E+04	Hypothetical.
β.NaKCl_4	1/s	4.00E+04	Hypothetical.
ε.NaKCl_PKC	none	2.00E+00	Hypothetical.
k.PKC_NaKCl	1/s	2.00E+01	Hypothetical.
PP.NaKCl_T	#/cell	1.00E+04	Assumed in 1:1 complex with NaKCl.T
k.PP_NaKCl	1/s	2.00E+01	Hypothetical.

k.PP_P_NaKCl	1/s	4.00E+01	Hypothetical.
k.PKA_PP_NaKCl	1/s	2.00E+01	Hypothetical.
k.PKG_PP_NaKCl	1/s	2.00E+01	Hypothetical.
k.PP_PP_NaKCl	1/s	2.00E+01	Hypothetical.
NCX			
NCX.T	#/cell	1.60E+03	Global fit.
K.NCX_Na	mM	1.00E+02	Hypothetical. 30 mM = ~(k.n1*k.n2*k.n3)^0.33 (Kang and Hilgemann, 2004)
K.NCX_Ca	µM	8.00E-02	Hypothetical. ~3 µM (Kang and Hilgemann, 2004)
α.NCX_0	1/s	3.00E+04	Hypothetical.
α.NCX_4	1/s	3.00E+04	(Kang and Hilgemann, 2004)
β.NCX_4	1/s	5.00E+04	Hypothetical.
K.NCX_act_Ca	µM	1.00E-01	Comparable parameter ~0.15 – 0.4 µM (Reeves et al., 2007).
n.NCX_act	none	2.00E+00	(Reeves et al., 2007)
NSCeet			
NSCeet.T	#/cell	4.00E+01	Global fit.
perm.NaNSCeet	cm^3/(#*s)	1.30E-13	Assumed equal to perm.KNSCeet.
perm.KNSCeet	cm^3/(#*s)	1.30E-13	From γ = 45 pS , symmetrical 98 mM KCl (Loukin et al., 2010).
perm.CaNSCeet	cm^3/(#*s)	9.00E-13	Based on p.Ca/p.Na = 6.9 (Voets et al., 2002).
K.NSCeet_EET	µM	5.00E-02	Local fit (Earley et al., 2005).
n.NSCeet	none	1.00E+00	Local fit (Earley et al., 2005).
V.NSCeet_min	mV	-1.00E+01	Local fit (Loukin et al., 2010)
V.NSCeet_max	mV	50	Local fit (Loukin et al., 2010)
ξ.NSCeet	mV	1.00E+01	Local fit (Loukin et al., 2010)
NSCne			
NSCne.T	#/cell	3.10E+01	Global fit.
perm.NaNSCne	cm^3/(#*s)	3.30E-14	From γ = 15 pS , symmetrical 126 mM Na^+/Cs^+ (Saleh et al., 2006).
perm.KNSCne	cm^3/(#*s)	3.30E-14	Assumed equal to perm.NaNSCne.
perm.CaNSCne	cm^3/(#*s)	1.50E-13	p.Ca/p.Na = 4.54 (Kapela et al., 2008).
K.NSCne_DAG	µM	1.20E+00	Hypothetical.
K.NSCne_Ca_act	µM	2.00E-01	Hypothetical.
K.NSCne_Ca_inh	µM	1.00E+00	Hypothetical.
n.NSCne	none	2.00E+00	Hypothetical.
NSCstr			
NSCstr.T	#/cell	2.61E+02	Global fit.
perm.NaNSCstr	cm^3/(#*s)	3.30E-14	Assumed to equal perm.NaNSCne
perm.KNSCstr	$cm^3$3/(#*s)	3.30E-14	Assumed to equal perm.KNSCne
perm.CaNSCstr	cm^3/(#*s)	1.50E-13	Assumed to equal perm.CaNSCne
bp.50	mm Hg	3.00E+02	Global fit.
K.NSCstr_DAG	µM	1.38E+00	Global fit.
K.NSCstr_Ca_act	µM	1.70E+00	Global fit.
K.NSCstr_Ca_inh	µM	1.00E+02	Global fit.
n.NSCstr_DAG	none	2	Global fit.
n.NSCstr_Ca	none	1.00E+00	Global fit.
n.NSCstr_bp	none	1.00E+00	Global fit.
K.NSCstr_PKC_Ca_act	µM	1.00E+00	Hypothetical.
K.NSCstr_PKG_Ca_act	µM	4.00E+00	Hypothetical.
k.PKC_NSCstr	1/s	3.00E+00	Hypothetical.

k.PKG_NSCstr	1/s	2.00E+01	Hypothetical.
k.PP_NSCstr		1.00E+01	Hypothetical.
PDE			
k.PKA_PDE	1/s	1.00E+01	Hypothetical.
k.PKG_PDE	1/s	1.00E+01	Hypothetical.
k.PP_PDE	1/s	1.00E+01	Hypothetical.
n.PDE	none	1.00E+00	Hill coefficient for activation of both PDEs
PDE.cAMP_T	μM	1.00E-02	Hypothetical.
K.PDE_cAMP	μM	8.00E+00	Hypothetical.
K.PDE_cAMP_P	μM	3.00E+00	Hypothetical.
k.PDE_cAMP	1/(μM*s)	1.00E+01	Hypothetical.
PDE.cGMP_T	μM	1.00E-02	Hypothetical.
K.PDE_cGMP	μM	8.00E+00	Hypothetical.
K.PDE_cGMP_P	μM	3.00E+00	Hypothetical.
k.PDE_cGMP	1/(μM*s)	1.00E+01	Hypothetical.
PKA_PKC_PKG_PKCe			
K.PKA_cAMP	μM	4.00E+00	In the range between basal and stimulated [cAMP] (Gesellchen et al., 2006).
n.PKA_cAMP	none	2.00E+00	Hill coefficient for activation. 1.6 in (Herberg et al., 1994).
K.PKC_DAG	μM	5.00E-01	
K.PKC_Ca	μM	2.00E-01	
n.PKC_Ca	none	2.00E+00	Added 6/3/13 to SM model 61.
K.PKG_cGMP	μM	3.00E+00	
n.PKG_cGMP	none	2.00E+00	Hill coeff for activation
K.PKCε_DAG	μM	1.70E+00	
K.PKD_DAG	μM	1.70E+00	
PLC			
PLC.T	#/cell	6.00E+03	Assumed equal to αAR.T.
k.PLC_PIP_on	cell/(#*s)	1.00E-06	Hypothetical basal rate. PLC is assumed to be membrane-bound.
k.PLC_PIP_off	1/s	1.00E+02	Hypothetical basal rate.
k.PLC_PIP_hyd	1/s	2.00E+01	Hypothetical basal rate.
k.PLC_Gq0_GTP_on	cell/(#*s)	2.00E-04	Local fit (Waldo et al., 2010). Both PLC and G_q are assumed to be membrane-bound and to diffuse and collide in two dimensions.
k.PLC_Gq0_GTP_off	1/s	2.00E-02	Local fit (Waldo et al., 2010).
k.PLC_Gq0_GTP_hyd	1/s	1.00E-01	Hypothetical.
k.PLC_Gq0_GTP_PIP_on	cell/(#*s)	3.00E-06	Hypothetical.
k.PLC_Gq0_GTP_PIP_off	1/s	1.00E+01	Hypothetical.
k.PLC_Gq0_GTP_PIP_hyd	1/S	8.00E+01	Hypothetical.
k.PKA_PLC_Gq0_GTP	1/s	1.00E+01	Hypothetical.
k.PKC_PLC_Gq0_GTP	1/S	1.00E+01	Hypothetical.
k.PLC_P_Gq0_GTP_on	cell/(#*s)	5.00E-06	Hypothetical.
k.PLC_P_Gq0_GTP_off	1/s	1	Hypothetical.
k.PP_PLC	1/s	2	Hypothetical.
PIP.T	#/cell	1.00E+07	Global fit.
k.met_DAG	1/s	0.09	Global fit. Unspecified pathway of metabolic removal.
k.met_IP3	1/s	0.09	Global fit. Unspecified pathway of metabolic removal.

PMCA			
I.PMCA_max	pA/cell	1.80E+01	Global fit.
K.PMCA_Ca	μM	4.00E-01	Local fit. (Brini and Carafoli, 2011)
n.PMCA_Ca	none	3.00E+00	Global fit.
P2XR			
P2XR.T	#/cell	1.00E+02	Global fit.
perm.NaP2XR	cm^3/s/cell	4.30E-14	From γ = 20 pS , symmetrical 130 mM Na^+ (Benham and Tsien, 1987).
perm.KP2XR	cm^3/s/cell	4.30E-14	Assumed equal to perm.NaP2XR
perm.CaP2XR	cm^3/s/cell	1.30E-13	p.Ca/p.Na = 3 (Benham and Tsien, 1987).
k.P2XR_0_on	$1/(s*\mu M^{nH)}$	1.00E+01	Local fit. EC50 for ATP = 0.67 μM (Lorinczi et al., 2012).
k.P2XR_3_off	1/s	1.00E+02	Calculated by microscopic reversibility in top cycle of reactions.
n_P2XR	none	2.00E+00	Local fit (Lorinczi et al., 2012).
k.P2XR_3_act	1/s	1.00E+02	Local fit (Lorinczi et al., 2012).
k.P2XR_3_deact	1/s	1.00E+01	Local fit (Lorinczi et al., 2012).
k.P2XR_3_act_desens	1/s	1.00E+00	Local fit. τ.desens ~ 250 ms (Lalo et al., 2011).
k.P2XD_3_resens	1/s	1.00E-02	Local fit.
k.P2XR_0_desens	1/s	1.00E-01	Local fit.
k.P2XD_0_resens	1/s	1.00E+00	Local fit.
k.P2XD_0_on	$1/(s*\mu M^{nH})$	1.00E+01	Local fit.
k.P2XD_3_off	1/s	1.00E-02	Local fit.
k.P2XD_0_PKD_on	$1/(s*\mu M^{nH})$	1.00E+00	Hypothetical.
k.P2XD_3_PKD_off	1/s	1.00E+00	Hypothetical.
k.PKD_P2XD_3	1/s	1.00E+00	Hypothetical.
k.PP_P2XD_0_PKD	1/s	1.00E+00	Hypothetical.
RyR.jun			
RyR.T	#/cell	3.00E+03	Global fit. ~15 per junction (Lifshitz et al., 2011).
perm.RyR	$cm^3/(s*\#)$	2.00E-13	From γ = 150 pS in symmetrical 50 mM Ca^{2+} (Meissner, 2004).
K.RyR_Ca_SR	μM	8.00E+02	Hypothetical.
n.RyR_Ca_SR	none	5.00E-01	Hypothetical.
K.RyR_Ca_jun_max	μM	1.00E+01	EC50_Ca.cyt ~ 10 μM (Guo et al., 2012).
K.RyR_Ca_jun_min	μM	4.00E+00	Hypothetical.
n.RyR_Ca_jun	none	2.00E+00	Hypothetical.
K.RyR_Ca_inh	μM	3.00E+00	Hypothetical. Assumed that RyR is saturated with calmodulin (Xu and Meissner, 2004).
n.RyR_Ca_inh	none	3.00E+00	Hypothetical.
k.PKA_RyR	1/s	4.00E+01	Hypothetical.
k.PKC_RyR	1/s	4.00E+01	Hypothetical.
k.PP_RyR	1/s	4.00E+01	Hypothetical.
f.RyR_PKA_min	none	4.00E-01	Hypothetical.
f.RyR_PKC_max	none	5.00E+00	Hypothetical.
SERCA			
SERCA.T	#/cell	1.00E+03	Arbitrary denominator in fractions of different forms of SERCA.
I.SERCA_max	pA/cell	8.00E-01	Global fit.
K.SERCA_Ca	μM	2.00E-01	0.31 μM for SERCA2a and 0.17 μM for SERCA2b (Missiaen et al., 1991).
n.SERCA	none	1.60E+00	Global fit.
K.SERCA_inh_Ca_SRce	μM	1.00E+02	Global fit.

n

K.SERCA_P_Ca	µM	1.00E-01	Global fit.
k.PKA_SERCA	1/s	2.00E+01	Hypothetical
k.PKC_SERCA	1/s	2.00E+01	Hypothetical
k.PKG_SERCA	1/s	2.00E+01	Hypothetical
k.PP_SERCA	1/s	2.00E+01	Hypothetical
sGC			
GC.T	µM	1.00E-02	
k.GC0_NO_on	1/(µM*s)	3.00E+02	Adjusted from 7E2 (1/(µM*s)) (Yang et al., 2005)
k.GC1_NO_off	1/s	2.00E+02	Adjusted from 1E2 (1/s) (Yang et al., 2005)
k.GC1_NO_on	1/(µM*s)	2.00E+02	Local fit
k.GC2_NO_off	1/s	2.00E+02	Local fit
k.GC1_act	1/s	1.00E+00	Local fit
k.GC1_deact	1/s	1.00E-01	Local fit
k.GC2_act	1/s	1.00E+01	Local fit
k.PKG_GC	1/s	1.00E+01	Hypothetical
k.PP_GC	1/s	1.00E+01	Hypothetical
k.GC_act_GTP	1/s	1.00E+01	Local fit
k.GC_basal_GTP	1/s	1.00E-01	Adjusted to yield basal [cGMP] ~ basal [cAMP] .
CAPAC & VOLS			
C.m	Farads/cell	2.50E-11	(Kapela et al., 2008)
VOL.cell	L/cell	1.00E-12	(Yang et al., 2005)
VOL.SRper	L/cell	5.60E-16	180 peripheral ER discs, radius 100 nm, height 100 nm (Moore et al., 2004)
VOL.jun	L/cell	1.30E-16	180 junctions, radius 100 nm, height 23 nm.
VOL.SRcen	L/cell	7.00E-14	Floyd and Wray (Floyd and Wray, 2007) state 1.5% to 7.5% of cell volume.
VOL.NSCstr	L/cell	6.30E-17	Approx. 260 hemispheres, 49 nm in radius.
BUFFERS			
BUF.T	µM	3.00E+02	Kapela et al: 100 µM calmodulin, 100 µM other Ca buffers
k.BUF_on	1/(µM*s)	2.20E+01	Geometric mean of k.on for calmodulin and calbindin sites (Keller et al., 2008).
k.BUF_off	1/s	7.70E+01	Geometric mean of k.off for calmodulin and calbindin sites (Keller et al., 2008).
BUF.jun_T	µM	3.00E+02	=BUF.T
BUF.NSCstr_T	µM	3.00E+02	=BUF.T
CSQ.SRcen_T	µM	3.00E+02	=BUF.T
CSQ.SRper_T	µM	3.00E+02	=BUF.T
k.CSQ_on	1/(µM*s)	2.00E+00	K.CSQ = 0.8 mM (Sobie et al., 2002)
k.CSQ_off	1/s	1.60E+03	= k.CSQ_on* K.CSQ
INTRACELL FLUX			
λ.jun_cyt	L/s	8.00E-13	Equilibration time-constant = VOL.jun/ λ.jun_cyt = ~160 µs
λ.cen_per	L/s	1.60E-14	Equilibration time-constant = VOL.per/ λ.cen_per = 35 ms
λ.NSCstr_cyt	L/s	4.00E-13	Equilibration time-constant = VOL.NSCstr/ λ.NSCstr_cyt = ~160 µs
IONS & T			
T	^{o}K	3.10E+02	(Knot and Nelson, 1998)
Na.ex	mM	1.43E+02	(Knot and Nelson, 1998)
K.ex	mM	5.90E+00	(Knot and Nelson, 1998)

Ca.ex	μM	1.60E+03	(Knot and Nelson, 1998)
Cl.ex	mM	1.27E+02	(Knot and Nelson, 1998)

Text preceded by a period in the table is subscripted in the program.

[a]$perm_x = RT\gamma_x/(z^2F^2c_x)$, where c_x is concentration of ion species x in mol/cm^3 at which γ_x, the single-channel conductance, was determined; conceptually, $perm_x = p_x/n_x$, where p_x is the permeability (cm/s) of a membrane to x due to a given channel and n_x is the number of these channels per cm^2 of membrane.

[b]Global fit to V.exp and Ca.exp vs pressure (Knot, 1998 #170).

[c]Local fit , at least qualitatively, to similar behavior in the referenced work, given the local model adopted here.

[d]Hypothetical indicates that the value of the parameter yields plausible behavior of the local model.

References

Bao, L., and D.H. Cox. 2005. Gating and ionic currents reveal how the BKCa channel's Ca2+ sensitivity is enhanced by its beta1 subunit. *The Journal of general physiology*. 126:393-412.

Benham, C.D., and R.W. Tsien. 1987. A novel receptor-operated Ca2+-permeable channel activated by ATP in smooth muscle. *Nature*. 328:275-278.

Bennett, M.R., L. Farnell, and W.G. Gibson. 2005. A quantitative description of the contraction of blood vessels following the release of noradrenaline from sympathetic varicosities. *Journal of theoretical biology*. 234:107-122.

Bergman, C., Kashiwaya, Y., and Veech, R.L. 2010. The Effect of pH and Free Mg2+ on ATP Linked Enzymes and the Calculation of Gibbs Free Energy of ATP Hydrolysis. *J. Phys. Chem. B*. 114:16137-16146.

Brini, M., and E. Carafoli. 2011. The plasma membrane Ca(2)+ ATPase and the plasma membrane sodium calcium exchanger cooperate in the regulation of cell calcium. *Cold Spring Harbor perspectives in biology*. 3.

Dessauer, C.W., and A.G. Gilman. 1997. The catalytic mechanism of mammalian adenylyl cyclase. Equilibrium binding and kinetic analysis of P-site inhibition. *The Journal of biological chemistry*. 272:27787-27795.

Earley, S., T.J. Heppner, M.T. Nelson, and J.E. Brayden. 2005. TRPV4 forms a novel Ca2+ signaling complex with ryanodine receptors and BKCa channels. *Circulation research*. 97:1270-1279.

Faber, J.E., N. Yang, and X. Xin. 2001. Expression of alpha-adrenoceptor subtypes by smooth muscle cells and adventitial fibroblasts in rat aorta and in cell culture. *The Journal of pharmacology and experimental therapeutics*. 298:441-452.

Floyd, R., and S. Wray. 2007. Calcium transporters and signalling in smooth muscles. *Cell calcium*. 42:467-476.

Garland, C.J., P.L. Yarova, F. Jimenez-Altayo, and K.A. Dora. 2011. Vascular hyperpolarization to beta-adrenoceptor agonists evokes spreading dilatation in rat isolated mesenteric arteries. *British journal of pharmacology*. 164:913-921.

Gesellchen, F., A. Prinz, B. Zimmermann, and F.W. Herberg. 2006. Quantification of cAMP antagonist action in vitro and in living cells. *European journal of cell biology*. 85:663-672.

Guo, T., D. Gillespie, and M. Fill. 2012. Ryanodine receptor current amplitude controls Ca2+ sparks in cardiac muscle. *Circulation research*. 111:28-36.

Herberg, F.W., W.R. Dostmann, M. Zorn, S.J. Davis, and S.S. Taylor. 1994. Crosstalk between domains in the regulatory subunit of cAMP-dependent protein kinase: influence of amino terminus on cAMP binding and holoenzyme formation. *Biochemistry*. 33:7485-7494.

Iancu, R.V., G. Ramamurthy, S. Warrier, V.O. Nikolaev, M.J. Lohse, S.W. Jones, and R.D. Harvey. 2008. Cytoplasmic cAMP concentrations in intact cardiac myocytes. *American journal of physiology. Cell physiology*. 295:C414-422.

Kang, T.M., and D.W. Hilgemann. 2004. Multiple transport modes of the cardiac Na+/Ca2+ exchanger. *Nature*. 427:544-548.

Kapela, A., A. Bezerianos, and N.M. Tsoukias. 2008. A mathematical model of Ca2+ dynamics in rat mesenteric smooth muscle cell: agonist and NO stimulation. *Journal of theoretical biology*. 253:238-260.

Keller, D.X., K.M. Franks, T.M. Bartol, Jr., and T.J. Sejnowski. 2008. Calmodulin activation by calcium transients in the postsynaptic density of dendritic spines. *PloS one*. 3:e2045.

Knot, H.J., and M.T. Nelson. 1998. Regulation of arterial diameter and wall [Ca2+] in cerebral arteries of rat by membrane potential and intravascular pressure. *The Journal of physiology*. 508 (Pt 1):199-209.

Kwan, D.C., D. Fedida, and S.J. Kehl. 2006. Single channel analysis reveals different modes of Kv1.5 gating behavior regulated by changes of external pH. *Biophysical journal*. 90:1212-1222.

Lalo, U., J.A. Roberts, and R.J. Evans. 2011. Identification of human P2X1 receptor-interacting proteins reveals a role of the cytoskeleton in receptor regulation. *The Journal of biological chemistry*. 286:30591-30599.

Ledwell, J.L., and R.W. Aldrich. 1999. Mutations in the S4 region isolate the final voltage-dependent cooperative step in potassium channel activation. *The Journal of general physiology*. 113:389-414.

Lifshitz, L.M., J.D. Carmichael, F.A. Lai, V. Sorrentino, K. Bellve, K.E. Fogarty, and R. ZhuGe. 2011. Spatial organization of RYRs and BK channels underlying the activation of STOCs by Ca(2+) sparks in airway myocytes. *The Journal of general physiology*. 138:195-209.

Lorinczi, E., Y. Bhargava, S.F. Marino, A. Taly, K. Kaczmarek-Hajek, A. Barrantes-Freer, S. Dutertre, T. Grutter, J. Rettinger, and A. Nicke. 2012. Involvement of the cysteine-rich head domain in activation and desensitization of the P2X1 receptor. *Proceedings of the National Academy of Sciences of the United States of America*. 109:11396-11401.

Loukin, S., X. Zhou, Z. Su, Y. Saimi, and C. Kung. 2010. Wild-type and brachyolmia-causing mutant TRPV4 channels respond directly to stretch force. *The Journal of biological chemistry*. 285:27176-27181.

Meissner, G. 2004. Molecular regulation of cardiac ryanodine receptor ion channel. *Cell calcium*. 35:621-628.

Missiaen, L., H. De Smedt, G. Droogmans, I. Declerck, L. Plessers, and R. Casteels. 1991. Uptake characteristics of the InsP3-sensitive and -insensitive Ca2+ pools in porcine aortic smooth-muscle cells: different Ca2+ sensitivity of the Ca2(+)-uptake mechanism. *Biochemical and biophysical research communications*. 174:1183-1188.

Mistry, D.K., and C.J. Garland. 1998. Nitric oxide (NO)-induced activation of large conductance Ca2+-dependent K+ channels (BK(Ca)) in smooth muscle cells isolated from the rat mesenteric artery. *British journal of pharmacology*. 124:1131-1140.

Moore, E.D., T. Voigt, Y.M. Kobayashi, G. Isenberg, F.S. Fay, M.F. Gallitelli, and C. Franzini-Armstrong. 2004. Organization of Ca2+ release units in excitable smooth muscle of the guinea-pig urinary bladder. *Biophysical journal*. 87:1836-1847.

Narayanan, D., A. Adebiyi, and J.H. Jaggar. 2012. Inositol trisphosphate receptors in smooth muscle cells. *American journal of physiology. Heart and circulatory physiology*. 302:H2190-2210.

Quayle, J.M., M.T. Nelson, and N.B. Standen. 1997. ATP-sensitive and inwardly rectifying potassium channels in smooth muscle. *Physiological reviews*. 77:1165-1232.

Reeves, J.P., M. Condrescu, J. Urbanczyk, and O. Chernysh. 2007. New modes of exchanger regulation: physiological implications. *Annals of the New York Academy of Sciences*. 1099:64-77.

Rubart, M., J.B. Patlak, and M.T. Nelson. 1996. Ca2+ currents in cerebral artery smooth muscle cells of rat at physiological Ca2+ concentrations. *The Journal of general physiology*. 107:459-472.

Saleh, S.N., A.P. Albert, C.M. Peppiatt, and W.A. Large. 2006. Angiotensin II activates two cation conductances with distinct TRPC1 and TRPC6 channel properties in rabbit mesenteric artery myocytes. *The Journal of physiology*. 577:479-495.

Schofl, C., G. Brabant, R.D. Hesch, A. von zur Muhlen, P.H. Cobbold, and K.S. Cuthbertson. 1993. Temporal patterns of alpha 1-receptor stimulation regulate amplitude and frequency of calcium transients. *The American journal of physiology*. 265:C1030-1036.

Sobie, E.A., K.W. Dilly, J. dos Santos Cruz, W.J. Lederer, and M.S. Jafri. 2002. Termination of cardiac Ca(2+) sparks: an investigative mathematical model of calcium-induced calcium release. *Biophysical journal*. 83:59-78.

Somasekharan, S., J. Tanis, and B. Forbush. 2012. Loop diuretic and ion-binding residues revealed by scanning mutagenesis of transmembrane helix 3 (TM3) of Na-K-Cl cotransporter (NKCC1). *The Journal of biological chemistry*. 287:17308-17317.

Tu, H., Z. Wang, and I. Bezprozvanny. 2005. Modulation of mammalian inositol 1,4,5-trisphosphate receptor isoforms by calcium: a role of calcium sensor region. *Biophysical journal*. 88:1056-1069.

Voets, T., J. Prenen, J. Vriens, H. Watanabe, A. Janssens, U. Wissenbach, M. Bodding, G. Droogmans, and B. Nilius. 2002. Molecular determinants of permeation through the cation channel TRPV4. *The Journal of biological chemistry*. 277:33704-33710.

Waldo, G.L., T.K. Ricks, S.N. Hicks, M.L. Cheever, T. Kawano, K. Tsuboi, X. Wang, C. Montell, T. Kozasa, J. Sondek, and T.K. Harden. 2010. Kinetic scaffolding mediated by a phospholipase C-beta and Gq signaling complex. *Science*. 330:974-980.

Wellman, G.C., and M.T. Nelson. 2003. Signaling between SR and plasmalemma in smooth muscle: sparks and the activation of Ca2+-sensitive ion channels. *Cell calcium*. 34:211-229.

Xu, L., and G. Meissner. 2004. Mechanism of calmodulin inhibition of cardiac sarcoplasmic reticulum Ca2+ release channel (ryanodine receptor). *Biophysical journal*. 86:797-804.

Yang, J., J.W. Clark, R.M. Bryan, and C.S. Robertson. 2005. Mathematical modeling of the nitric oxide/cGMP pathway in the vascular smooth muscle cell. *American journal of physiology. Heart and circulatory physiology*. 289:H886-897.

Yang, Y.D., H. Cho, J.Y. Koo, M.H. Tak, Y. Cho, W.S. Shim, S.P. Park, J. Lee, B. Lee, B.M. Kim, R. Raouf, Y.K. Shin, and U. Oh. 2008. TMEM16A confers receptor-activated calcium-dependent chloride conductance. *Nature*. 455:1210-1215.

Zhang, S., S.J. Kehl, and D. Fedida. 2001. Modulation of Kv1.5 potassium channel gating by extracellular zinc. *Biophysical journal*. 81:125-136.

SUPPLEMENTARY REACTION SCHEMES

α-Adrenergic signaling

$$\alpha A + \alpha AR_0 \underset{k_{\alpha AR\_off}}{\overset{k_{\alpha AR\_on}}{\rightleftharpoons}} \alpha AR_1 \xrightarrow{k_{\alpha AR\_P}} \alpha AR_P \xrightarrow{k_{\alpha AR\_endo}} \alpha AR_{in} \xrightarrow{k_{\alpha AR\_recyc}} \alpha AR_0$$

$$\alpha AR_1 + G_{q0\_GDP} \underset{k_{Gq1\_GDP\_\alpha AR\_off}}{\overset{k_{Gq0\_GDP\_\alpha AR\_on}}{\rightleftharpoons}} G_{q1\_GDP}$$

$$G_{q1\_GDP} \xrightarrow{k_{Gq1\_GDP\_GTP\_exch}, +GTP} G_{q0\_GTP} + GDP + \alpha AR_1$$

$$G_{q0\_GTP} \xrightarrow{k_{Gq\_GTPase}} G_{q0\_GDP}$$

$$G_{q0\_GTP} + PLC \underset{k_{PLC\_Gq0\_GTP\_off}}{\overset{k_{PLC\_Gq0\_GTP\_on}}{\rightleftharpoons}} PLC_{Gq0\_GTP}$$

$$PLC_{Gq0\_GTP} \xrightarrow{k_{PLC\_Gq0\_GTP\_hyd}} PLC + G_{q0\_GDP} + GDP$$

$$PLC + PIP \underset{k_{PLC\_PIP\_off}}{\overset{k_{PLC\_PIP\_on}}{\rightleftharpoons}} PLC_{PIP} \xrightarrow{k_{PLC\_PIP\_hyd}} PLC + DAG + IP3$$

$$PLC_{Gq0\_GTP} + PIP \underset{k_{PLC\_Gq0\_GTP\_PIP\_off}}{\overset{k_{PLC\_Gq0\_GTP\_PIP\_on}}{\rightleftharpoons}} PLC_{Gq0\_GTP\_PIP}$$

$$PLC_{Gq0\_GTP\_PIP} \xrightarrow{k_{PLC\_Gq0\_GTP\_PIP\_hyd}} PLC_{Gq0\_GTP} + DAG + IP3$$

$$PLC_{Gq0\_GTP} \xrightarrow{k_{PKA\_PLC\_Gq0\_GTP}, PKA} PLC_{P\_Gq0\_GTP}$$

$$PLC_{Gq0\_GTP} \xrightarrow{k_{PKC\_PLC\_Gq0\_GTP}, PKC} PLC_{P\_Gq0GTP}$$

$$PLC_{P\_Gq0\_GTP} \underset{k_{PLC\_P\_Gq0\_GTP\_on}}{\overset{k_{PLC\_P\_Gq0\_GTP\_off}}{\rightleftharpoons}} PLC_P + G_{q0GTP}$$

$$PLC_P \xrightarrow{k_{PP\_PLC\_P}, PP} PLC$$

$$DAG \xrightarrow{k_{met\_DAG}} products$$

$$IP3 \xrightarrow{k_{met\_IP3}} products$$

β-Adrenergic signaling

$$\beta A + \beta AR_0 \underset{k_{\beta AR\_off}}{\overset{k_{\beta AR\_on}}{\rightleftharpoons}} \beta AR_1 \xrightarrow{k_{\beta AR\_P}} \beta AR_P \xrightarrow{k_{\beta AR\_endo}} \beta AR_{in} \xrightarrow{k_{\beta AR\_recyc}} \beta AR_0$$

$$\beta AR_1 + G_{s0\_GDP} \underset{k_{Gs\_GDP\_\beta AR\_off}}{\overset{k_{Gs\_GDP\_\beta AR\_on}}{\rightleftharpoons}} G_{s1\_GDP}$$

$$G_{s1\_GDP} \xrightarrow{k_{Gs1\_GDP\_GTP\_exch}, +GTP} G_{s0\_GTP} + GDP + \beta AR_1$$

$$G_{s0\_GTP} \xrightarrow{k_{Gs\_GTPase}} G_{s0\_GDP}$$

$$G_{s0\_GTP} + AC_0 \underset{k_{AC1\_Gs\_off}}{\overset{k_{AC0\_Gs\_on}}{\rightleftharpoons}} AC_1 \xrightarrow{k_{AC\_ATP}, +ATP} AC_1 + cAMP$$

$$AC_0 \underset{k_{PP\_AC}, PP}{\overset{k_{PKA\_AC}, PKA_{cAMP}}{\rightleftharpoons}} AC_1$$

$$n_{PKA\_cAMP} \cdot cAMP + PKA \xleftrightarrow{K_{PKA\_cAMP}} PKA_{cAMP}$$

$$n_{PDE} \cdot cAMP + PDE_{cAMP} \xleftrightarrow{K_{PDE\_cAMP}} PDE_{cAMP\_act} \xrightarrow{k_{PDE\_cAMP}, +cAMP} AMP$$

$$PDE_{cAMP} \underset{PP}{\overset{k_{PKA\_PDE}, PKA_{cAMP}}{\rightleftharpoons}} PDE_{cAMP\_P}$$

$$PDE_{cAMP} \underset{PP}{\overset{k_{PKG\_PDE}, PKG_{cGMP}}{\rightleftharpoons}} PDE_{cAMP\_P}$$

$$n_{PDE} \cdot cAMP + PDE_{cAMP\_P} \xleftrightarrow{K_{PDE\_cAMP\_P}} PDE_{cAMP\_P\_act} \xrightarrow{k_{PDE\_cAMP}, +cAMP} AMP$$

NaKCl co-transporter

$$
\begin{array}{ccc}
 & X_0 \quad \underset{\beta_{NaKCl\_0}}{\overset{\alpha_{NaKCl\_0}}{\rightleftharpoons}} \quad Y_0 & \\
L_{NaKCl\_Na}, +Na_{ex} \downarrow\uparrow -Na_{ex} & & -Na_{in} \uparrow\downarrow L_{NaKCl\_Na}, +Na_{in} \\
 & X_1 \qquad\qquad Y_1 & \\
L_{NaKCl\_Cl}, +Cl_{ex} \downarrow\uparrow -Cl_{ex} & & -Cl_{in} \uparrow\downarrow L_{NaKCl\_Cl}, +Cl_{in} \\
 & X_2 \qquad\qquad Y_2 & \\
L_{NaKCl\_K}, +K_{ex} \downarrow\uparrow -K_{ex} & & -K_{in} \uparrow\downarrow L_{NaKCl\_K}, +K_{in} \\
 & X_3 \qquad\qquad Y_3 & \\
L_{NaKCl\_Cl}, +Cl_{ex} \downarrow\uparrow -Cl_{ex} & & -Cl_{in} \uparrow\downarrow L_{NaKCl\_Cl}, +Cl_{in} \\
 & X_4 \quad \underset{\beta_{NaKCl\_4}}{\overset{\alpha_{NaKCl\_4}}{\rightleftharpoons}} \quad Y_4 &
\end{array}
$$

where X is the NaKCl co-transporter with the ion binding sites accessible to the extracellular medium and Y is NaKCl with the ion binding sites accessible to the intracellular medium, the L are equilibrium dissociation constants, and the α are rate constants for the isomerizations of the ion binding sites from outside-accessible to inside accessible and the β are rate constants for the opposite isomerizations. In addition, NaKCl is phosphorylated and dephosphorylated.

$$NaKCl \xrightarrow{k_{PKC\_NaKCl}, PKC_{Ca\_DAG}} NaKCl_{PKC}$$

$$PP_{NaKCl} \xrightarrow{k_{PKA\_PP\_NaKCl}, PKA_{cAMP}} PP_{P\_NaKCl} \xrightarrow{k_{PP\_PP\_NaKCl}, PP} PP_{NaKCl}$$

$$PP_{NaKCl} \xrightarrow{k_{PKG\_PP\_NaKCl}, PKG_{cGMP}} PP_{P\_NaKCl} \xrightarrow{k_{PP\_PP\_NaKCl}, PP} PP_{NaKCl}$$

$$NaKCl_{PKC} \xrightarrow{k_{PP\_NaKCl}, PP_{NaKCl}} NaKCl$$

$$NaKCl_{PKC} \xrightarrow{k_{PP\_P\_NaKCl}, PP_{P\_NaKCl}} NaKCl$$

NCX exchanger

$$NCX_{inact} + n \cdot Ca \underset{}{\overset{K_{NCX\_act\_Ca}}{\rightleftharpoons}} NCX_{act}$$

$$X_0 \quad \underset{\beta'_{NCX\_0}}{\overset{\alpha'_{NCX\_0}}{\rightleftharpoons}} \quad Y_0$$

$$1/3 \cdot K_{NCX\_Na}, + Na_{ex} \downarrow\uparrow -Na_{ex} \qquad -Na_{in} \uparrow\downarrow 1/3 \cdot K_{NCX\_Na}, + Na_{in}$$

$$X_1 \qquad\qquad Y_1$$

$$K_{NCX\_Na}, + Na_{ex} \downarrow\uparrow -Na_{ex} \qquad -Na_{in} \uparrow\downarrow K_{NCX\_Na}, + Na_{in}$$

$$X_2 \qquad\qquad Y_2$$

$$3K_{NCX\_Na}, + Na_{ex} \downarrow\uparrow -Na_{ex} \qquad -Na_{in} \uparrow\downarrow 3K_{NCX\_Na}, + Na_{in}$$

$$X_3 \qquad\qquad Y_3$$

$$K_{NCX\_Ca}, + Ca_{in} \downarrow\uparrow -Ca_{in} \qquad -Ca_{ex} \uparrow\downarrow K_{NCX\_Ca}, + Ca_{ex}$$

$$X_4 \quad \underset{\beta_{NCX\_4}}{\overset{\alpha_{NCX\_4}}{\rightleftharpoons}} \quad Y_4$$

$$\alpha'_{NCX\_0} = \alpha_{NCX\_0} \cdot \exp[F \cdot V_m / (2RT)]$$
$$\beta'_{NCX\_0} = \beta_{NCX\_0} \cdot \exp[-F \cdot V_m / (2RT)]$$

NCX_T is the total of all forms of the exchanger, and NCX_{act} is the total of all X_i and Y_i, the active forms of of NCX. In X three Na binding sites are accessible to the extracellular medium and one Ca binding site is accessible to the intracellular medium and in Y these sites have the opposite accessibilities. The K are equilibrium dissocation constants, and α and β are isomerization rate constants. It is assumed that X_0 and Y_0 have one net negative charge that moves; i.e., three negative charges associated with the three Na binding sites and, on the opposite side of the membrane, two negative charges associated with the Ca binding site. These drop through one-half of the transmembrane potential to reach the transition state during the change in accessibilities, hence the forms of α' and β'. The fully occupied X_4 and Y_4 are assumed to have no net moving charge.

P2XR

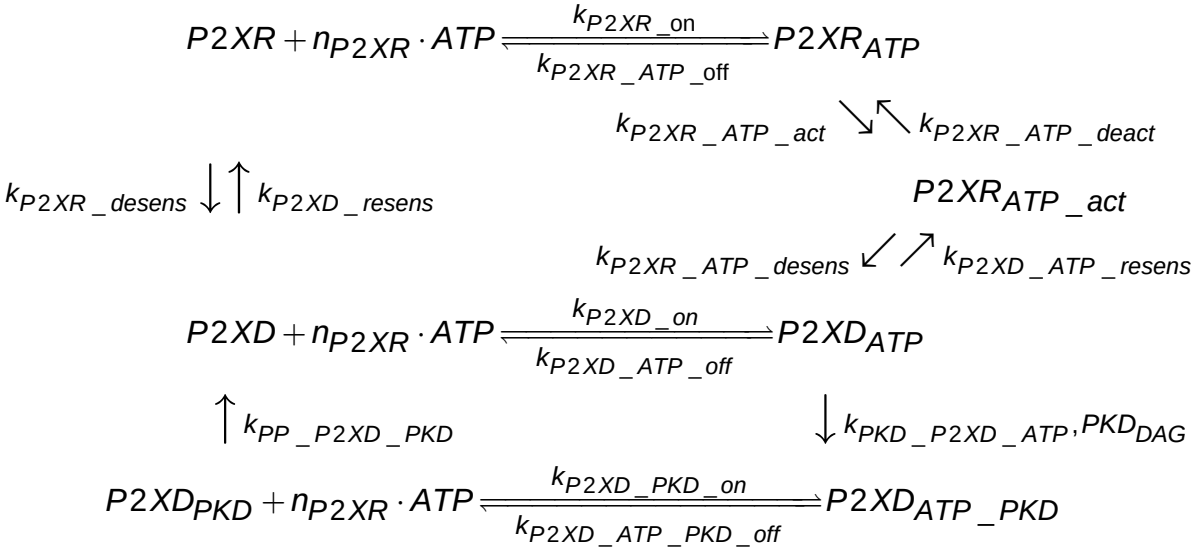
$P2XR + n_{P2XR} \cdot ATP \rightleftharpoons P2XR_{ATP}$
k_{P2XR_on}
$k_{P2XR\_ATP\_off}$
$k_{P2XR\_ATP\_act}$
$k_{P2XR\_ATP\_deact}$
k_{P2XR_desens}
k_{P2XD_resens}
$P2XR_{ATP\_act}$
$k_{P2XR\_ATP\_desens}$
$k_{P2XD\_ATP\_resens}$
$P2XD + n_{P2XR} \cdot ATP \rightleftharpoons P2XD_{ATP}$
k_{P2XD_on}
$k_{P2XD\_ATP\_off}$
$k_{PP\_P2XD\_PKD}$
$k_{PKD\_P2XD\_ATP}, PKD_{DAG}$
$P2XD_{PKD} + n_{P2XR} \cdot ATP \rightleftharpoons P2XD_{ATP\_PKD}$
$k_{P2XD\_PKD\_on}$
$k_{P2XD\_ATP\_PKD\_off}$

sGC

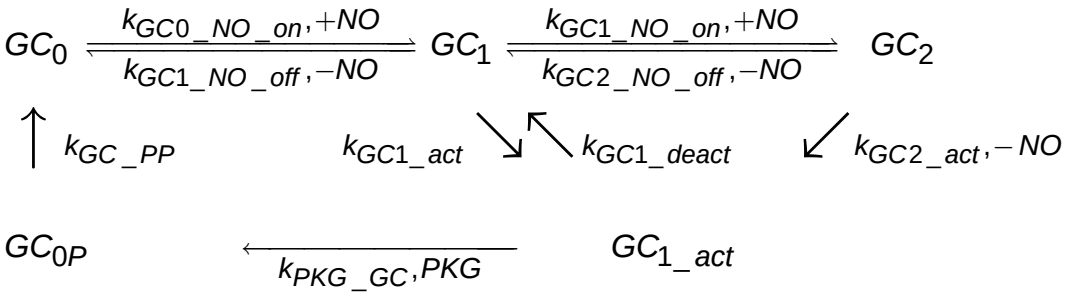
GC_0
$k_{GC0\_NO\_on}, +NO$
$k_{GC1\_NO\_off}, -NO$
GC_1
$k_{GC1\_NO\_on}, +NO$
$k_{GC2\_NO\_off}, -NO$
GC_2
k_{GC_PP}
k_{GC1_act}
k_{GC1_deact}
$k_{GC2\_act}, -NO$
GC_{0P}
k_{PKG_GC}, PKG
GC_{1_act}

SUPPLEMENTARY EQUATIONS

Parameters values are entered in Excel and copied to Mathcad (see below). Results obtained with each set of parameters are copied back to Excel. Units of variables are mV for electrostatic potential, μM for concentrations of all soluble components including Ca, and mM for Na, K, and Cl. Total fluxes are in fmol/s, and total currents are in pA. Parameter units are listed in the table of normal parameters (Table S1).

Comments are in Arial font; Mathcad statements are in Times New Roman font.

A. Effector concentrations

These are copied from Excel as row vectors and converted to column vectors. Ordinarily, the concentration (or pressure) of only one effector will change in a run. As written, six intravascular pressures are input, but any number can be input. The concentrations of the other effectors are constant (in this case zero)..

ATP. extracellular

[Seq.A.1] $ATP1\_excel := (0 \;\; 0 \;\; 0 \;\; 0 \;\; 0 \;\; 0)$

[Seq.A.2] $atp1 := ATP1\_excel^{T}$

β1-adrenergic receptor agonist

[Seq.A.5] $betaA1\_excel := (0 \;\; 0 \;\; 0 \;\; 0 \;\; 0 \;\; 0)$

[Seq.A.6] $betaA1 := betaA1\_excel^{T}$

Epoxyeicosatrienoic acid

[Seq.A.9] $eet1\_excel := (0 \;\; 0 \;\; 0 \;\; 0 \;\; 0 \;\; 0)$

[Seq.A.10] $eet1 := eet1\_excel^{T}$

α1-adrenergic receptor agonist

[Seq.A.3] $alphaA1\_excel := (0 \;\; 0 \;\; 0 \;\; 0 \;\; 0 \;\; 0)$

[Seq.A.4] $alphaA1 := alphaA1\_excel^{T}$

Intravascular pressure

[Seq.A.7] $bp1\_excel := (10 \;\; 20 \;\; 40 \;\; 60 \;\; 80 \;\; 100)$

[Seq.A.8] $bp1 := bp1\_excel^{T}$

Nitric oxide

[Seq.A.11] $nox1\_excel := (0 \;\; 0 \;\; 0 \;\; 0 \;\; 0 \;\; 0)$

[Seq.A.12] $nox1 := nox1\_excel^{T}$

For simulations at multiple effector concentrations or intravascular pressures, one of the above vectors is assigned to the effector concentration vector, eff_conc1. The parameter name of the effector that varies (ATP_1, αA_1, βA_1, BP_1, EET_1, or NO_1] must be the argument of W( ). Only the effector vector assigned to eff_conc1 is called and this vector can be of any length greater or equal to 1. A second effector can co-vary if set equal to, or a multiple of, the first.

Define eff_conc1

[Seq.A.13] $\text{eff\_conc1} := \text{bp1}$

In the EFFECTORS vector below, each effector is assigned two concentrations; $conc_0$ and $conc_1$. The effector is at $conc_0$ from t=0 to t=τ_1, rises to $conc_1$ from τ_1 to τ_2, is steady from τ_2 to τ_3, and then falls to $conc_0$. These are the fixed concentrations of the effectors not specified as the varying argument of W( ) (see solve block). The application of multiple pulses requires additional parameters specifying the number of pulses and the pulse duration and the inter-pulse interval. Solutions for multiple $conc_1$ for a given effector, specified by eff_conc_1, are obtained by automatic successive runs. During these runs (or one run if eff_conc1 has a single value), any of the other effectors can also be added but at the same concentrations in successive runs.

[Seq.A.14]

0	αA_0
0	αA_1
4.00E+01	$\tau_{\alpha A1}$
5.00E+01	$\tau_{\alpha A2}$
3.00E+02	$\tau_{\alpha A3}$
2	$\kappa_{\alpha A1}$
2	$\kappa_{\alpha A2}$
0	ATP_0
0	ATP_1
100	τ_{pulse_init}
1	$\Delta\tau_{pulse\_on}$
9	$\Delta\tau_{pulse\_off}$
20	n_{cycles}
4.00E+01	τ_{atp1}
5.00E+01	τ_{atp2}
3.00E+02	τ_{atp3}
2	
2	
0.00E+00	

[Seq.A.15]

Knot & Nelson, 1998 data

[Seq.A.16]

$$BP_{exp} := \begin{pmatrix} 10 \\ 20 \\ 40 \\ 60 \\ 80 \\ 100 \end{pmatrix}$$

[Seq.A.17]

$$Ca_{exp} := \begin{pmatrix} .119 \\ .140 \\ .160 \\ .190 \\ .215 \\ .245 \end{pmatrix}$$

[Seq.A.18]

$$V_{exp} := \begin{pmatrix} -63 \\ -59 \\ -51 \\ -45 \\ -41 \\ -37 \end{pmatrix}$$

$$\text{EFFECTORS} := \begin{pmatrix} 0 \\ 4.00\text{E+}01 \\ 5.00\text{E+}01 \\ 3.00\text{E+}02 \\ 2 \\ 2 \\ 0.00\text{E+}00 \\ 10 \\ 1.00\text{E+}01 \\ 1.50\text{E+}01 \\ 3.00\text{E+}02 \\ 2 \\ 2 \\ 0 \\ 0 \\ 4.00\text{E+}01 \\ 6.00\text{E+}01 \\ 3.00\text{E+}02 \\ 2.00\text{E-}01 \\ 2.00\text{E+}00 \\ 0 \\ 0 \\ 4.00\text{E+}01 \\ 5.00\text{E+}01 \\ 3.00\text{E+}02 \\ 2 \\ 2 \end{pmatrix} \quad \begin{vmatrix} \kappa_{atp1} \\ \kappa_{atp2} \\ \beta A_0 \\ \beta A_1 \\ \tau_{\beta A1} \\ \tau_{\beta A2} \\ \tau_{\beta A3} \\ \kappa_{\beta A1} \\ \kappa_{\beta A2} \\ BP_0 \\ BP_1 \\ \tau_{bp1} \\ \tau_{bp2} \\ \tau_{bp3} \\ \kappa_{bp1} \\ \kappa_{bp2} \\ EET_0 \\ EET_1 \\ \tau_{eet1} \\ \tau_{eet2} \\ \tau_{eet3} \\ \kappa_{eet1} \\ \kappa_{eet2} \\ NO_0 \\ NO_1 \\ \tau_{no1} \\ \tau_{no2} \end{vmatrix} := \text{EFFECTORS}$$

$$\begin{pmatrix} \tau_{no3} \\ \kappa_{no1} \\ \kappa_{no2} \end{pmatrix}$$

[Seq.A.19]

$$EFF\_NAMES := \begin{pmatrix} "\alpha A.0" \\ "\alpha A.1" \\ "\tau.\alpha A1" \\ "\tau.\alpha A2" \\ "\tau.\alpha A3" \\ "\kappa.\alpha A1" \\ "\kappa.\alpha A2" \\ "ATP.0" \\ "ATP.1" \\ "\tau.pulse\_init" \\ "\Delta\tau.pulse\_on" \\ "\Delta\tau.pulse\_off" \\ "n.cycles" \\ "\tau.atp1" \\ "\tau.atp2" \\ "\tau.atp3" \\ "\kappa.atp1" \\ "\kappa.atp2" \\ "\beta A.0" \\ "\beta A.1" \\ "\tau.\beta A1" \\ "\tau.\beta A2" \\ "\tau.\beta A3" \\ "\kappa.\beta A1" \\ "\kappa.\beta A2" \end{pmatrix}$$

"BP.0"
"BP.1"
"τ.bp1"
"τ.bp2"
"τ.bp3"
"κ.bp1"
"κ.bp2"
"EET.0"
"EET.1"
"τ.eet1"
"τ.eet2"
"τ.eet3"
"κ.eet1"
"κ.eet2"
"NO.0"
"NO.1"
"τ.no1"
"τ.no2"
"τ.no3"
"κ.no1"
"κ.no2"

A table, EFF_NAMES_VALUES, is generated showing the effector parameter names and values.

[Seq.A.20] EFF_NAMES_VALUES := augment(EFF_NAMES, EFFECTORS)

[Seq.A.21]

$$EFF\_NAMES\_VALUES = \begin{pmatrix} "\alpha A.0" & 0E{+}000 \\ "\alpha A.1" & 0E{+}000 \\ "\tau.\alpha A1" & 4E{+}001 \\ "\tau.\alpha A2" & 5E{+}001 \\ "\tau.\alpha A3" & 3E{+}002 \\ "\kappa.\alpha A1" & 2E{+}000 \\ "\kappa.\alpha A2" & 2E{+}000 \\ "ATP.0" & 0E{+}000 \\ "ATP.1" & 0E{+}000 \\ "\tau.pulse\_init" & 1E{+}002 \\ "\Delta\tau.pulse\_on" & 1E{+}000 \\ "\Delta\tau.pulse\_off" & 9E{+}000 \\ "n.cycles" & 2E{+}001 \\ "\tau.atp1" & 4E{+}001 \\ "\tau.atp2" & 5E{+}001 \\ "\tau.atp3" & 3E{+}002 \\ "\kappa.atp1" & 2E{+}000 \\ "\kappa.atp2" & 2E{+}000 \\ "\beta A.0" & 0E{+}000 \\ "\beta A.1" & 0E{+}000 \\ "\tau.\beta A1" & 4E{+}001 \\ "\tau.\beta A2" & 5E{+}001 \\ "\tau.\beta A3" & 3E{+}002 \\ "\kappa.\beta A1" & 2E{+}000 \\ "\kappa.\beta A2" & 2E{+}000 \\ "BP.0" & 0E{+}000 \\ "BP.1" & 1E{+}001 \\ "\tau.bp1" & 1E{+}001 \\ "\tau.bp2" & 1.5E{+}001 \\ "\tau.bp3" & 3E{+}002 \\ "\kappa.bp1" & 2E{+}000 \\ "\kappa.bp2" & 2E{+}000 \\ "EET.0" & 0E{+}000 \end{pmatrix}$$

"EET.1"	0E+000
"τ.eet1"	4E+001
"τ.eet2"	6E+001
"τ.eet3"	3E+002
"κ.eet1"	2E-001
"κ.eet2"	2E+000
"NO.0"	0E+000
"NO.1"	0E+000
"τ.no1"	4E+001
"τ.no2"	5E+001
"τ.no3"	3E+002
"κ.no1"	2E+000
"κ.no2"	2E+000

B. All other parameters

These parameters, which are copied from Excel into the PARAS column vector, are used in the steady-state equations and the differential equations.

[Seq.B.1]

[Seq.B.2]

300	"t1"
12000	"N1"
1.00E-05	"TOL"
1.00E-03	"CTOL"
250	"a (integration start time)"
300	"b (integration stop time)"
""	""
""	"αAR"
6.00E+03	"αAR.T"
1.00E+00	"k.αAR_on"
1.00E+01	"k.αAR_off"
2.00E-02	"k.αAR_P"
2.00E-02	"k.αAR_endo"
1.00E-02	"k.αAR_recyc"
""	""
""	"AC"
6.00E+03	"AC.T"
4.00E-05	"k.AC0_Gs_on"
5.00E-01	"k.AC1_Gs_off"
2.00E+02	"k.AC1_ATP"
1.00E-02	"k.PKA_AC"
1.00E-02	"k.PP_AC"
1.00E-01	"k.AC0_ATP"
""	"βAR"
6.00E+03	"βAR.T"
2.00E-01	"k.βAR_on"
4.00E+00	"k.βAR_off"
4.00E-03	"k.βAR_P"
4.00E-03	"k.βAR_endo"
4.00E-03	"k.βAR_recyc"
""	""
""	
1.50E+03	

4.00E-13	"BK"
4.72E+00	"BK.T"
8.00E-01	"perm.BK"
–3.40E+01	"K.BK_closed"
8.00E+01	"K.BK_open"
0.57	"V.BK_open"
4.10E-01	"V.BK_closed"
2.50E-06	"z.BK_J"
7.50E-06	"z.BK_L"
8.33E-07	"L.BK"
7.50E-06	"L.BK_PKA"
2.00E+01	"L.BK_PKC"
2.00E+01	"L.BK_PKG"
4.00E+01	"k.PKA_BK"
2.00E+01	"k.PKC_BK"
""	"k.PKG_BK"
""	"k.PP_BK"
3.00E+03	""
1.21E-13	"CaV"
6.20E+00	"CaV.T"
9.30E+00	"perm.CaV"
1.20E+00	"V.CaV_act"
1.12E+01	"ξ.CaV_act"
1.20E+00	"V.CaV_PKC_act"
2.00E+01	"V.CaV_PKG_act"
4.00E+01	"K.CaV_inh"
2.00E+01	"k.PKC_CaV"
""	"k.PKG_CaV"
""	"k.PP_CaV"
""	""
""	""
""	""
""	""

2.50E+03	""
1.60E-14	"Cl.A=Cl(Ca)"
2.00E+00	"Cl.AT"
0.00E+00	"perm.ClA"
4.10E+00	"zeta.ClA"
3.00E-01	"V.ClA"
4.00E+01	"K.ClA_Ca_act_max"
2.60E+00	"K.ClA_Ca_act_min"
""	"K.ClA_Ca_inh"
""	"n.ClA"
""	""
""	""
""	""
""	""
""	""
""	""
""	""
""	""
""	""
6.00E+03	""
2.00E-05	"G.q"
1.00E+00	"G.qT"
1.00E+00	"k.Gq0_GDP_αAR_on"
5.00E-02	"k.Gq1_GDP_αAR_off"
""	"k.Gq1_GDP_GTP_exch"
""	"k.Gq_GTPase"
6.00E+03	""
1.00E-05	"Gs"
5.00E-01	"G.sT"
1.00E+00	"k.Gs0_GDP_βAR_on"
5.00E-02	"k.Gs1_GDP_βAR_off"
""	"k.Gs1_GDP_GTP_exch"
""	"k.Gs_GTPase"
	""

2.00E+03	
1.10E-13	"IP3R"
3.50E-01	"IP3.T"
8.00E-01	"perm.IP3R"
3.00E+00	"K.IP3R_IP3"
1.00E+00	"K.IP3R_IRAG_PKG_IP3"
1.00E-01	"n.IP3R_IP3"
3.00E-01	"K.IP3R_Ca_max"
2.50E+00	"K.IP3R_Ca_min"
1.40E+02	"K.IP3R_Ca_inh"
2.50E+00	"n.IP3R_Ca_inh"
3.00E+00	"K.IP3R_CaSR"
2.00E+01	"n.IP3R_CaSR"
2.00E+01	"n.IP3R_Ca_act"
""	"k.PKG_IP3R_IRAG"
""	"k.PP_IP3R_IRAG_PKG"
3.00E+02	""
5.00E-03	"KATP"
1.20E-01	"KATP.T"
2.00E+00	"P.open_KATP"
2.00E+00	"P.open_KATP_PKA"
2.00E-01	"k.PKA_KATP"
2.00E-01	"k.PKCε_KATP"
7.00E-14	"k.PP_KATP_PKA"
""	"k.PP_KATP_PKCε"
""	"perm.KATP"
""	""
2.70E+02	""
2.50E-14	"Kv"
–2.00E+01	"Kv.T"
7.00E+00	"perm.Kv"
""	"V.Kv"
0.00E+00	"x.Kv"

1.00E-15	"LEAKS"
2.00E+01	"Na.leakT"
1.00E-15	"perm.Na_leak"
2.20E+01	"K.leakT"
1.00E-15	"perm.K_leak"
1.30E+01	"Cl.leakT"
1.00E-14	"perm.Cl_leak"
""	"Ca.leakT"
6.00E+01	"perm.Ca_leak"
1.60E+00	"NaK"
2.20E+01	"I.NaKmax"
2.50E+00	"K.NaK_Kex"
1.10E+00	"K.NaK_Nain"
−5.00E+04	"n.NaK_Na"
""	"n.NaK_K"
""	"delta-mu.ATP"
1.00E+04	""
3.20E+01	"NaKCl"
2.70E+01	"NaKCl.T"
6.30E+01	"L.NaKCl_Na"
5.00E+04	"L.NaKCl_K"
5.00E+04	"L.NaKCl_Cl"
4.00E+04	"α.NaKCl_4"
2.00E+00	"β.NaKCl_0"
2.00E+01	"β.NaKCl_4"
1.00E+04	"ε.NaKCl_PKC"
2.00E+01	"k.PKC_NaKCl"
4.00E+01	"PP.NaKCl_T"
2.00E+01	"k.PP_NaKCl"
2.00E+01	"k.PP_P_NaKCl"
2.00E+01	"k.PKA_PP_NaKCl"
""	"k.PKG_PP_NaKCl"
""	"k.PP_PP_NaKCl"

PARAS :=	1.60E+03	PARA_NAMES :=	""
	1.00E+02		"NCX"
	8.00E-02		"NCX.T"
	3.00E+04		"K.NCX_Na"
	3.00E+04		"K.NCX_Ca"
	5.00E+04		"α.NCX_0"
	1.00E-01		"α.NCX_4"
	2.00E+00		"β.NCX_4"
	""		"K.NCX_act_Ca"
	""		"n.NCX_act"
	4.00E+01		""
	1.30E-13		"NSCeet"
	1.30E-13		"NSCeet.T"
	9.00E-13		"perm.NaNSCeet"
	5.00E-02		"perm.KNSCeet"
	1.00E+00		"perm.CaNSCeet"
	–1.00E+01		"K.NSCeet_EET"
	50		"n.NSCeet"
	1.00E+01		"V.NSCeet_min"
	""		"V.NSCeet_max"
	3.10E+01		"ξ.NSCeet"
	3.30E-14		"NSCne"
	3.30E-14		"NSCne.T"
	1.50E-13		"perm.NaNSCne"
	1.20E+00		"perm.KNSCne"
	2.00E-01		"perm.CaNSCne"
	1.00E+00		"K.NSCne_DAG"
	2.00E+00		"K.NSCne_Ca_act"
	""		"K.NSCne_Ca_inh"
	""		"n.NSCne"
	2.61E+02		""
	3.30E-14		"NSCstr"
	3.30E-14		"NSCstr.T"

	"perm.NaNSCstr"
1.50E-13	"perm.KNSCstr"
3.00E+02	"perm.CaNSCstr"
1.38E+00	"bp.50"
1.70E+00	"K.NSCstr_DAG"
1.00E+02	"K.NSCstr_Ca_act"
2	"K.NSCstr_Ca_inh"
1.00E+00	"n.NSCstr_DAG"
1.00E+00	"n.NSCstr_Ca"
1.00E+00	"n.NSCstr_bp"
4.00E+00	"K.NSCstr_PKC_Ca_act"
3.00E+00	"K.NSCstr_PKG_Ca_act"
2.00E+01	"k.PKC_NSCstr"
1.00E+01	"k.PKG_NSCstr"
""	"k.PP_NSCstr"
""	""
1.00E+01	"PDE"
1.00E+01	"k.PKA_PDE"
1.00E+01	"k.PKG_PDE"
1.00E+00	"k.PP_PDE"
1.00E-02	"n.PDE"
8.00E+00	"PDE.cAMP_T"
3.00E+00	"K.PDE_cAMP"
1.00E+01	"K.PDE_cAMP_P"
1.00E-02	"k.PDE_cAMP"
8.00E+00	"PDE.cGMP_T"
3.00E+00	"K.PDE_cGMP"
1.00E+01	"K.PDE_cGMP_P"
""	"k.PDE_cGMP"
""	""
4.00E+00	"PKA_PKC_PKG_PKCe"
2.00E+00	"K.PKA_cAMP"
5.00E-01	" n.PKA AMP"

2.00E-01	
2.00E+00	"K.PKC_DAG"
3.00E+00	"K.PKC_Ca"
2.00E+00	"n.PKC_Ca"
1.70E+00	"K.PKG_cGMP"
1.70E+00	"n.PKG_cGMP"
""	"K.PKCε_DAG"
6.00E+03	"K.PKD_DAG"
1.00E-06	"PLC"
1.00E+02	"PLC.T"
2.00E+01	"k.PLC_PIP_on"
2.00E-04	"k.PLC_PIP_off"
2.00E-02	"k.PLC_PIP_hyd"
1.00E-01	"k.PLC_Gq0_GTP_on"
3.00E-06	"k.PLC_Gq0_GTP_off"
1.00E+01	"k.PLC_Gq0_GTP_hyd"
8.00E+01	"k.PLC_Gq0_GTP_PIP_on"
1.00E+01	"k.PLC_Gq0_GTP_PIP_off"
1.00E+01	"k.PLC_Gq0_GTP_PIP_hyd"
5.00E-06	"k.PKA_PLC_Gq0_GTP"
1	"k.PKC_PLC_Gq0_GTP"
2	"k.PLC_P_Gq0_GTP_on"
1.00E+07	"k.PLC_P_Gq0_GTP_off"
0.09	"k.PP_PLC"
0.09	"PIP.T"
""	"k.met_DAG"
1.80E+01	"k.met_IP3"
4.00E-01	"PMCA"
3.00E+00	"I.PMCA_max"
""	"K.PMCA_Ca"
""	"n.PMCA_Ca"
1.00E+02	""
4.30E-14	"P2XR"

4.30E-14	"P2XR.T"
1.30E-13	"perm.NaP2XR"
1.00E+01	"perm.KP2XR"
1.00E+02	"perm.CaP2XR"
2.00E+00	"k.P2XR_0_on"
1.00E+02	"k.P2XR_3_off"
1.00E+01	"n_P2XR"
1.00E+00	"k.P2XR_3_act"
1.00E-02	"k.P2XR_3_deact"
1.00E-01	"k.P2XR_3_act_desens"
1.00E+00	"k.P2XD_3_resens"
1.00E+01	"k.P2XR_0_desens"
1.00E-02	"k.P2XD_0_resens"
1.00E+00	"k.P2XD_0_on"
1.00E+00	"k.P2XD_3_off"
1.00E+00	"k.P2XD_0_PKD_on"
1.00E+00	"k.P2XD_3_PKD_off"
""	"k.PKD_P2XD_3"
""	"k.PP_P2XD_0_PKD"
""	""
3.00E+03	""
2.00E-13	"RyR"
8.00E+02	"RyR.T"
5.00E-01	"perm.RyR"
1.00E+01	"K.RyR_Ca_SR"
4.00E+00	"n.RyR_Ca_SR"
2.00E+00	"K.RyR_Ca_jun_max"
3.00E+00	"K.RyR_Ca_jun_min"
3.00E+00	"n.RyR_Ca_jun"
4.00E+01	"K.RyR_Ca_inh"
4.00E+01	"n.RyR_Ca_inh"
4.00E+01	"k.PKA_RyR"
4.00E-01	"k.PKC_RyR"

5.00E+00	"k.PP_RyR"
""	"f.RyR_PKA_min"
""	"f.RyR_PKC_max"
1.00E+03	""
8.00E-01	"SERCA"
2.00E-01	"SERCA.T"
1.60E+00	"I.SERCA_max"
1.00E+02	"K.SERCA_Ca"
1.00E-01	"n.SERCA"
2.00E+01	"K.SERCA_inh_Ca_SRcen"
2.00E+01	"K.SERCA_P_Ca"
2.00E+01	"k.PKA_SERCA"
2.00E+01	"k.PKC_SERCA"
""	"k.PKG_SERCA"
""	"k.PP_SERCA"
1.00E-02	""
3.00E+02	"sGC"
2.00E+02	"GC.T"
2.00E+02	"k.GC0_NO_on"
2.00E+02	"k.GC1_NO_off"
1.00E+00	"k.GC1_NO_on"
1.00E-01	"k.GC2_NO_off"
1.00E+01	"k.GC1_act"
1.00E+01	"k.GC1_deact"
1.00E+01	"k.GC2_act"
1.00E+01	"k.PKG_GC"
1.00E-01	"k.PP_GC"
""	"k.GC_act_GTP"
""	"k.GC_basal_GTP"
2.50E-11	""
1.00E-12	"CAPAC & VOLS"
5.60E-16	"C.m"
1.30E-16	"VOL cell"

7.00E-14	"VOL.SRper"
6.30E-17	"VOL.jun"
""	"VOL.SRcen"
""	"VOL.NSCstr"
""	""
3.00E+02	""
2.20E+01	"BUFFERS"
7.70E+01	"BUF.T"
3.00E+02	"k.BUF_on"
3.00E+02	"k.BUF_off"
3.00E+02	"BUF.jun_T"
3.00E+02	"BUF.NSCstr_T"
2.00E+00	"CSQ.SRcen_T"
1.60E+03	"CSQ.SRper_T"
""	"k.CSQ_on"
""	"k.CSQ_off"
8.00E-13	""
1.60E-14	"INTRACELL FLUX"
4.00E-13	"lambda.jun_cyt"
""	"lambda.cen_per"
""	"lambda.NSCstr_cyt"
3.10E+02	""
1.43E+02	"IONS & T"
5.90E+00	"T"
1.60E+03	"Na.ex"
1.27E+02	"K.ex"
	"Ca.ex"
	"Cl.ex"

[Seq.B.3] PARA_AUGMENT := augment(PARA_NAMES, PARAS)

[Seq.B.4]

Click on table and use scroll bar to see entire table.

PARA_AUGMENT =

	0	1
0	"t1"	3E+002
1	"N1"	1.2E+004
2	"TOL"	1E-005
3	"CTOL"	1E-003
4	"a (integration start time)"	2.5E+002
5	"b (integration stop time)"	3E+002
6	""	""
7	"αAR"	""
8	"αAR.T"	6E+003
9	"k.αAR_on"	1E+000
10	"k.αAR_off"	1E+001
11	"k.αAR_P"	2E-002
12	"k.αAR_endo"	2E-002
13	"k.αAR_recyc"	1E-002
14	""	""
15	"AC"	""
16	"AC.T"	6E+003
17	"k.AC0_Gs_on"	4E-005
18	"k.AC1_Gs_off"	5E-001
19	"k.AC1_ATP"	2E+002
20	"k.PKA_AC"	1E-002
21	"k.PP_AC"	1E-002
22	"k.AC0_ATP"	1E-001
23	"βAR"	""
24	"βAR.T"	6E+003
25	"k.βAR_on"	2E-001
26	"k.βAR_off"	4E+000
27	"k.βAR_P"	4E-003
28	"k.βAR_endo"	4E-003
29	"k.βAR_recyc"	...

Assignment of parameter values, as sub-matrices of PARAS, to parameters

[Seq.B.5]

$$SOLVE\_PARAS := submatrix(PARAS, 0, 5, 0, 0)$$

[Seq.B.6]

$$\alpha AR := submatrix(PARAS, 8, 13, 0, 0)$$

[Seq.B.7]

$$AC := submatrix(PARAS, 16, 22, 0, 0)$$

[Seq.B.8]

$$\begin{pmatrix} t1 \\ N1 \\ TOL \\ CTOL \\ a \\ b \end{pmatrix} := SOLVE\_PARAS$$

[Seq.B.9]

$$\begin{pmatrix} \alpha AR_T \\ k_{\alpha AR\_on} \\ k_{\alpha AR\_off} \\ k_{\alpha AR\_P} \\ k_{\alpha AR\_endo} \\ k_{\alpha AR\_recyc} \end{pmatrix} := \alpha AR$$

[Seq.B.10]

$$\begin{pmatrix} AC_T \\ k_{AC0\_Gs\_on} \\ k_{AC1\_Gs\_off} \\ k_{AC1\_ATP} \\ k_{PKA\_AC} \\ k_{PP\_AC} \\ k_{AC0\_ATP} \end{pmatrix} := AC$$

[Seq.B.11]

$$\beta AR := submatrix(PARAS, 24, 29, 0, 0)$$

[Seq.B.12]

$$BK := submatrix(PARAS, 32, 47, 0, 0)$$

[Seq.B.13]

$$CaV := submatrix(PARAS, 50, 59, 0, 0)$$

[Seq.B.14] $\begin{pmatrix} \beta AR_T \\ k_{\beta AR\_on} \\ k_{\beta AR\_off} \\ k_{\beta AR\_P} \\ k_{\beta AR\_endo} \\ k_{\beta AR\_recyc} \end{pmatrix} := \beta AR$

[Seq.B.15] $\begin{pmatrix} BK_T \\ perm_{BK} \\ K_{BK\_closed} \\ K_{BK\_open} \\ V_{BK\_open} \\ V_{BK\_closed} \\ z_{BK\_J} \\ z_{BK\_L} \\ L_{BK} \\ L_{BK\_PKA} \\ L_{BK\_PKC} \\ L_{BK\_PKG} \\ k_{PKA\_BK} \\ k_{PKC\_BK} \\ k_{PKG\_BK} \\ k_{PP\_BK} \end{pmatrix} := BK$

[Seq.B.16] $\begin{pmatrix} CaV_T \\ perm_{CaV} \\ V_{CaV\_act} \\ \xi_{CaV\_act} \\ V_{CaV\_PKC\_act} \\ V_{CaV\_PKG\_act} \\ K_{CaV\_inh} \\ k_{PKC\_CaV} \\ k_{PKG\_CaV} \\ k_{PP\_CaV} \end{pmatrix} := CaV$

[Seq.B17]

$Cl_A := \text{submatrix}(PARAS, 66, 73, 0, 0)$

[Seq.B.18]

$G_q := \text{submatrix}(PARAS, 84, 88, 0, 0)$

[Seq.B.19]
$$\begin{pmatrix} Cl_{AT} \\ perm_{ClA} \\ \zeta_{ClA} \\ V_{ClA} \\ K_{ClA\_Ca\_act\_max} \\ K_{ClA\_Ca\_act\_min} \\ K_{ClA\_Ca\_inh} \\ n_{ClA} \end{pmatrix} := Cl_A$$

[Seq.B.20]
$$\begin{pmatrix} G_{qT} \\ k_{Gq0\_GDP\_\alpha AR\_on} \\ k_{Gq1\_GDP\_\alpha AR\_off} \\ k_{Gq1\_GDP\_GTP\_exch} \\ k_{Gq\_GTPase} \end{pmatrix} := G_q$$

[Seq.B.21]

$$G_s := \text{submatrix}(PARAS, 91, 95, 0, 0)$$

[Seq.B.22]

$$IP3R := \text{submatrix}(PARAS, 98, 111, 0, 0)$$

[Seq.B.23]

$$KATP := \text{submatrix}(PARAS, 114, 121, 0, 0)$$

[Seq.B.24]
$$\begin{pmatrix} G_{sT} \\ k_{Gs0\_GDP\_\beta AR\_on} \\ k_{Gs1\_GDP\_\beta AR\_off} \\ k_{Gs1\_GDP\_GTP\_exch} \\ k_{Gs\_GTPase} \end{pmatrix} := G_s$$

[Seq.B.25]
$$\begin{pmatrix} IP3R_T \\ perm_{IP3R} \\ K_{IP3R\_IP3} \\ K_{IP3R\_IRAG\_PKG\_IP3} \\ n_{IP3R\_IP3} \\ K_{IP3R\_Ca\_max} \\ K_{IP3R\_Ca\_min} \\ K_{IP3R\_Ca\_inh} \\ n_{IP3R\_Ca\_inh} \\ K_{IP3R\_CaSR} \\ n_{IP3R\_CaSR} \\ n_{IP3R\_Ca\_act} \\ k_{PKG\_IP3R\_IRAG} \\ k_{PP\_IP3R\_IRAG\_PKG} \end{pmatrix} := IP3R$$

[Seq.B.26]
$$\begin{pmatrix} KATP_T \\ P_{open\_KATP} \\ P_{open\_KATP\_PKA} \\ k_{PKA\_KATP} \\ k_{PKC\varepsilon\_KATP} \\ k_{PP\_KATP\_PKA} \\ k_{PP\_KATP\_PKC\varepsilon} \\ perm_{KATP} \end{pmatrix} := KATP$$

[Seq.B.27]

$$K_V := \text{submatrix}(PARAS, 125, 128, 0, 0)$$

[Seq.B.28]

$$LEAKS := \text{submatrix}(PARAS, 130, 137, 0, 0)$$

[Seq.B.29]

$$NaK := \text{submatrix}(PARAS, 139, 144, 0, 0)$$

[Seq.B.30]

$$\begin{pmatrix} Kv_T \\ perm_{Kv} \\ V_{Kv} \\ \xi_{Kv} \end{pmatrix} := K_V$$

[Seq.B.31]

$$\begin{pmatrix} Na_{leakT} \\ perm_{Na\_leak} \\ K_{leakT} \\ perm_{K\_leak} \\ Cl_{leakT} \\ perm_{Cl\_leak} \\ Ca_{leakT} \\ perm_{Ca\_leak} \end{pmatrix} := LEAKS$$

[Seq.B.32]

$$\begin{pmatrix} I_{NaKmax} \\ K_{NaK\_Kex} \\ K_{NaK\_Nain} \\ n_{NaK\_Na} \\ n_{NaK\_K} \\ \Delta\mu_{ATP} \end{pmatrix} := NaK$$

[Seq.B.33]

$$NaKCl := \text{submatrix}(PARAS, 147, 161, 0, 0)$$

[Seq.B.34]

$$NCX := \text{submatrix}(PARAS, 164, 171, 0, 0)$$

[Seq.B.35]

$$NSCeet := \text{submatrix}(PARAS, 174, 182, 0, 0)$$

[Seq.B.36]
$$\begin{pmatrix} NaKCl_T \\ L_{NaKCl\_Na} \\ L_{NaKCl\_K} \\ L_{NaKCl\_Cl} \\ \alpha_{NaKCl\_4} \\ \beta_{NaKCl\_0} \\ \beta_{NaKCl\_4} \\ \varepsilon_{NaKCl\_PKC} \\ k_{PKC\_NaKCl} \\ PP_{NaKCl\_T} \\ k_{PP\_NaKCl} \\ k_{PP\_P\_NaKCl} \\ k_{PKA\_PP\_NaKCl} \\ k_{PKG\_PP\_NaKCl} \\ k_{PP\_PP\_NaKCl} \end{pmatrix} := NaKCl$$

[Seq.B.37]
$$\begin{pmatrix} NCX_T \\ K_{NCX\_Na} \\ K_{NCX\_Ca} \\ \alpha_{NCX\_0} \\ \alpha_{NCX\_4} \\ \beta_{NCX\_4} \\ K_{NCX\_act\_Ca} \\ n_{NCX\_act} \end{pmatrix} := NCX$$

[Seq.B.38]
$$\begin{pmatrix} NSCeet_T \\ perm_{NaNSCeet} \\ perm_{KNSCeet} \\ perm_{CaNSCeet} \\ K_{NSCeet\_EET} \\ n_{NSCeet} \\ V_{NSCeet\_min} \\ V_{NSCeet\_max} \\ \xi_{NSCeet} \end{pmatrix} := NSCeet$$

[Seq.B.39]

$$NSCne := submatrix(PARAS, 184, 191, 0, 0)$$

[Seq.B.40]

$$NSCstr := submatrix(PARAS, 194, 209, 0, 0)$$

[Seq.B.41]

$$PDE := submatrix(PARAS, 212, 223, 0, 0)$$

[Seq.B.42] $\begin{pmatrix} NSCne_T \\ perm_{NaNSCne} \\ perm_{KNSCne} \\ perm_{CaNSCne} \\ K_{NSCne\_DAG} \\ K_{NSCne\_Ca\_act} \\ K_{NSCne\_Ca\_inh} \\ n_{NSCne} \end{pmatrix} := NSCne$

[Seq.B.43] $\begin{pmatrix} NSCstr_T \\ perm_{NaNSCstr} \\ perm_{KNSCstr} \\ perm_{CaNSCstr} \\ bp_{50} \\ K_{NSCstr\_DAG} \\ K_{NSCstr\_Ca\_act} \\ K_{NSCstr\_Ca\_inh} \\ n_{NSCstr\_DAG} \\ n_{NSCstr\_Ca} \\ n_{NSCstr\_bp} \\ K_{NSCstr\_PKC\_Ca\_act} \\ K_{NSCstr\_PKG\_Ca\_act} \\ k_{PKC\_NSCstr} \\ k_{PKG\_NSCstr} \\ k_{PP\_NSCstr} \end{pmatrix} := NSCstr$

[Seq.B.44] $\begin{pmatrix} k_{PKA\_PDE} \\ k_{PKG\_PDE} \\ k_{PP\_PDE} \\ n_{PDE} \\ PDE_{cAMP\_T} \\ K_{PDE\_cAMP} \\ K_{PDE\_cAMP\_P} \\ k_{PDE\_cAMP} \\ PDE_{cGMP\_T} \\ K_{PDE\_cGMP} \\ K_{PDE\_cGMP\_P} \\ k_{PDE\_cGMP} \end{pmatrix} := PDE$

[Seq.B.45]

$PKA\_PKC\_PKG := submatrix(PARAS, 226, 234, 0, 0)$

[Seq.B.46]

$PLC\beta := submatrix(PARAS, 236, 253, 0, 0)$

[Seq.B.47]

$PMCA := submatrix(PARAS, 255, 257, 0, 0)$

[Seq.B.48] $\begin{pmatrix} K_{PKA\_cAMP} \\ n_{PKA\_cAMP} \\ K_{PKC\_DAG} \\ K_{PKC\_Ca} \\ n_{PKC\_Ca} \\ K_{PKG\_cGMP} \\ n_{PKG\_cGMP} \\ K_{PKC\varepsilon\_DAG} \\ K_{PKD\_DAG} \end{pmatrix} := PKA\_PKC\_PKG$

[Seq.B.49] $\begin{pmatrix} PLC_T \\ k_{PLC\_PIP\_on} \\ k_{PLC\_PIP\_off} \\ k_{PLC\_PIP\_hyd} \\ k_{PLC\_Gq0\_GTP\_on} \\ k_{PLC\_Gq0\_GTP\_off} \\ k_{PLC\_Gq0\_GTP\_hyd} \\ k_{PLC\_Gq0\_GTP\_PIP\_on} \\ k_{PLC\_Gq0\_GTP\_PIP\_off} \\ k_{PLC\_Gq0\_GTP\_PIP\_hyd} \\ k_{PKA\_PLC\_Gq0\_GTP} \\ k_{PKC\_PLC\_Gq0\_GTP} \\ k_{PLC\_P\_Gq0\_GTP\_on} \\ k_{PLC\_P\_Gq0\_GTP\_off} \\ k_{PP\_PLC} \\ PIP_T \\ k_{met\_DAG} \\ k_{met\_IP3} \end{pmatrix} := PLC\beta$

[Seq.B.50] $\begin{pmatrix} I_{PMCA\_max} \\ K_{PMCA\_Ca} \\ n_{PMCA\_Ca} \end{pmatrix} := PMCA$

[Seq.B.51]

$P2XR := submatrix(PARAS, 260, 278, 0, 0)$

[Seq.B.52]

$RyR := submatrix(PARAS, 282, 295, 0, 0)$

[Seq.B.53]

$SERCA := submatrix(PARAS, 298, 307, 0, 0)$

[Seq.B.54] $\begin{pmatrix} P2XR_T \\ perm_{NaP2XR} \\ perm_{KP2XR} \\ perm_{CaP2XR} \\ k_{P2XR\_0\_on} \\ k_{P2XR\_3\_off} \\ n\_P2XR \\ k_{P2XR\_3\_act} \\ k_{P2XR\_3\_deact} \\ k_{P2XR\_3\_act\_desens} \\ k_{P2XD\_3\_resens} \\ k_{P2XR\_0\_desens} \\ k_{P2XD\_0\_resens} \\ k_{P2XD\_0\_on} \\ k_{P2XD\_3\_off} \\ k_{P2XD\_0\_PKD\_on} \\ k_{P2XD\_3\_PKD\_off} \\ k_{PKD\_P2XD\_3} \\ k_{PP\_P2XD\_0\_PKD} \end{pmatrix} := P2XR$

[Seq.B.55] $\begin{pmatrix} RyR_T \\ perm_{RyR} \\ K_{RyR\_Ca\_SR} \\ n_{RyR\_Ca\_SR} \\ K_{RyR\_Ca\_jun\_max} \\ K_{RyR\_Ca\_jun\_min} \\ n_{RyR\_Ca\_jun} \\ K_{RyR\_Ca\_inh} \\ n_{RyR\_Ca\_inh} \\ k_{PKA\_RyR} \\ k_{PKC\_RyR} \\ k_{PP\_RyR} \\ f_{RyR\_PKA\_min} \\ f_{RyR\_PKC\_max} \end{pmatrix} := RyR$

[Seq.B.56] $\begin{pmatrix} SERCA_T \\ I_{SERCA\_max} \\ K_{SERCA\_Ca} \\ n_{SERCA} \\ K_{SERCA\_inh\_Ca\_SRcen} \\ K_{SERCA\_P\_Ca} \\ k_{PKA\_SERCA} \\ k_{PKC\_SERCA} \\ k_{PKG\_SERCA} \\ k_{PP\_SERCA} \end{pmatrix} := SERCA$

[Seq.B.57]

$sGC := submatrix(PARAS, 310, 321, 0, 0)$

[Seq.B.58]

$BUFFERS := submatrix(PARAS, 333, 341, 0, 0)$

[Seq.B.59]
$$\begin{pmatrix} GC_T \\ k_{GC0\_NO\_on} \\ k_{GC1\_NO\_off} \\ k_{GC1\_NO\_on} \\ k_{GC2\_NO\_off} \\ k_{GC1\_act} \\ k_{GC1\_deact} \\ k_{GC2\_act} \\ k_{PKG\_GC} \\ k_{PP\_GC} \\ k_{GC\_act\_GTP} \\ k_{GC\_basal\_GTP} \end{pmatrix} := sGC$$

[Seq.B.60]
$$\begin{pmatrix} BUF_T \\ k_{BUF\_on} \\ k_{BUF\_off} \\ BUF_{jun\_T} \\ BUF_{NSCstr\_T} \\ CSQ_{SRcen\_T} \\ CSQ_{SRper\_T} \\ k_{CSQ\_on} \\ k_{CSQ\_off} \end{pmatrix} := BUFFERS$$

[Seq.B.61]
$$CAPAC\_VOLS := submatrix(PARAS, 324, 329, 0, 0)$$

[Seq.B.62]
$$INTRACELL\_FLUX := submatrix(PARAS, 344, 346, 0, 0)$$

[Seq.B.63]
$$IONS\_T\_\beta := submatrix(PARAS, 349, 353, 0, 0)$$

[Seq.B.64]
$$\begin{pmatrix} C_m \\ VOL_{cell} \\ VOL_{SRper} \\ VOL_{jun} \\ VOL_{SRcen} \\ VOL_{NSCstr} \end{pmatrix} := CAPAC\_VOLS$$

[Seq.B.65]
$$\begin{pmatrix} \lambda_{jun\_cyt} \\ \lambda_{cen\_per} \\ \lambda_{NSCstr\_cyt} \end{pmatrix} := INTRACELL\_FLUX$$

[Seq.B.66]
$$\begin{pmatrix} T \\ Na_{ex} \\ K_{ex} \\ Ca_{ex} \\ Cl_{ex} \end{pmatrix} := IONS\_T\_\beta$$

Physical constants

[Seq.B.67-73] $N_A := 6.022 \cdot 10^{23}$ $R := 8.314$ $F := 96487$ $z_{Na} := 1$ $z_K := 1$ $z_{Ca} := 2$ $z_{Cl} := -1$

Frequently used combinations

[Seq.B.74] $\nu := N_A \cdot VOL_{cell}$

[Seq.B.75] $\beta := \frac{F}{(1000 \cdot R \cdot T)}$

C. APPLICATION OF EFFECTORS

Change in concentration of αA from αA_0 to αA_1 and its return to αA_0.

$\tau_{\alpha A1}$, start application; $\tau_{\alpha A2}$, start plateau; $\tau_{\alpha A3}$, start wash-out; $\kappa_{\alpha A1}$, rise rate constant; $\kappa_{\alpha A2}$, wash-out rate constant. Power of 2 rounds the corners.

[Seq.C.1]

$$\alpha A\_steady(\alpha A_0, \alpha A_1, t) := \begin{cases} \alpha A_0 & \text{if } 0 \le t < \tau_{\alpha A1} \\ \alpha A_0 + (\alpha A_1 - \alpha A_0) \cdot \left[1 - e^{-\kappa_{\alpha A1} \cdot (t - \tau_{\alpha A1})}\right]^2 & \text{if } \tau_{\alpha A1} \le t < \tau_{\alpha A2} \\ \alpha A_0 + (\alpha A_1 - \alpha A_0) \cdot \left[1 - e^{-\kappa_{\alpha A1} \cdot (\tau_{\alpha A2} - \tau_{\alpha A1})}\right]^2 & \text{if } \tau_{\alpha A2} \le t < \tau_{\alpha A3} \\ \alpha A_0 + (\alpha A_1 - \alpha A_0) \cdot \left[1 - e^{-\kappa_{\alpha A1} \cdot (\tau_{\alpha A2} - \tau_{\alpha A1})}\right]^2 \cdot e^{-\kappa_{\alpha A2} \cdot (t - \tau_{\alpha A3})} & \text{if } \tau_{\alpha A3} \le t \end{cases}$$

Pulsatile application of αA, raising concentration from αA_0 to αA_1.

τ_{pulse_init}, initial pulse start; $\Delta\tau_{pulse\_on}$, pulse-on duration; $\Delta\tau_{pulse\_off}$, pulse-off duration; n_{cycles}, number of on-off cycles.

[Seq.C2] $cycle\_period := \Delta\tau_{pulse\_on} + \Delta\tau_{pulse\_off}$

[Seq.C3] $t_{cycles\_end} := n_{cycles} \cdot cycle\_period + \tau_{pulse\_init}$

Define pulse_number(t) that returns which pulse, if any, t is in, and pulse_start(t) that returns the start time of that pulse. pulse_number(t) can exceed n.cycles, the specified number of cycles, but only n.cycles will occur before $t > t_{cycles\_end}$.

[Seq.C4] $$\text{pulse\_number}(t) := \text{floor}\left(\frac{t - \tau_{\text{pulse\_init}}}{\text{cycle\_period}}\right) + 1$$

[Seq.C5] $$\text{pulse\_start}(t) := \tau_{\text{pulse\_init}} + (\text{pulse\_number}(t) - 1)\cdot\text{cycle\_period}$$

[Seq.C6] $$\alpha A\_\text{rise}\left(\alpha A_0, \alpha A_1, t\right) := \alpha A_0 + \left(\alpha A_1 - \alpha A_0\right)\cdot\left[1 - e^{-\kappa_{\alpha A1}\cdot(t - \text{pulse\_start}(t))}\right]^2$$

[Seq.C7] $$\alpha A\_\text{fall}\left(\alpha A_0, \alpha A_1, t\right) := \alpha A_0 + \left(\alpha A_1 - \alpha A_0\right)\cdot\left(1 - e^{-\kappa_{\alpha A1}\cdot\Delta\tau_{\text{pulse\_on}}}\right)^2 \cdot e^{-\kappa_{\alpha A2}\cdot\left(t - \text{pulse\_start}(t) - \Delta\tau_{\text{pulse\_on}}\right)}$$

[Seq.C8]
$$\alpha A\_\text{pulse}\left(\alpha A_0, \alpha A_1, t\right) := \begin{cases} \text{alphaA} \leftarrow \alpha A\_\text{rise}\left(\alpha A_0, \alpha A_1, t\right) & \text{if } \left(\tau_{\text{pulse\_init}} \le t \le t_{\text{cycles\_end}} \wedge 0 \le t - \text{pulse\_start}(t) \le \Delta\tau_{\text{pulse\_on}}\right) \\ \text{alphaA} \leftarrow \alpha A\_\text{fall}\left(\alpha A_0, \alpha A_1, t\right) & \text{if } \left(\tau_{\text{pulse\_init}} \le t \le t_{\text{cycles\_end}} \wedge 0 < t - \text{pulse\_start}(t) - \Delta\tau_{\text{pulse\_on}} \le \Delta\tau_{\text{pulse\_off}}\right) \\ \text{alphaA} \leftarrow \alpha A_0 & \text{otherwise} \end{cases}$$

Change in concentration of ATP from ATP_0 to ATP_1 and its return to ATP_0.

[Seq.C9]
$$\text{ATP\_steady}\left(ATP_0, ATP_1, t\right) := \begin{cases} ATP_0 & \text{if } 0 \le t < \tau_{\text{atp1}} \\ ATP_0 + \left(ATP_1 - ATP_0\right)\cdot\left[1 - e^{-\kappa_{\text{atp1}}\cdot\left(t - \tau_{\text{atp1}}\right)}\right]^2 & \text{if } \tau_{\text{atp1}} \le t < \tau_{\text{atp2}} \\ ATP_0 + \left(ATP_1 - ATP_0\right)\cdot\left[1 - e^{-\kappa_{\text{atp1}}\cdot\left(\tau_{\text{atp2}} - \tau_{\text{atp1}}\right)}\right]^2 & \text{if } \tau_{\text{atp2}} \le t < \tau_{\text{atp3}} \\ ATP_0 + \left(ATP_1 - ATP_0\right)\cdot\left[1 - e^{-\kappa_{\text{atp1}}\cdot\left(\tau_{\text{atp2}} - \tau_{\text{atp1}}\right)}\right]^2 \cdot e^{-\kappa_{\text{atp2}}\cdot\left(t - \tau_{\text{atp3}}\right)} & \text{if } \tau_{\text{atp3}} \le t \end{cases}$$

Pulsatile application of ATPex (co-ordinated with pulsatile application of αA)

[Seq.C10]
$$\mathrm{ATP\_rise}(\mathrm{ATP}_0,\mathrm{ATP}_1,t) := \mathrm{ATP}_0 + (\mathrm{ATP}_1 - \mathrm{ATP}_0)\cdot\left[1 - e^{-\kappa_{atp1}\cdot(t-\mathrm{pulse\_start}(t))}\right]^2$$

[Seq.C11]
$$\mathrm{ATP\_fall}(\mathrm{ATP}_0,\mathrm{ATP}_1,t) := \mathrm{ATP}_0 + (\mathrm{ATP}_1 - \mathrm{ATP}_0)\cdot\left(1 - e^{-\kappa_{atp1}\cdot\Delta\tau_{pulse\_on}}\right)^2\cdot e^{-\kappa_{atp2}\cdot\left(t-\mathrm{pulse\_start}(t)-\Delta\tau_{pulse\_on}\right)}$$

[Seq.C12]
$$\mathrm{ATP\_pulse}(\mathrm{ATP}_0,\mathrm{ATP}_1,t) := \begin{cases} \mathrm{ATP} \leftarrow \mathrm{ATP\_rise}(\mathrm{ATP}_0,\mathrm{ATP}_1,t) & \text{if } \left(\tau_{pulse\_init} \le t \le t_{cycles\_end} \wedge 0 \le t - \mathrm{pulse\_start}(t) \le \Delta\tau_{pulse\_on}\right) \\ \mathrm{ATP} \leftarrow \mathrm{ATP\_fall}(\mathrm{ATP}_0,\mathrm{ATP}_1,t) & \text{if } \left(\tau_{pulse\_init} \le t \le t_{cycles\_end} \wedge 0 < t - \mathrm{pulse\_start}(t) - \Delta\tau_{pulse\_on} \le \Delta\tau_{pulse\_off}\right) \\ \mathrm{ATP} \leftarrow \mathrm{ATP}_0 & \text{otherwise} \end{cases}$$

Change in concentration of βA from βA_0 to βA_1 and its return to βA_0.

[Seq.C13]
$$\beta A(\beta A_0,\beta A_1,t) := \begin{cases} \beta A_0 & \text{if } 0 \le t < \tau_{\beta A1} \\ \beta A_0 + (\beta A_1 - \beta A_0)\cdot\left[1 - e^{-\kappa_{\beta A1}\cdot(t-\tau_{\beta A1})}\right]^2 & \text{if } \tau_{\beta A1} \le t < \tau_{\beta A2} \\ \beta A_0 + (\beta A_1 - \beta A_0)\cdot\left[1 - e^{-\kappa_{\beta A1}\cdot(\tau_{\beta A2}-\tau_{\beta A1})}\right]^2 & \text{if } \tau_{\beta A2} \le t < \tau_{\beta A3} \\ \beta A_0 + (\beta A_1 - \beta A_0)\cdot\left[1 - e^{-\kappa_{\beta A1}\cdot(\tau_{\beta A2}-\tau_{\beta A1})}\right]^2\cdot e^{-\kappa_{\beta A2}\cdot(t-\tau_{\beta A3})} & \text{if } \tau_{\beta A3} \le t \end{cases}$$

Change in intravascular pressure, BP, from BP_0 to BP_1 and its return to BP_0.

[Seq.C14]

$$BP(BP_0, BP_1, t) := \begin{cases} BP_0 \ \text{ if } \ 0 \le t < \tau_{bp1} \\ BP_0 + (BP_1 - BP_0)\cdot\left[1 - e^{-\kappa_{bp1}\cdot(t-\tau_{bp1})}\right]^2 \ \text{ if } \ \tau_{bp1} \le t < \tau_{bp2} \\ BP_0 + (BP_1 - BP_0)\cdot\left[1 - e^{-\kappa_{bp1}\cdot(\tau_{bp2}-\tau_{bp1})}\right]^2 \ \text{ if } \ \tau_{bp2} \le t < \tau_{bp3} \\ BP_0 + (BP_1 - BP_0)\cdot\left[1 - e^{-\kappa_{bp1}\cdot(\tau_{bp2}-\tau_{bp1})}\right]^2 \cdot e^{-\kappa_{bp2}\cdot(t-\tau_{bp3})} \ \text{ if } \ \tau_{bp3} \le t \end{cases}$$

Change in concentration of EET from EET_0 to EET_1 and its return to EET_0.

[Seq.C15]

$$EET(EET_0, EET_1, t) := \begin{cases} EET_0 \ \text{ if } \ 0 \le t < \tau_{eet1} \\ EET_0 + (EET_1 - EET_0)\cdot\left[1 - e^{-\kappa_{eet1}\cdot(t-\tau_{eet1})}\right]^2 \ \text{ if } \ \tau_{eet1} \le t < \tau_{eet2} \\ EET_0 + (EET_1 - EET_0)\cdot\left[1 - e^{-\kappa_{eet1}\cdot(\tau_{eet2}-\tau_{eet1})}\right]^2 \ \text{ if } \ \tau_{eet2} \le t < \tau_{eet3} \\ EET_0 + (EET_1 - EET_0)\cdot\left[1 - e^{-\kappa_{eet1}\cdot(\tau_{eet2}-\tau_{eet1})}\right]^2 \cdot e^{-\kappa_{eet2}\cdot(t-\tau_{eet3})} \ \text{ if } \ \tau_{eet3} \le t \end{cases}$$

Change in concentration of NO from NO_0 to NO_1 and its return to NO_0.

[Seq.C16]

$$NO(NO_0, NO_1, t) := \begin{cases} NO_0 \ \text{ if } \ 0 \le t < \tau_{no1} \\ NO_0 + (NO_1 - NO_0)\cdot\left[1 - e^{-\kappa_{no1}\cdot(t-\tau_{no1})}\right]^2 \ \text{ if } \ \tau_{no1} \le t < \tau_{no2} \\ NO_0 + (NO_1 - NO_0)\cdot\left[1 - e^{-\kappa_{no1}\cdot(\tau_{no2}-\tau_{no1})}\right]^2 \ \text{ if } \ \tau_{no2} \le t < \tau_{no3} \\ NO_0 + (NO_1 - NO_0)\cdot\left[1 - e^{-\kappa_{no1}\cdot(\tau_{no2}-\tau_{no1})}\right]^2 \cdot e^{-\kappa_{no2}\cdot(t-\tau_{no3})} \ \text{ if } \ \tau_{no3} \le t \end{cases}$$

D. DIFFUSION OF Ca BETWEEN COMPARTMENTS

In the steady-state equations below, the variable c = Ca_{in} is the uniform concentration of Ca in the cytoplasm.

Total flux of Ca between all junctions and the cytoplasm

[Seq.D1] $J_{jun\_cyt}(Ca_{jun}, c) := 10^9 \cdot \lambda_{jun\_cyt} \cdot (Ca_{jun} - c)$ (fmol/(s*cell) ; conc in μM)

Total flux between total central SR and peripheral SR

[Seq.D2] $J_{cen\_per}(Ca_{SRcen}, Ca_{SRper}) := 10^9 \cdot \lambda_{cen\_per} \cdot (Ca_{SRcen} - Ca_{SRper})$

Total flux between NSCstr micordomains and the cytoplasm

[Seq.D3] $J_{CaNSCstr\_cyt}(Ca_{NSC\_str}, c) := 10^9 \cdot \lambda_{NSCstr\_cyt} \cdot (Ca_{NSC\_str} - c)$

E. SARCOLEMMAL CHANNELS OPEN PROBABILITIES, FLUXES, AND CURRENTS

Fluxes into the cytoplasm from the extracellular medium or from intracellular compartments are taken as positive; positive currents away from the cytoplasm to the extracellular medium or to intracellular compartments are taken as positive. Fluxes between intracellular compartments are also expressed as currents for comparison of their magnitudes with currents across the plasma membrane.

BK CHANNELS

Open probability of BK

[Seq.E1] $$X_{BK}(v) := \frac{\left[1 + \exp\left[z_{BK\_J} \cdot \beta \cdot (v - V_{BK\_closed})\right]\right]}{\left[1 + \exp\left[z_{BK\_J} \cdot \beta \cdot (v - V_{BK\_open})\right]\right]}$$

[Seq.E2] $$Y_{BK}(c) := \frac{\left(1 + \frac{c}{K_{BK\_closed}}\right)}{\left(1 + \frac{c}{K_{BK\_open}}\right)}$$

[Seq.E3] $$P_{BK}(v, c) := \frac{1}{1 + X_{BK}(v)^4 \cdot Y_{BK}(c)^8 \cdot \left(\frac{1}{L_{BK}}\right) \cdot \exp(-z_{BK\_L} \cdot \beta \cdot v)}$$

BK flux and current

[Seq.E4] $$J_{BK}(v,c,K_{in}) := \begin{cases} J \leftarrow 10^9 \cdot BK_T \cdot perm_{BK} \cdot P_{BK}(v,c)\left(K_{ex} - K_{in}\right) & \text{if } v = 0 \\ J \leftarrow 10^9 \cdot BK_T \cdot perm_{BK} \cdot P_{BK}(v,c) \cdot z_K \cdot \beta \cdot v \dfrac{\left(K_{ex} - K_{in} \cdot \exp\left(z_K \cdot \beta \cdot v\right)\right)}{\left(\exp\left(z_K \cdot \beta \cdot v\right) - 1\right)} & \text{if } v \neq 0 \end{cases}$$ (fmol/(cell*s)).

[Seq.E5] $$I_{BK}(v,c,K_{in}) := \frac{-z_K \cdot F \cdot J_{BK}(v,c,K_{in})}{1000}$$ (pA/cell)

Open probability of BK phosphorylated by PKA (BK_{PKA})

The enhancement is assumed to be due to an increase in $L_{BK,}$ now $L_{BK\_PKA.}$

[Seq.E6] $$P_{BK\_PKA}(v,c) := \frac{1}{1 + X_{BK}(v)^4 \cdot Y_{BK}(c)^8 \cdot \left(\frac{1}{L_{BK\_PKA}}\right) \cdot \exp\left(-z_{BK\_L} \cdot \beta \cdot v\right)}$$

BK_PKA flux and current

[Seq.E7] $$J_{BK\_PKA}(v,c,K_{in}) := \begin{cases} J \leftarrow 10^9 \cdot BK_T \cdot perm_{BK} \cdot P_{BK\_PKA}(v,c)\left(K_{ex} - K_{in}\right) & \text{if } v = 0 \\ J \leftarrow 10^9 \cdot BK_T \cdot perm_{BK} \cdot P_{BK\_PKA}(v,c) \cdot z_K \cdot \beta \cdot v \dfrac{\left(K_{ex} - K_{in} \cdot \exp\left(z_K \cdot \beta \cdot v\right)\right)}{\left(\exp\left(z_K \cdot \beta \cdot v\right) - 1\right)} & \text{if } v \neq 0 \end{cases}$$

[Seq.E8] $$I_{BK\_PKA}(v,c,K_{in}) := \frac{-z_K \cdot F \cdot J_{BK\_PKA}(v,c,K_{in})}{1000}$$

Open probability of BK phosphorylated by PKC (BK_{PKC})

The suppression is assumed to be due to a decrease in $L_{BK,}$ now $L_{BK\_PKC.}$

[Seq.E9] $$P_{BK\_PKC}(v,c) := \frac{1}{1 + X_{BK}(v)^4 \cdot Y_{BK}(c)^8 \cdot \left(\frac{1}{L_{BK\_PKC}}\right) \cdot \exp\left(-z_{BK\_L} \cdot \beta \cdot v\right)}$$

BK_PKC flux and current

[Seq.E10]
$$J_{BK\_PKC}(v,c,K_{in}) := \begin{cases} J \leftarrow 10^9 \cdot BK_T \cdot perm_{BK} \cdot P_{BK\_PKC}(v,c)\left(K_{ex} - K_{in}\right) & \text{if } v = 0 \\ J \leftarrow 10^9 \cdot BK_T \cdot perm_{BK} \cdot P_{BK\_PKC}(v,c) \cdot z_K \cdot \beta \cdot v \dfrac{\left(K_{ex} - K_{in} \cdot \exp\left(z_K \cdot \beta \cdot v\right)\right)}{\left(\exp\left(z_K \cdot \beta \cdot v\right) - 1\right)} & \text{if } v \neq 0 \end{cases}$$

[Seq.E11]
$$I_{BK\_PKC}(v,c,K_{in}) := -\frac{z_K \cdot F \cdot J_{BK\_PKC}(v,c,K_{in})}{1000}$$

Open probability of BK phosphorylated by PKG (BK_{PKG})

The enhancement is assumed to be due to an increase in $L_{BK,}$ now $L_{BK\_PKG.}$

[Seq.E12]
$$P_{BK\_PKG}(v,c) := \frac{1}{1 + X_{BK}(v)^4 \cdot Y_{BK}(c)^8 \cdot \left(\dfrac{1}{L_{BK\_PKG}}\right) \cdot \exp\left(-z_{BK\_L} \cdot \beta \cdot v\right)}$$

BK_PKG flux and current

[Seq.E13]
$$J_{BK\_PKG}(v,c,K_{in}) := \begin{cases} J \leftarrow 10^9 \cdot BK_T \cdot perm_{BK} \cdot P_{BK\_PKG}(v,c)\left(K_{ex} - K_{in}\right) & \text{if } v = 0 \\ J \leftarrow 10^9 \cdot BK_T \cdot perm_{BK} \cdot P_{BK\_PKG}(v,c) \cdot z_K \cdot \beta \cdot v \dfrac{\left(K_{ex} - K_{in} \cdot \exp\left(z_K \cdot \beta \cdot v\right)\right)}{\left(\exp\left(z_K \cdot \beta \cdot v\right) - 1\right)} & \text{if } v \neq 0 \end{cases}$$

[Seq.E14]
$$I_{BK\_PKG}(v,c,K_{in}) := \frac{-z_K \cdot F \cdot J_{BK\_PKG}(v,c,K_{in})}{1000}$$

Total flux and current due to BK and PKA-, PKG- and PKC-phosphorylated BK

[Seq.E15]
$$I_{BK\_ALL}(v,c,K_{in},BK,BK_{PKA},BK_{PKC},BK_{PKG}) := \frac{1}{BK_T} \cdot \begin{pmatrix} BK \cdot I_{BK}(v,c,K_{in}) + BK_{PKC} \cdot I_{BK\_PKC}(v,c,K_{in}) \ldots \\ + BK_{PKA} \cdot I_{BK\_PKA}(v,c,K_{in}) + BK_{PKG} \cdot I_{BK\_PKG}(v,c,K_{in}) \end{pmatrix}$$

[Seq.E16]
$$J_{BK\_ALL}(v,c,K_{in},BK,BK_{PKA},BK_{PKC},BK_{PKG}) := \frac{-1000}{F} \cdot I_{BK\_ALL}(v,c,K_{in},BK,BK_{PKA},BK_{PKC},BK_{PKG})$$

CaV CHANNELS

Open probability of CaV

[Seq.E17] $$X_{CaVa}(v) := \frac{1}{1 + \exp\left[\frac{-\left(v - V_{CaV\_act}\right)}{\xi_{CaV\_act}}\right]}$$

[Seq.E18] $$Y_{CaVi}(v,c) := \frac{1}{1 + \frac{c}{K_{CaV\_inh}}}$$

[Seq.E19] $$P_{CaV}(v,c) := X_{CaVa}(v)\cdot Y_{CaVi}(v,c)$$

CaV flux and current

[Seq.E20] $$J_{CaV}(v,c) := \begin{cases} J \leftarrow 10^{6}\cdot CaV_T\cdot perm_{CaV}\cdot P_{CaV}(v,c)\left(Ca_{ex} - c\right) & \text{if } v = 0 \\ J \leftarrow 10^{6}\cdot CaV_T\cdot perm_{CaV}\cdot P_{CaV}(v,c)\cdot z_{Ca}\cdot\beta\cdot v\,\frac{\left(Ca_{ex} - c\cdot\exp\left(z_{Ca}\cdot\beta\cdot v\right)\right)}{\exp\left(z_{Ca}\cdot\beta\cdot v\right) - 1} & \text{if } v \neq 0 \end{cases}$$

[Seq.E21] $$I_{CaV}(v,c) := \frac{-z_{Ca}\cdot F\cdot J_{CaV}(v,c)}{1000}$$

Open probability of CaV_{PKC}

[Seq.E22] $$X_{CaV\_PKC\_a}(v) := \frac{1}{1 + \exp\left[\frac{-\left[v - \left(V_{CaV\_PKC\_act}\right)\right]}{\xi_{CaV\_act}}\right]}$$

[Seq.E23] $$P_{CaV\_PKC}(v,c) := X_{CaV\_PKC\_a}(v)\cdot Y_{CaVi}(v,c)$$

CaV_{PKC} flux and current

[Seq.E24] $$J_{CaV\_PKC}(v,c) := \begin{cases} J \leftarrow 10^{6}\cdot CaV_T\cdot perm_{CaV}\cdot P_{CaV\_PKC}(v,c)\left(Ca_{ex} - c\right) & \text{if } v = 0 \\ J \leftarrow 10^{6}\cdot CaV_T\cdot perm_{CaV}\cdot P_{CaV\_PKC}(v,c)\cdot z_{Ca}\cdot\beta\cdot v\,\frac{\left(Ca_{ex} - c\cdot\exp\left(z_{Ca}\cdot\beta\cdot v\right)\right)}{\left(\exp\left(z_{Ca}\cdot\beta\cdot v\right) - 1\right)} & \text{if } v \neq 0 \end{cases}$$

[Seq.E25] $$I_{CaV\_PKC}(v,c) := \frac{-z_{Ca}\cdot F\cdot J_{CaV\_PKC}(v,c)}{1000}$$

Open probability of CaV_{PKG}

[Seq.E26] $$X_{CaV\_PKG\_a}(v) := \frac{1}{1 + \exp\left[\frac{-\left[v - \left(V_{CaV\_PKG\_act}\right)\right]}{\xi_{CaV\_act}}\right]}$$

[Seq.E27] $$P_{CaV\_PKG}(v,c) := X_{CaV\_PKG\_a}(v) \cdot Y_{CaVi}(v,c)$$

CaV_{PKG} flux and current

[Seq.E28] $$J_{CaV\_PKG}(v,c) := \begin{cases} J \leftarrow 10^6 \cdot CaV_T \cdot perm_{CaV} \cdot P_{CaV\_PKG}(v,c)\left(Ca_{ex} - c\right) & \text{if } v = 0 \\ J \leftarrow 10^6 \cdot CaV_T \cdot perm_{CaV} \cdot P_{CaV\_PKG}(v,c) \cdot z_{Ca} \cdot \beta \cdot v \dfrac{\left(Ca_{ex} - c \cdot \exp\left(z_{Ca} \cdot \beta \cdot v\right)\right)}{\left(\exp\left(z_{Ca} \cdot \beta \cdot v\right) - 1\right)} & \text{if } v \neq 0 \end{cases}$$

[Seq.E29] $$I_{CaV\_PKG}(v,c) := \frac{-z_{Ca} \cdot F \cdot J_{CaV\_PKG}(v,c)}{1000}$$

Total current due to CaV + $CaV_{.PKC}$ + CaV_{PKG}

[Seq.E30] $$I_{CaV\_ALL}\left(v,c,CaV,CaV_{PKC},CaV_{PKG}\right) := \frac{\left(CaV \cdot I_{CaV}(v,c) + CaV_{PKC} \cdot I_{CaV\_PKC}(v,c) + CaV_{PKG} \cdot I_{CaV\_PKG}(v,c)\right)}{CaV_T}$$

CIA CHANNELS

Open probability of CIA

Assume that $K_{ClA\_Ca\_act}$ decreases with V with an effective moving charge of ζ_{ClA}..

[Seq.E31] $$X_{ClA}(v) := \frac{1}{1 + \exp\left[-\zeta_{ClA}\cdot\beta\cdot\left(v - V_{ClA}\right)\right]}$$

[Seq.E32] $$K_{ClA\_Ca\_act}(v) := \frac{1}{\frac{1}{K_{ClA\_Ca\_act\_max}} + X_{ClA}(v)\cdot\left(\frac{1}{K_{ClA\_Ca\_act\_min}} - \frac{1}{K_{ClA\_Ca\_act\_max}}\right)}$$

[Seq.E33] $$P_{ClA}\left(v, Ca_{NSC\_str}\right) := \frac{Ca_{NSC\_str}^{\ n_{ClA}}}{Ca_{NSC\_str}^{\ n_{ClA}} + K_{ClA\_Ca\_act}(v)^{n_{ClA}}}\cdot\left(\frac{K_{ClA\_Ca\_inh}^{\ n_{ClA}}}{Ca_{NSC\_str}^{\ n_{ClA}} + K_{ClA\_Ca\_inh}^{\ n_{ClA}}}\right)$$

ClA flux and current

[Seq.E34] $$\xi_{Cl}\left(v, Cl_{in}\right) := z_{Cl}\cdot\beta\cdot v\,\frac{\left(Cl_{ex} - Cl_{in}\cdot\exp\left(z_{Cl}\cdot\beta\cdot v\right)\right)}{\exp\left(z_{Cl}\cdot\beta\cdot v\right) - 1}$$

[Seq.E35] $$J_{ClA}\left(v, Ca_{NSC\_str}, Cl_{in}\right) := \begin{cases} J \leftarrow 10^{9}\cdot Cl_{AT}\cdot perm_{ClA}\cdot P_{ClA}\left(v, Ca_{NSC\_str}\right)\left(Cl_{ex} - Cl_{in}\right) & \text{if } v = 0 \\ J \leftarrow 10^{9}\cdot Cl_{AT}\cdot perm_{ClA}\cdot P_{ClA}\left(v, Ca_{NSC\_str}\right)\cdot\xi_{Cl}\left(v, Cl_{in}\right) & \text{if } v \neq 0 \end{cases}$$

[Seq.E36] $$I_{ClA}\left(v, Ca_{NSC\_str}, Cl_{in}\right) := \frac{-z_{Cl}\cdot F\cdot J_{ClA}\left(v, Ca_{NSC\_str}, Cl_{in}\right)}{1000}$$

KATP CHANNELS

KATP open probability

KATP flux & current

[Seq.E37]

$$J_{KATP}(v, K_{in}, KATP) := \begin{cases} J \leftarrow 10^{9} \cdot KATP \cdot perm_{KATP} \cdot P_{open\_KATP}(K_{ex} - K_{in}) & \text{if } v = 0 \\ J \leftarrow 10^{9} \cdot KATP \cdot perm_{KATP} \cdot P_{open\_KATP} \cdot z_K \cdot \beta \cdot v \dfrac{(K_{ex} - K_{in} \cdot \exp(z_K \cdot \beta \cdot v))}{\exp(z_K \cdot \beta \cdot v) - 1} & \text{if } v \neq 0 \end{cases}$$

[Seq.E38]

$$I_{KATP}(v, K_{in}, KATP) := \frac{-z_K \cdot F \cdot J_{KATP}(v, K_{in}, KATP)}{1000}$$

KATP_PKA flux & current

[Seq.E39]

$$J_{KATP\_PKA}(v, K_{in}, KATP_{PKA}) := \begin{cases} J \leftarrow 10^{9} \cdot KATP_{PKA} \cdot perm_{KATP} \cdot P_{open\_KATP\_PKA}(K_{ex} - K_{in}) & \text{if } v = 0 \\ J \leftarrow 10^{9} \cdot KATP_{PKA} \cdot perm_{KATP} \cdot P_{open\_KATP\_PKA} \cdot z_K \cdot \beta \cdot v \dfrac{(K_{ex} - K_{in} \cdot \exp(z_K \cdot \beta \cdot v))}{\exp(z_K \cdot \beta \cdot v) - 1} & \text{if } v \neq 0 \end{cases}$$

[Seq.E40]

$$I_{KATP\_PKA}(v, K_{in}, KATP_{PKA}) := \frac{-z_K \cdot F \cdot J_{KATP\_PKA}(v, K_{in}, KATP_{PKA})}{1000}$$

KATP_ALL flux & current

[Seq.E41]

$$J_{KATP\_ALL}(v, K_{in}, KATP, KATP_{PKA}) := J_{KATP}(v, K_{in}, KATP) + J_{KATP\_PKA}(v, K_{in}, KATP_{PKA})$$

[Seq.E42]

$$I_{KATP\_ALL}(v, K_{in}, KATP, KATP_{PKA}) := I_{KATP}(v, K_{in}, KATP) + I_{KATP\_PKA}(v, K_{in}, KATP_{PKA})$$

Kv CHANNELS

Kv open probability

[Seq.E43] $$P_{Kv}(v) := \frac{1}{1 + \exp\left[\frac{-(v - V_{Kv})}{\xi_{Kv}}\right]}$$

Kv flux & current

[Seq.E44] $$J_{Kv}(v, K_{in}) := \begin{cases} J \leftarrow 10^9 \cdot Kv_T \cdot perm_{Kv} \cdot P_{Kv}(v)(K_{ex} - K_{in}) & \text{if } v = 0 \\ J \leftarrow 10^9 \cdot Kv_T \cdot perm_{Kv} \cdot P_{Kv}(v) \cdot z_K \cdot \beta \cdot v \dfrac{(K_{ex} - K_{in} \cdot \exp(z_K \cdot \beta \cdot v))}{\exp(z_K \cdot \beta \cdot v) - 1} & \text{if } v \neq 0 \end{cases}$$

[Seq.E45] $$I_{Kv}(v, K_{in}) := \frac{-z_K \cdot F \cdot J_{Kv}(v, K_{in})}{1000}$$

LEAKS

Cl leak flux & current

[Seq.E46] $$J_{Cl\_leak}(v, Cl_{in}) := \begin{cases} J \leftarrow 10^9 \cdot Cl_{leakT} \cdot perm_{Cl\_leak} \cdot (Cl_{ex} - Cl_{in}) & \text{if } v = 0 \\ J \leftarrow 10^9 \cdot Cl_{leakT} \cdot perm_{Cl\_leak} \cdot z_{Cl} \cdot \beta \cdot v \dfrac{(Cl_{ex} - Cl_{in} \cdot \exp(z_{Cl} \cdot \beta \cdot v))}{\exp(z_{Cl} \cdot \beta \cdot v) - 1} & \text{if } v \neq 0 \end{cases}$$

[Seq.E47] $$I_{Cl\_leak}(v, Cl_{in}) := \frac{-z_{Cl} \cdot F \cdot J_{Cl\_leak}(v, Cl_{in})}{1000}$$

K leak flux & current

[Seq.E48] $$J_{K\_leak}(v, K_{in}) := \begin{cases} J \leftarrow 10^9 \cdot K_{leakT} \cdot perm_{K\_leak} \cdot (K_{ex} - K_{in}) & \text{if } v = 0 \\ J \leftarrow 10^9 \cdot K_{leakT} \cdot perm_{K\_leak} \cdot z_K \cdot \beta \cdot v \dfrac{(K_{ex} - K_{in} \cdot \exp(z_K \cdot \beta \cdot v))}{\exp(z_K \cdot \beta \cdot v) - 1} & \text{if } v \neq 0 \end{cases}$$

[Seq.E49] $$I_{K\_leak}(v, K_{in}) := \frac{-z_K \cdot F \cdot J_{K\_leak}(v, K_{in})}{1000}$$

Na leak flux & current

[Seq.E50] $$J_{Na\_leak}(v, Na_{in}) := \begin{cases} J \leftarrow 10^9 \cdot Na_{leakT} \cdot perm_{Na\_leak} \cdot (Na_{ex} - Na_{in}) & \text{if } v = 0 \\ J \leftarrow 10^9 Na_{leakT} \cdot perm_{Na\_leak} \cdot z_{Na} \cdot \beta \cdot v \dfrac{(Na_{ex} - Na_{in} \cdot \exp(z_{Na} \cdot \beta \cdot v))}{\exp(z_{Na} \cdot \beta \cdot v) - 1} & \text{if } v \neq 0 \end{cases}$$

[Seq.E51] $$I_{Na\_leak}(v, Na_{in}) := \frac{-z_{Na} \cdot F \cdot J_{Na\_leak}(v, Na_{in})}{1000}$$

Ca leak flux & current

[Seq.E52] $$J_{Ca\_leak}(v, Ca_{in}) := \begin{cases} J \leftarrow \left[10^6 \cdot Ca_{leakT} \cdot perm_{Ca\_leak} \cdot (Ca_{ex} - Ca_{in})\right] & \text{if } v = 0 \\ J \leftarrow 10^6 Ca_{leakT} \cdot perm_{Ca\_leak} \cdot z_{Ca} \cdot \beta \cdot v \dfrac{(Ca_{ex} - Ca_{in} \cdot \exp(z_{Ca} \cdot \beta \cdot v))}{\exp(z_{Ca} \cdot \beta \cdot v) - 1} & \text{if } v \neq 0 \end{cases}$$

[Seq.E53] $$I_{Ca\_leak}(v, Ca_{in}) := \frac{-z_{Ca} \cdot F \cdot J_{Ca\_leak}(v, Ca_{in})}{1000}$$

Total leak current

[Seq.E54] $$I_{ALL\_leak}(v, K_{in}, Na_{in}, Cl_{in}, Ca_{in}) := I_{K\_leak}(v, K_{in}) + I_{Na\_leak}(v, Na_{in}) + I_{Cl\_leak}(v, Cl_{in}) + I_{Ca\_leak}(v, Ca_{in})$$

NSCeet CHANNELS

Open probability of NSCeet channels

[Seq.E55] $$V_{NSCeet}(eet) := \left(V_{NSCeet\_min} - V_{NSCeet\_max}\right)\cdot\left(\frac{eet}{eet + K_{NSCeet\_EET}}\right) + V_{NSCeet\_max}$$

[Seq.E56] $$P_{NSCeet}(v, eet) := \frac{1}{1 + \exp\left[\frac{-\left(v - V_{NSCeet}(eet)\right)}{\xi_{NSCeet}}\right]}\cdot\left(\frac{eet}{eet + K_{NSCeet\_EET}}\right)$$

NSCeet fluxes and currents NSCeet

[Seq.E57] $$J_{NaNSCeet}\left(v, eet, Na_{in}\right) := \begin{cases} J \leftarrow 10^{9}\cdot NSCeet_{T}\cdot perm_{NaNSCeet}\cdot P_{NSCeet}(v, eet)\left(Na_{ex} - Na_{in}\right) & \text{if } v = 0 \\ J \leftarrow 10^{9}\cdot NSCeet_{T}\cdot perm_{NaNSCeet}\cdot P_{NSCeet}(v, eet)\cdot z_{Na}\cdot\beta\cdot v\,\frac{\left(Na_{ex} - Na_{in}\cdot\exp\left(z_{Na}\cdot\beta\cdot v\right)\right)}{\exp\left(z_{Na}\cdot\beta\cdot v\right) - 1} & \text{if } v \neq 0 \end{cases}$$

[Seq.E58] $$I_{NaNSCeet}\left(v, eet, Na_{in}\right) := \frac{-z_{Na}\cdot F\cdot J_{NaNSCeet}\left(v, eet, Na_{in}\right)}{1000}$$

[Seq.E59] $$J_{KNSCeet}\left(v, eet, K_{in}\right) := \begin{cases} J \leftarrow 10^{9}\cdot NSCeet_{T}\cdot perm_{KNSCeet}\cdot P_{NSCeet}(v, eet)\left(K_{ex} - K_{in}\right) & \text{if } v = 0 \\ J \leftarrow 10^{9}\cdot NSCeet_{T}\cdot perm_{KNSCeet}\cdot P_{NSCeet}(v, eet)\cdot z_{K}\cdot\beta\cdot v\,\frac{\left(K_{ex} - K_{in}\cdot\exp\left(z_{K}\cdot\beta\cdot v\right)\right)}{\exp\left(z_{K}\cdot\beta\cdot v\right) - 1} & \text{if } v \neq 0 \end{cases}$$

[Seq.E60] $$I_{KNSCeet}\left(v, eet, K_{in}\right) := \frac{-z_{K}\cdot F\cdot J_{KNSCeet}\left(v, eet, K_{in}\right)}{1000}$$

[Seq.E61] $$J_{CaNSCeet}\left(v, eet, ca_{jun}\right) := \begin{cases} J \leftarrow 10^{6}\cdot NSCeet_{T}\cdot perm_{CaNSCeet}\cdot P_{NSCeet}(v, eet)\left(Ca_{ex} - ca_{jun}\right) & \text{if } v = 0 \\ J \leftarrow 10^{6}\cdot NSCeet_{T}\cdot perm_{CaNSCeet}\cdot P_{NSCeet}(v, eet)\cdot z_{Ca}\cdot\beta\cdot v\,\frac{\left(Ca_{ex} - ca_{jun}\cdot\exp\left(z_{Ca}\cdot\beta\cdot v\right)\right)}{\exp\left(z_{Ca}\cdot\beta\cdot v\right) - 1} & \text{if } v \neq 0 \end{cases}$$

[Seq.E62] $$I_{CaNSCeet}(v, eet, ca_{jun}) := \frac{-z_{Ca} \cdot F \cdot J_{CaNSCeet}(v, eet, ca_{jun})}{1000}$$

[Seq.E63] $$I_{NSCeet\_ALL}(v, eet, Na_{in}, K_{in}, ca_{jun}) := I_{NaNSCeet}(v, eet, Na_{in}) + I_{KNSCeet}(v, eet, K_{in}) + I_{CaNSCeet}(v, eet, ca_{jun})$$

NSCne CHANNELS

Open probability of NSCne channels

[Seq.E64] $$P_{NSCne}(DAG, c) := \left(\frac{DAG^{n_{NSCne}}}{DAG^{n_{NSCne}} + K_{NSCne\_DAG}^{n_{NSCne}}} \frac{c^{n_{NSCne}}}{c^{n_{NSCne}} + K_{NSCne\_Ca\_act}^{n_{NSCne}}} \right) \cdot \left(\frac{1}{1 + \frac{c^{n_{NSCne}}}{K_{NSCne\_Ca\_inh}^{n_{NSCne}}}} \right)$$

NSCne fluxes & currents

[Seq.E65] $$J_{NaNSCne}(v, DAG, Na_{in}, c) := \begin{cases} J \leftarrow 10^9 \cdot NSCne_T \cdot perm_{NaNSCne} \cdot P_{NSCne}(DAG, c)(Na_{ex} - Na_{in}) & \text{if } v = 0 \\ J \leftarrow 10^9 \cdot NSCne_T \cdot perm_{NaNSCne} \cdot P_{NSCne}(DAG, c) \cdot z_{Na} \cdot \beta \cdot v \frac{(Na_{ex} - Na_{in} \cdot \exp(z_{Na} \cdot \beta \cdot v))}{\exp(z_{Na} \cdot \beta \cdot v) - 1} & \text{if } v \neq 0 \end{cases}$$

[Seq.E66] $$I_{NaNSCne}(v, DAG, Na_{in}, c) := \frac{-z_{Na} \cdot F \cdot J_{NaNSCne}(v, DAG, Na_{in}, c)}{1000}$$

[Seq.E67] $$J_{KNSCne}(v, DAG, K_{in}, c) := \begin{cases} J \leftarrow 10^9 \cdot NSCne_T \cdot perm_{KNSCne} \cdot P_{NSCne}(DAG, c)(K_{ex} - K_{in}) & \text{if } v = 0 \\ J \leftarrow 10^9 \cdot NSCne_T \cdot perm_{KNSCne} \cdot P_{NSCne}(DAG, c) \cdot z_K \cdot \beta \cdot v \frac{(K_{ex} - K_{in} \cdot \exp(z_K \cdot \beta \cdot v))}{\exp(z_K \cdot \beta \cdot v) - 1} & \text{if } v \neq 0 \end{cases}$$

[Seq.E68] $$I_{KNSCne}(v, DAG, K_{in}, c) := \frac{-z_K \cdot F \cdot J_{KNSCne}(v, DAG, K_{in}, c)}{1000}$$

[Seq.E69] $$J_{CaNSCne}(v, DAG, c) := \begin{cases} J \leftarrow 10^6 \cdot NSCne_T \cdot perm_{CaNSCne} \cdot P_{NSCne}(DAG, c)\left(Ca_{ex} - c\right) & \text{if } v = 0 \\ J \leftarrow 10^6 \cdot NSCne_T \cdot perm_{CaNSCne} \cdot P_{NSCne}(DAG, c) \cdot z_{Ca} \cdot \beta \cdot v \dfrac{\left(Ca_{ex} - c \cdot \exp\left(z_{Ca} \cdot \beta \cdot v\right)\right)}{\exp\left(z_{Ca} \cdot \beta \cdot v\right) - 1} & \text{if } v \neq 0 \end{cases}$$

[Seq.E70] $$I_{CaNSCne}(v, DAG, c) := \frac{-z_{Ca} \cdot F \cdot J_{CaNSCne}(v, DAG, c)}{1000}$$

[Seq.E71] $$I_{NSCne\_ALL}(v, DAG, Na_{in}, K_{in}, c) := I_{NaNSCne}(v, DAG, Na_{in}, c) + I_{KNSCne}(v, DAG, K_{in}, c) + I_{CaNSCne}(v, DAG, c)$$

NSCstr CHANNELS

Open probability for NSCstr channels

[Seq.E72] $$S_{NSCstr\_act}(DAG, bp) := \left(\frac{DAG^{n_{NSCstr\_DAG}}}{DAG^{n_{NSCstr\_DAG}} + K_{NSCstr\_DAG}^{n_{NSCstr\_DAG}}}\right) \cdot \left(\frac{bp^{n_{NSCstr\_bp}}}{bp^{n_{NSCstr\_bp}} + bp_{50}^{n_{NSCstr\_bp}}}\right)$$

[Seq.E73] $$X_{NSCstr\_act}(Ca_{NSC\_str}) := \left(\frac{Ca_{NSC\_str}^{n_{NSCstr\_Ca}}}{Ca_{NSC\_str}^{n_{NSCstr\_Ca}} + K_{NSCstr\_Ca\_act}^{n_{NSCstr\_Ca}}}\right)$$

[Seq.E74] $$X_{NSCstr\_PKC\_act}(Ca_{NSC\_str}) := \left(\frac{Ca_{NSC\_str}^{n_{NSCstr\_Ca}}}{Ca_{NSC\_str}^{n_{NSCstr\_Ca}} + K_{NSCstr\_PKC\_Ca\_act}^{n_{NSCstr\_Ca}}}\right)$$

[Seq.E75] $$X_{NSCstr\_PKG\_act}\left(Ca_{NSC\_str}\right) := \left(\frac{Ca_{NSC\_str}^{\,n_{NSCstr\_Ca}}}{Ca_{NSC\_str}^{\,n_{NSCstr\_Ca}} + K_{NSCstr\_PKG\_Ca\_act}^{\,n_{NSCstr\_Ca}}} \right)$$

[Seq.E76] $$Y_{NSCstr\_inh}\left(Ca_{NSC\_str}\right) := \left(\frac{K_{NSCstr\_Ca\_inh}^{\,n_{NSCstr\_Ca}}}{K_{NSCstr\_Ca\_inh}^{\,n_{NSCstr\_Ca}} + Ca_{NSC\_str}^{\,n_{NSCstr\_Ca}}} \right)$$

[Seq.E77] $$P_{NSCstr}\left(DAG, Ca_{NSC\_str}, bp\right) := S_{NSCstr\_act}(DAG, bp) \cdot X_{NSCstr\_act}\left(Ca_{NSC\_str}\right) \cdot Y_{NSCstr\_inh}\left(Ca_{NSC\_str}\right)$$

[Seq.E78] $$P_{NSCstr\_PKC}\left(DAG, Ca_{NSC\_str}, bp\right) := S_{NSCstr\_act}(DAG, bp) \cdot X_{NSCstr\_PKC\_act}\left(Ca_{NSC\_str}\right) \cdot Y_{NSCstr\_inh}\left(Ca_{NSC\_str}\right)$$

[Seq.E79] $$P_{NSCstr\_PKG}\left(DAG, Ca_{NSC\_str}, bp\right) := S_{NSCstr\_act}(DAG, bp) \cdot X_{NSCstr\_PKG\_act}\left(Ca_{NSC\_str}\right) \cdot Y_{NSCstr\_inh}\left(Ca_{NSC\_str}\right)$$

NSCstr Na^+ flux and current

[Seq.E80] $$\xi_{Na}\left(v, Na_{in}\right) := z_{Na} \cdot \beta \cdot v \, \frac{\left(Na_{ex} - Na_{in} \cdot \exp\left(z_{Na} \cdot \beta \cdot v\right)\right)}{\left(\exp\left(z_{Na} \cdot \beta \cdot v\right) - 1\right)}$$

[Seq.E81] $$J_{NaNSCstr}\left(v, DAG, Na_{in}, Ca_{NSC\_str}, bp, NSCstr\right) := \begin{cases} J \leftarrow 10^9 \cdot NSCstr \cdot perm_{NaNSCstr} \cdot P_{NSCstr}\left(DAG, Ca_{NSC\_str}, bp\right)\left(Na_{ex} - Na_{in}\right) & \text{if } v = 0 \\ J \leftarrow 10^9 \cdot NSCstr \cdot perm_{NaNSCstr} \cdot P_{NSCstr}\left(DAG, Ca_{NSC\_str}, bp\right) \cdot \xi_{Na}\left(v, Na_{in}\right) & \text{if } v \neq 0 \end{cases}$$

[Seq.E82]

$$J_{NaNSCstr\_PKC}\left(v, DAG, Na_{in}, Ca_{NSC\_str}, bp, NSCstr\_PKC\right) := \begin{cases} J \leftarrow 10^9 \cdot NSCstr\_PKC \cdot perm_{NaNSCstr} \cdot P_{NSCstr\_PKC}\left(DAG, Ca_{NSC\_str}, bp\right)\left(Na_{ex} - Na_{in}\right) & \text{if } v = 0 \\ J \leftarrow 10^9 \cdot NSCstr\_PKC \cdot perm_{NaNSCstr} \cdot P_{NSCstr\_PKC}\left(DAG, Ca_{NSC\_str}, bp\right) \cdot \xi_{Na}\left(v, Na_{in}\right) & \text{if } v \neq 0 \end{cases}$$

[Seq.E83]

$$J_{NaNSCstr\_PKG}(v, DAG, Na_{in}, Ca_{NSC\_str}, bp, NSCstr\_PKG) := \begin{cases} J \leftarrow 10^9 \cdot NSCstr\_PKG \cdot perm_{NaNSCstr} \cdot P_{NSCstr\_PKG}(DAG, Ca_{NSC\_str}, bp)(Na_{ex} - Na_{in}) & \text{if } v = 0 \\ J \leftarrow 10^9 \cdot NSCstr\_PKG \cdot perm_{NaNSCstr} \cdot P_{NSCstr\_PKG}(DAG, Ca_{NSC\_str}, bp) \cdot \xi_{Na}(v, Na_{in}) & \text{if } v \neq 0 \end{cases}$$

[Seq.E84] $$I_{NaNSCstr}(v, DAG, Na_{in}, Ca_{NSC\_str}, bp, NSCstr) := \frac{-z_{Na} \cdot F \cdot J_{NaNSCstr}(v, DAG, Na_{in}, Ca_{NSC\_str}, bp, NSCstr)}{1000}$$

[Seq.E85] $$I_{NaNSCstr\_PKC}(v, DAG, Na_{in}, Ca_{NSC\_str}, bp, NSCstr\_PKC) := \frac{-z_{Na} \cdot F \cdot J_{NaNSCstr\_PKC}(v, DAG, Na_{in}, Ca_{NSC\_str}, bp, NSCstr\_PKC)}{1000}$$

[Seq.E86] $$I_{NaNSCstr\_PKG}(v, DAG, Na_{in}, Ca_{NSC\_str}, bp, NSCstr\_PKG) := \frac{-z_{Na} \cdot F \cdot J_{NaNSCstr\_PKG}(v, DAG, Na_{in}, Ca_{NSC\_str}, bp, NSCstr\_PKG)}{1000}$$

[Seq.E87]
$$\begin{aligned} I_{NaNSCstr\_ALL}(v, DAG, Na_{in}, Ca_{NSC\_str}, bp, NSCstr, NSCstr\_PKC, NSCstr\_PKG) := {} & I_{NaNSCstr}(v, DAG, Na_{in}, Ca_{NSC\_str}, bp, NSCstr) \ldots \\ & + I_{NaNSCstr\_PKC}(v, DAG, Na_{in}, Ca_{NSC\_str}, bp, NSCstr\_PKC) \ldots \\ & + I_{NaNSCstr\_PKG}(v, DAG, Na_{in}, Ca_{NSC\_str}, bp, NSCstr\_PKG) \end{aligned}$$

NSCstr K^+ flux and current

[Seq.E88] $$\xi_K(v, K_{in}) := z_K \cdot \beta \cdot v \frac{(K_{ex} - K_{in} \cdot \exp(z_K \cdot \beta \cdot v))}{(\exp(z_K \cdot \beta \cdot v) - 1)}$$

[Seq.E89] $$J_{KNSCstr}(v, DAG, K_{in}, Ca_{NSC\_str}, bp, NSCstr) := \begin{cases} J \leftarrow 10^9 \cdot NSCstr \cdot perm_{KNSCstr} \cdot P_{NSCstr}(DAG, Ca_{NSC\_str}, bp)(K_{ex} - K_{in}) & \text{if } v = 0 \\ J \leftarrow 10^9 \cdot NSCstr \cdot perm_{KNSCstr} \cdot P_{NSCstr}(DAG, Ca_{NSC\_str}, bp) \cdot \xi_K(v, K_{in}) & \text{if } v \neq 0 \end{cases}$$

[Seq.E90]

$$J_{KNSCstr\_PKC}(v, DAG, K_{in}, Ca_{NSC\_str}, bp, NSCstr\_PKC) := \begin{cases} J \leftarrow 10^9 \cdot NSCstr\_PKC \cdot perm_{KNSCstr} \cdot P_{NSCstr\_PKC}(DAG, Ca_{NSC\_str}, bp)(K_{ex} - K_{in}) & \text{if } v = 0 \\ J \leftarrow 10^9 \cdot NSCstr\_PKC \cdot perm_{KNSCstr} \cdot P_{NSCstr\_PKC}(DAG, Ca_{NSC\_str}, bp) \cdot \xi_K(v, K_{in}) & \text{if } v \neq 0 \end{cases}$$

[Seq.E91]

$$J_{KNSCstr\_PKG}(v, DAG, K_{in}, Ca_{NSC\_str}, bp, NSCstr\_PKG) := \begin{cases} J \leftarrow 10^{9} \cdot NSCstr\_PKG \cdot perm_{KNSCstr} \cdot P_{NSCstr\_PKG}(DAG, Ca_{NSC\_str}, bp)(K_{ex} - K_{in}) & \text{if } v = 0 \\ J \leftarrow 10^{9} \cdot NSCstr\_PKG \cdot perm_{KNSCstr} \cdot P_{NSCstr\_PKG}(DAG, Ca_{NSC\_str}, bp) \cdot \xi_K(v, K_{in}) & \text{if } v \neq 0 \end{cases}$$

[Seq.E92] $$I_{KNSCstr}(v, DAG, K_{in}, Ca_{NSC\_str}, bp, NSCstr) := \frac{-z_K \cdot F \cdot J_{KNSCstr}(v, DAG, K_{in}, Ca_{NSC\_str}, bp, NSCstr)}{1000}$$

[Seq.E93] $$I_{KNSCstr\_PKC}(v, DAG, K_{in}, Ca_{NSC\_str}, bp, NSCstr\_PKC) := \frac{-z_K \cdot F \cdot J_{KNSCstr\_PKC}(v, DAG, K_{in}, Ca_{NSC\_str}, bp, NSCstr\_PKC)}{1000}$$

[Seq.E94] $$I_{KNSCstr\_PKG}(v, DAG, K_{in}, Ca_{NSC\_str}, bp, NSCstr\_PKG) := \frac{-z_K \cdot F \cdot J_{KNSCstr\_PKG}(v, DAG, K_{in}, Ca_{NSC\_str}, bp, NSCstr\_PKG)}{1000}$$

[Seq.E95] $$I_{KNSCstr\_ALL}(v, DAG, K_{in}, Ca_{NSC\_str}, bp, NSCstr, NSCstr\_PKC, NSCstr\_PKG) := I_{KNSCstr}(v, DAG, K_{in}, Ca_{NSC\_str}, bp, NSCstr) \ldots + I_{KNSCstr\_PKC}(v, DAG, K_{in}, Ca_{NSC\_str}, bp, NSCstr\_PKC) \ldots + I_{KNSCstr\_PKG}(v, DAG, K_{in}, Ca_{NSC\_str}, bp, NSCstr\_PKG)$$

NSCstr Ca^{2+} flux and current

[Seq.E96] $$\xi_{Ca}(v, Ca_{NSC\_str}) := z_{Ca} \cdot \beta \cdot v \frac{(Ca_{ex} - Ca_{NSC\_str} \cdot \exp(z_{Ca} \cdot \beta \cdot v))}{(\exp(z_{Ca} \cdot \beta \cdot v) - 1)}$$

[Seq.E97] $$J_{CaNSCstr}(v, DAG, Ca_{NSC\_str}, bp, NSCstr) := \begin{cases} J \leftarrow 10^{6} \cdot NSCstr \cdot perm_{CaNSCstr} \cdot P_{NSCstr}(DAG, Ca_{NSC\_str}, bp)(Ca_{ex} - Ca_{NSC\_str}) & \text{if } v = 0 \\ J \leftarrow 10^{6} \cdot NSCstr \cdot perm_{CaNSCstr} \cdot P_{NSCstr}(DAG, Ca_{NSC\_str}, bp) \cdot \xi_{Ca}(v, Ca_{NSC\_str}) & \text{if } v \neq 0 \end{cases}$$

[Seq.E98]

$$J_{CaNSCstr\_PKC}(v, DAG, Ca_{NSC\_str}, bp, NSCstr\_PKC) := \begin{cases} J \leftarrow 10^6 \cdot NSCstr\_PKC \cdot perm_{CaNSCstr} \cdot P_{NSCstr\_PKC}(DAG, Ca_{NSC\_str}, bp)(Ca_{ex} - Ca_{NSC\_str}) & \text{if } v = 0 \\ J \leftarrow 10^6 \cdot NSCstr\_PKC \cdot perm_{CaNSCstr} \cdot P_{NSCstr\_PKC}(DAG, Ca_{NSC\_str}, bp) \cdot \xi_{Ca}(v, Ca_{NSC\_str}) & \text{if } v \neq 0 \end{cases}$$

[Seq.E99]

$$J_{CaNSCstr\_PKG}(v, DAG, Ca_{NSC\_str}, bp, NSCstr\_PKG) := \begin{cases} J \leftarrow 10^6 \cdot NSCstr\_PKG \cdot perm_{CaNSCstr} \cdot P_{NSCstr\_PKG}(DAG, Ca_{NSC\_str}, bp)(Ca_{ex} - Ca_{NSC\_str}) & \text{if } v = 0 \\ J \leftarrow 10^6 \cdot NSCstr\_PKG \cdot perm_{CaNSCstr} \cdot P_{NSCstr\_PKG}(DAG, Ca_{NSC\_str}, bp) \cdot \xi_{Ca}(v, Ca_{NSC\_str}) & \text{if } v \neq 0 \end{cases}$$

[Seq.E100]

$$\begin{aligned} J_{CaNSCstr\_ALL}(v, DAG, Ca_{NSC\_str}, bp, NSCstr, NSCstr\_PKC, NSCstr\_PKG) := {} & J_{CaNSCstr}(v, DAG, Ca_{NSC\_str}, bp, NSCstr) \ldots \\ & + J_{CaNSCstr\_PKC}(v, DAG, Ca_{NSC\_str}, bp, NSCstr\_PKC) \ldots \\ & + J_{CaNSCstr\_PKG}(v, DAG, Ca_{NSC\_str}, bp, NSCstr\_PKG) \end{aligned}$$

[Seq.E101]

$$I_{CaNSCstr}(v, DAG, Ca_{NSC\_str}, bp, NSCstr) := \frac{-z_{Ca} \cdot F \cdot J_{CaNSCstr}(v, DAG, Ca_{NSC\_str}, bp, NSCstr)}{1000}$$

[Seq.E102]

$$I_{CaNSCstr\_PKC}(v, DAG, Ca_{NSC\_str}, bp, NSCstr\_PKC) := \frac{-z_{Ca} \cdot F \cdot J_{CaNSCstr\_PKC}(v, DAG, Ca_{NSC\_str}, bp, NSCstr\_PKC)}{1000}$$

[Seq.E103]

$$I_{CaNSCstr\_PKG}(v, DAG, Ca_{NSC\_str}, bp, NSCstr\_PKG) := \frac{-z_{Ca} \cdot F \cdot J_{CaNSCstr\_PKG}(v, DAG, Ca_{NSC\_str}, bp, NSCstr\_PKG)}{1000}$$

[Seq.E104]

$$\begin{aligned} I_{CaNSCstr\_ALL}(v, DAG, Ca_{NSC\_str}, bp, NSCstr, NSCstr\_PKC, NSCstr\_PKG) := {} & I_{CaNSCstr}(v, DAG, Ca_{NSC\_str}, bp, NSCstr) \ldots \\ & + I_{CaNSCstr\_PKC}(v, DAG, Ca_{NSC\_str}, bp, NSCstr\_PKC) \ldots \\ & + I_{CaNSCstr\_PKG}(v, DAG, Ca_{NSC\_str}, bp, NSCstr\_PKG) \end{aligned}$$

NSCstr Na^+ + K^+ + Ca^{2+} currents

[Seq.E105]

$$\begin{aligned} I_{NSCstr\_ALL}(v, DAG, Na_{in}, K_{in}, Ca_{NSC\_str}, bp, NSCstr, NSCstr\_PKC, NSCstr\_PKG) := {} & I_{NaNSCstr\_ALL}(v, DAG, Na_{in}, Ca_{NSC\_str}, bp, NSCstr, NSCstr\_PKC, NSCstr\_PKG) \ldots \\ & + I_{KNSCstr\_ALL}(v, DAG, K_{in}, Ca_{NSC\_str}, bp, NSCstr, NSCstr\_PKC, NSCstr\_PKG) \ldots \\ & + I_{CaNSCstr\_ALL}(v, DAG, Ca_{NSC\_str}, bp, NSCstr, NSCstr\_PKC, NSCstr\_PKG) \end{aligned}$$

P2X1 RECEPTOR

P2X1R fluxes & currents

[Seq.E106]
$$J_{NaP2XR}(v, Na_{in}, P2XR\_3\_act) := \begin{cases} J \leftarrow 10^{9} \cdot P2XR\_3\_act \cdot perm_{NaP2XR} \cdot (Na_{ex} - Na_{in}) & \text{if } v = 0 \\ J \leftarrow 10^{9} \cdot P2XR\_3\_act \cdot perm_{NaP2XR} \cdot z_{Na} \cdot \beta \cdot v \dfrac{(Na_{ex} - Na_{in} \cdot \exp(z_{Na} \cdot \beta \cdot v))}{\exp(z_{Na} \cdot \beta \cdot v) - 1} & \text{if } v \neq 0 \end{cases}$$

[Seq.E107]
$$I_{NaP2XR}(v, Na_{in}, P2XR\_3\_act) := \frac{-z_{Na} \cdot F \cdot J_{NaP2XR}(v, Na_{in}, P2XR\_3\_act)}{1000}$$

[Seq.E108]
$$J_{KP2XR}(v, K_{in}, P2XR\_3\_act) := \begin{cases} J \leftarrow 10^{9} \cdot P2XR\_3\_act \cdot perm_{KP2XR} \cdot (K_{ex} - K_{in}) & \text{if } v = 0 \\ J \leftarrow 10^{9} \cdot P2XR\_3\_act \cdot perm_{KP2XR} \cdot z_{K} \cdot \beta \cdot v \dfrac{(K_{ex} - K_{in} \cdot \exp(z_{K} \cdot \beta \cdot v))}{\exp(z_{K} \cdot \beta \cdot v) - 1} & \text{if } v \neq 0 \end{cases}$$

[Seq.E109]
$$I_{KP2XR}(v, K_{in}, P2XR\_3\_act) := \frac{-z_{K} \cdot F \cdot J_{KP2XR}(v, K_{in}, P2XR\_3\_act)}{1000}$$

[Seq.E110]
$$J_{CaP2XR}(v, c, P2XR\_3\_act) := \begin{cases} J \leftarrow 10^{6} \cdot P2XR\_3\_act \cdot perm_{CaP2XR} \cdot (Ca_{ex} - c) & \text{if } v = 0 \\ J \leftarrow 10^{6} \cdot P2XR\_3\_act \cdot perm_{CaP2XR} \cdot z_{Ca} \cdot \beta \cdot v \dfrac{(Ca_{ex} - c \cdot \exp(z_{Ca} \cdot \beta \cdot v))}{\exp(z_{Ca} \cdot \beta \cdot v) - 1} & \text{if } v \neq 0 \end{cases}$$

[Seq.E111]
$$I_{CaP2XR}(v, c, P2XR\_3\_act) := \frac{-z_{Ca} \cdot F \cdot J_{CaP2XR}(v, c, P2XR\_3\_act)}{1000}$$

[Seq.E112]
$$I_{P2XR\_ALL}(v, Na_{in}, K_{in}, c, P2XR\_3\_act) := I_{NaP2XR}(v, Na_{in}, P2XR\_3\_act) + I_{KP2XR}(v, K_{in}, P2XR\_3\_act) + I_{CaP2XR}(v, c, P2XR\_3\_act)$$

F. SR CHANNELS OPEN PROBABILITIES, FLUXES, AND CURRENTS

IP3R

Binding of IP3 to IP3R and to IP3R_IRAG_PKG

[Seq.F1]
$$X_{IP3R}(IP3) := \frac{(IP3)^{n_{IP3R\_IP3}}}{(IP3)^{n_{IP3R\_IP3}} + K_{IP3R\_IP3}{}^{n_{IP3R\_IP3}}}$$

[Seq.F2]
$$X_{IP3R\_IRAG\_PKG}(IP3) := \frac{(IP3)^{n_{IP3R\_IP3}}}{(IP3)^{n_{IP3R\_IP3}} + K_{IP3R\_IRAG\_PKG\_IP3}{}^{n_{IP3R\_IP3}}}$$

Regulation of affinity of cytosolic activation site for Ca by IP3 binding

[Seq.F3]
$$K_{IP3R\_Ca\_act}(IP3) := \frac{1}{\frac{1}{K_{IP3R\_Ca\_max}} + X_{IP3R}(IP3)\left(\frac{1}{K_{IP3R\_Ca\_min}} - \frac{1}{K_{IP3R\_Ca\_max}}\right)}$$

[Seq.F4]
$$K_{IP3R\_IRAG\_PKG\_Ca\_act}(IP3) := \frac{1}{\frac{1}{K_{IP3R\_Ca\_max}} + X_{IP3R\_IRAG\_PKG}(IP3)\left(\frac{1}{K_{IP3R\_Ca\_min}} - \frac{1}{K_{IP3R\_Ca\_max}}\right)}$$

Ca binding to cytosolic inhibitory site

[Seq.F5]
$$Y_{IP3\_Ca\_inh}(c) := \frac{1}{1 + \left(\frac{c}{K_{IP3R\_Ca\_inh}}\right)^{n_{IP3R\_Ca\_inh}}}$$

Ca binding to SR lumenal activation site

[Seq.F6] $$Z_{IP3R\_CaSR}\left(Ca_{SRcen}\right) := \frac{Ca_{SRcen}^{\,n_{IP3R\_CaSR}}}{Ca_{SRcen}^{\,n_{IP3R\_CaSR}} + K_{IP3R\_CaSR}^{\,n_{IP3R\_CaSR}}}$$

IP3R and IP3R_IRAG_PKG open probabilities

[Seq.F7] $$P_{IP3R}\left(c, IP3, Ca_{SRcen}\right) := \frac{c^{n_{IP3R\_Ca\_act}}}{c^{n_{IP3R\_Ca\_act}} + K_{IP3R\_Ca\_act}(IP3)^{n_{IP3R\_Ca\_act}}} \cdot Y_{IP3\_Ca\_inh}(c) \cdot Z_{IP3R\_CaSR}\left(Ca_{SRcen}\right)$$

[Seq.F8] $$P_{IP3R\_IRAG\_PKG}\left(c, IP3, Ca_{SRcen}\right) := \frac{c^{n_{IP3R\_Ca\_act}}}{c^{n_{IP3R\_Ca\_act}} + K_{IP3R\_IRAG\_PKG\_Ca\_act}(IP3)^{n_{IP3R\_Ca\_act}}} \cdot Y_{IP3\_Ca\_inh}(c) \cdot Z_{IP3R\_CaSR}\left(Ca_{SRcen}\right)$$

Flux & currents via IP3R & IP3R_IRAG_PKG

[Seq.F9] $$J_{IP3R}\left(c, IP3, Ca_{SRcen}, IP3R\right) := 10^{6} \cdot IP3R \cdot perm_{IP3R} \cdot P_{IP3R}\left(c, IP3, Ca_{SRcen}\right) \cdot \left(Ca_{SRcen} - c\right)$$

[Seq.F10] $$J_{IP3R\_IRAG\_PKG}\left(c, IP3, Ca_{SRcen}, IP3R_{IRAG\_PKG}\right) := 10^{6} \cdot IP3R_{IRAG\_PKG} \cdot perm_{IP3R} \cdot P_{IP3R\_IRAG\_PKG}\left(c, IP3, Ca_{SRcen}\right) \cdot \left(Ca_{SRcen} - c\right)$$

[Seq.F11] $$J_{IP3R\_ALL}\left(c, IP3, Ca_{SRcen}, IP3R, IP3R_{IRAG\_PKG}\right) := J_{IP3R}\left(c, IP3, Ca_{SRcen}, IP3R\right) + J_{IP3R\_IRAG\_PKG}\left(c, IP3, Ca_{SRcen}, IP3R_{IRAG\_PKG}\right)$$

[Seq.F12] $$I_{IP3R\_ALL}\left(c, IP3, Ca_{SRcen}, IP3R, IP3R_{IRAG\_PKG}\right) := -\frac{z_{Ca} \cdot F}{1000} \cdot J_{IP3R\_ALL}\left(c, IP3, Ca_{SRcen}, IP3R, IP3R_{IRAG\_PKG}\right)$$

RyR

Ca binding to sensitizing sites facing peripheral SR lumen increases afffinity of junctional sites.

[Seq.F13] $$X_{RyR\_Ca\_SR}\left(Ca_{SRper}\right) := \frac{Ca_{SRper}^{\,n_{RyR\_Ca\_SR}}}{Ca_{SRper}^{\,n_{RyR\_Ca\_SR}} + K_{RyR\_Ca\_SR}^{\,n_{RyR\_Ca\_SR}}}$$

[Seq.F14] $$K_{RyR\_Ca\_jun}\left(Ca_{SRper}\right) := \frac{1}{\frac{1}{K_{RyR\_Ca\_jun\_max}} + X_{RyR\_Ca\_SR}\left(Ca_{SRper}\right)\cdot\left(\frac{1}{K_{RyR\_Ca\_jun\_min}} - \frac{1}{K_{RyR\_Ca\_jun\_max}}\right)}$$

Occupation of inhibitory junctional sites decreases open probability.

[Seq.F15] $$Y_{RyR\_Ca\_jun}\left(Ca_{jun}\right) := \frac{1}{1 + \left(\frac{Ca_{jun}}{K_{RyR\_Ca\_inh}}\right)^{n_{RyR\_Ca\_inh}}}$$

RyR open probability

[Seq.F16] $$P_{RyR}\left(Ca_{jun}, Ca_{SRper}\right) := \frac{Ca_{jun}^{\,n_{RyR\_Ca\_jun}}}{Ca_{jun}^{\,n_{RyR\_Ca\_jun}} + K_{RyR\_Ca\_jun}\left(Ca_{SRper}\right)^{n_{RyR\_Ca\_jun}}}\cdot Y_{RyR\_Ca\_jun}\left(Ca_{jun}\right)$$

RyR_{PKA} open probability

[Seq.F17] $$Z_{RyR\_PKA}\left(RyR_{PKA}\right) := \frac{RyR_{PKA}}{RyR_T}$$

[Seq.F18] $$f_{RyR\_PKA}\left(RyR_{PKA}\right) := 1 - \left(1 - f_{RyR\_PKA\_min}\right)\cdot Z_{RyR\_PKA}\left(RyR_{PKA}\right)^2$$

[Seq.F19] $$P_{RyR\_PKA}\left(Ca_{jun}, Ca_{SRper}, RyR_{PKA}\right) := \frac{Ca_{jun}^{\,n_{RyR\_Ca\_jun}}}{Ca_{jun}^{\,n_{RyR\_Ca\_jun}} + \left(f_{RyR\_PKA}\left(RyR_{PKA}\right)\cdot K_{RyR\_Ca\_jun}\left(Ca_{SRper}\right)\right)^{n_{RyR\_Ca\_jun}}}\cdot Y_{RyR\_Ca\_jun}\left(Ca_{jun}\right)$$

RyR.$_{PKC}$ open probability

[Seq.F20] $$Z_{RyR\_PKC}\left(RyR_{PKC}\right) := \frac{RyR_{PKC}}{RyR_T}$$

[Seq.F21] $$f_{RyR\_PKC}\left(RyR_{PKC}\right) := 1 - \left(1 - f_{RyR\_PKC\_max}\right)\cdot Z_{RyR\_PKC}\left(RyR_{PKC}\right)^2$$

[Seq.F22] $$P_{RyR\_PKC}\left(Ca_{jun}, Ca_{SRper}, RyR_{PKC}\right) := \frac{Ca_{jun}^{\,n_{RyR\_Ca\_jun}}}{Ca_{jun}^{\,n_{RyR\_Ca\_jun}} + \left(f_{RyR\_PKC}\left(RyR_{PKC}\right)\cdot K_{RyR\_Ca\_jun}\left(Ca_{SRper}\right)\right)^{n_{RyR\_Ca\_jun}}}\cdot Y_{RyR\_Ca\_jun}\left(Ca_{jun}\right)$$

RyR flux into junction

[Seq.F23]

$$J_{RyR}\left(Ca_{jun}, Ca_{SRper}, RyR_{PKA}, RyR_{PKC}\right) := 10^6\cdot\left(1 - Z_{RyR\_PKA}\left(RyR_{PKA}\right) - Z_{RyR\_PKC}\left(RyR_{PKC}\right)\right)\cdot RyR_T\cdot perm_{RyR}\cdot P_{RyR}\left(Ca_{jun}, Ca_{SRper}\right)\cdot\left(Ca_{SRper} - Ca_{jun}\right)$$

RyR$_{PKA}$ flux into junction

[Seq.F24] $$J_{RyR\_PKA}\left(Ca_{jun}, Ca_{SRper}, RyR_{PKA}\right) := 10^6\cdot Z_{RyR\_PKA}\left(RyR_{PKA}\right)\cdot RyR_T\cdot perm_{RyR}\cdot P_{RyR\_PKA}\left(Ca_{jun}, Ca_{SRper}, RyR_{PKA}\right)\cdot\left(Ca_{SRper} - Ca_{jun}\right)$$

RyR$_{PKC}$ flux into junction

[Seq.F25] $$J_{RyR\_PKC}(Ca_{jun}, Ca_{SRper}, RyR_{PKC}) := 10^6 \cdot Z_{RyR\_PKC}(RyR_{PKC}) \cdot RyR_T \cdot perm_{RyR} \cdot P_{RyR\_PKC}(Ca_{jun}, Ca_{SRper}, RyR_{PKC}) \cdot (Ca_{SRper} - Ca_{jun})$$

RyR + RyR_{PKA} + RyR_{PKC} flux into junction

[Seq.F26] $$J_{RyR\_ALL}(Ca_{jun}, Ca_{SRper}, RyR_{PKA}, RyR_{PKC}) := J_{RyR}(Ca_{jun}, Ca_{SRper}, RyR_{PKA}, RyR_{PKC}) + J_{RyR\_PKA}(Ca_{jun}, Ca_{SRper}, RyR_{PKA}) \ldots + J_{RyR\_PKC}(Ca_{jun}, Ca_{SRper}, RyR_{PKC})$$

RyR + RyR_{PKA} + RyR_{PKC} current

[Seq.F27] $$I_{RyR\_ALL}(Ca_{jun}, Ca_{SRper}, RyR_{PKA}, RyR_{PKC}) := -\frac{z_{Ca} \cdot F}{1000} \cdot J_{RyR\_ALL}(Ca_{jun}, Ca_{SRper}, RyR_{PKA}, RyR_{PKC})$$

G. TRANSPORTERS

Na,K ATPase

[Seq.G1] $$rel\Delta\mu_{NaK}(v, Na_{in}, K_{in}) := \frac{3 \cdot R \cdot T \cdot \ln\left(\frac{Na_{ex}}{Na_{in}}\right) + 2 \cdot R \cdot T \cdot \ln\left(\frac{K_{in}}{K_{ex}}\right) - F \cdot \frac{v}{1000} + \Delta\mu_{ATP}}{\Delta\mu_{ATP}}$$

[Seq.G2] $$I_{NaK}(v, Na_{in}, K_{in}) := I_{NaKmax} \cdot \left(\frac{K_{ex}^{\,n_{NaK\_K}}}{K_{ex}^{\,n_{NaK\_K}} + K_{NaK\_Kex}^{\,n_{NaK\_K}}}\right) \cdot \left(\frac{Na_{in}^{\,n_{NaK\_Na}}}{Na_{in}^{\,n_{NaK\_Na}} + K_{NaK\_Nain}^{\,n_{NaK\_Na}}}\right) \cdot rel\Delta\mu_{NaK}(v, Na_{in}, K_{in})$$

NaKCl cotransporter

Flux of fully occupied NaKCl and PKC-phosphorylated NaKCl_PKC

[Seq.G3] $$\alpha_{NaKCl\_0} := \frac{\beta_{NaKCl\_0} \cdot \alpha_{NaKCl\_4}}{\beta_{NaKCl\_4}}$$

[Seq.G4] $$Q\left(Na_{in}, K_{in}, Cl_{in}\right) := \frac{\alpha_{NaKCl\_4} + \alpha_{NaKCl\_0} \cdot \frac{L_{NaKCl\_Na} \cdot L_{NaKCl\_K} \cdot L_{NaKCl\_Cl}^{2}}{Na_{ex} \cdot K_{ex} \cdot Cl_{ex}^{2}}}{\beta_{NaKCl\_4} + \beta_{NaKCl\_0} \cdot \frac{L_{NaKCl\_Na} \cdot L_{NaKCl\_K} \cdot L_{NaKCl\_Cl}^{2}}{Na_{in} \cdot K_{in} \cdot Cl_{in}^{2}}}$$

[Seq.G5] $$D_1 := 1 + \frac{L_{NaKCl\_Cl}}{Cl_{ex}} + \frac{L_{NaKCl\_K} \cdot L_{NaKCl\_Cl}}{K_{ex} \cdot Cl_{ex}} + \frac{L_{NaKCl\_K} \cdot L_{NaKCl\_Cl}^{2}}{K_{ex} \cdot Cl_{ex}^{2}} + \frac{L_{NaKCl\_Na} \cdot L_{NaKCl\_K} \cdot L_{NaKCl\_Cl}^{2}}{Na_{ex} \cdot K_{ex} \cdot Cl_{ex}^{2}}$$

[Seq.G6] $$D_2\left(Na_{in}, K_{in}, Cl_{in}\right) := 1 + \frac{L_{NaKCl\_Na}}{Na_{in}} + \frac{L_{NaKCl\_Na} \cdot L_{NaKCl\_Cl}}{Na_{in} \cdot Cl_{in}} + \frac{L_{NaKCl\_Na} \cdot L_{NaKCl\_Cl} \cdot L_{NaKCl\_K}}{Na_{in} \cdot Cl_{in} \cdot K_{in}} + \frac{L_{NaKCl\_Na} \cdot L_{NaKCl\_Cl}^{2} \cdot L_{NaKCl\_K}}{Na_{in} \cdot Cl_{in}^{2} \cdot K_{in}}$$

[Seq.G7] $$J_{4\_NaKCl}\left(NaKCl, Na_{in}, K_{in}, Cl_{in}\right) := \frac{NaKCl}{\left(D_1 + Q\left(Na_{in}, K_{in}, Cl_{in}\right) \cdot D_2\left(Na_{in}, K_{in}, Cl_{in}\right)\right)} \cdot \left(\alpha_{NaKCl\_4} - \beta_{NaKCl\_4} \cdot Q\left(Na_{in}, K_{in}, Cl_{in}\right)\right)$$

[Seq.G8] $$J_{4\_NaKCl\_PKC}\left(NaKCl_{PKC}, Na_{in}, K_{in}, Cl_{in}\right) := \frac{\varepsilon_{NaKCl\_PKC} \cdot NaKCl_{PKC}}{\left(D_1 + Q\left(Na_{in}, K_{in}, Cl_{in}\right) \cdot D_2\left(Na_{in}, K_{in}, Cl_{in}\right)\right)} \cdot \left(\alpha_{NaKCl\_4} - \beta_{NaKCl\_4} \cdot Q\left(Na_{in}, K_{in}, Cl_{in}\right)\right)$$

[Seq.G9] $$J_{4\_NaKCl\_ALL}\left(NaKCl, NaKCl_{PKC}, Na_{in}, K_{in}, Cl_{in}\right) := J_{4\_NaKCl}\left(NaKCl, Na_{in}, K_{in}, Cl_{in}\right) + J_{4\_NaKCl\_PKC}\left(NaKCl_{PKC}, Na_{in}, K_{in}, Cl_{in}\right)$$

Cl flux

[Seq.G10] $$J_{NaK\_Cl}(NaKCl, NaKCl_{PKC}, Na_{in}, K_{in}, Cl_{in}) := \frac{2 \cdot 10^{15}}{N_A} \cdot J_{4\_NaKCl\_ALL}(NaKCl, NaKCl_{PKC}, Na_{in}, K_{in}, Cl_{in})$$

Na flux

[Seq.G11] $$J_{KCl\_Na}(NaKCl, NaKCl_{PKC}, Na_{in}, K_{in}, Cl_{in}) := \frac{10^{15}}{N_A} \cdot J_{4\_NaKCl\_ALL}(NaKCl, NaKCl_{PKC}, Na_{in}, K_{in}, Cl_{in})$$

K flux

[Seq.G12] $$J_{NaCl\_K}(NaKCl, NaKCl_{PKC}, Na_{in}, K_{in}, Cl_{in}) := \frac{10^{15}}{N_A} \cdot J_{4\_NaKCl\_ALL}(NaKCl, NaKCl_{PKC}, Na_{in}, K_{in}, Cl_{in})$$

Cl current (currents of Na,K, & Cl add to zero)

[Seq.G13] $$I_{NaK\_Cl}(NaKCl, NaKCl_{PKC}, Na_{in}, K_{in}, Cl_{in}) := \frac{-z_{Cl} \cdot F}{1000} \cdot J_{NaK\_Cl}(NaKCl, NaKCl_{PKC}, Na_{in}, K_{in}, Cl_{in})$$

NCX

Microscopic reversibility applied to binding and isomerizations at V_m =0, assuming that the Na affinities and the Ca affinities are the same for inward and outward facing sites, yields:

[Seq.G14] $$\beta_{NCX\_0} := \frac{\alpha_{NCX\_0} \cdot \beta_{NCX\_4}}{\alpha_{NCX\_4}}$$

[Seq.G15] $$Z_{NCX\_act}(Ca_{in}) := \frac{Ca_{in}^{n_{NCX\_act}}}{K_{NCX\_act\_Ca}^{n_{NCX\_act}} + Ca_{in}^{n_{NCX\_act}}}$$

[Seq.G16]
$$QQ(v, Ca_{in}, Na_{in}) := \frac{\alpha_{NCX\_4} + \alpha_{NCX\_0} \cdot \frac{K_{NCX\_Ca} \cdot K_{NCX\_Na}^{3} \cdot \exp\left(\frac{F \cdot v}{2000 \cdot R \cdot T}\right)}{Ca_{in} \cdot Na_{ex}^{3}}}{\beta_{NCX\_4} + \beta_{NCX\_0} \cdot \frac{K_{NCX\_Ca} \cdot K_{NCX\_Na}^{3} \cdot \exp\left(\frac{-F \cdot v}{2000 \cdot R \cdot T}\right)}{Ca_{ex} \cdot Na_{in}^{3}}}$$

[Seq.G17]
$$DD_1(Ca_{in}) := 1 + \frac{K_{NCX\_Ca}}{Ca_{in}} + \frac{3K_{NCX\_Na} \cdot K_{NCX\_Ca}}{Na_{ex} \cdot Ca_{in}} + \frac{3 \cdot K_{NCX\_Na}^{2} \cdot K_{NCX\_Ca}}{Na_{ex}^{2} \cdot Ca_{in}} + \frac{K_{NCX\_Na}^{3}}{Na_{ex}^{3}} \cdot \frac{K_{NCX\_Ca}}{Ca_{in}}$$

[Seq.G18]
$$DD_2(Na_{in}) := 1 + \frac{K_{NCX\_Ca}}{Ca_{ex}} + \frac{3K_{NCX\_Na} \cdot K_{NCX\_Ca}}{Na_{in} \cdot Ca_{ex}} + \frac{3 \cdot K_{NCX\_Na}^{2} \cdot K_{NCX\_Ca}}{Na_{in}^{2} \cdot Ca_{ex}} + \frac{K_{NCX\_Na}^{3}}{Na_{in}^{3}} \cdot \frac{K_{NCX\_Ca}}{Ca_{ex}}$$

Net isomerization rate of transporter from 3 Na out and 1 Ca in to 3 Na in and 1 Ca out

[Seq.G19]
$$S_4(v, Ca_{in}, Na_{in}) := \left(\alpha_{NCX\_4} - QQ(v, Ca_{in}, Na_{in}) \cdot \beta_{NCX\_4}\right) \cdot \frac{Z_{NCX\_act}(Ca_{in}) \cdot NCX_T}{DD_1(Ca_{in}) + QQ(v, Ca_{in}, Na_{in}) \cdot DD_2(Na_{in})}$$

Net current

[Seq.G20]
$$I_{NCX}(v, Ca_{in}, Na_{in}) := \frac{-10^{12} \cdot F}{N_A} \cdot S_4(v, Ca_{in}, Na_{in})$$

Plasma Membrane CaATPase

Relative free energy difference

[Seq.G21] $$rel\Delta\mu_{PMCA}(v,c) := \frac{\left(-F\cdot\frac{v}{1000} + R\cdot T\cdot\ln\left(\frac{Ca_{ex}}{c}\right)\right) + \Delta\mu_{ATP}}{\Delta\mu_{ATP}}$$

[Seq.G22] $$I_{PMCA}(v,c) := I_{PMCA\_max}\cdot\frac{c^{n_{PMCA\_Ca}}}{c^{n_{PMCA\_Ca}} + K_{PMCA\_Ca}^{n_{PMCA\_Ca}}}\cdot rel\Delta\mu_{PMCA}(v,c)$$

SERCA

Relative activities of SERCA and phosphorylated SERCA

[Seq.G23] $$relSERCA(c,Ca_{SRcen}) := \frac{c^{n_{SERCA}}}{c^{n_{SERCA}} + K_{SERCA\_Ca}^{n_{SERCA}}}\cdot\left[\frac{1}{1 + \left(\frac{Ca_{SRcen}}{K_{SERCA\_inh\_Ca\_SRcen}}\right)^{n_{SERCA}}}\right]$$

[Seq.G24] $$relSERCA\_P(c,Ca_{SRcen}) := \frac{c^{n_{SERCA}}}{c^{n_{SERCA}} + K_{SERCA\_P\_Ca}^{n_{SERCA}}}\cdot\left[\frac{1}{1 + \left(\frac{Ca_{SRcen}}{K_{SERCA\_inh\_Ca\_SRcen}}\right)^{n_{SERCA}}}\right]$$

SERCA & SERCA_P fluxes & current

[Seq.G25] $$rel\Delta\mu_{SERCA}(c,Ca_{SRcen}) := \frac{2R\cdot T\cdot\ln\left(\frac{Ca_{SRcen}}{c}\right) + \Delta\mu_{ATP}}{\Delta\mu_{ATP}}$$

2 Ca^{2+} countered by 2 H^+ per ATP
gives 2 net charges transported per cycle
or 1 Ca^{2+} per charge transported.

[Seq.G26] $$J_{SERCA}(c,Ca_{SRcen}) := \frac{-1\cdot 10^3}{F}\cdot I_{SERCA\_max}\cdot relSERCA(c,Ca_{SRcen})\cdot rel\Delta\mu_{SERCA}(c,Ca_{SRcen})$$

[Seq.G27] $$J_{SERCA\_P}(c,Ca_{SRcen}) := \frac{-1\cdot 10^3}{F}\cdot I_{SERCA\_max}\cdot relSERCA\_P(c,Ca_{SRcen})\cdot rel\Delta\mu_{SERCA}(c,Ca_{SRcen})$$

[Seq.G28] $$J_{SERCA\_ALL}(c, Ca_{SRcen}, SERCA, SERCA\_P) := \frac{SERCA \cdot J_{SERCA}(c, Ca_{SRcen}) + SERCA\_P \cdot J_{SERCA\_P}(c, Ca_{SRcen})}{SERCA_T}$$

[Seq.G29] $$I_{SERCA\_ALL}(c, Ca_{SRcen}, SERCA, SERCA\_P) := -\frac{F}{1000} \cdot J_{SERCA\_ALL}(c, Ca_{SRcen}, SERCA, SERCA\_P)$$

H. ENZYMES

PHOSPHODIESTERASES (PDE)

Active fraction of cAMP-specific PDE

[Seq.H1] $$relPDE_{cAMP}(cAMP) := \frac{cAMP^{n_{PDE}}}{cAMP^{n_{PDE}} + K_{PDE\_cAMP}{}^{n_{PDE}}}$$

Active fraction of phosphorylated cAMP-specific PDE

[Seq.H2] $$relPDE_{cAMP\_P}(cAMP) := \frac{cAMP^{n_{PDE}}}{cAMP^{n_{PDE}} + K_{PDE\_cAMP\_P}{}^{n_{PDE}}}$$

Active fraction of cGMP-specific PDE

[Seq.H3] $$relPDE_{cGMP}(cGMP) := \frac{cGMP^{n_{PDE}}}{cGMP^{n_{PDE}} + K_{PDE\_cGMP}{}^{n_{PDE}}}$$

Active fraction of phosphorylated cGMP-specific PDE

[Seq.H4] $$relPDE_{cGMP\_P}(cGMP) := \frac{cGMP^{n_{PDE}}}{cGMP^{n_{PDE}} + K_{PDE\_cGMP\_P}{}^{n_{PDE}}}$$

PROTEIN KINASES

Active fraction of PKA

[Seq.H5] $$relPKA_1(cAMP) := \frac{cAMP^{n_{PKA\_cAMP}}}{cAMP^{n_{PKA\_cAMP}} + K_{PKA\_cAMP}^{n_{PKA\_cAMP}}}$$

Active fraction of PKC

[Seq.H6] $$relPKC_{11}(DAG, c) := \left(\frac{DAG}{DAG + K_{PKC\_DAG}}\right) \cdot \left(\frac{c^{n_{PKC\_Ca}}}{c^{n_{PKC\_Ca}} + K_{PKC\_Ca}^{n_{PKC\_Ca}}}\right)$$

Active fraction of PKCε

[Seq.H7] $$relPKC\varepsilon_{DAG}(DAG) := \left(\frac{DAG}{DAG + K_{PKC\varepsilon\_DAG}}\right)$$

Active fraction of PKD

[Seq.H8] $$relPKD_{DAG}(DAG) := \left(\frac{DAG}{DAG + K_{PKD\_DAG}}\right)$$

Active fraction of PKG

[Seq.H9] $$relPKG_1(cGMP) := \frac{cGMP^{n_{PKG\_cGMP}}}{cGMP^{n_{PKG\_cGMP}} + K_{PKG\_cGMP}^{n_{PKG\_cGMP}}}$$

J. SOLVE BLOCK FOR ALGEBRAIC & DIFFERENTIAL EQUATIONS

[Seq.J1] $t0 := 0$

Given

[Seq.J2] $$\frac{d}{dt}cGMP(t) = k_{GC\_act\_GTP}\cdot GC_{1\_act}(t) + k_{GC\_basal\_GTP}\cdot\left(GC_T - GC_{1\_act}(t)\right) \ldots + (-1)\cdot\left[k_{PDE\_cGMP}\cdot cGMP(t)\cdot\left(PDE_{cGMP}(t)\cdot relPDE_{cGMP}(cGMP(t)) + PDE_{cGMP\_P}(t)\cdot relPDE_{cGMP\_P}(cGMP(t))\right)\right]$$

[Seq.J3] $$\frac{d}{dt}GC_0(t) = -\left(k_{GC0\_NO\_on}\right)\cdot GC_0(t)\cdot NO\left(NO_0, NO_1, t\right) + \left(k_{GC1\_NO\_off}\right)\cdot GC_1(t) + k_{PP\_GC}\cdot GC_{0P}(t)$$

[Seq.J4] $$\frac{d}{dt}GC_1(t) = \left(k_{GC0\_NO\_on}\right)\cdot GC_0(t)\cdot NO\left(NO_0, NO_1, t\right) - k_{GC1\_NO\_off}\cdot GC_1(t) - k_{GC1\_act}\cdot GC_1(t) \ldots + k_{GC1\_deact}\cdot GC_{1\_act}(t) - k_{GC1\_NO\_on}\cdot NO\left(NO_0, NO_1, t\right)\cdot GC_1(t) + k_{GC2\_NO\_off}\cdot GC_2(t)$$

[Seq.J5] $$\frac{d}{dt}GC_2(t) = k_{GC1\_NO\_on}\cdot NO\left(NO_0, NO_1, t\right)\cdot GC_1(t) - k_{GC2\_NO\_off}\cdot GC_2(t) - k_{GC2\_act}\cdot GC_2(t)$$

[Seq.J6] $$\frac{d}{dt}GC_{1\_act}(t) = k_{GC1\_act}\cdot GC_1(t) - k_{GC1\_deact}\cdot GC_{1\_act}(t) + k_{GC2\_act}\cdot GC_2(t) - k_{PKG\_GC}\cdot relPKG_1(cGMP(t))\cdot GC_{1\_act}(t)$$

[Seq.J7] $$GC_T = GC_0(t) + GC_1(t) + GC_{1\_act}(t) + GC_{0P}(t) + GC_2(t)$$

[Seq.J8] $$\frac{d}{dt}AC_P(t) = k_{PKA\_AC}\cdot relPKA_1(cAMP(t))\cdot AC_0(t) - k_{PP\_AC}\cdot AC_P(t)$$

[Seq.J9] $$\frac{d}{dt}AC_1(t) = k_{AC0\_Gs\_on}\cdot AC_0(t)\cdot G_{s0\_GTP}(t) - k_{AC1\_Gs\_off}\cdot AC_1(t) - k_{Gs\_GTPase}\cdot AC_1(t)$$

[Seq.J10] $$\frac{d}{dt}cAMP(t) = \frac{10^6\cdot k_{AC1\_ATP}}{\nu}\cdot AC_1(t) + \frac{10^6\cdot k_{AC0\_ATP}}{\nu}\cdot AC_0(t) \ldots + (-1)\cdot\left[k_{PDE\_cAMP}\cdot cAMP(t)\cdot\left(PDE_{cAMP}(t)\cdot relPDE_{cAMP}(cAMP(t)) + PDE_{cAMP\_P}(t)\cdot relPDE_{cAMP\_P}(cAMP(t))\right)\right]$$

[Seq.J11] $$\frac{d}{dt}\alpha AR_1(t) = k_{\alpha AR\_on}\cdot\alpha A\_steady\left(\alpha A_0,\alpha A_1,t\right)\cdot\alpha AR_0(t) - \left(k_{\alpha AR\_off} + k_{Gq0\_GDP\_\alpha AR\_on}\cdot G_{q0\_GDP}(t) + k_{\alpha AR\_P}\right)\cdot\alpha AR_1(t) \ldots + \left(k_{Gq1\_GDP\_\alpha AR\_off} + k_{Gq1\_GDP\_GTP\_exch}\right)\cdot G_{q1\_GDP}(t)$$

[Seq.J12] $$\frac{d}{dt}\alpha AR_0(t) = -k_{\alpha AR\_on}\cdot\alpha A\_steady\left(\alpha A_0,\alpha A_1,t\right)\cdot\alpha AR_0(t) + k_{\alpha AR\_off}\cdot\alpha AR_1(t) + k_{\alpha AR\_recyc}\cdot\alpha AR_{in}(t)$$

[Seq.J13] $$\frac{d}{dt}\alpha AR_P(t) = k_{\alpha AR\_P}\cdot\alpha AR_1(t) - k_{\alpha AR\_endo}\cdot\alpha AR_P(t)$$

[Seq.J14] $$\frac{d}{dt}G_{q0\_GTP}(t) = k_{Gq1\_GDP\_GTP\_exch}\cdot G_{q1\_GDP}(t) - k_{Gq\_GTPase}\cdot G_{q0\_GTP}(t) - k_{PLC\_Gq0\_GTP\_on}\cdot G_{q0\_GTP}(t)\cdot PLC(t) \ldots + k_{PLC\_Gq0\_GTP\_off}\cdot PLC_{Gq0\_GTP}(t) - k_{PLC\_P\_Gq0\_GTP\_on}\cdot PLC_P(t)\cdot G_{q0\_GTP}(t) + k_{PLC\_P\_Gq0\_GTP\_off}\cdot PLC_{P\_Gq0\_GTP}(t)$$

[Seq.J15] $$\frac{d}{dt}G_{q1\_GDP}(t) = k_{Gq0\_GDP\_\alpha AR\_on}\cdot G_{q0\_GDP}(t)\cdot\alpha AR_1(t) - k_{Gq1\_GDP\_\alpha AR\_off}\cdot G_{q1\_GDP}(t) - k_{Gq1\_GDP\_GTP\_exch}\cdot G_{q1\_GDP}(t)$$

[Seq.J16] $$\frac{d}{dt}PLC_{PIP}(t) = k_{PLC\_PIP\_on}\cdot PLC(t)\cdot PIP_T - \left(k_{PLC\_PIP\_off} + k_{PLC\_PIP\_hyd}\right)\cdot PLC_{PIP}(t)$$

[Seq.J17] $$\frac{d}{dt}PLC_{Gq0\_GTP}(t) = k_{PLC\_Gq0\_GTP\_on}\cdot PLC(t)\cdot G_{q0\_GTP}(t) - k_{PLC\_Gq0\_GTP\_off}\cdot PLC_{Gq0\_GTP}(t) - k_{PLC\_Gq0\_GTP\_hyd}\cdot PLC_{Gq0\_GTP}(t) \ldots + \left(-k_{PLC\_Gq0\_GTP\_PIP\_on}\cdot PLC_{Gq0\_GTP}(t)\cdot PIP_T\right) + k_{PLC\_Gq0\_GTP\_PIP\_off}\cdot PLC_{Gq0\_GTP\_PIP}(t) \ldots + k_{PLC\_Gq0\_GTP\_PIP\_hyd}\cdot PLC_{Gq0\_GTP\_PIP}(t) - \left(k_{PKA\_PLC\_Gq0\_GTP}\cdot relPKA_1(cAMP(t))\cdot PLC_{Gq0\_GTP}(t)\right) \ldots + \left(-k_{PKC\_PLC\_Gq0\_GTP}\cdot relPKC_{11}\left(DAG(t),Ca_{in}(t)\right)\cdot PLC_{Gq0\_GTP}(t)\right)$$

[Seq.J18] $$\frac{d}{dt}PLC_{Gq0\_GTP\_PIP}(t) = k_{PLC\_Gq0\_GTP\_PIP\_on}\cdot PLC_{Gq0\_GTP}(t)\cdot PIP_T - k_{PLC\_Gq0\_GTP\_PIP\_off}\cdot PLC_{Gq0\_GTP\_PIP}(t) \ldots + \left(-k_{PLC\_Gq0\_GTP\_PIP\_hyd}\cdot PLC_{Gq0\_GTP\_PIP}(t)\right)$$

[Seq.J19] $$\frac{d}{dt}PLC_{P\_Gq0\_GTP}(t) = \left(k_{PKA\_PLC\_Gq0\_GTP}\cdot relPKA_1(cAMP(t)) + k_{PKC\_PLC\_Gq0\_GTP}\cdot relPKC_{11}\left(DAG(t),Ca_{in}(t)\right)\right)\cdot PLC_{Gq0\_GTP}(t) \ldots + k_{PLC\_P\_Gq0\_GTP\_on}\cdot PLC_P(t)\cdot G_{q0\_GTP}(t) - k_{PLC\_P\_Gq0\_GTP\_off}\cdot PLC_{P\_Gq0\_GTP}(t)$$

[Seq.J20] $$\frac{d}{dt}PLC_P(t) = -k_{PLC\_P\_Gq0\_GTP\_on}\cdot PLC_P(t)\cdot G_{q0\_GTP}(t) + k_{PLC\_P\_Gq0\_GTP\_off}\cdot PLC_{P\_Gq0\_GTP}(t) - k_{PP\_PLC}\cdot PLC_P(t)$$

[Seq.J21] $$\frac{d}{dt}IP3(t) = \frac{10^6}{\nu}\cdot\left(k_{PLC\_Gq0\_GTP\_PIP\_hyd}\cdot PLC_{Gq0\_GTP\_PIP}(t) + k_{PLC\_PIP\_hyd}\cdot PLC_{PIP}(t)\right) - k_{met\_IP3}\cdot IP3(t)$$

[Seq.J22] $$\frac{d}{dt}BK_{PKC}(t) = k_{PKC\_BK}\cdot relPKC_{11}\left(DAG(t), Ca_{jun}(t)\right)\cdot BK(t) - k_{PP\_BK}\cdot BK_{PKC}(t)$$

[Seq.J23] $$\frac{d}{dt}BK_{PKA}(t) = k_{PKA\_BK}\cdot relPKA_{1}(cAMP(t))\cdot BK(t) - k_{PP\_BK}\cdot BK_{PKA}(t)$$

[Seq.J24] $$\frac{d}{dt}BK_{PKG}(t) = k_{PKG\_BK}\cdot relPKG_{1}(cGMP(t))\cdot BK(t) - k_{PP\_BK}\cdot BK_{PKG}(t)$$

[Seq.J25] $$\alpha AR_0(t) + \alpha AR_1(t) + \alpha AR_P(t) + \alpha AR_{in}(t) + G_{q1\_GDP}(t) = \alpha AR_T$$

[Seq.J26] $$G_{q0\_GDP}(t) + G_{q0\_GTP}(t) + G_{q1\_GDP}(t) + PLC_{Gq0\_GTP}(t) + PLC_{Gq0\_GTP\_PIP}(t) + PLC_{P\_Gq0\_GTP}(t) = G_{qT}$$

[Seq.J27] $$BK(t) + BK_{PKC}(t) + BK_{PKA}(t) + BK_{PKG}(t) = BK_T$$

[Seq.J28] $$PLC(t) + PLC_{Gq0\_GTP}(t) + PLC_{PIP}(t) + PLC_{Gq0\_GTP\_PIP}(t) + PLC_P(t) + PLC_{P\_Gq0\_GTP}(t) = PLC_T$$

[Seq.J29] $$\frac{d}{dt}DAG(t) = \frac{10^6}{\nu}\cdot\left(k_{PLC\_Gq0\_GTP\_PIP\_hyd}\cdot PLC_{Gq0\_GTP\_PIP}(t) + k_{PLC\_PIP\_hyd}\cdot PLC_{PIP}(t)\right) - k_{met\_DAG}\cdot DAG(t)$$

[Seq.J30]

$$\frac{d}{dt}V(t) = \frac{-1\cdot 10^{-9}}{C_m}\left(\begin{array}{l} I_{P2XR\_ALL}\left(V(t), Na_{in}(t), K_{in}(t), Ca_{in}(t), P2XR\_3\_act(t)\right) + I_{KATP\_ALL}\left(V(t), K_{in}(t), KATP(t), KATP_{PKA}(t)\right) \ldots \\ + I_{NSCne\_ALL}\left(V(t), DAG(t), Na_{in}(t), K_{in}(t), Ca_{in}(t)\right) + I_{BK\_ALL}\left(V(t), Ca_{jun}(t), K_{in}(t), BK(t), BK_{PKA}(t), BK_{PKC}(t), BK_{PKG}(t)\right) \ldots \\ + I_{CaV\_ALL}\left(V(t), Ca_{in}(t), CaV(t), CaV_{PKC}(t), CaV_{PKG}(t)\right) + I_{Kv}\left(V(t), K_{in}(t)\right) + I_{PMCA}\left(V(t), Ca_{in}(t)\right) + I_{NCX}\left(V(t), Ca_{in}(t), Na_{in}(t)\right) \ldots \\ + I_{NaK}\left(V(t), Na_{in}(t), K_{in}(t)\right) \ldots \\ + I_{NSCstr\_ALL}\left(V(t), DAG(t), Na_{in}(t), K_{in}(t), Ca_{NSCstr}(t), BP\left(BP_0, BP_1, t\right), NSCstr(t), NSCstr\_PKC(t), NSCstr\_PKG(t)\right) \ldots \\ + I_{ClA}\left(V(t), Ca_{NSCstr}(t), Cl_{in}(t)\right) \ldots \\ + I_{NSCeet\_ALL}\left(V(t), EET\left(EET_0, EET_1, t\right), Na_{in}(t), K_{in}(t), Ca_{jun}(t)\right) + I_{ALL\_leak}\left(V(t), K_{in}(t), Na_{in}(t), Cl_{in}(t), Ca_{in}(t)\right) \end{array}\right)$$

[Seq.J31]
$$\frac{d}{dt}Cl_{in}(t) = \left(\frac{-10^{-9}}{z_{Cl}\cdot F\cdot VOL_{cell}}\right)\cdot\left(I_{ClA}\left(V(t),Ca_{NSCstr}(t),Cl_{in}(t)\right) + I_{Cl\_leak}\left(V(t),Cl_{in}(t)\right)\right) \ldots + \frac{10^{-12}}{VOL_{cell}}\cdot J_{NaK\_Cl}\left(NaKCl(t),NaKCl_{PKC}(t),Na_{in}(t),K_{in}(t),Cl_{in}(t)\right)$$

[Seq.J32]
$$\frac{d}{dt}BUF_1(t) = k_{BUF\_on}\cdot Ca_{in}(t)\cdot\left(BUF_T - BUF_1(t)\right) - k_{BUF\_off}\cdot BUF_1(t)$$

[Seq.J33]
$$\frac{d}{dt}BUF_{jun1}(t) = k_{BUF\_on}\cdot Ca_{jun}(t)\cdot\left(BUF_{jun\_T} - BUF_{jun1}(t)\right) - k_{BUF\_off}\cdot BUF_{jun1}(t)$$

[Seq.J34]
$$\frac{d}{dt}CSQ_{SRper1}(t) = k_{CSQ\_on}\cdot Ca_{SRper}(t)\cdot\left(CSQ_{SRper\_T} - CSQ_{SRper1}(t)\right) - k_{CSQ\_off}\cdot CSQ_{SRper1}(t)$$

[Seq.J35]
$$\frac{d}{dt}CSQ_{SRcen1}(t) = k_{CSQ\_on}\cdot Ca_{SRcen}(t)\cdot\left(CSQ_{SRcen\_T} - CSQ_{SRcen1}(t)\right) - k_{CSQ\_off}\cdot CSQ_{SRcen1}(t)$$

[Seq.J36]
$$\frac{d}{dt}Na_{in}(t) = \frac{-10^{-9}}{z_{Na}\cdot F\cdot VOL_{cell}}\cdot\left(\begin{array}{l} I_{NaP2XR}\left(V(t),Na_{in}(t),P2XR\_3\_act(t)\right) + I_{NaNSCne}\left(V(t),DAG(t),Na_{in}(t),Ca_{in}(t)\right) \ldots \\ + I_{NaNSCstr\_ALL}\left(V(t),DAG(t),Na_{in}(t),Ca_{NSCstr}(t),BP\left(BP_0,BP_1,t\right),NSCstr(t),NSCstr\_PKC(t),NSCstr\_PKG(t)\right) \ldots \\ + 3\cdot I_{NCX}\left(V(t),Ca_{in}(t),Na_{in}(t)\right) + 3\cdot I_{NaK}\left(V(t),Na_{in}(t),K_{in}(t)\right) + I_{NaNSCeet}\left(V(t),EET\left(EET_0,EET_1,t\right),Na_{in}(t)\right) \ldots \\ + I_{Na\_leak}\left(V(t),Na_{in}(t)\right) \end{array}\right) \ldots + \frac{10^{-12}}{VOL_{cell}}\cdot J_{KCl\_Na}\left(NaKCl(t),NaKCl_{PKC}(t),Na_{in}(t),K_{in}(t),Cl_{in}(t)\right)$$

[Seq.J37]

$$\frac{d}{dt}K_{in}(t) = \frac{-10^{-9}}{z_K \cdot F \cdot VOL_{cell}} \cdot \left(\begin{array}{l} I_{KP2XR}\left(V(t), K_{in}(t), P2XR\_3\_act(t)\right) + I_{KATP\_ALL}\left(V(t), K_{in}(t), KATP(t), KATP_{PKA}(t)\right) \ldots \\ + I_{BK\_ALL}\left(V(t), Ca_{jun}(t), K_{in}(t), BK(t), BK_{PKA}(t), BK_{PKC}(t), BK_{PKG}(t)\right) \ldots \\ + I_{KNSCne}\left(V(t), DAG(t), K_{in}(t), Ca_{in}(t)\right) \ldots \\ + I_{KNSCstr\_ALL}\left(V(t), DAG(t), K_{in}(t), Ca_{NSCstr}(t), BP\left(BP_0, BP_1, t\right), NSCstr(t), NSCstr\_PKC(t), NSCstr\_PKG(t)\right) \ldots \\ + I_{KNSCeet}\left(V(t), EET\left(EET_0, EET_1, t\right), K_{in}(t)\right) + I_{Kv}\left(V(t), K_{in}(t)\right) - 2 \cdot I_{NaK}\left(V(t), Na_{in}(t), K_{in}(t)\right) + I_{K\_leak}\left(V(t), K_{in}(t)\right) \end{array} \right) \ldots$$

$$+ \frac{10^{-12}}{VOL_{cell}} \cdot J_{NaCl\_K}\left(NaKCl(t), NaKCl_{PKC}(t), Na_{in}(t), K_{in}(t), Cl_{in}(t)\right)$$

[Seq.J38]

$$\frac{d}{dt}Ca_{in}(t) = \frac{-10^{-6}}{z_{Ca} \cdot F \cdot VOL_{cell}} \cdot \left(I_{CaP2XR}\left(V(t), Ca_{in}(t), P2XR\_3\_act(t)\right) + I_{CaV\_ALL}\left(V(t), Ca_{in}(t), CaV(t), CaV_{PKC}(t), CaV_{PKG}(t)\right)\right) \ldots$$

$$+ \frac{-10^{-6}}{z_{Ca} \cdot F \cdot VOL_{cell}} \cdot \left(I_{CaNSCne}\left(V(t), DAG(t), Ca_{in}(t)\right) + I_{Ca\_leak}\left(V(t), Ca_{in}(t)\right)\right) \ldots$$

$$+ \left(\frac{-10^{-6}}{F \cdot VOL_{cell}}\right) \cdot \left(I_{PMCA}\left(V(t), Ca_{in}(t)\right) - I_{NCX}\left(V(t), Ca_{in}(t), Na_{in}(t)\right)\right) + \frac{10^{-9}}{VOL_{cell}} \cdot J_{SERCA\_ALL}\left(Ca_{in}(t), Ca_{SRcen}(t), SERCA(t), SERCA\_P(t)\right) \ldots$$

$$+ \frac{10^{-9}}{VOL_{cell}} \cdot J_{jun\_cyt}\left(Ca_{jun}(t), Ca_{in}(t)\right) - \left[k_{BUF\_on} \cdot Ca_{in}(t) \cdot \left(BUF_T - BUF_1(t)\right) - k_{BUF\_off} \cdot BUF_1(t)\right] \ldots$$

$$+ \frac{10^{-9}}{VOL_{cell}} \cdot J_{IP3R\_ALL}\left(Ca_{in}(t), IP3(t), Ca_{SRcen}(t), IP3R(t), IP3R_{IRAG\_PKG}(t)\right) + \frac{10^{-9}}{VOL_{cell}} \cdot J_{CaNSCstr\_cyt}\left(Ca_{NSCstr}(t), Ca_{in}(t)\right)$$

[Seq.J39]

$$\frac{d}{dt}Ca_{jun}(t) = \frac{10^{-9}}{VOL_{jun}}\cdot J_{RyR\_ALL}\left(Ca_{jun}(t), Ca_{SRper}(t), RyR_{PKA}(t), RyR_{PKC}(t)\right) - \frac{10^{-9}}{VOL_{jun}}\cdot J_{jun\_cyt}\left(Ca_{jun}(t), Ca_{in}(t)\right) \ldots$$
$$+ k_{BUF\_off}\cdot BUF_{jun1}(t) + \left(\frac{-10^{-6}}{z_{Ca}\cdot F\cdot VOL_{jun}}\right)\cdot I_{CaNSCeet}\left(V(t), EET\left(EET_0, EET_1, t\right), Ca_{jun}(t)\right) - k_{BUF\_on}\cdot Ca_{jun}(t)\cdot\left(BUF_{jun\_T} - BUF_{jun1}(t)\right)$$

[Seq.J40]
$$\frac{d}{dt}Ca_{SRper}(t) = \frac{10^{-9}}{VOL_{SRper}}\cdot\left(-J_{RyR\_ALL}\left(Ca_{jun}(t), Ca_{SRper}(t), RyR_{PKA}(t), RyR_{PKC}(t)\right) + J_{cen\_per}\left(Ca_{SRcen}(t), Ca_{SRper}(t)\right)\right) \ldots$$
$$+\left[-k_{CSQ\_on}\cdot Ca_{SRper}(t)\cdot\left(CSQ_{SRper\_T} - CSQ_{SRper1}(t)\right) + k_{CSQ\_off}\cdot CSQ_{SRper1}(t)\right]$$

[Seq.J41]
$$\frac{d}{dt}Ca_{SRcen}(t) = \frac{-10^{-9}}{VOL_{SRcen}}\cdot\left[\begin{array}{l}\left(J_{SERCA\_ALL}\left(Ca_{in}(t), Ca_{SRcen}(t), SERCA(t), SERCA\_P(t)\right) + J_{cen\_per}\left(Ca_{SRcen}(t), Ca_{SRper}(t)\right)\right) \ldots \\ + J_{IP3R\_ALL}\left(Ca_{in}(t), IP3(t), Ca_{SRcen}(t), IP3R(t), IP3R_{IRAG\_PKG}(t)\right)\end{array}\right] \ldots$$
$$+\left[-k_{CSQ\_on}\cdot Ca_{SRcen}(t)\cdot\left(CSQ_{SRcen\_T} - CSQ_{SRcen1}(t)\right) + k_{CSQ\_off}\cdot CSQ_{SRcen1}(t)\right]$$

[Seq.J42]
$$\frac{d}{dt}\beta AR_1(t) = k_{\beta AR\_on}\cdot\beta A\left(\beta A_0, \beta A_1, t\right)\cdot\beta AR_0(t) - \left(k_{\beta AR\_off} + k_{Gs0\_GDP\_\beta AR\_on}\cdot G_{s0\_GDP}(t) + k_{\beta AR\_P}\right)\cdot\beta AR_1(t) \ldots$$
$$+\left(k_{Gs1\_GDP\_\beta AR\_off} + k_{Gs1\_GDP\_GTP\_exch}\right)\cdot G_{s1\_GDP}(t)$$

[Seq.J43]
$$\frac{d}{dt}\beta AR_0(t) = -k_{\beta AR\_on}\cdot\beta A\left(\beta A_0, \beta A_1, t\right)\cdot\beta AR_0(t) + k_{\beta AR\_off}\cdot\beta AR_1(t) + k_{\beta AR\_recyc}\cdot\beta AR_{in}(t)$$

[Seq.J44]
$$\frac{d}{dt}\beta AR_P(t) = k_{\beta AR\_P}\cdot\beta AR_1(t) - k_{\beta AR\_endo}\cdot\beta AR_P(t)$$

[Seq.J45]
$$\beta AR_0(t) + \beta AR_1(t) + \beta AR_P(t) + \beta AR_{in}(t) + G_{s1\_GDP}(t) = \beta AR_T$$

[Seq.J46]
$$\frac{d}{dt}G_{s0\_GTP}(t) = k_{Gs1\_GDP\_GTP\_exch}\cdot G_{s1\_GDP}(t) - k_{Gs\_GTPase}\cdot G_{s0\_GTP}(t) - k_{AC0\_Gs\_on}\cdot AC_0(t)\cdot G_{s0\_GTP}(t) + k_{AC1\_Gs\_off}\cdot AC_1(t)$$

[Seq.J47]
$$\frac{d}{dt}G_{s1\_GDP}(t) = k_{Gs0\_GDP\_\beta AR\_on}\cdot G_{s0\_GDP}(t)\cdot\beta AR_1(t) - k_{Gs1\_GDP\_\beta AR\_off}\cdot G_{s1\_GDP}(t) - k_{Gs1\_GDP\_GTP\_exch}\cdot G_{s1\_GDP}(t)$$

[Seq.J48]
$$G_{s0\_GDP}(t) + G_{s0\_GTP}(t) + G_{s1\_GDP}(t) + AC_1(t) = G_{sT}$$

[Seq.J49] $$AC_0(t) + AC_1(t) + AC_P(t) = AC_T$$

[Seq.J50] $$\frac{d}{dt}IP3R_{IRAG\_PKG}(t) = k_{PKG\_IP3R\_IRAG}\cdot relPKG_1(cGMP(t))\cdot IP3R(t) - k_{PP\_IP3R\_IRAG\_PKG}\cdot IP3R_{IRAG\_PKG}(t)$$

[Seq.J51] $$IP3R(t) + IP3R_{IRAG\_PKG}(t) = IP3R_T$$

[Seq.J52] $$\frac{d}{dt}Ca_{NSCstr}(t) = \frac{10^{-9}}{VOL_{NSCstr}}\cdot\left[\begin{array}{l} J_{CaNSCstr\_ALL}\left(V(t), DAG(t), Ca_{NSCstr}(t), BP\left(BP_0, BP_1, t\right), NSCstr(t), NSCstr\_PKC(t), NSCstr\_PKG(t)\right) \ldots \\ +\left(-J_{CaNSCstr\_cyt}\left(Ca_{NSCstr}(t), Ca_{in}(t)\right)\right) \end{array}\right] \ldots$$
$$+\left[-k_{BUF\_on}\cdot Ca_{NSCstr}(t)\cdot\left(BUF_{NSCstr\_T} - BUF_{NSCstr1}(t)\right) + k_{BUF\_off}\cdot BUF_{NSCstr1}(t)\right]$$

[Seq.J53] $$\frac{d}{dt}BUF_{NSCstr1}(t) = k_{BUF\_on}\cdot Ca_{NSCstr}(t)\cdot\left(BUF_{NSCstr\_T} - BUF_{NSCstr1}(t)\right) - k_{BUF\_off}\cdot BUF_{NSCstr1}(t)$$

[Seq.J54] $$\frac{d}{dt}RyR_{PKA}(t) = k_{PKA\_RyR}\cdot relPKA_1(cAMP(t))\cdot RyR(t) - k_{PP\_RyR}\cdot RyR_{PKA}(t)$$

[Seq.J55] $$\frac{d}{dt}RyR_{PKC}(t) = k_{PKC\_RyR}\cdot relPKC_{11}\left(DAG(t), Ca_{jun}(t)\right)\cdot RyR(t) - k_{PP\_RyR}\cdot RyR_{PKC}(t)$$

[Seq.J56] $$RyR(t) + RyR_{PKA}(t) + RyR_{PKC}(t) = RyR_T$$

[Seq.J57] $$\frac{d}{dt}CaV_{PKC}(t) = k_{PKC\_CaV}\cdot relPKC_{11}\left(DAG(t), Ca_{in}(t)\right)\cdot CaV(t) - k_{PP\_CaV}\cdot CaV_{PKC}(t)$$

[Seq.J58] $$\frac{d}{dt}CaV_{PKG}(t) = k_{PKG\_CaV}\cdot relPKG_1(cGMP(t))\cdot CaV(t) - k_{PP\_CaV}\cdot CaV_{PKG}(t)$$

[Seq.J59] $$CaV(t) + CaV_{PKC}(t) + CaV_{PKG}(t) = CaV_T$$

[Seq.J60] $$\frac{d}{dt}SERCA\_P(t) = \left(k_{PKA\_SERCA}\cdot relPKA_1(cAMP(t)) + k_{PKG\_SERCA}\cdot relPKG_1(cGMP(t)) + k_{PKC\_SERCA}\cdot relPKC_{11}\left(DAG(t), Ca_{in}(t)\right)\right)\cdot SERCA(t)$$
$$+\left(-k_{PP\_SERCA}\cdot SERCA\_P(t)\right)$$

[Seq.J61] $$SERCA(t) + SERCA\_P(t) = SERCA_T$$

[Seq.J62] $$\frac{d}{dt}PDE_{cAMP\_P}(t) = \left(k_{PKA\_PDE}\cdot relPKA_1(cAMP(t)) + k_{PKG\_PDE}\cdot relPKG_1(cGMP(t))\right)\cdot PDE_{cAMP}(t) - k_{PP\_PDE}\cdot PDE_{cAMP\_P}(t)$$

[Seq.J63] $$PDE_{cAMP}(t) + PDE_{cAMP\_P}(t) = PDE_{cAMP\_T}$$

[Seq.J64] $$\frac{d}{dt}PDE_{cGMP\_P}(t) = \left(k_{PKA\_PDE}\cdot relPKA_1(cAMP(t)) + k_{PKG\_PDE}\cdot relPKG_1(cGMP(t))\right)\cdot PDE_{cGMP}(t) - k_{PP\_PDE}\cdot PDE_{cGMP\_P}(t)$$

[Seq.J65] $$PDE_{cGMP}(t) + PDE_{cGMP\_P}(t) = PDE_{cGMP\_T}$$

[Seq.J66] $$NaKCl(t) + NaKCl_{PKC}(t) = NaKCl_T$$

[Seq.J67] $$\frac{d}{dt}NaKCl_{PKC}(t) = k_{PKC\_NaKCl}\cdot relPKC_{11}\left(DAG(t), Ca_{in}(t)\right)\cdot NaKCl(t) - k_{PP\_NaKCl}\cdot\frac{PP_{NaKCl}(t)}{PP_{NaKCl\_T}}\cdot NaKCl_{PKC}(t) - k_{PP\_P\_NaKCl}\cdot\frac{PP_{P\_NaKCl}(t)}{PP_{NaKCl\_T}}\cdot NaKCl_{PKC}(t)$$

[Seq.J68] $$PP_{NaKCl}(t) + PP_{P\_NaKCl}(t) = PP_{NaKCl\_T}$$

[Seq.J69] $$\frac{d}{dt}PP_{P\_NaKCl}(t) = k_{PKA\_PP\_NaKCl}\cdot relPKA_1(cAMP(t))\cdot PP_{NaKCl}(t) + k_{PKG\_PP\_NaKCl}\cdot relPKG_1(cGMP(t))\cdot PP_{NaKCl}(t) - k_{PP\_PP\_NaKCl}\cdot PP_{P\_NaKCl}(t)$$

[Seq.J70] $$\frac{d}{dt}NSCstr\_PKC(t) = k_{PKC\_NSCstr}\cdot relPKC_{11}\left(DAG(t), Ca_{NSCstr}(t)\right)\cdot NSCstr(t) - k_{PP\_NSCstr}\cdot NSCstr\_PKC(t)$$

[Seq.J71] $$\frac{d}{dt}NSCstr\_PKG(t) = k_{PKG\_NSCstr}\cdot relPKG_1(cGMP(t))\cdot NSCstr(t) - k_{PP\_NSCstr}\cdot NSCstr\_PKG(t)$$

[Seq.J72] $$NSCstr(t) + NSCstr\_PKC(t) + NSCstr\_PKG(t) = NSCstr_T$$

[Seq.J73] $$KATP(t) + KATP_{PKA}(t) + KATP_{PKC\varepsilon}(t) = KATP_T$$

[Seq.J74] $$\frac{d}{dt}KATP_{PKA}(t) = k_{PKA\_KATP}\cdot relPKA_1(cAMP(t))\cdot KATP(t) - k_{PP\_KATP\_PKA}\cdot KATP_{PKA}(t)$$

[Seq.J75] $$\frac{d}{dt}KATP_{PKC\varepsilon}(t) = k_{PKC\varepsilon\_KATP}\cdot relPKC\varepsilon_{DAG}(DAG(t))\cdot KATP(t) - k_{PP\_KATP\_PKC\varepsilon}\cdot KATP_{PKC\varepsilon}(t)$$

[Seq.J76] $$P2XR\_0(t) + P2XR\_3(t) + P2XR\_3\_act(t) + P2XD\_0(t) + P2XD\_3(t) + P2XD\_0\_PKD(t) + P2XD\_3\_PKD(t) = P2XR_T$$

[Seq.J77] $$\frac{d}{dt}P2XR\_3(t) = k_{P2XR\_0\_on}\cdot ATP\_steady\left(ATP_0,\alpha A_1,t\right)^{n\_P2XR}\cdot P2XR\_0(t) - k_{P2XR\_3\_off}\cdot P2XR\_3(t) - k_{P2XR\_3\_act}\cdot P2XR\_3(t) \ldots + k_{P2XR\_3\_deact}\cdot P2XR\_3\_act(t)$$

[Seq.J78] $$\frac{d}{dt}P2XR\_3\_act(t) = k_{P2XR\_3\_act}\cdot P2XR\_3(t) - k_{P2XR\_3\_deact}\cdot P2XR\_3\_act(t) - k_{P2XR\_3\_act\_desens}\cdot P2XR\_3\_act(t) + k_{P2XD\_3\_resens}\cdot P2XD\_3(t)$$

[Seq.J79] $$\frac{d}{dt}P2XD\_0(t) = k_{P2XR\_0\_desens}\cdot P2XR\_0(t) - k_{P2XD\_0\_resens}\cdot P2XD\_0(t) \ldots + k_{PP\_P2XD\_0\_PKD}\cdot P2XD\_0\_PKD(t) - k_{P2XD\_0\_on}\cdot ATP\_steady\left(ATP_0,\alpha A_1,t\right)^{n\_P2XR}\cdot P2XD\_0(t) + k_{P2XD\_3\_off}\cdot P2XD\_3(t)$$

[Seq.J80] $$\frac{d}{dt}P2XD\_3(t) = k_{P2XR\_3\_act\_desens}\cdot P2XR\_3\_act(t) - k_{P2XD\_3\_resens}\cdot P2XD\_3(t) \ldots + k_{P2XD\_0\_on}\cdot ATP\_steady\left(ATP_0,\alpha A_1,t\right)^{n\_P2XR}\cdot P2XD\_0(t) - k_{P2XD\_3\_off}\cdot P2XD\_3(t) - k_{PKD\_P2XD\_3}\cdot relPKD_{DAG}(DAG(t))\cdot P2XD\_3(t)$$

[Seq.J81] $$\frac{d}{dt}P2XD\_0\_PKD(t) = -k_{P2XD\_0\_PKD\_on}\cdot ATP\_steady\left(ATP_0,\alpha A_1,t\right)^{n\_P2XR}\cdot P2XD\_0\_PKD(t) \ldots + k_{P2XD\_3\_PKD\_off}\cdot P2XD\_3\_PKD(t) - k_{PP\_P2XD\_0\_PKD}\cdot P2XD\_0\_PKD(t)$$

[Seq.J82] $$\frac{d}{dt}P2XD\_3\_PKD(t) = k_{PKD\_P2XD\_3}\cdot relPKD_{DAG}(DAG(t))\cdot P2XD\_3(t) \ldots + k_{P2XD\_0\_PKD\_on}\cdot ATP\_steady\left(ATP_0,\alpha A_1,t\right)^{n\_P2XR}\cdot P2XD\_0\_PKD(t) - k_{P2XD\_3\_PKD\_off}\cdot P2XD\_3\_PKD(t)$$

Initial conditions

[Seq.J83-89] $$\beta AR_0(t0) = \beta AR_T \quad \beta AR_1(t0) = 0 \quad \beta AR_P(t0) = 0 \quad \beta AR_{in}(t0) = 0 \quad G_{s0\_GDP}(t0) = G_{sT} \quad G_{s0\_GTP}(t0) = 0 \quad G_{s1\_GDP}(t0) = 0$$

[Seq.J90-96] $G_{q0\_GTP}(t0) = 0$ $GC_0(t0) = GC_T$ $GC_1(t0) = 0$ $GC_2(t0) = 0$ $GC_{1\_act}(t0) = 0$ $GC_{0P}(t0) = 0$ $cGMP(t0) = 0$

[Seq.J97-103] $\alpha AR_0(t0) = \alpha AR_T$ $\alpha AR_1(t0) = 0$ $\alpha AR_P(t0) = 0$ $\alpha AR_{in}(t0) = 0$ $G_{q0\_GDP}(t0) = G_{qT}$ $G_{q1\_GDP}(t0) = 0$ $PLC(t0) = PLC_T$

[Seq.J104-110] $PLC_{Gq0\_GTP}(t0) = 0$ $PLC_{Gq0\_GTP\_PIP}(t0) = 0$ $PLC_{PIP}(t0) = 0$ $PLC_P(t0) = 0$ $PLC_{P\_Gq0\_GTP}(t0) = 0$ $IP3(t0) = 0$ $DAG(t0) = 0$

[Seq.J111-117] $AC_1(t0) = 0$ $AC_0(t0) = AC_T$ $AC_P(t0) = 0$ $cAMP(t0) = 0$ $PDE_{cGMP}(t0) = PDE_{cGMP\_T}$ $PDE_{cGMP\_P}(t0) = 0$ $PDE_{cAMP}(t0) = PDE_{cAMP\_T}$

[Seq.J118-123] $PDE_{cAMP\_P}(t0) = 0$ $IP3R(t0) = IP3R_T$ $IP3R_{IRAG\_PKG}(t0) = 0$ $NSCstr(t0) = NSCstr_T$ $NSCstr\_PKC(t0) = 0$ $NSCstr\_PKG(t0) = 0$

[Seq.J124-130] $BK_{PKC}(t0) = 0$ $BK_{PKA}(t0) = 0$ $BK(t0) = BK_T$ $BK_{PKG}(t0) = 0$ $RyR_{PKA}(t0) = 0$ $RyR_{PKC}(t0) = 0$ $RyR(t0) = RyR_T$

[Seq.J131-136] $CaV(t0) = CaV_T$ $CaV_{PKC}(t0) = 0$ $CaV_{PKG}(t0) = 0$ $SERCA(t0) = SERCA_T$ $SERCA\_P(t0) = 0$ $NaKCl(t0) = NaKCl_T$

[Seq.J137-143] $NaKCl_{PKC}(t0) = 0$ $PP_{NaKCl}(t0) = PP_{NaKCl\_T}$ $PP_{P\_NaKCl}(t0) = 0$ $V(t0) = -60$ $Na_{in}(t0) = 7$ $K_{in}(t0) = 140$ $Ca_{in}(t0) = 0.1$

[Seq.J144-150] $Cl_{in}(t0) = 50$ $Ca_{jun}(t0) = 0.1$ $Ca_{SRper}(t0) = 100$ $KATP(t0) = KATP_T$ $KATP_{PKA}(t0) = 0$ $KATP_{PKC\varepsilon}(t0) = 0$ $BUF_1(t0) = 2.6$

[Seq.J151-156] $BUF_{jun1}(t0) = 2.6$ $BUF_{NSCstr1}(t0) = 2.6$ $Ca_{SRcen}(t0) = 100$ $CSQ_{SRper1}(t0) = 33$ $Ca_{NSCstr}(t0) = 0.1$ $CSQ_{SRcen1}(t0) = 33$

[Seq.J157-163] $P2XR\_0(t0) = P2XR_T$ $P2XR\_3(t0) = 0$ $P2XR\_3\_act(t0) = 0$ $P2XD\_0(t0) = 0$ $P2XD\_3(t0) = 0$ $P2XD\_0\_PKD(t0) = 0$ $P2XD\_3\_PKD(t0) = 0$

Solve function

$$\begin{bmatrix} \alpha AR_0 \\ \alpha AR_1 \\ \alpha AR_P \\ \alpha AR_{in} \\ G_{q0\_GDP} \\ G_{q1\_GDP} \\ G_{q0\_GTP} \\ PLC \\ PLC_{Gq0\_GTP} \\ PLC_{Gq0\_GTP\_PIP} \\ PLC_{PIP} \\ IP3 \\ DAG \\ V \\ Na_{in} \\ K_{in} \\ Ca_{in} \\ BUF_1 \\ Cl_{in} \\ BK \\ BK_{PKA} \\ BK_{PKC} \\ BK_{PKG} \\ RyR \\ RyR_{PKA} \\ RyR_{PKC} \\ CaV \\ CaV_{PKC} \end{bmatrix}$$

[Seq.J164]

$$W(BP_1) := \text{Odesolve}\left(\begin{matrix} CaV_{PKG} \\ SERCA \\ SERCA\_P \\ Ca_{jun} \\ BUF_{jun1} \\ Ca_{SRper} \\ CSQ_{SRper1} \\ Ca_{SRcen} \\ CSQ_{SRcen1} \\ GC_0 \\ GC_1 \\ GC_2 \\ GC_{1\_act} \\ GC_{0P} \\ cGMP \\ \beta AR_0 \\ \beta AR_1 \\ \beta AR_P \\ \beta AR_{in} \\ G_{s0\_GDP} \\ G_{s1\_GDP} \\ G_{s0\_GTP} \\ AC_0 \\ AC_1 \\ AC_P \\ cAMP \\ PDE_{cAMP} \end{matrix}, t, t1, N1\right)$$

$$\begin{bmatrix} \begin{pmatrix} PDE_{cAMP\_P} \\ PDE_{cGMP} \\ PDE_{cGMP\_P} \\ IP3R \\ IP3R_{IRAG\_PKG} \\ Ca_{NSCstr} \\ BUF_{NSCstr1} \\ NaKCl \\ NaKCl_{PKC} \\ PP_{NaKCl} \\ PP_{P\_NaKCl} \\ NSCstr \\ NSCstr\_PKC \\ NSCstr\_PKG \\ PLC_{P} \\ PLC_{P\_Gq0\_GTP} \\ KATP \\ KATP_{PKA} \\ KATP_{PKC\varepsilon} \\ P2XR\_0 \\ P2XR\_3 \\ P2XR\_3\_act \\ P2XD\_0 \\ P2XD\_3 \\ P2XD\_0\_PKD \\ P2XD\_3\_PKD \end{pmatrix} \end{bmatrix}$$

Number of variables

[Seq.J165] $num\_var := 81$

Vector of N1 +1 time points

[Seq.J166] $j := 0 .. N1$

$tt_j := j \cdot \frac{t1}{N1}$

Number of effector concentrations

[Seq.J167] $num\_eff\_conc := length(eff\_conc1)$

[Seq.J168]

$$ALLDATA := \left(\begin{array}{l} \text{for } i \in 0 .. num\_eff\_conc - 1 \\ \quad p \leftarrow eff\_conc1_i \\ \quad Z \leftarrow W(p) \\ \quad \text{for } k \in 0 .. num\_var - 1 \\ \quad\quad F \leftarrow Z_k \\ \quad\quad mm^{\langle k+i \cdot num\_var \rangle} \leftarrow \overrightarrow{F(tt)} \\ mm \end{array} \right)$$

p = each pressure or conc, in turn, of the varied effector.

Z is the vector of num_var functions of t for p = the i^{th}+1 effector pressure or conc.

These functions are obtained by the call of W(p) to the solve block above. The k^{th}+1 function is passed to F, which is evaluated at N1+1 times specified in the tt vector, defined above. These values form the N1+1 rows of column k + i*num_var of ALLDATA. In the present case, in which there are 81 functions of t returned by W(p) and 6 values of p, ALLDATA consists of 12001 rows by 6*81 (=486) columns, such that the first 81 columns correspond to the first value of p, the next 81 columns correspond to the second value of p, etc. (Note that vectors & matrices are indexed from 0.)

Click on the table and use scroll bars to access the entire table.

[Seq.J169] ALLDATA =

	0	1	2	3
0	6E+003	0E+000	0E+000	0E+000
1	6E+003	0E+000	0E+000	0E+000
2	6E+003	0E+000	0E+000	0E+000
3	6E+003	0E+000	0E+000	0E+000
4	6E+003	0E+000	0E+000	0E+000
5	6E+003	0E+000	0E+000	0E+000
6	6E+003	0E+000	0E+000	0E+000
7	6E+003	0E+000	0E+000	0E+000
8	6E+003	0E+000	0E+000	0E+000
9	6E+003	0E+000	0E+000	0E+000
10	6E+003	0E+000	0E+000	0E+000
11	6E+003	0E+000	0E+000	0E+000
12	6E+003	0E+000	0E+000	0E+000
13	6E+003	0E+000	0E+000	0E+000
14	6E+003	0E+000	0E+000	0E+000
15	6E+003	0E+000	0E+000	...

ALLDATA6 is a compression in which every 6 time points in ALLDATA are averaged. It is convenient for copying to Excel for later processing and plotting.

[Seq.J170]

$$\text{ALLDATA6} := \left| \begin{array}{l} \text{for } j \in 0 \,..\, \text{num\_eff\_conc} \cdot \text{num\_var} - 1 \\ \quad \text{for } i \in 0 \,..\, \frac{N1}{6} - 1 \\ \quad\quad \left| \begin{array}{l} \text{TIME\_POINTS} \leftarrow \text{submatrix}(\text{ALLDATA}, 6 \cdot i, 6 \cdot i + 5, j, j) \\ M_{i,j} \leftarrow \text{mean}(\text{TIME\_POINTS}) \end{array} \right. \\ M \end{array} \right.$$

[Seq.J171]

ALLDATA6 =

	0	1	2	3
0	6E+003	0E+000	0E+000	0E+000
1	6E+003	0E+000	0E+000	0E+000
2	6E+003	0E+000	0E+000	0E+000
3	6E+003	0E+000	0E+000	0E+000
4	6E+003	0E+000	0E+000	0E+000
5	6E+003	0E+000	0E+000	0E+000
6	6E+003	0E+000	0E+000	0E+000
7	6E+003	0E+000	0E+000	0E+000
8	6E+003	0E+000	0E+000	0E+000
9	6E+003	0E+000	0E+000	0E+000
10	6E+003	0E+000	0E+000	0E+000
11	6E+003	0E+000	0E+000	0E+000
12	6E+003	0E+000	0E+000	0E+000
13	6E+003	0E+000	0E+000	0E+000
14	6E+003	0E+000	0E+000	0E+000
15	6E+003	0E+000	0E+000	...

K. EXTRACTING VARIABLES AS FUNCTIONS OF TIME FROM ALLDATA

[Seq.K1]

$$\text{VARIABLE}(k) := \left| \begin{array}{l} \text{variable} \leftarrow \text{ALLDATA}^{\langle k \rangle} \\ \text{for } i \in 1 .. \text{num\_eff\_conc} - 1 \\ \quad \text{variable} \leftarrow \text{augment}\left(\text{variable}, \text{ALLDATA}^{\langle k+i \cdot \text{num\_var} \rangle}\right) \\ \text{variable} \end{array} \right.$$

To simplify defining plot variables, VARIABLE(k) is a submatrix of ALLDATA corresponding to the variable with index k, as determined by the order of variables in the vector following Odesolve above. The first column of variable is the k^{th} column of ALLDATA, which is augmented, for all i, by the k^{th}+ i*num_var column. In the current case, for example, VARIABLE (14) corresponds to variable V and consists of 6 columns, corresponding to the 6 values of BP_1, and N1+1 rows of V(t) values.These submatrices are assigned modified names to distinguish them from the variables in the solve block.

VARIABLE(k) for some k

[Seq.K2-6] VV := VARIABLE(13) Ca_in := VARIABLE(16) Ca_jun := VARIABLE(31) Ca_NSCstr := VARIABLE(60) Ca_SRcen := VARIABLE(35)

[Seq.K7-11] Ca_SRper := VARIABLE(33) Na_in := VARIABLE(14) K_in := VARIABLE(15) Cl_in := VARIABLE(18) NSC_str := VARIABLE(66)

[Seq.K12-15] NSC_str_PKC := VARIABLE(67) NSC_str_PKG := VARIABLE(68) Ca_V := VARIABLE(26) Ca_V_PKC := VARIABLE(27)

[Seq.K16-20] Ca_V_PKG := VARIABLE(28) BK := VARIABLE(19) BK_PKA := VARIABLE(20) BK_PKC := VARIABLE(21) BK_PKG := VARIABLE(22)

[Seq.K21-25] RYR := VARIABLE(23) RYR_PKA := VARIABLE(24) RYR_PKC := VARIABLE(25) SERCA := VARIABLE(29) SERCA_P := VARIABLE(30)

[Seq.K26-30] DAG := VARIABLE(12) IP_3 := VARIABLE(11) c_AMP := VARIABLE(53) c_GMP := VARIABLE(42) IP3_R := VARIABLE(58)

[Seq.K31-35] IP3_R_PKG := VARIABLE(59) αAR_0 := VARIABLE(0) αAR_1 := VARIABLE(1) αAR_p := VARIABLE(2) αAR_in := VARIABLE(3)

[Seq.K36-39] Gq0_GTP := VARIABLE(6) PLC_Gq0_GTP_PIP := VARIABLE(9) P2X1R_0 := VARIABLE(74) P2X1R_3 := VARIABLE(75)

[Seq.K40-43] P2X1R_3_act := VARIABLE(76) P2X1D_0 := VARIABLE(77) P2X1D_3 := VARIABLE(78) P2X1D_0_PKD := VARIABLE(79)

[Seq.K44] P2X1D_3_PKD := VARIABLE(80)

L. EFFECTOR CONCENTRATIONS & CURRENTS AS FUNCTIONS OF TIME

Currents that are functions of the above variables are tabulated such that the columns correspond to the different effector pressures or concentrations and the rows are the values at N1+1 times. The currents are defined as steady-state equations above the solve block. In some cases, the currents depend on effector concentrations. For each effector, a matrix with N1+1 rows and num_eff_conc columns is generated. For the effector that is varied, the i^{th}+1 column contains the concentrations at N1+1 times for the i^{th} nominal concentration of the effector. For the other effectors all colums are identrical.

Effector concentrations or pressures as functions of time

.

$i := 0 .. num\_eff\_conc - 1$

[Seq.L1-3] $\alpha AA_{j,i} := \alpha A\_steady(\alpha A_0, alphaA1_i, tt_j)$ $\beta AA_{j,i} := \beta A(\beta A_0, betaA1_i, tt_j)$ $B\_Press_{j,i} := BP(BP_0, bp1_i, tt_j)$

[Seq.L4-6] $EETT_{j,i} := EET(EET_0, eet1_i, tt_j)$ $NOX_{j,i} := NO(NO_0, nox1_i, tt_j)$ $ATPP_{j,i} := ATP\_steady(ATP_0, alphaA1_i, tt_j)$

Currents as functions of time

$i := 0 .. num\_eff\_conc - 1$

[Seq.L7] $I\_NSCstr\_ALL^{\langle i \rangle} := \overrightarrow{I_{NSCstr\_ALL}(VV^{\langle i \rangle}, DAG^{\langle i \rangle}, Na\_in^{\langle i \rangle}, K\_in^{\langle i \rangle}, Ca\_NSCstr^{\langle i \rangle}, B\_Press^{\langle i \rangle}, NSC\_str^{\langle i \rangle}, NSC\_str\_PKC^{\langle i \rangle}, NSC\_str\_PKG^{\langle i \rangle})}$

[Seq.L8] $I\_ClA^{\langle i \rangle} := \overrightarrow{I_{ClA}(VV^{\langle i \rangle}, Ca\_NSCstr^{\langle i \rangle}, Cl\_in^{\langle i \rangle})}$

[Seq.L9] $I\_CaV\_ALL^{\langle i \rangle} := \overrightarrow{I_{CaV\_ALL}(VV^{\langle i \rangle}, Ca\_in^{\langle i \rangle}, Ca\_V^{\langle i \rangle}, Ca\_V\_PKC^{\langle i \rangle}, Ca\_V\_PKG^{\langle i \rangle})}$

[Seq.L10] $I\_RyR\_ALL^{\langle i \rangle} := \overrightarrow{I_{RyR\_ALL}(Ca\_jun^{\langle i \rangle}, Ca\_SRper^{\langle i \rangle}, RYR\_PKA^{\langle i \rangle}, RYR\_PKC^{\langle i \rangle})}$

[Seq.L11] $I\_BK\_ALL^{\langle i \rangle} := \overrightarrow{I_{BK\_ALL}(VV^{\langle i \rangle}, Ca\_jun^{\langle i \rangle}, K\_in^{\langle i \rangle}, BK^{\langle i \rangle}, BK\_PKA^{\langle i \rangle}, BK\_PKC^{\langle i \rangle}, BK\_PKG^{\langle i \rangle})}$

[Seq.L12] $I\_PMCA^{\langle i \rangle} := \overrightarrow{I_{PMCA}\left(VV^{\langle i \rangle}, Ca\_in^{\langle i \rangle}\right)}$

[Seq.L13] $I\_NaK^{\langle i \rangle} := \overrightarrow{I_{NaK}\left(VV^{\langle i \rangle}, Na\_in^{\langle i \rangle}, K\_in^{\langle i \rangle}\right)}$

[Seq.L14] $I\_SERCA\_ALL^{\langle i \rangle} := \overrightarrow{I_{SERCA\_ALL}\left(Ca\_in^{\langle i \rangle}, Ca\_SRcen^{\langle i \rangle}, SERCA^{\langle i \rangle}, SERCA\_P^{\langle i \rangle}\right)}$

[Seq.L15] $I\_IP3R\_ALL^{\langle i \rangle} := \overrightarrow{I_{IP3R\_ALL}\left(Ca\_in^{\langle i \rangle}, IP\_3^{\langle i \rangle}, Ca\_SRcen^{\langle i \rangle}, IP3\_R^{\langle i \rangle}, IP3\_R\_PKG^{\langle i \rangle}\right)}$

[Seq.L16] $I\_NSCeet\_ALL^{\langle i \rangle} := \overrightarrow{I_{NSCeet\_ALL}\left(VV^{\langle i \rangle}, EETT^{\langle i \rangle}, Na\_in^{\langle i \rangle}, K\_in^{\langle i \rangle}, Ca\_jun^{\langle i \rangle}\right)}$

[Seq.L17] $I\_P2X1R\_ALL^{\langle i \rangle} := \overrightarrow{I_{P2XR\_ALL}\left(VV^{\langle i \rangle}, Na\_in^{\langle i \rangle}, K\_in^{\langle i \rangle}, Ca\_in^{\langle i \rangle}, P2X1R\_3\_act^{\langle i \rangle}\right)}$

[Seq.L18] $I\_Kv^{\langle i \rangle} := \overrightarrow{I_{Kv}\left(VV^{\langle i \rangle}, K\_in^{\langle i \rangle}\right)}$

M. PLOTS OF SOME VARIABLES AND FUNCTIONS OF VARIABLES VERSUS TIME

The column index <i> refers to the i^{th} +1 intravascular pressure; e.g., <0> refers to 10 mm Hg, <1> to 20 mm Hg, etc.

[Splot M1-3]

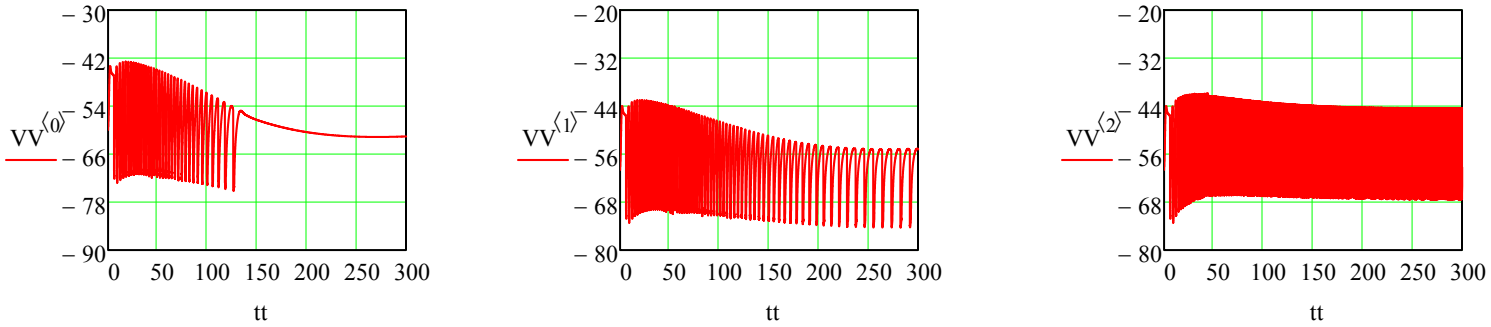

[Splot M4-6]

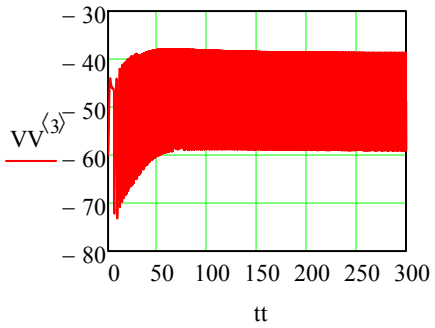

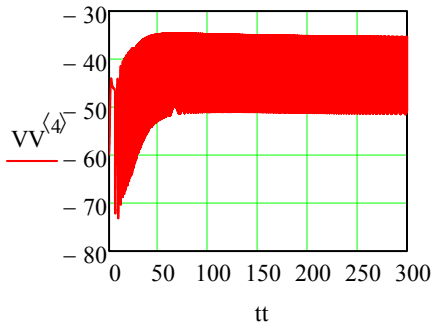

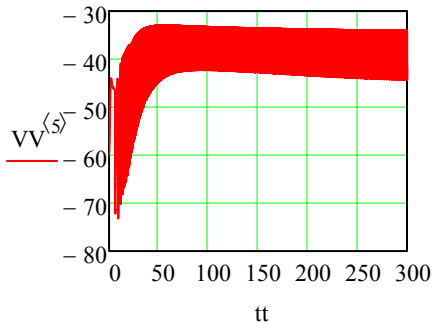

[Splot M7-9]

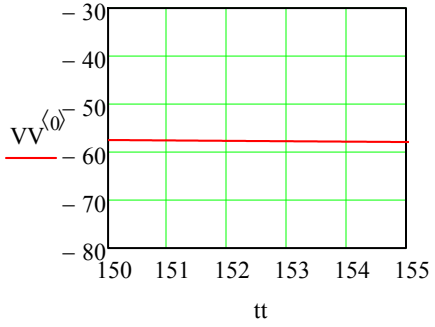

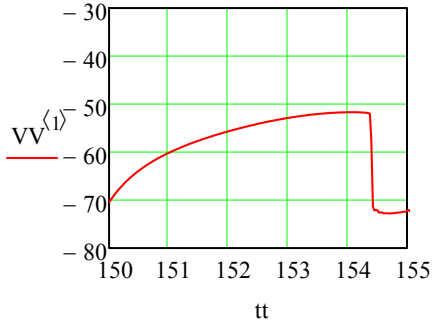

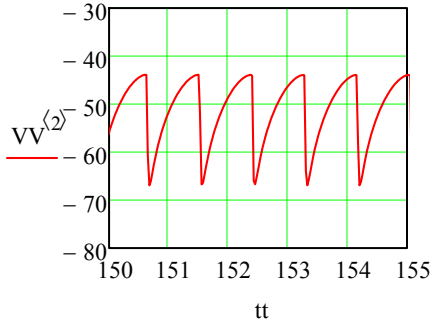

[Splot M10-12]

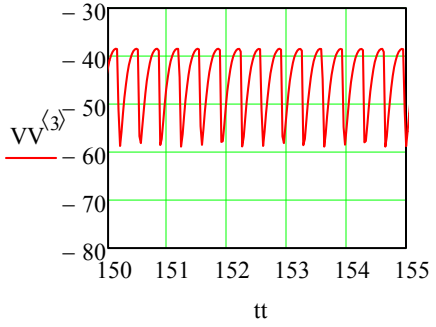

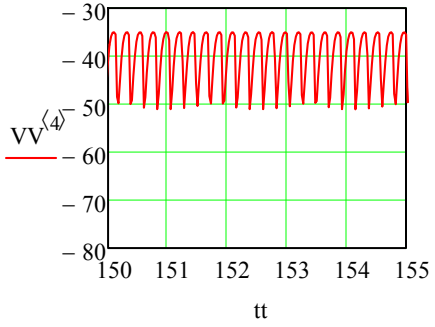

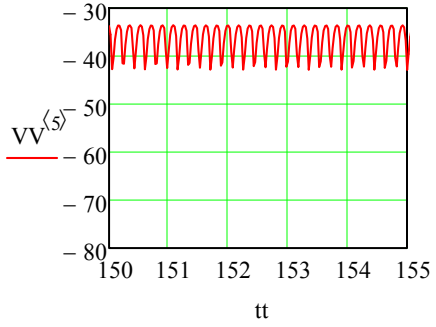

[Splot M13-15]

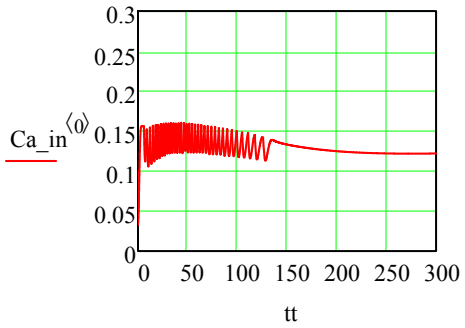

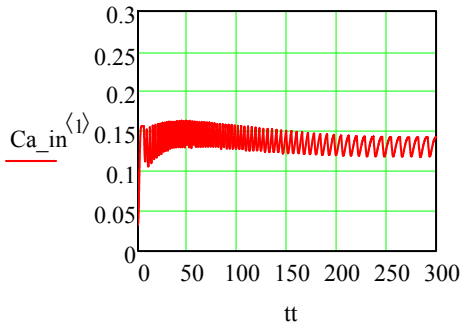

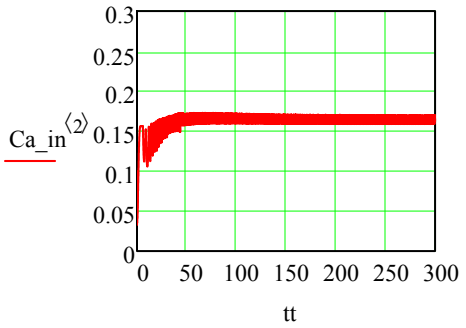

[Splot M16-18]

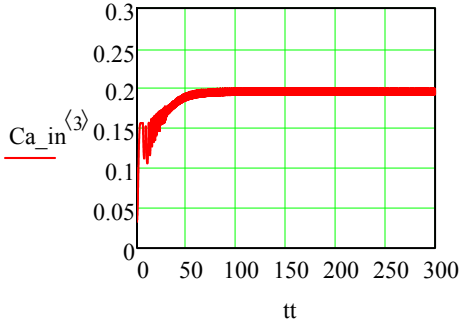

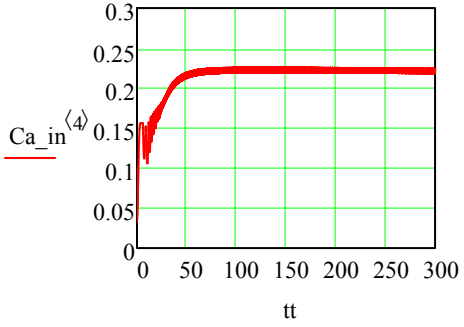

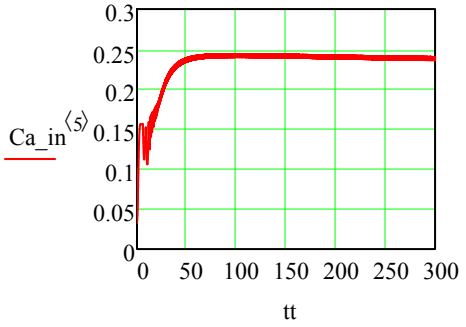

[Splot M19-21]

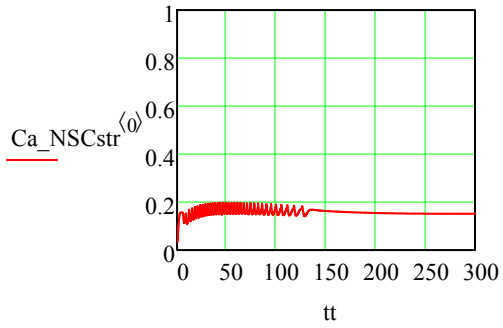

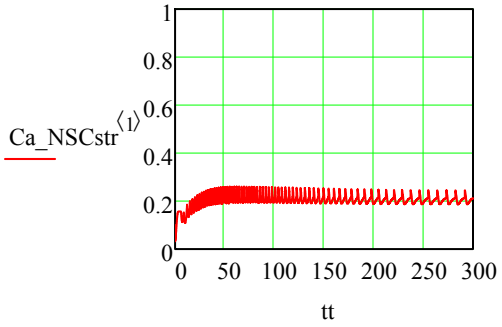

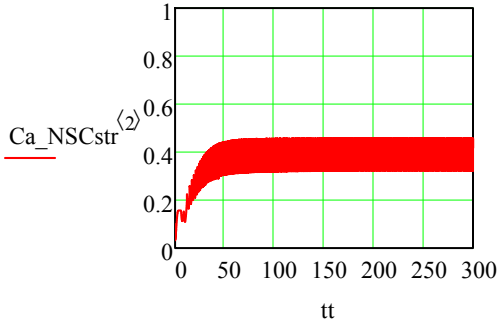

[Splot M22-24]

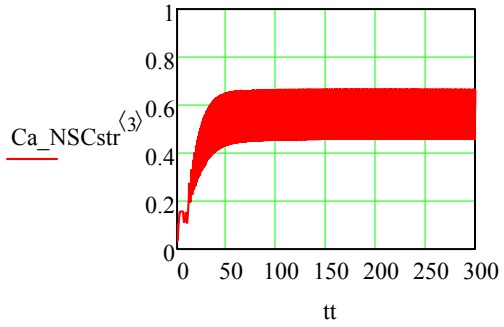

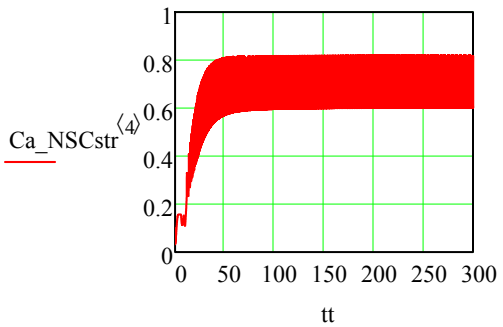

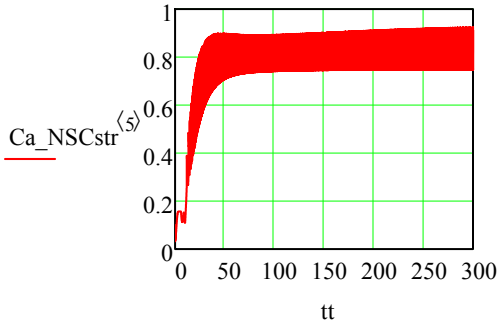

[Splot M25-27]

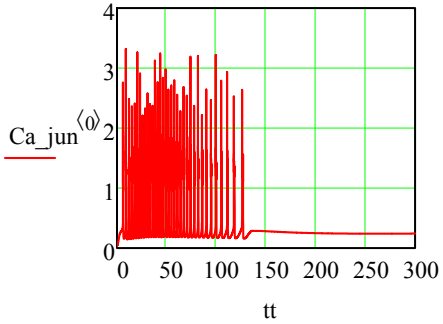

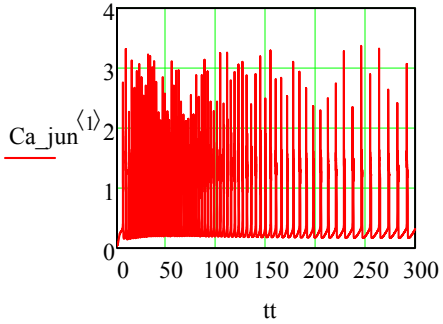

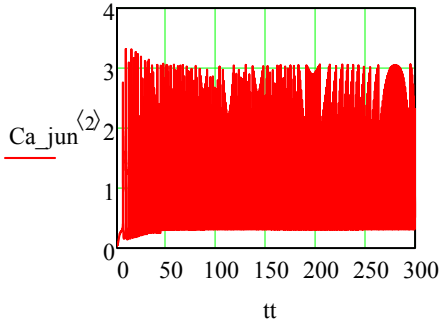

[Splot M28-30]

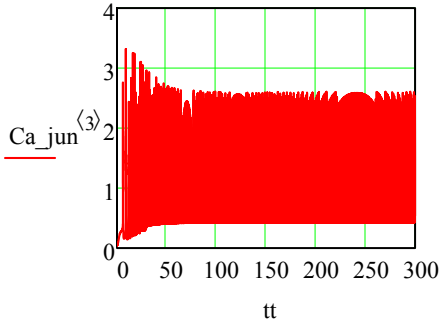

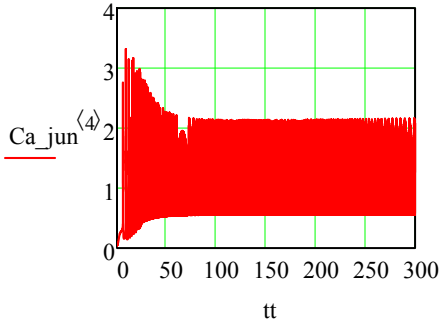

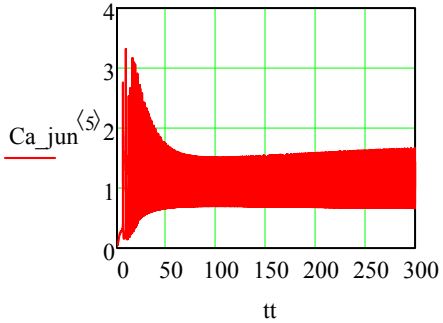

[Splot M31-33]

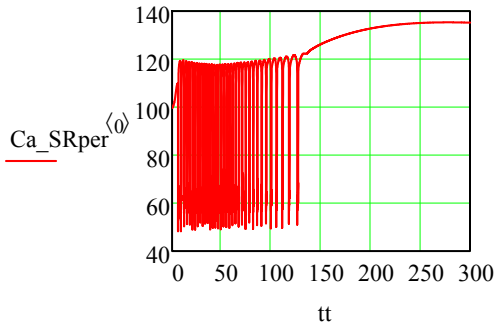

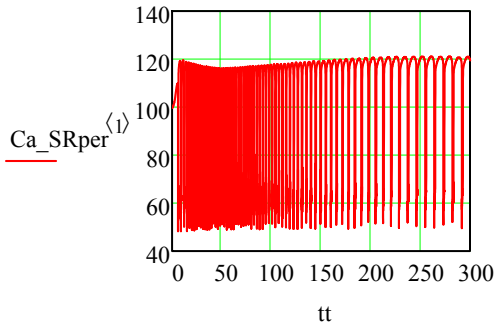

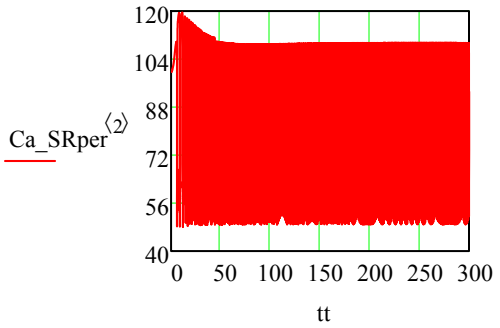

[Splot M34-36]

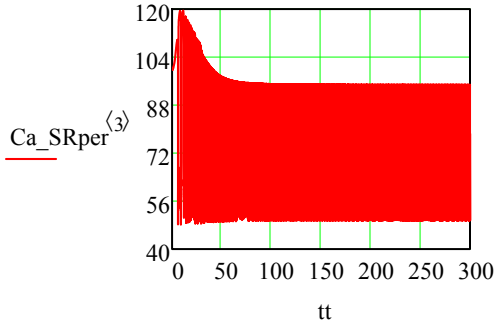

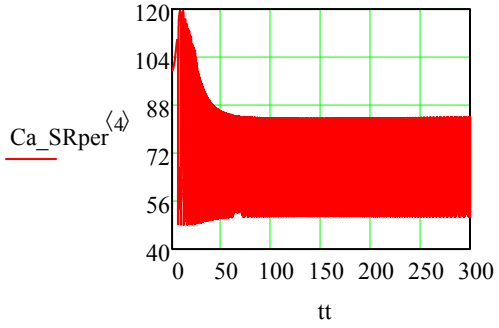

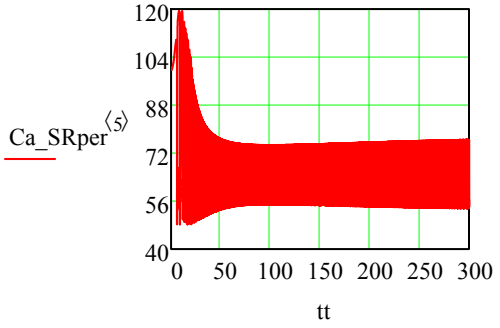

[Splot M37-39]

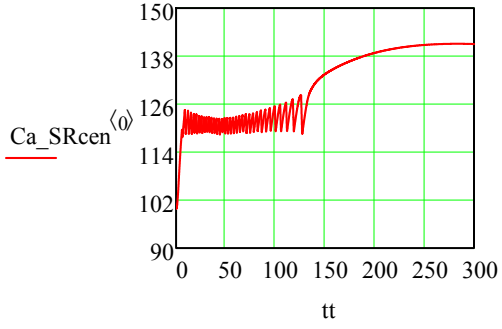

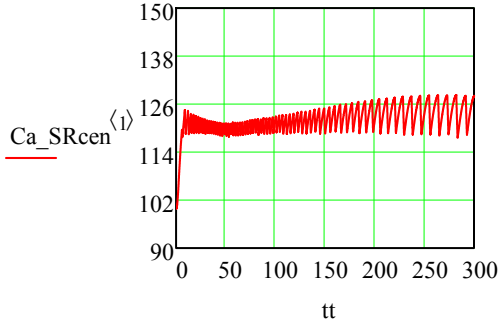

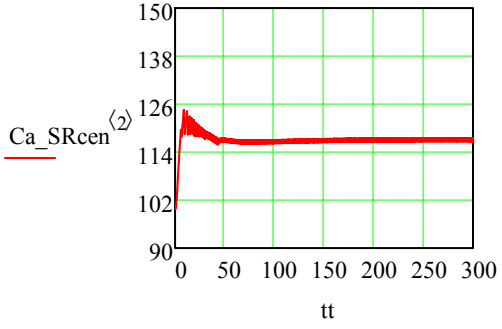

[Splot M40-42]

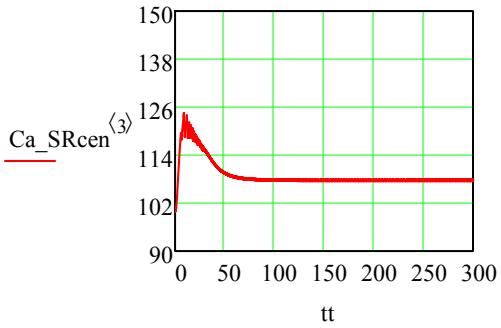

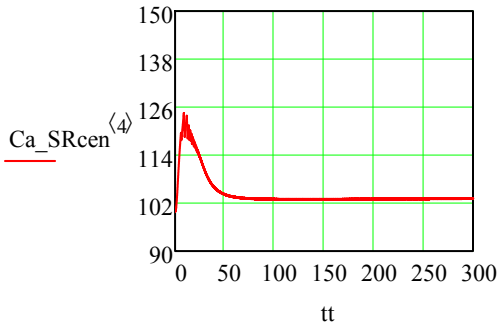

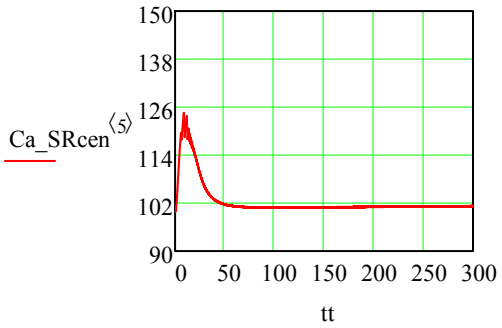

[Splot M43-45]

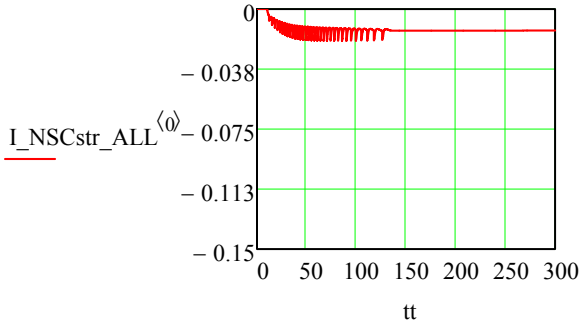

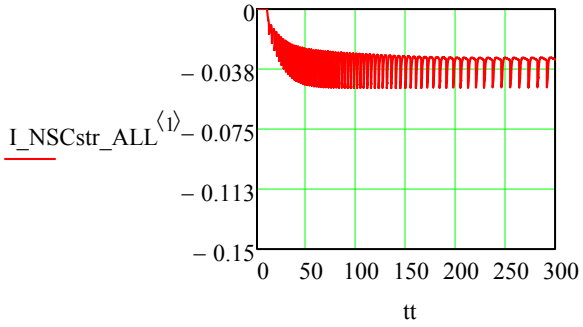

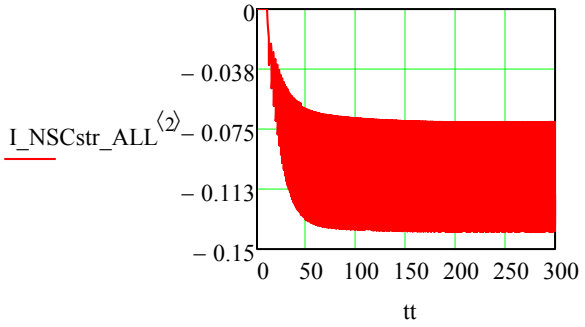

[Splot M46-48]

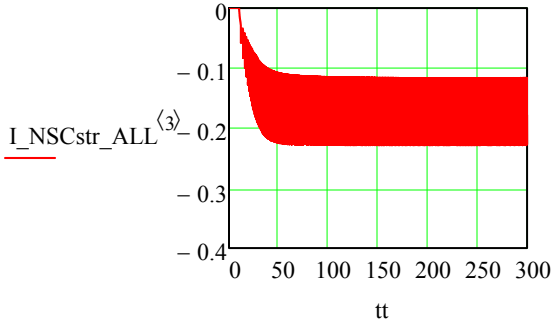

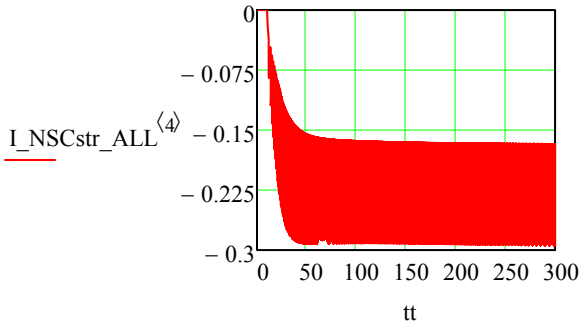

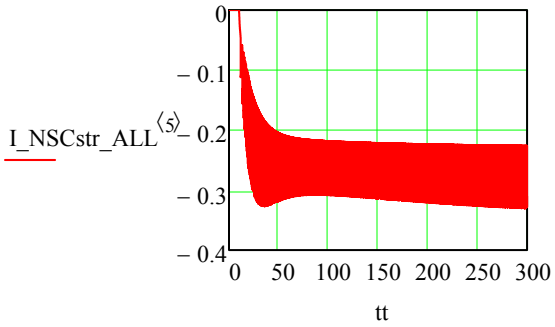

[Splot M49-51]

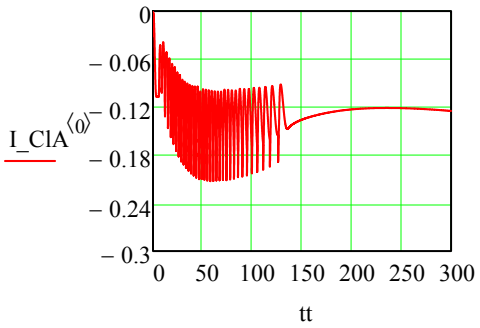

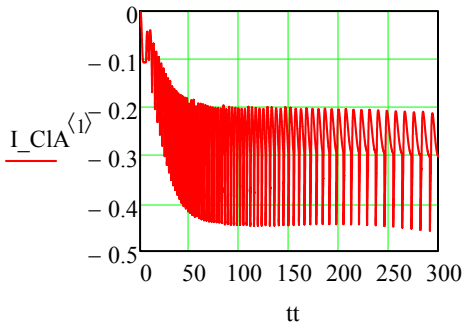

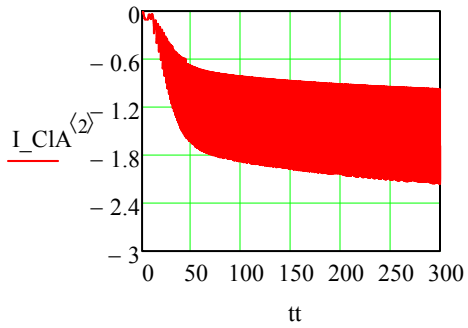

[Splot M52-54]

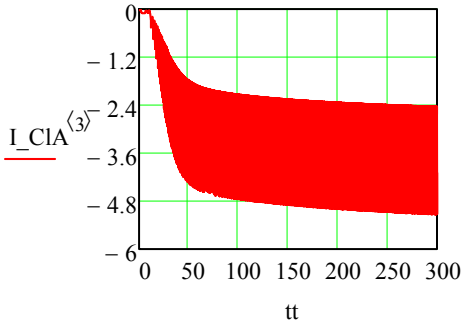

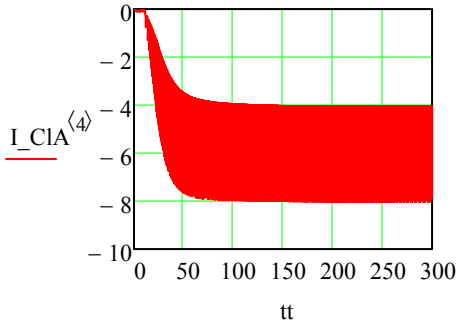

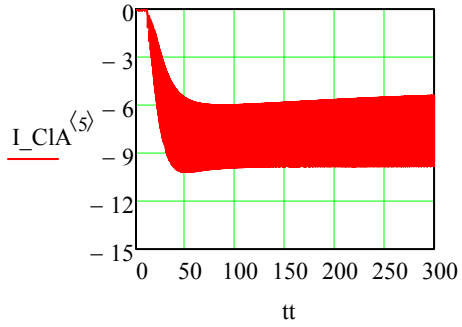

[Splot M55-57]

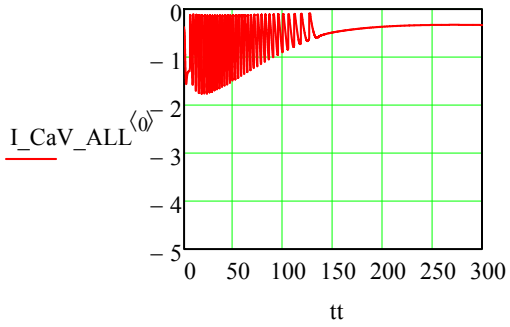

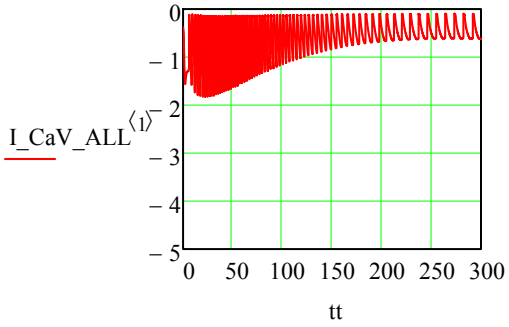

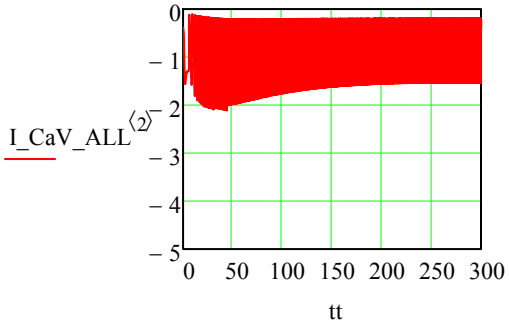

[Splot M58-60]

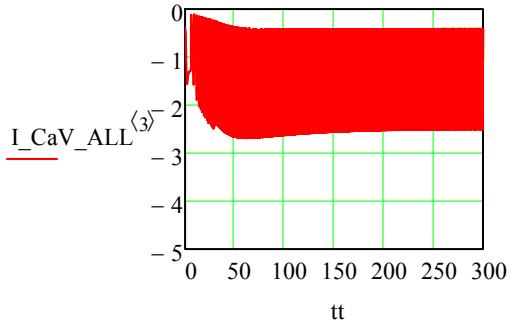

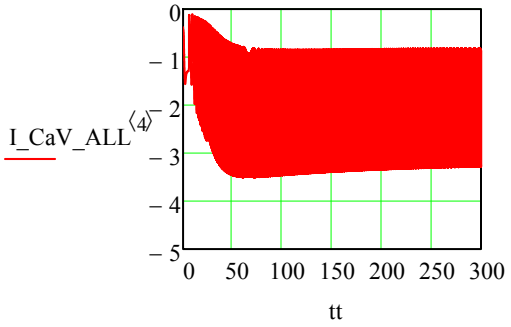

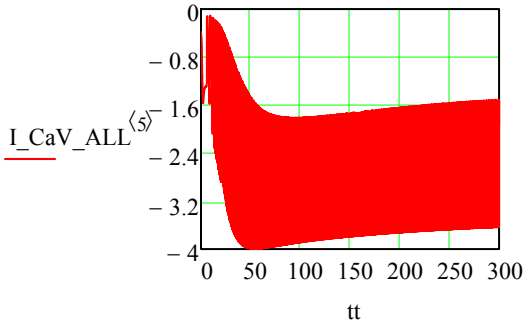

[Splot M61-63]

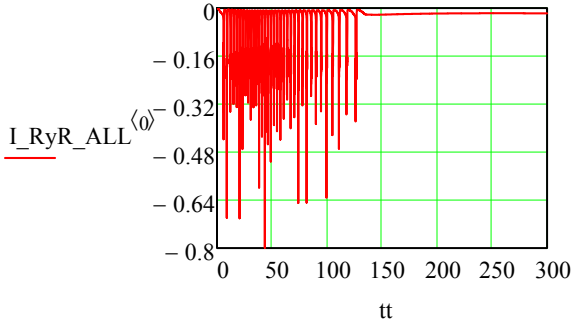

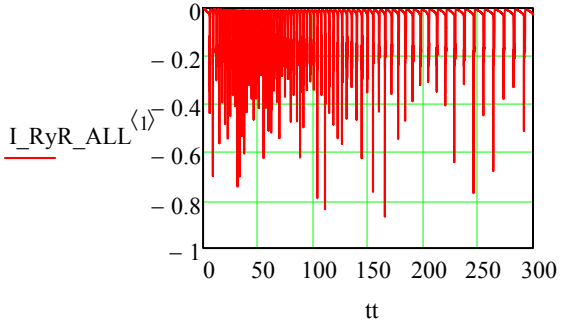

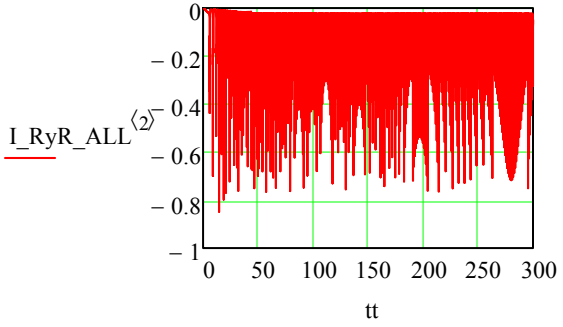

[Splot M64-66]

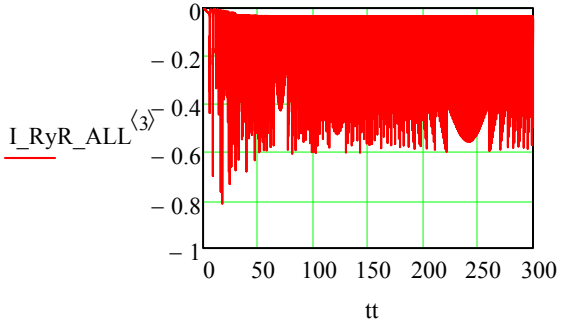

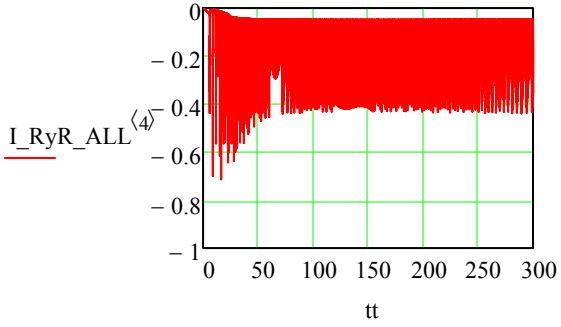

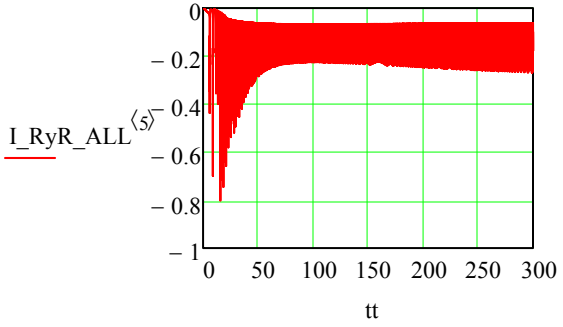

[Splot M67-69]

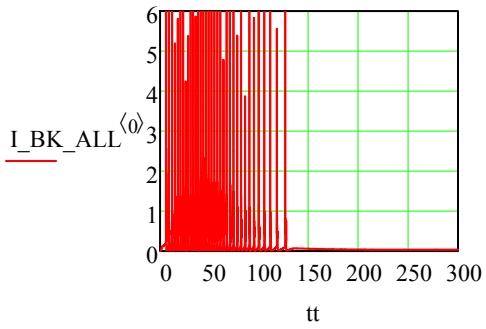

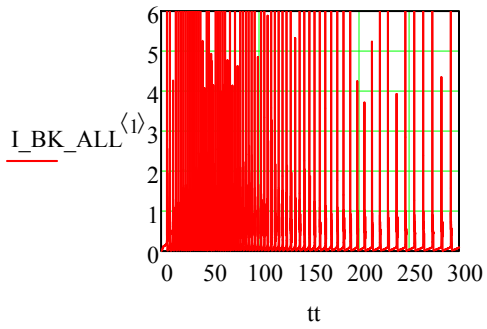

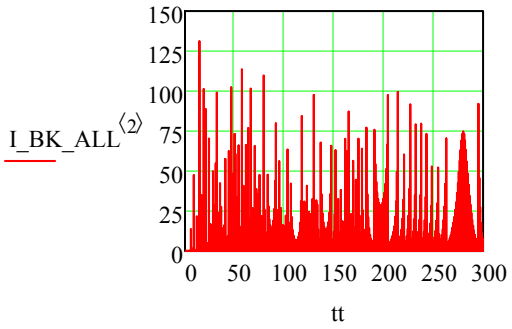

[Splot M70-72]

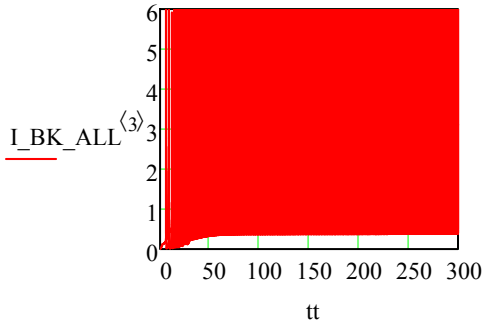

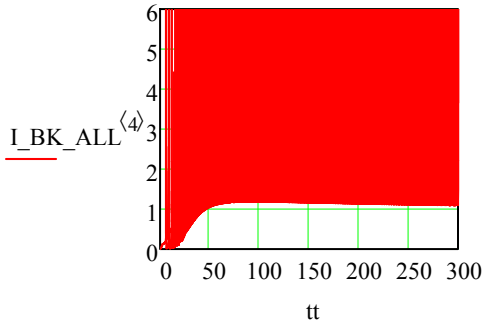

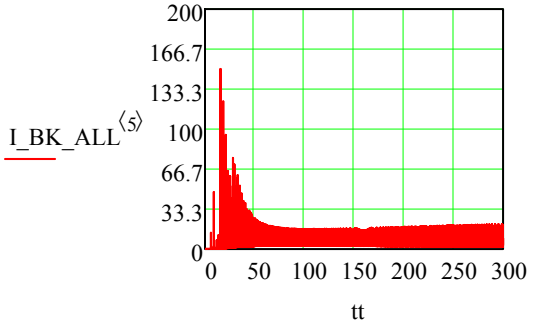

[Splot M73-75]

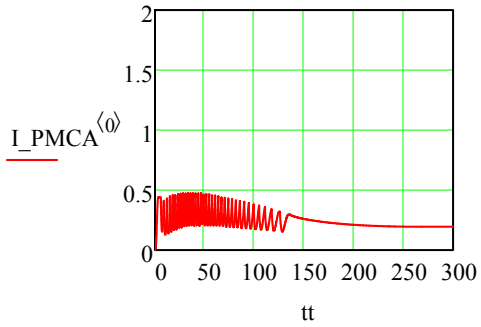

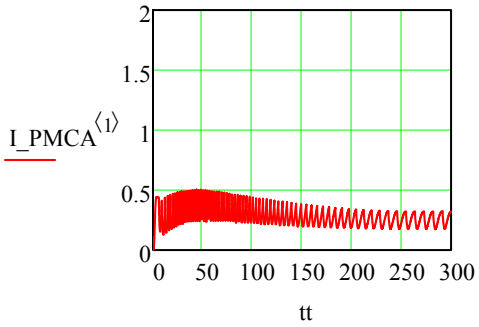

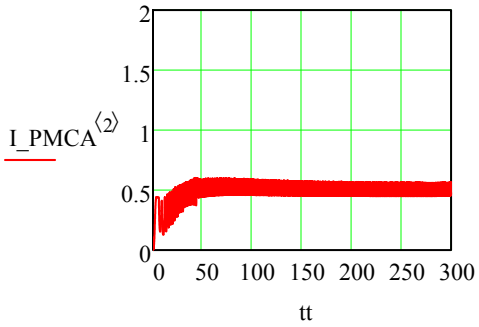

[Splot M76-78]

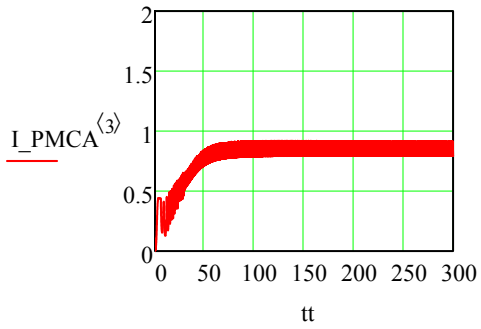

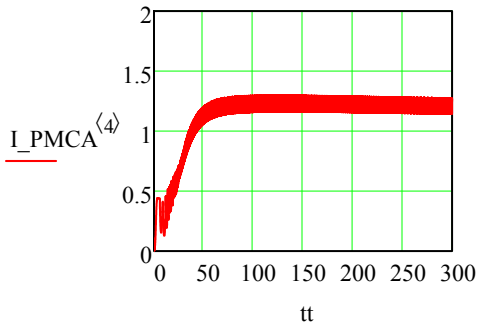

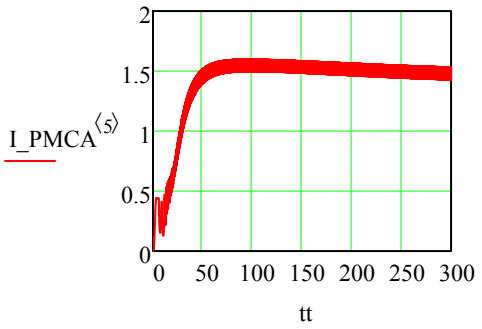

[Splot M79-81]

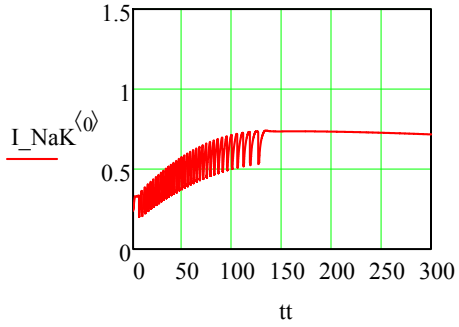

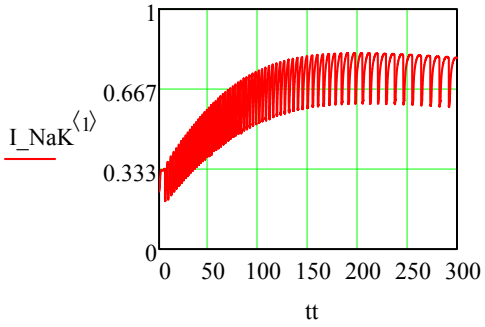

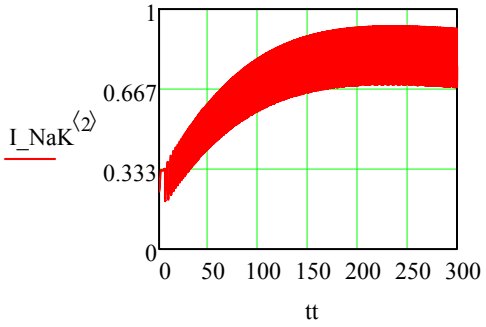

[Splot M82-84]

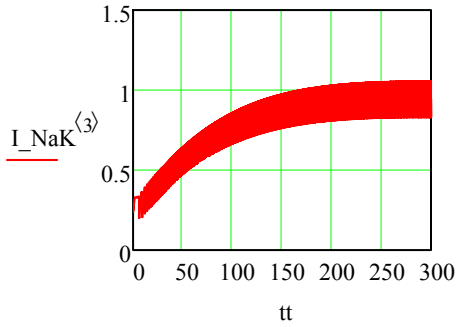

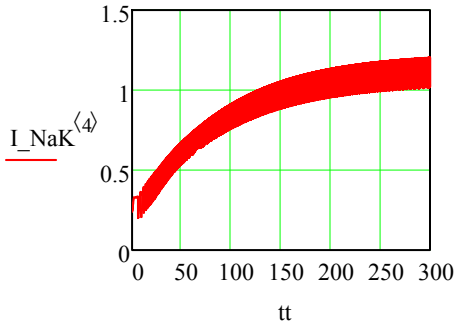

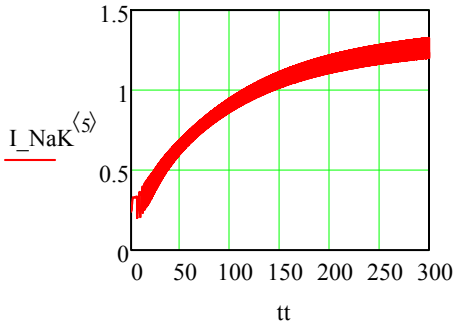

[Splot M85-87]

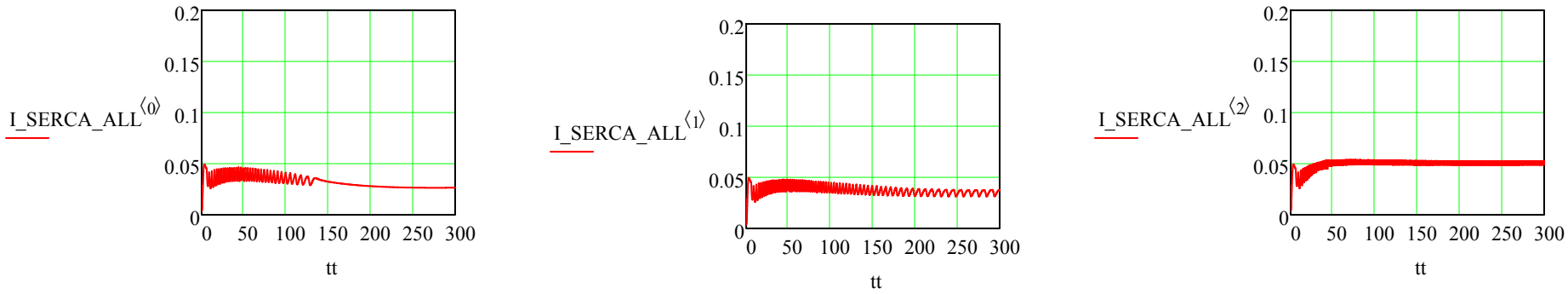

[Splot M88-90]

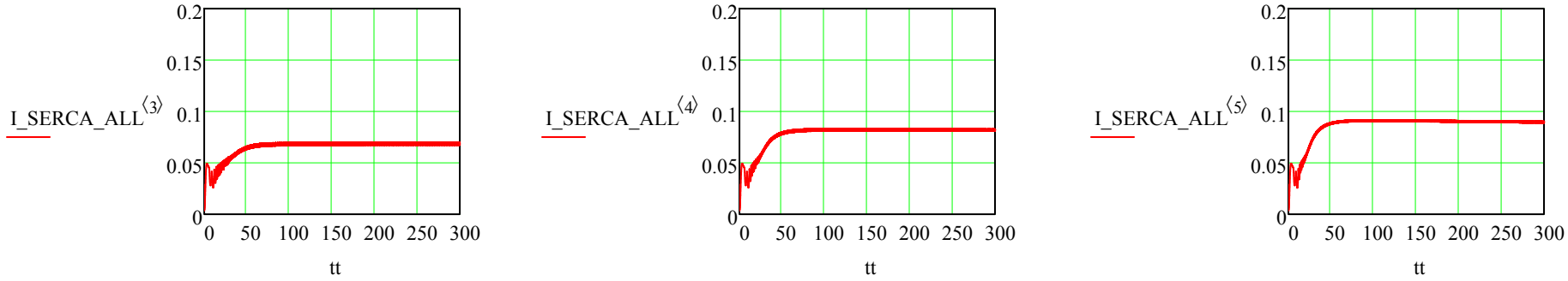

N. MEANS OF VARIABLES AND FUNCTIONS OF VARIABLES

The period over which the means are taken is given by the input parameters, a and b. Sub-vectors of ALLDATA columns are formed containing the values to to be averaged. In addition, sub-vectors of currents are calculated with sub-vectors of ALLDATA and sub-vectors of effector concentrations as arguments.

Indices of rows corresponding to a and b:

[Seq.N1-2] $j1 := \frac{a}{t1} \cdot N1$ $j2 := \frac{b}{t1} \cdot N1$

The number of points from a to b, including a:

[Seq.N3] $NN1 := j2 - j1 + 1$

Sub-matrices of effector values from j1 to j2:

[Seq.N4-5] $\alpha AA\_a\_b := submatrix(\alpha AA, j1, j2, 0, num\_eff\_conc - 1)$ $\beta AA\_a\_b := submatrix(\beta AA, j1, j2, 0, num\_eff\_conc - 1)$

[Seq.N6-7] $BP\_a\_b := submatrix(B\_Press, j1, j2, 0, num\_eff\_conc - 1)$ $EETT\_a\_b := submatrix(EETT, j1, j2, 0, num\_eff\_conc - 1)$

[Seq.N8-9] $NOX\_a\_b := submatrix(NOX, j1, j2, 0, num\_eff\_conc - 1)$ $ATP\_a\_b := submatrix(ATPP, j1, j2, 0, num\_eff\_conc - 1)$

Calculate means of selected variables and steady-state functions.

[Seq.N10] $MM :=$ for $i \in 0 .. num\_eff\_conc - 1$

$vv \leftarrow submatrix(ALLDATA, j1, j2, 13 + num\_var \cdot i, 13 + num\_var \cdot i)$

$ca \leftarrow submatrix(ALLDATA, j1, j2, 16 + num\_var \cdot i, 16 + num\_var \cdot i)$

$na \leftarrow submatrix(ALLDATA, j1, j2, 14 + num\_var \cdot i, 14 + num\_var \cdot i)$

$kk \leftarrow submatrix(ALLDATA, j1, j2, 15 + num\_var \cdot i, 15 + num\_var \cdot i)$

$cl \leftarrow submatrix(ALLDATA, j1, j2, 18 + num\_var \cdot i, 18 + num\_var \cdot i)$

$ca\_jun \leftarrow submatrix(ALLDATA, j1, j2, 31 + num\_var \cdot i, 31 + num\_var \cdot i)$

$ca\_nsc\_str \leftarrow submatrix(ALLDATA, j1, j2, 60 + num\_var \cdot i, 60 + num\_var \cdot i)$

$ca\_per \leftarrow submatrix(ALLDATA, j1, j2, 33 + num\_var \cdot i, 33 + num\_var \cdot i)$

$ca\_cen \leftarrow submatrix(ALLDATA, j1, j2, 35 + num\_var \cdot i, 35 + num\_var \cdot i)$

$bk \leftarrow submatrix(ALLDATA, j1, j2, 19 + num\_var \cdot i, 19 + num\_var \cdot i)$

$bk\_pka \leftarrow submatrix(ALLDATA, j1, j2, 20 + num\_var \cdot i, 20 + num\_var \cdot i)$

$bk\_pkc \leftarrow submatrix(ALLDATA, j1, j2, 21 + num\_var \cdot i, 21 + num\_var \cdot i)$

$bk\_pkg \leftarrow submatrix(ALLDATA, j1, j2, 22 + num\_var \cdot i, 22 + num\_var \cdot i)$

$ryr \leftarrow submatrix(ALLDATA, j1, j2, 23 + num\_var \cdot i, 23 + num\_var \cdot i)$

$ryr\_pka \leftarrow submatrix(ALLDATA, j1, j2, 24 + num\_var \cdot i, 24 + num\_var \cdot i)$

$ryr\_pkc \leftarrow submatrix(ALLDATA, j1, j2, 25 + num\_var \cdot i, 25 + num\_var \cdot i)$

$cav \leftarrow submatrix(ALLDATA, j1, j2, 26 + num\_var \cdot i, 26 + num\_var \cdot i)$

cav_pkc ← submatrix(ALLDATA, j1, j2, 27 + num_var·i, 27 + num_var·i)
cav_pkg ← submatrix(ALLDATA, j1, j2, 28 + num_var·i, 28 + num_var·i)
serca ← submatrix(ALLDATA, j1, j2, 29 + num_var·i, 29 + num_var·i)
serca_p ← submatrix(ALLDATA, j1, j2, 30 + num_var·i, 30 + num_var·i)
cgmp ← submatrix(ALLDATA, j1, j2, 42 + num_var·i, 42 + num_var·i)
camp ← submatrix(ALLDATA, j1, j2, 53 + num_var·i, 53 + num_var·i)
alpha_ar1 ← submatrix(ALLDATA, j1, j2, 1 + num_var·i, 1 + num_var·i)
gq1_gdp ← submatrix(ALLDATA, j1, j2, 5 + num_var·i, 5 + num_var·i)
gq0_gtp ← submatrix(ALLDATA, j1, j2, 6 + num_var·i, 6 + num_var·i)
plc_pip ← submatrix(ALLDATA, j1, j2, 10 + num_var·i, 10 + num_var·i)
plc_gq0gtp_pip ← submatrix(ALLDATA, j1, j2, 9 + num_var·i, 9 + num_var·i)
dag ← submatrix(ALLDATA, j1, j2, 12 + num_var·i, 12 + num_var·i)
ip3 ← submatrix(ALLDATA, j1, j2, 11 + num_var·i, 11 + num_var·i)
ip3r ← submatrix(ALLDATA, j1, j2, 58 + num_var·i, 58 + num_var·i)
ip3r_irag_pkg ← submatrix(ALLDATA, j1, j2, 59 + num_var·i, 59 + num_var·i)
nakcl ← submatrix(ALLDATA, j1, j2, 62 + num_var·i, 62 + num_var·i)
nakcl_pkc ← submatrix(ALLDATA, j1, j2, 63 + num_var·i, 63 + num_var·i)
pp_nakcl ← submatrix(ALLDATA, j1, j2, 64 + num_var·i, 64 + num_var·i)
pp_p_nakcl ← submatrix(ALLDATA, j1, j2, 65 + num_var·i, 65 + num_var·i)
nsc_str ← submatrix(ALLDATA, j1, j2, 66 + num_var·i, 66 + num_var·i)
nsc_str_pkc ← submatrix(ALLDATA, j1, j2, 67 + num_var·i, 67 + num_var·i)
nsc_str_pkg ← submatrix(ALLDATA, j1, j2, 68 + num_var·i, 68 + num_var·i)
plc_p ← submatrix(ALLDATA, j1, j2, 69 + num_var·i, 69 + num_var·i)
gc0 ← submatrix(ALLDATA, j1, j2, 37 + num_var·i, 37 + num_var·i)
gc1 ← submatrix(ALLDATA, j1, j2, 38 + num_var·i, 38 + num_var·i)
gc2 ← submatrix(ALLDATA, j1, j2, 39 + num_var·i, 39 + num_var·i)
gc1_act ← submatrix(ALLDATA, j1, j2, 40 + num_var·i, 40 + num_var·i)
gc0_p ← submatrix(ALLDATA, j1, j2, 41 + num_var·i, 41 + num_var·i)
βr0 ← submatrix(ALLDATA, j1, j2, 43 + num_var·i, 43 + num_var·i)
βr1 ← submatrix(ALLDATA, j1, j2, 44 + num_var·i, 44 + num_var·i)
βr_p ← submatrix(ALLDATA, j1, j2, 45 + num_var·i, 45 + num_var·i)
βr_in ← submatrix(ALLDATA, j1, j2, 46 + num_var·i, 46 + num_var·i)
g_s0_gdp ← submatrix(ALLDATA, j1, j2, 47 + num_var·i, 47 + num_var·i)

g_s1_gdp ← submatrix(ALLDATA, j1, j2, 48 + num_var·i, 48 + num_var·i)

g_s0_gtp ← submatrix(ALLDATA, j1, j2, 49 + num_var·i, 49 + num_var·i)

ac0 ← submatrix(ALLDATA, j1, j2, 50 + num_var·i, 50 + num_var·i)

ac1 ← submatrix(ALLDATA, j1, j2, 51 + num_var·i, 51 + num_var·i)

ac_p ← submatrix(ALLDATA, j1, j2, 52 + num_var·i, 52 + num_var·i)

pde_camp ← submatrix(ALLDATA, j1, j2, 54 + num_var·i, 54 + num_var·i)

pde_camp_p ← submatrix(ALLDATA, j1, j2, 55 + num_var·i, 55 + num_var·i)

pde_cgmp ← submatrix(ALLDATA, j1, j2, 56 + num_var·i, 56 + num_var·i)

pde_cgmp_p ← submatrix(ALLDATA, j1, j2, 57 + num_var·i, 57 + num_var·i)

katp ← submatrix(ALLDATA, j1, j2, 71 + num_var·i, 71 + num_var·i)

katp_pka ← submatrix(ALLDATA, j1, j2, 72 + num_var·i, 72 + num_var·i)

katp_pkcε ← submatrix(ALLDATA, j1, j2, 73 + num_var·i, 73 + num_var·i)

p2xr_0 ← submatrix(ALLDATA, j1, j2, 74 + num_var·i, 74 + num_var·i)

p2xr_3 ← submatrix(ALLDATA, j1, j2, 75 + num_var·i, 75 + num_var·i)

p2xr_3_act ← submatrix(ALLDATA, j1, j2, 76 + num_var·i, 76 + num_var·i)

p2xd_0 ← submatrix(ALLDATA, j1, j2, 77 + num_var·i, 77 + num_var·i)

p2xd_3 ← submatrix(ALLDATA, j1, j2, 78 + num_var·i, 78 + num_var·i)

p2xd_0_pkd ← submatrix(ALLDATA, j1, j2, 79 + num_var·i, 79 + num_var·i)

p2xd_3_pkd ← submatrix(ALLDATA, j1, j2, 80 + num_var·i, 80 + num_var·i)

for $j \in 0 .. j2 - j1$

$ii\_bk\_all_j \leftarrow I_{BK\_ALL}(vv_j, ca\_jun_j, kk_j, bk_j, bk\_pka_j, bk\_pkc_j, bk\_pkg_j)$

$ii\_cav\_all_j \leftarrow I_{CaV\_ALL}(vv_j, ca_j, cav_j, cav\_pkc_j, cav\_pkg_j)$

$ii\_cl\_a_j \leftarrow I_{ClA}(vv_j, ca\_nsc\_str_j, cl_j)$

$ii\_kv_j \leftarrow I_{Kv}(vv_j, kk_j)$

$ii\_all\_leak_j \leftarrow I_{ALL\_leak}(vv_j, kk_j, na_j, cl_j, ca_j)$

$ii\_nak_j \leftarrow I_{NaK}(vv_j, na_j, kk_j)$

$ii\_ncx_j \leftarrow I_{NCX}(vv_j, ca_j, na_j)$

$ii\_nsc\_str\_all_j \leftarrow I_{NSCstr\_ALL}(vv_j, dag_j, na_j, kk_j, ca\_nsc\_str_j, BP\_a\_b_{j,i}, nsc\_str_j, nsc\_str\_pkc_j, nsc\_str\_pkg_j)$

$ii\_PMCA_j \leftarrow I_{PMCA}(vv_j, ca_j)$

ii_serca_all ← I[illegible](ca, ca_cen, serca, serca_p)

$$ii\_serca\_all_j \leftarrow I_{SERCA\_ALL}\left(ca_j, ca\_cen_j, serca_j, serca\_p_j\right)$$

$$ii\_ryr\_all_j \leftarrow I_{RyR\_ALL}\left(ca\_jun_j, ca\_per_j, ryr\_pka_j, ryr\_pkc_j\right)$$

$$ii\_ip3r\_all_j \leftarrow I_{IP3R\_ALL}\left(ca_j, ip3_j, ca\_cen_j, ip3r_j, ip3r\_irag\_pkg_j\right)$$

$$ii\_nsc\_eet\_all_j \leftarrow I_{NSCeet\_ALL}\left(vv_j, EETT\_a\_b_{j,i}, na_j, kk_j, ca\_jun_j\right)$$

$$ii\_nsc\_ne\_all_j \leftarrow I_{NSCne\_ALL}\left(vv_j, dag_j, na_j, kk_j, ca_j\right)$$

$$ii\_nak\_cl_j \leftarrow I_{NaK\_Cl}\left(nakcl_j, nakcl\_pkc_j, na_j, kk_j, cl_j\right)$$

$$rel\_pkc_j \leftarrow relPKC_{11}\left(dag_j, ca_j\right)$$

$$rel\_pka_j \leftarrow relPKA_1\left(camp_j\right)$$

$$rel\_pkg_j \leftarrow relPKG_1\left(cgmp_j\right)$$

$$rel\_pkc\varepsilon_j \leftarrow relPKC\varepsilon_{DAG}\left(dag_j\right)$$

$$rel\_pkd_j \leftarrow relPKD_{DAG}\left(dag_j\right)$$

$$ii\_katp\_all_j \leftarrow I_{KATP\_ALL}\left(vv_j, kk_j, katp_j, katp\_pka_j\right)$$

$$ii\_p2xr\_all_j \leftarrow I_{P2XR\_ALL}\left(vv_j, na_j, kk_j, ca_j, p2xr\_3\_act_j\right)$$

$$ii\_ca\_p2xr_j \leftarrow I_{CaP2XR}\left(vv_j, ca_j, p2xr\_3\_act_j\right)$$

$$ii\_ca\_leak_j \leftarrow I_{Ca\_leak}\left(vv_j, ca_j\right)$$

$$ii\_cl\_leak_j \leftarrow I_{Cl\_leak}\left(vv_j, cl_j\right)$$

$$ii\_kk\_leak_j \leftarrow I_{K\_leak}\left(vv_j, kk_j\right)$$

$$MEAN_{i,0} \leftarrow mean(vv)$$

$$MEAN_{i,1} \leftarrow mean(ca)$$

$$MEAN_{i,2} \leftarrow mean(ca\_nsc\_str)$$

$$MEAN_{i,3} \leftarrow mean(ca\_jun)$$

$$MEAN_{i,4} \leftarrow mean(ii\_bk\_all)$$

$$MEAN_{i,5} \leftarrow mean(ii\_cav\_all)$$

$$MEAN_{i,6} \leftarrow mean(ii\_cl\_a)$$

$$MEAN_{i,7} \leftarrow mean(ii\_kv)$$

$MEAN_{i,8} \leftarrow \text{mean}(\text{ii\_all\_leak})$

$MEAN_{i,9} \leftarrow \text{mean}(\text{ii\_nak})$

$MEAN_{i,10} \leftarrow \text{mean}(\text{ii\_ncx})$

$MEAN_{i,11} \leftarrow \text{mean}(\text{ii\_nsc\_str\_all})$

$MEAN_{i,12} \leftarrow \text{mean}(\text{ii\_PMCA})$

$MEAN_{i,13} \leftarrow \text{mean}(\text{ii\_serca\_all})$

$MEAN_{i,14} \leftarrow \text{mean}(\text{ii\_ryr\_all})$

$MEAN_{i,15} \leftarrow \text{mean}(\text{ca\_per})$

$MEAN_{i,16} \leftarrow \text{mean}(\text{ca\_cen})$

$MEAN_{i,17} \leftarrow \text{mean}(\text{cl})$

$MEAN_{i,18} \leftarrow \text{mean}(\text{kk})$

$MEAN_{i,19} \leftarrow \text{mean}(\text{na})$

$MEAN_{i,20} \leftarrow \text{mean}(\text{ii\_ca\_leak})$

$MEAN_{i,21} \leftarrow \text{mean}(\text{ii\_ip3r\_all})$

$MEAN_{i,22} \leftarrow \text{mean}(\text{ii\_nsc\_eet\_all})$

$MEAN_{i,23} \leftarrow \text{mean}(\text{ii\_nsc\_ne\_all})$

$MEAN_{i,24} \leftarrow \text{mean}(\text{ii\_nak\_cl})$

$MEAN_{i,25} \leftarrow \text{mean}(\text{alpha\_ar1})$

$MEAN_{i,26} \leftarrow \text{mean}(\text{gq1\_gdp})$

$MEAN_{i,27} \leftarrow \text{mean}(\text{gq0\_gtp})$

$MEAN_{i,28} \leftarrow \text{mean}(\text{plc\_pip})$

$MEAN_{i,29} \leftarrow \text{mean}(\text{ip3})$

$MEAN_{i,30} \leftarrow \text{mean}(\text{dag})$

$MEAN_{i,31} \leftarrow \text{mean}(\text{rel\_pkc})$

$MEAN_{i,32} \leftarrow \text{mean}(\text{plc\_gq0gtp\_pip})$

$MEAN_{i,33} \leftarrow \text{mean}(\text{plc\_p})$

$MEAN_{i,34} \leftarrow \text{mean}(\text{gc0})$

$MEAN_{i,35} \leftarrow \text{mean}(\text{gc1})$

$MEAN_{i,36} \leftarrow \text{mean}(\text{gc2})$

$MEAN_{i,37} \leftarrow \text{mean}(\text{gc1\_act})$

$MEAN_{i,38} \leftarrow \text{mean}(\text{gc0\_p})$

$MEAN_{i,39} \leftarrow \text{mean}(\text{cgmp})$

$MEAN_{i,40} \leftarrow \text{mean}(\beta\text{r0})$

$MEAN_{i,41} \leftarrow \text{mean}(\beta\text{r1})$

$MEAN_{i,42} \leftarrow \text{mean}(\beta\text{r\_p})$

$MEAN_{i,43} \leftarrow \text{mean}(\beta\text{r\_in})$

$MEAN_{i,44} \leftarrow \text{mean}(\text{g\_s0\_gdp})$

$MEAN_{i,45} \leftarrow \text{mean}(\text{g\_s1\_gdp})$

$MEAN_{i,46} \leftarrow \text{mean}(\text{g\_s0\_gtp})$

$MEAN_{i,47} \leftarrow \text{mean}(\text{ac0})$

$MEAN_{i,48} \leftarrow \text{mean}(\text{ac1})$

$MEAN_{i,49} \leftarrow \text{mean}(\text{ac\_p})$

$MEAN_{i,50} \leftarrow \text{mean}(\text{camp})$

$MEAN_{i,51} \leftarrow \text{mean}(\text{pde\_camp})$

$MEAN_{i,52} \leftarrow \text{mean}(\text{pde\_camp\_p})$

$MEAN_{i,53} \leftarrow \text{mean}(\text{pde\_cgmp})$

$MEAN_{i,54} \leftarrow \text{mean}(\text{pde\_cgmp\_p})$

$MEAN_{i,55} \leftarrow \text{mean}(\text{rel\_pka})$

$MEAN_{i,56} \leftarrow \text{mean}(\text{rel\_pkg})$

$MEAN_{i,57} \leftarrow \text{mean}(\text{bk})$

$MEAN_{i,58} \leftarrow \text{mean}(\text{bk\_pka})$

$MEAN_{i,59} \leftarrow \text{mean}(\text{bk\_pkc})$

$MEAN_{i,60} \leftarrow \text{mean}(\text{bk\_pkg})$

$MEAN_{i,61} \leftarrow \text{mean}(\text{cav})$

$MEAN_{i,62} \leftarrow \text{mean}(\text{cav\_pkc})$

$MEAN_{i,63} \leftarrow \text{mean}(\text{cav\_pkg})$

$MEAN_{i,64} \leftarrow \text{mean}(\text{ii\_cl\_leak})$

$MEAN_{i,65} \leftarrow \text{mean}(\text{nakcl})$

$MEAN_{i,66} \leftarrow \text{mean}(\text{nakcl\_pkc})$

$MEAN_{i,67} \leftarrow \text{mean}(\text{nsc\_str})$

$MEAN_{i,68} \leftarrow \text{mean}(\text{nsc\_str\_pkc})$

$MEAN_{i,69} \leftarrow \text{mean}(\text{nsc\_str\_pkg})$

$MEAN_{i,70} \leftarrow \text{mean}(\text{pp\_nakcl})$

$MEAN_{i,71} \leftarrow \text{mean}(\text{pp\_p\_nakcl})$

$MEAN_{i,72} \leftarrow \text{mean}(\text{ip3r})$

$MEAN_{i,73} \leftarrow \text{mean}(\text{ip3r\_irag\_pkg})$

$MEAN_{i,74} \leftarrow \text{mean}(\text{serca})$

$MEAN_{i,75} \leftarrow \text{mean}(\text{serca\_p})$

$MEAN_{i,76} \leftarrow \text{mean}(\text{rel\_pkc}\varepsilon)$

$MEAN_{i,77} \leftarrow \text{mean}(\text{katp})$

$MEAN_{i,78} \leftarrow \text{mean}(\text{katp\_pka})$

$MEAN_{i,79} \leftarrow \text{mean}(\text{katp\_pkc}\varepsilon)$

$MEAN_{i,80} \leftarrow \text{mean}(\text{ii\_katp\_all})$

$MEAN_{i,81} \leftarrow \text{mean}(\text{rel\_pkd})$

$MEAN_{i,82} \leftarrow \text{mean}(\text{p2xr\_0})$

$MEAN_{i,83} \leftarrow mean(p2xr\_3)$

$MEAN_{i,84} \leftarrow mean(p2xr\_3\_act)$

$MEAN_{i,85} \leftarrow mean(p2xd\_0)$

$MEAN_{i,86} \leftarrow mean(p2xd\_3)$

$MEAN_{i,87} \leftarrow mean(p2xd\_0\_pkd)$

$MEAN_{i,88} \leftarrow mean(p2xd\_3\_pkd)$

$MEAN_{i,89} \leftarrow mean(ii\_p2xr\_all)$

$MEAN_{i,90} \leftarrow mean(ii\_ca\_p2xr)$

$MEAN_{i,91} \leftarrow mean(ii\_kk\_leak)$

MEAN

The transposed matrix of means from a run is copied to Excel file aligned with the parameters of the run.

	0	1	2	3	4
0	-6.1724E+001	-5.9241E+001	-5.1801E+001	-4.5342E+001	-4.0469E+001
1	1.2166E-001	1.3199E-001	1.6264E-001	1.947E-001	2.2091E-001
2	1.5074E-001	2.0375E-001	3.5952E-001	5.3243E-001	6.8262E-001
3	2.3747E-001	3.6341E-001	5.1121E-001	7.003E-001	8.4063E-001
4	3.0989E-002	1.4031E-001	1.0896E+000	2.3384E+000	3.7859E+000
5	-3.3269E-001	-4.698E-001	-9.453E-001	-1.6404E+000	-2.3561E+000
6	-1.2299E-001	-2.7564E-001	-1.235E+000	-3.3042E+000	-5.5241E+000

[Seq.N11] $MM^{1} =$

7	3.7951E-002	8.9672E-002	3.9222E-001	1.1312E+000	2.1059E+000
8	-4.1204E-001	-3.8268E-001	-2.9295E-001	-2.0594E-001	-1.3674E-001
9	7.2104E-001	7.5714E-001	8.4594E-001	9.7927E-001	1.1312E+000
10	-8.5613E-002	-8.9856E-002	-9.8867E-002	-9.376E-002	-7.9484E-002
11	-1.3542E-002	-3.3336E-002	-9.0782E-002	-1.5453E-001	-2.1015E-001
12	1.931E-001	2.5382E-001	4.8358E-001	8.3392E-001	1.2038E+000
13	2.6346E-002	3.5044E-002	5.0047E-002	6.8173E-002	8.1635E-002
14	-1.7878E-002	-3.5637E-002	-5.4534E-002	-7.7982E-002	-9.5826E-002
15	1.3517E+002	1.1268E+002	9.987E+001	8.2321E+001	7.2116E+001
16	1.4096E+002	1.2428E+002	1.1698E+002	1.0762E+002	...

Define vectors for plotting means

[Seq.N12-16] $meanV := MM^{\langle 0 \rangle}$ $meanCa\_in := MM^{\langle 1 \rangle}$ $meanCa\_NSCstr := MM^{\langle 2 \rangle}$ $meanCa\_jun := MM^{\langle 3 \rangle}$ $meanI\_BK\_ALL := MM^{\langle 4 \rangle}$

[Seq.N17-21] $meanI\_CaV\_ALL := MM^{\langle 5 \rangle}$ $meanI\_ClA := MM^{\langle 6 \rangle}$ $meanI\_Kv := MM^{\langle 7 \rangle}$ $meanI\_ALL\_leak := MM^{\langle 8 \rangle}$ $meanI\_NaK := MM^{\langle 9 \rangle}$

[Seq.N22-26] $meanI\_NCX := MM^{\langle 10 \rangle}$ $meanI\_NSCstr\_ALL := MM^{\langle 11 \rangle}$ $meanI\_PMCA := MM^{\langle 12 \rangle}$ $meanI\_SERCA\_ALL := MM^{\langle 13 \rangle}$ $meanI\_RyR\_ALL := MM^{\langle 14 \rangle}$

[Seq.N27-31] $meanCa\_SRper := MM^{\langle 15 \rangle}$ $meanCa\_SRcen := MM^{\langle 16 \rangle}$ $meanCl\_in := MM^{\langle 17 \rangle}$ $meanK\_in := MM^{\langle 18 \rangle}$ $meanNa\_in := MM^{\langle 19 \rangle}$

[Seq.N32-36] $meanI\_Ca\_leak := MM^{\langle 20 \rangle}$ $meanI\_IP3R\_ALL := MM^{\langle 21 \rangle}$ $meanI\_NSCeet\_ALL := MM^{\langle 22 \rangle}$ $meanI\_NSCne\_ALL := MM^{\langle 23 \rangle}$ $meanI\_NaK\_Cl := MM^{\langle 24 \rangle}$

[Seq.N37-41] $mean\_\alpha AR1 := MM^{\langle 25 \rangle}$ $meanIP3 := MM^{\langle 29 \rangle}$ $meanGq0\_GTP := MM^{\langle 27 \rangle}$ $meanPLC\_PIP := MM^{\langle 28 \rangle}$ $meanGq1\_GDP := MM^{\langle 26 \rangle}$

[Seq.N42-45] $meanDAG := MM^{\langle 30 \rangle}$ $mean\_rel\_PKC := MM^{\langle 31 \rangle}$ $meanPLC\_Gq0\_GTP\_PIP := MM^{\langle 32 \rangle}$ $meanPLC\_P := MM^{\langle 33 \rangle}$

[Seq.N46-50] $meanGC\_0 := MM^{\langle 34 \rangle}$ $meanGC\_1 := MM^{\langle 35 \rangle}$ $meanGC\_2 := MM^{\langle 36 \rangle}$ $meanGC\_1\_act := MM^{\langle 37 \rangle}$ $meanGC\_0P := MM^{\langle 38 \rangle}$

[Seq.N51-55] $mean\_cGMP := MM^{\langle 39 \rangle}$ $mean\_\beta AR\_0 := MM^{\langle 40 \rangle}$ $mean\_\beta AR\_1 := MM^{\langle 41 \rangle}$ $mean\_\beta AR\_P := MM^{\langle 42 \rangle}$ $mean\_\beta AR\_in := MM^{\langle 43 \rangle}$

[Seq.N56-60] meanGs0_GDP := MM⟨44⟩ meanGs1_GDP := MM⟨45⟩ meanGs0_GTP := MM⟨46⟩ meanAC_0 := MM⟨47⟩ meanAC_1 := MM⟨48⟩

[Seq.N61-65] meanAC_P := MM⟨49⟩ mean_cAMP := MM⟨50⟩ meanPDE_cAMP := MM⟨51⟩ meanPDE_cAMP_P := MM⟨52⟩ mean_PDE_cGMP := MM⟨53⟩

[Seq.N66-70] meanPDE_cGMP_P := MM⟨54⟩ mean_rel_PKA := MM⟨55⟩ mean_rel_PKG := MM⟨56⟩ mean_rel_PKCε := MM⟨76⟩ mean_rel_PKD := MM⟨81⟩

[Seq.N71-75] meanK_ATP := MM⟨77⟩ meanK_ATP_PKA := MM⟨78⟩ meanK_ATP_PKCε := MM⟨79⟩ meanI_KATP_ALL := MM⟨80⟩ meanI_Cl_leak := MM⟨64⟩

[Seq.N76-80] meanP2XR_0 := MM⟨82⟩ meanP2XR_3 := MM⟨83⟩ meanP2XR_3_act := MM⟨84⟩ meanP2XD_0 := MM⟨85⟩ meanP2XD_3 := MM⟨86⟩

[Seq.N81-85] meanP2XD_0_PKD := MM⟨87⟩ meanP2XD_3_PKD := MM⟨88⟩ meanI_P2XR_ALL := MM⟨89⟩ meanI_CaP2XR := MM⟨90⟩ meanI_K_leak := MM⟨91⟩

P. PLOTS OF SOME MEANS VERSUS INTRAVASCULAR PRESSURES or EFFECTOR CONCENTRATIONS

(Membrane potential is in mV; Ca concentrations are in μM; Na, K, and Cl concentrations are in mM; currents are in pA; intravascular pressure, bp1, is in mm mg.)

[Splot P1-3]

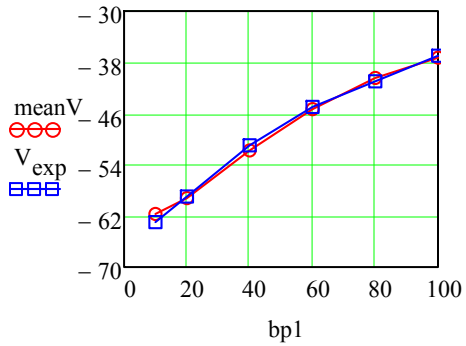

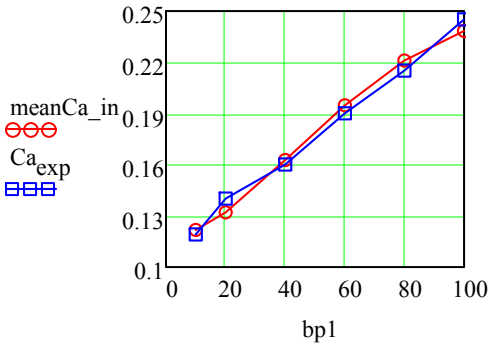

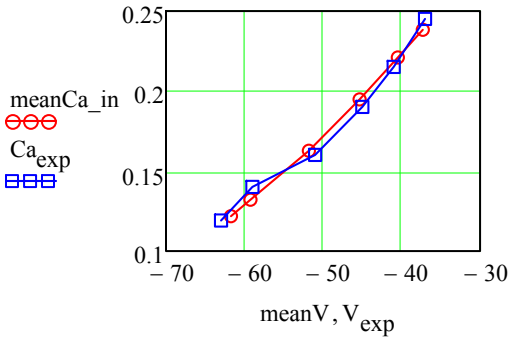

[Splot P4-6]

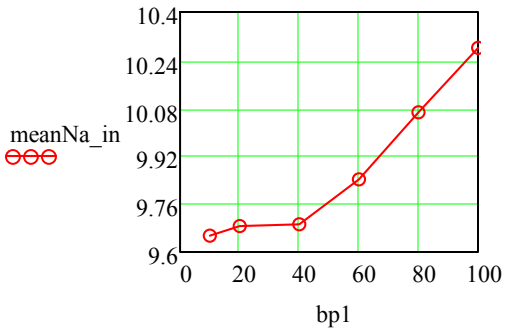

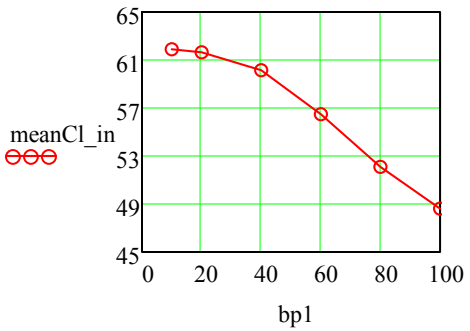

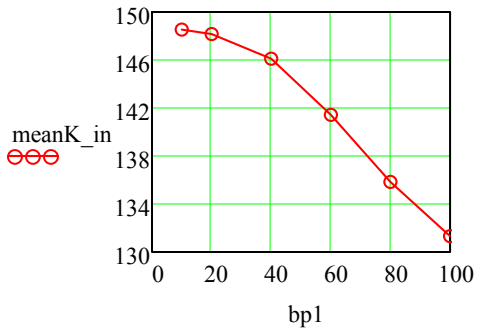

[Splot P7-9]

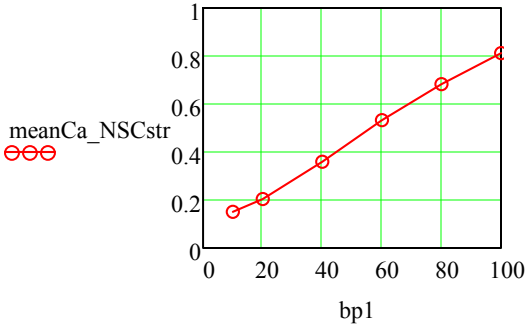

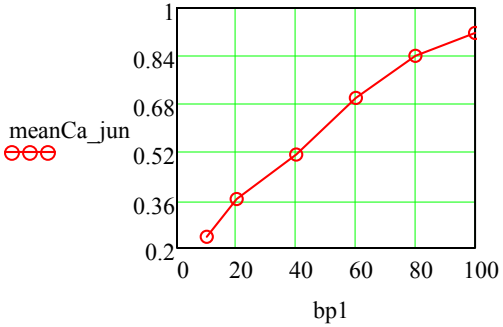

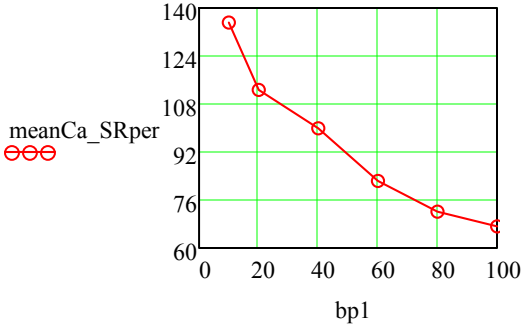

[Splot P10-12]

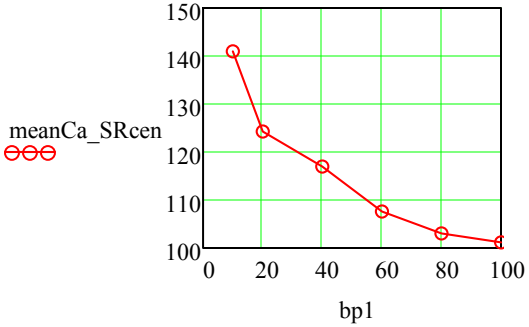

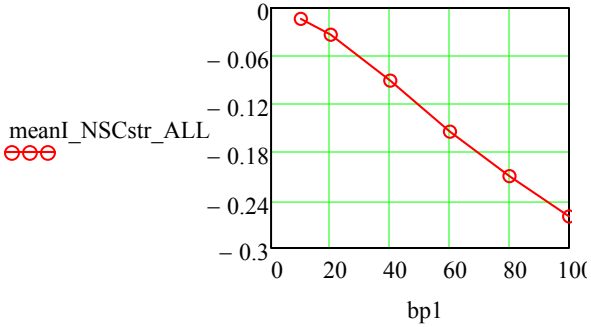

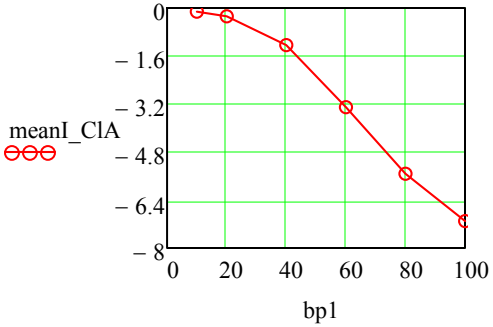

[Splot P13-15]

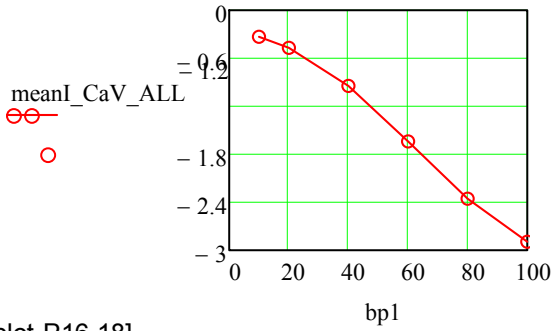

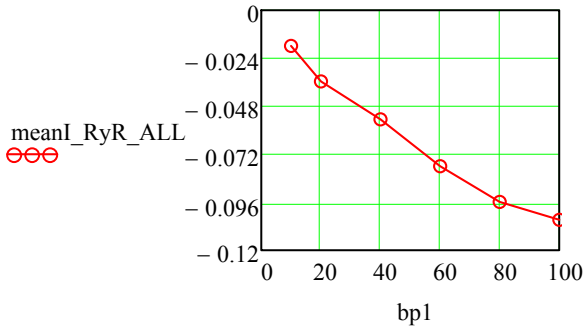

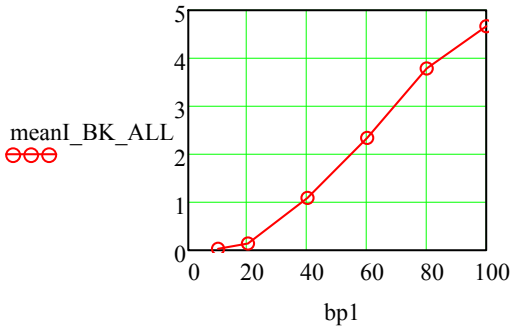

[Splot P16-18]

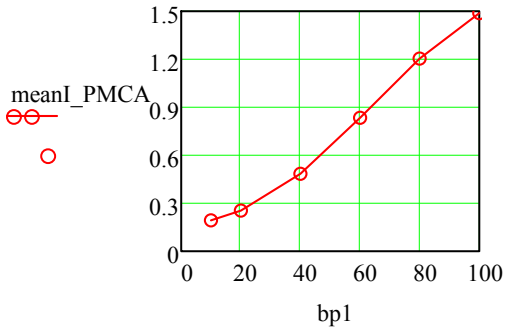

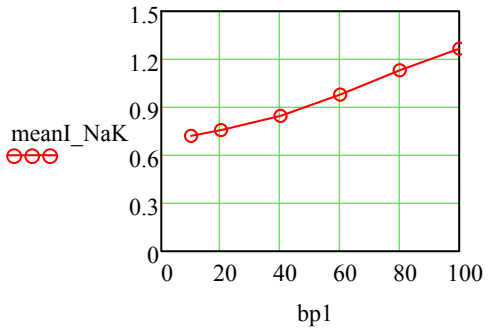

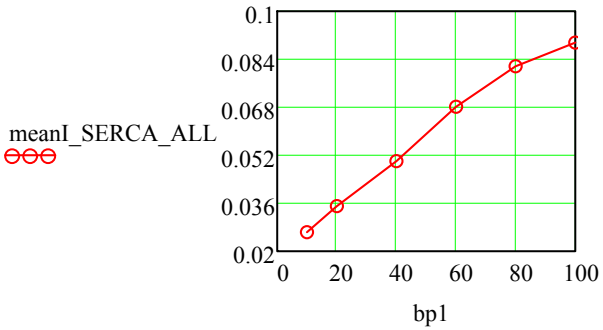

[Splot P19-21]

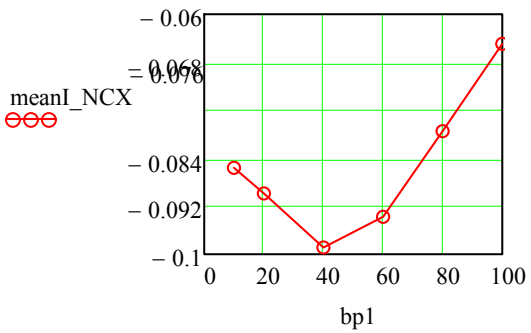

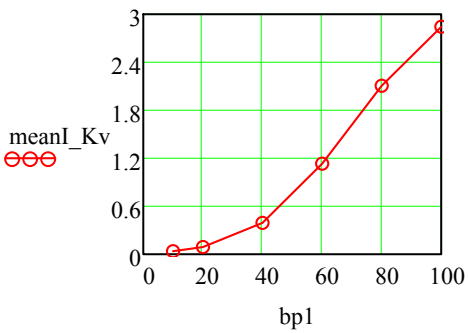

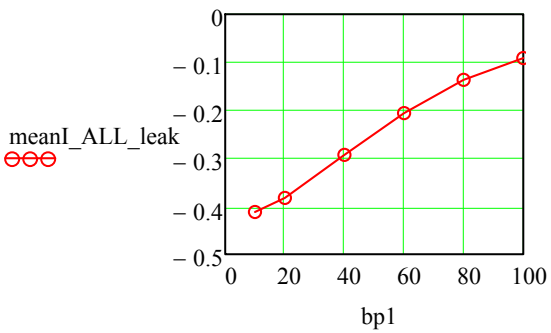

[Splot P22-24]

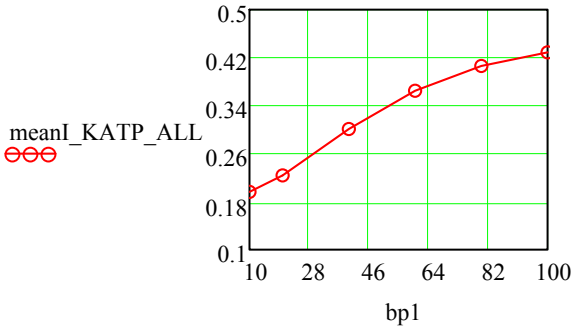

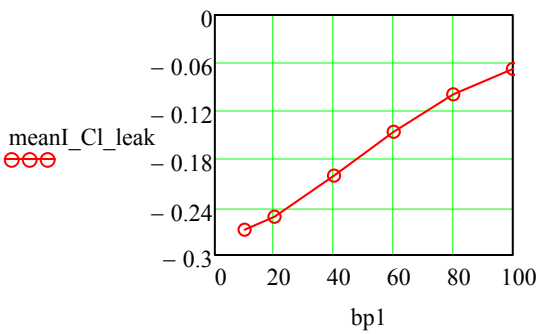

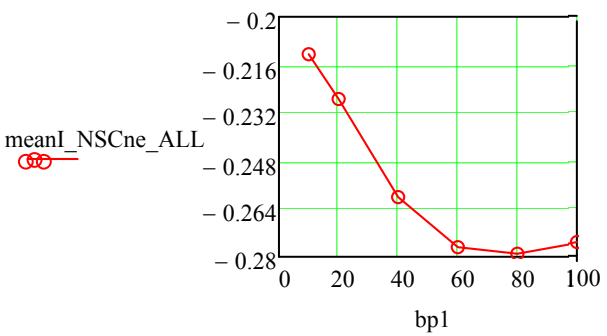

[Splot P25-27]

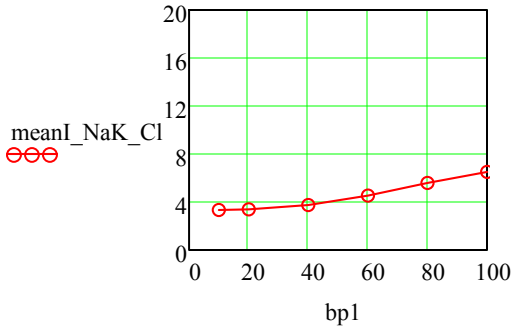

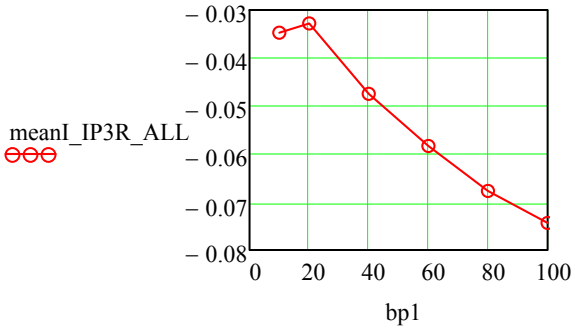

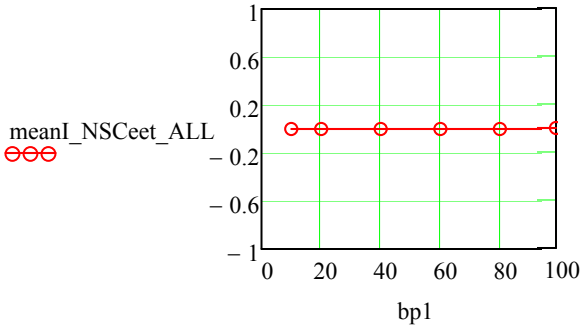

[Splot P28-30]

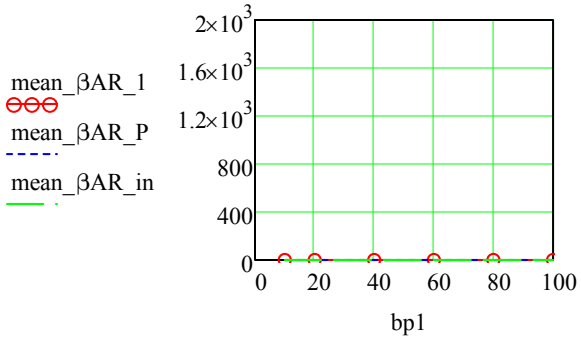

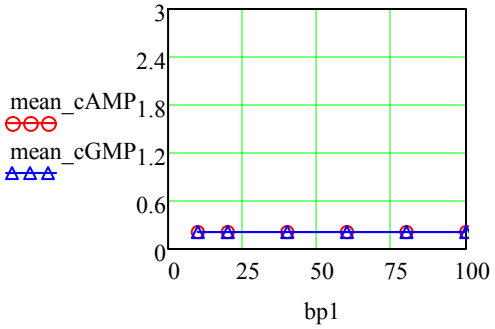

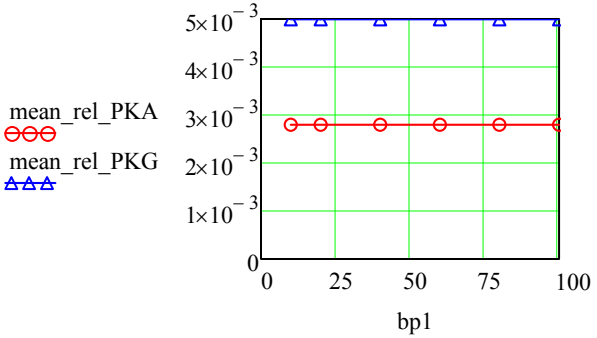

[Splot P31-33]

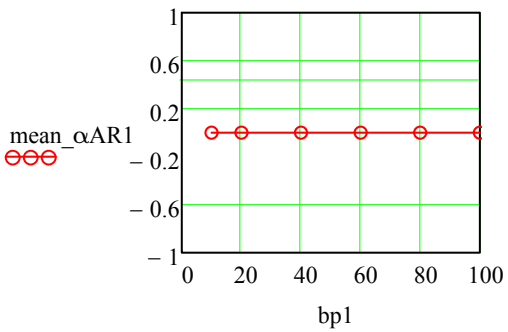

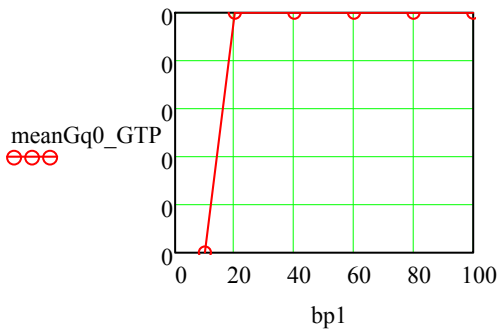

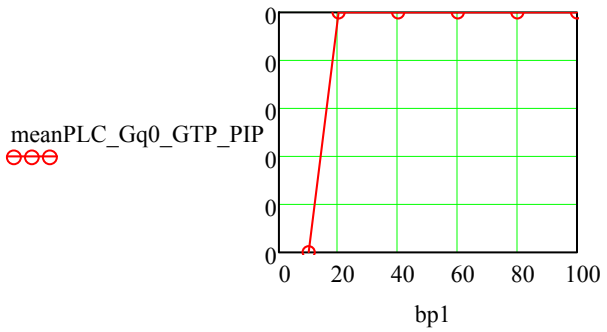

[Splot P34-36]